

EFFECTS OF SOIL REINFORCEMENT ON SEISMIC PERFORMANCE
OF LOW-TO-MEDIUM RISE BUILDINGS

by

Yusuf Ali Akçay

B.S., Civil Engineering, Karadeniz Technical University, 2014

Submitted to the Institute for Graduate Studies in
Science and Engineering in partial fulfillment of
the requirements for the degree of
Master of Science

Master Program in Earthquake Engineering

Boğaziçi University

2021

ACKNOWLEDGEMENTS

I would like to sincerely state my gratitude to Prof. Ayşe Edinçliler for her support, guidance and help during the preparation of the thesis. I would like to thank for her patience approach during this process.

I would like to thank experts and technicians, who helped me during my experiments in KOERI Shaking Table Laboratory.

In the realization of this thesis, the exoerinfrastructure supported by the Boğaziçi University Research Fund (Project No. BAP8084) was used. I thank BÜ-BAP for making this thesis possible.

And, I would like to express my deepest gratitude to my parents for their invaluable support, love and encouragement. I could never achieve without their priceless assistance.

ABSTRACT

EFFECTS OF SOIL REINFORCEMENT ON SEISMIC PERFORMANCE OF LOW-TO-MEDIUM RISE BUILDINGS

Soil reinforcement is used to improve the stiffness and strength of soil. The benefits of reinforcement inclusions within soil mass to increase the bearing capacity and reduce the settlement of soil foundation have been widely studied. The principle of geosynthetic reinforced soil method briefly is to deploy horizontal layers of closely spaced tensile inclusion in the fill material to achieve stability of a soil mass. This study aimed to determine the applicability and effectiveness of a proposed geogrid reinforcement system for low-rise and mid-rise buildings under earthquake loadings to mitigate earthquake effects. In order to observe the effectiveness of the proposed reinforcement system, a set of shaking table experiments were carried out with and without soil reinforcement. To determine structure and soil behavior together, an experimental set-up was designed. The effects of the number of the story, the number of geogrids layers and ground motion characteristic were evaluated and the effects of all these parameters on system were investigated. There are many experimental studies showing that the ratio of geogrid length (L) to building foundation width (B) affects experimental results under static loads. In this study, the L/B ratio was taken as 2.3. This value is the highest possible L/B ratio due to limitations in the experimental setup. When the results of experiments are evaluated, it is clearly seen that proposed reinforcement system can reduce the horizontal accelerations, horizontal drifts in the soil, story displacement of the building. The seismic energy transmitted from ground to the structure without geogrid reinforcement system in the soil can be decreased through this system. Therefore, proposed geogrid reinforcement system can be used to improve the seismic resistance capacity of the structures against strong ground motions.

ÖZET

ZEMİN DONATISININ DÜŞÜK VE ORTA KATLI BİNALARIN SİSMİK PERFORMANSI ÜZERİNDE ETKİLERİ

Zemin donatısı, zeminin rijitliği ve mukavemetini arttırmak için kullanılır. Taşıma kapasitesini artırmak ve zemin temelini oturmasını azaltmak için geogrid yardımıyla yapılacak bir zemin güçlendirmesi geniş çapta incelenmiştir. Geosentetik takviyeli zemin yönteminin kısaca prensibi, zemin içerisinde yatay olarak oluşturulan katmanların zeminin çekme gerilmesini azaltmasıyla gerçekleşmesidir. Bu çalışma, deprem etkilerinin azaltılması için deprem yükleri altında az ve orta katlı binalar için önerilen bir geogrid güçlendirme sisteminin uygulanabilirliğini ve etkinliğini belirlemeyi amaçlamıştır. Önerilen zemin donatısı sisteminin etkinliğini gözlemlemek için zemin güçlendirilerek ve güçlendirilmeden bir seri sarsma masası deneyleri yapılmıştır. Yapı ve zemin davranışını birlikte belirlemek için bir deney düzeneği tasarlanmıştır. Kat sayısı, geogrid katman sayısı ve yer hareketi karakteristiğinin etkileri değerlendirilmiş ve tüm bu parametrelerin sistem üzerindeki etkileri araştırılmıştır. Geogrid uzunluğunun (L) bina temel genişliğine (B) oranının statik yükler altında deneysel sonuçları etkilediğini gösteren birçok deneysel çalışma bulunmaktadır. Bu çalışmada L/B oranı 2.3 olarak alınmıştır. Bu değer, deney düzeneğindeki sınırlamalar nedeniyle mümkün olan en yüksek L/B oranıdır. Deney sonuçları değerlendirildiğinde, önerilen donatı sisteminin binanın yatay ivmelerini, zemindeki yatay yer değiştirmeleri, ve kat yer değiştirmesini azaltabileceği açıkça görülmektedir. Bu sistem sayesinde zeminde geogrid donatı sistemi olmadan zeminden yapıya aktarılan sismik enerji azaltılabilir. Bu nedenle, önerilen geogrid donatı sistemi, yapıların kuvvetli yer hareketlerine karşı sismik direnç kapasitesini geliştirmek için kullanılabilir.

TABLE OF CONTENTS

ACKNOWLEDGEMENTS	iii
ABSTRACT.....	iv
ÖZET	v
LIST OF FIGURES	xi
LIST OF TABLES	xxv
LIST OF SYMBOLS	xxxii
LIST OF ACRONYMS/ABBREVIATIONS	xxxiii
1. INTRODUCTION	1
1.1. General	1
1.2. Objectives And Problem Statement	2
2. LITERATURE REVIEW	4
2.1. What is Soil Reinforcement	4
2.2. Types Of Soil Reinforcement.....	6
2.2.1. Soil-Fill Matrix.....	6
2.2.2. Reinforcement or Anchor System	6
2.2.3. Geosynthetics	6
2.3. Techniques of Soil Reinforcement.....	7
2.3.1. In-situ Reinforcement	8
2.3.1.1. Soil Nailing	8
2.3.1.1. Soil Dowelling.....	8
2.3.2. Constructed Soil Reinforcement Technique.....	8
2.4. Geosynthetics in Soil Reinforcement.....	9
2.4.1. Geogrid Reinforcement	10
2.5. Literature Review	12

2.5.1. Experimental Studies	12
2.5.2. Numerical Studies	20
3. MATERIALS AND METHODS	28
3.1. Experimental Model Properties	28
3.1.1. Shaking Table	28
3.1.2. Measuring Instruments	29
3.1.3. Laminar Box	29
3.1.4. Scaled Building Models	33
3.2. Materials	35
3.2.1. Soil Material	35
3.2.2. Geogrid Material	36
3.3. Input Seismic Motions	37
3.4. Determination of the Number and Location of Geogrid Layers	39
3.4.1. The Number and Location of Geogrid Layers	40
3.4.2. The Location of Sensors on Scaled Building Model and in Soil	42
3.4.3. The Scaled Input Motions	46
3.4.4. Sample Preparation	48
4. RESULTS OF SHAKING TABLE TESTS	53
4.1. Experimental Program	53
4.2. 5-Story Building Model on Geogrid Reinforced Soil	56
4.2.1. Seismic Response of 5-Story Model under Kobe Earthquake Motion (PGA=0.74 g)	56
4.2.2. Seismic Response of 5-Story Model under Kobe Earthquake Motion (PGA=0.89 g)	63
4.2.3. Seismic Response of 5-Story Model under Kocaeli Earthquake Motion (PGA=0.21 g)	70

4.2.4. Seismic Response of 5-Story Model under Kocaeli Earthquake Motion (PGA=0.51 g)	77
4.2.5. Seismic Response of 5-Story Model under El Centro Earthquake Motion (PGA=0.35 g)	84
4.2.6. Seismic Response of 5-Story Model under El Centro Earthquake Motion (PGA=0.55 g)	91
4.2.7. Seismic Response of 5-Story Model under El Centro Earthquake Motion (PGA=0.89 g)	98
4.3. 3-Story Building Model on Geogrid Reinforced Soil	105
4.3.1. Seismic Response of 3-Story Model under Kobe Earthquake Motion (PGA=0.74 g)	105
4.3.2. Seismic Response of 3-Story Model under Kobe Earthquake Motion (PGA=0.89 g)	112
4.3.3. Seismic Response of 3-Story Model under Kocaeli Earthquake Motion (PGA=0.21 g)	119
4.4.3. Seismic Response of 3-Story Model under Kocaeli Earthquake Motion (PGA=0.51 g)	126
4.3.5. Seismic Response of 3-Story Model under El Centro Earthquake Motion (PGA=0.35 g)	133
4.3.6. Seismic Response of 3-Story Model under El Centro Earthquake Motion (PGA=0.55 g)	140
4.3.7. Seismic Response of 3-Story Model under El Centro Earthquake Motion (PGA=0.89 g)	147
4.4. Free-Surface Tests for Geogrid Reinforced Soil	154
4.4.1. Seismic Response of Free-Surface under Kobe Earthquake Motion (PGA=0.89 g)	155
4.4.2. Seismic Response of Free-Surface under Kobe Earthquake Motion (PGA=0.99 g)	158

4.4.3. Seismic Response of Free-Surface under Kocaeli Earthquake Motion (PGA=0.16 g)	161
4.4.4. Seismic Response of Free-Surface under Kocaeli Earthquake Motion (PGA=0.25 g)	164
4.4.5. Seismic Response of Free-Surface under El Centro Earthquake (PGA=0.35g) .	167
4.5. Cyclic Sinusoidal Motions with Natural Frequencies.....	170
4.5.1. Seismic Response of 5-Story Building Model under 8.58 Hz Cyclic Sinusoidal Motion (PGA=0.35 g)	170
4.5.2. Seismic Response of 3-Story Building Model under 12.46Hz Cyclic Sinusoidal Motion (PGA=0.4 g)	177
5. DISCUSSION.....	184
5.1. Effects of The Proposed Geogrid Reinforcement System under Earthquake Motions with Real PGA, Earthquake Motions with Increasing PGA and Cyclic Sinusoidal Motion	184
5.1.1. Seismic Response of The Cases For 5-Story Model	184
5.1.1.1. Effects of Proposed Geogrid Reinforcement System on Top Floor Acceleration for 5-Story Model.....	185
5.1.1.2. Effects of Proposed Geogrid Reinforcement System on First Floor Acceleration for 5-Story Model.....	186
5.1.1.3. Effects of Proposed Geogrid Reinforcement System on Top Floor Displacement for 5-Story Model	187
5.1.1.4. Effects of Proposed Geogrid Reinforcement System on First Floor Displacement for 5-Story Model	189
5.1.1.5. Effects of Proposed Geogrid Reinforcement System on Foundation Acceleration for 5-Story Model.....	190
5.1.1.6. Effects of Proposed Geogrid Reinforcement System on Soil Acceleration for 5-Story Model	192
5.1.1.7. Effects of Proposed Geogrid Reinforcement System on Top Floor Arias Intensity for 5-Story Model	193

5.1.1.8. Effects of Proposed Geogrid Reinforcement System on Foundation Arias Intensity For 5-Story Model	195
5.1.2. Seismic Response of The Cases For 3-Story Model	197
5.1.2.1. Effects of Proposed Geogrid Reinforcement System on Top Floor Acceleration for 3-Story Model.....	197
5.1.2.2. Effects of Proposed Geogrid Reinforcement System on First Floor Acceleration for 3-Story Model.....	198
5.1.2.3. Effects of Proposed Geogrid Reinforcement System on Top Floor Displacement for 3-Story Model	199
5.1.2.4. Effects of Proposed Geogrid Reinforcement System on First Floor Displacement for 3-Story Model.	201
5.1.2.5. Effects of Proposed Geogrid Reinforcement System on Foundation Acceleration for 3-Story Model.....	202
5.1.2.6. Effects of Proposed Geogrid Reinforcement System on Soil Acceleration for 3-Story Model.	204
5.1.2.7. Effects of Proposed Geogrid Reinforcement System on Top Floor Arias Intensity for 3-Story Model.	205
5.1.2.8. Effects of Proposed Geogrid Reinforcement System on Foundation Arias Intensity For 3-Story Model.	207
6. SUMMARY AND CONCLUSIONS	209
6.1. Summary	209
6.2. Conclusions.....	211

LIST OF FIGURES

Figure 2.1. The slope stability with Geosynthetic (Geosyntheticsmagazine, 2019).....	5
Figure 2.2. Soil Reinforcement with Geosynthetic (Geosyntheticsmagazine, 2019).....	5
Figure 2.3. Overview of Geosynthetic Categories (Designing with Geosynthetics, Koerner R. M. 2012).....	7
Figure 2.4. General View of Uniaxial Geogrid (https://mainlinematerials.com).....	11
Figure 2.5. General View of Biaxial Geogrid (https://indiamart.com).....	11
Figure 2.6. General View of Triaxial Geogrid (https://indiamart.com).....	12
Figure 2.7. Sketches of Strip and Square Foundations used in the study (Omar & Das, 1993).	13
Figure 2.8. Geometric Parameters of Reinforced Foundation (Yetimoglu & Saglamer, 1994	14
Figure 2.9. The general View of Strip Foundation on Geogrid-Reinforced Sand (Shin et al., 2000).....	15
Figure 2.10. A General View of Shallow Strip Foundation on Geogrid Reinforced Sand for Model Test (Patra et al., 2000)	16
Figure 2.11. General View of Model Plate supported by Geogrid Reinforced over Collapsible Soil (H.A. Alawaji et al., 2000).....	17
Figure 2.12. A General View of the Model Test Setup (Yabu & Tripathi, 2013).....	19

Figure 2.13. A general View of Building Model and Sections (Ruoshi & Behzad, 2018).....	21
Figure 2.14. Adopted Soil-Structure System with Layers (Ruoshi & Behzad, 2018).....	21
Figure 2.15. Finite Element Modelling for 5 storey Model (Edinçliler et al., 2017).....	22
Figure 2.16. A general View of The Footing Model, generated Mesh and Boundary Condi- ons. (Tahmaz et al., 2017).....	24
Figure 2.17. A general View of Geosynthetic Layers in The Model Tests (Latha & Somwan-shi, 2008).....	25
Figure 3.1. A General View of Shaking Table and Laminar Box.....	28
Figure 3.2. Accelerometer and Displacement meter.....	29
Figure 3.3. A Profile View of Laminar Box.....	31
Figure 3.4. The Friction Forces of Laminar Box.....	32
Figure 3.5. The Profile View of 5 Storey Scaled Building Model.....	34
Figure 3.6. The Profile View of 3 Storey Scaled Building Model.....	35
Figure 3.7. The Grain-Size Distribution of Silivri Sand.....	36
Figure 3.8. A Sample Piece of Geogrid Material (80 cm x 80 cm).....	37
Figure 3.9. Time-Acceleration Records of (a) El Centro, (b) Kobe and (c) Kocaeli Earth- quakes.....	39

Figure 3.10. Variation with Number of Geogrid Reinforcement Layers (Omar et al. 1993).	40
Figure 3.11. Variation with Number of Geogrid Reinforcement Layers (Yetimoglu et al. 1994).....	41
Figure 3.12. A General View of Experimental Model).....	42
Figure 3.13. General View of Accelerometer's Locations in Soil (Sekman, 2016)	43
Figure 3.14. The Sketch of Scaled Building Model and Sensors For 5-Storey.....	44
Figure 3.15. The Sketch of Scaled Building Model and Sensors For 3-Storey.....	45
Figure 3.16. A View of The Scaled Building Model with Projection of Sensors.....	46
Figure 3.17. Soil Preparation Process of Experimental Model (a) Without Geogrid Reinforcement, (b) With Geogrid Reinforcement.....	49
Figure 3.18. Soil Preparation Process of Model.....	50
Figure 3.19. Soil Preparation Process of Model (a) With an Accelerometer and Geogrid Reinforcement in Soil, (b) Measurement of Soil Level, (c) With Complete Soil Container.....	51
Figure 3.20. 5-Storey and 3-Storey Scaled Building Models.....	52
Figure 4.1. Acceleration Measurements and FAS of 1st and 5th Floors under Kobe Earthquake Motion (PGA= 0.74 g).....	58
Figure 4.2. Displacement Measurements and FAS of 1st and 5th Floors under Kobe Earthquake Motion (PGA= 0.74 g).....	59

Figure 4.3. The Acceleration Improvement Graphs in Accordance with Story and Reinforcement Layers for (a) Foundation, (b) 1st Floor, (c) 5th Floor under Kobe Earthquake Motion (PGA= 0.74 g).....	60
Figure 4.4. The Displacement Improvement Graphs in Accordance with Story and Reinforcement Layers for (a) 1st Floor, (b) 5th Floor under Kobe Earthquake Motion (PGA= 0.74 g).....	61
Figure 4.5. Improvement Ratios considering (a) Story Drifts and (b) Arias Intensity under Kobe Earthquake Motion (PGA= 0.74 g).....	63
Figure 4.6. Acceleration Measurements and FAS of 1st and 5th Floors under Kobe Earthquake Motion (PGA= 0.89 g).....	65
Figure 4.7. Displacement Measurements and FAS of 1st and 5th Floors under Kobe Earthquake Motion (PGA= 0.89 g).....	66
Figure 4.8. The Acceleration Improvement Graphs in Accordance with Story and Reinforcement Layers for (a) Foundation, (b) 1st Floor, (c) 5th Floor under Kobe Earthquake Motion (PGA= 0.89 g).....	67
Figure 4.9. The Displacement Improvement Graphs in Accordance with Story and Reinforcement Layers for (a) 1st Floor, (b) 5th Floor under Kobe Earthquake Motion (PGA= 0.89 g).....	68
Figure 4.10. Improvement Ratios considering (a) Story Drifts and (b) Arias Intensity under Kobe Earthquake Motion (PGA= 0.89 g).....	70
Figure 4.11. Acceleration Measurements and FAS of 1st and 5th Floors under Kocaeli Earthquake Motion (PGA= 0.21 g).....	72
Figure 4.12. Displacement Measurements and FAS of 1st and 5th Floors under Kocaeli Earthquake Motion (PGA= 0.21 g).....	73

Figure 4.13. The Acceleration Improvement Graphs in Accordance with Story and Reinforcement Layers for (a) Foundation, (b) 1st Floor, (c) 5th Floor under Kocaeli Earthquake Motion (PGA= 0.21 g).....74

Figure 4.14. The Displacement Improvement Graphs in Accordance with Story and Reinforcement Layers for (a) 1st Floor, (b) 5th Floor under Kocaeli Earthquake Motion (PGA= 0.89 g).....75

Figure 4.15. Improvement Ratios considering (a) Story Drifts and (b) Arias Intensity under Kocaeli Earthquake Motion (PGA= 0.21 g).....77

Figure 4.16. Acceleration Measurements and FAS of 1st and 5th Floors under Kocaeli Earthquake Motion (PGA= 0.51 g).....79

Figure 4.17. Displacement Measurements and FAS of 1st and 5th Floors under Kocaeli Earthquake Motion (PGA= 0.51 g).....80

Figure 4.18. The Acceleration Improvement Graphs in Accordance with Story and Reinforcement Layers for (a) Foundation, (b) 1st Floor, (c) 5th Floor under Kocaeli Earthquake Motion (PGA= 0.51 g).....81

Figure 4.19. The Displacement Improvement Graphs in Accordance with Story and Reinforcement Layers for (a) 1st Floor, (b) 5th Floor under Kocaeli Earthquake Motion (PGA= 0.51 g).....82

Figure 4.20. Improvement Ratios considering (a) Story Drifts and (b) Arias Intensity under Kocaeli Earthquake Motion (PGA= 0.51 g).....84

Figure 4.21. Acceleration Measurements and FAS of 1st and 5th Floors under El Centro Earthquake Motion (PGA= 0.35 g).....86

Figure 4.22. Displacement Measurements and FAS of 1st and 5th Floors under El Centro Earthquake Motion (PGA= 0.35 g).....87

Figure 4.23. The Acceleration Improvement Graphs in Accordance with Story and Reinforcement Layers for (a) Foundation, (b) 1st Floor, (c) 5th Floor under El Centro Earthquake Motion (PGA= 0.35 g).....	88
Figure 4.24. The Displacement Improvement Graphs in Accordance with Story and Reinforcement Layers for (a) 1st Floor, (b) 5th Floor under El Centro Earthquake Motion (PGA= 0.35 g).....	89
Figure 4.25. Improvement Ratios considering (a) Story Drifts and (b) Arias Intensity under El Centro Earthquake Motion (PGA= 0.35 g).....	91
Figure 4.26. Acceleration Measurements and FAS of 1st and 5th Floors under El Centro Earthquake Motion (PGA= 0.55 g).....	93
Figure 4.27. Displacement Measurements and FAS of 1st and 5th Floors under El Centro Earthquake Motion (PGA= 0.55 g).....	94
Figure 4.28. The Acceleration Improvement Graphs in Accordance with Story and Reinforcement Layers for (a) Foundation, (b) 1st Floor, (c) 5th Floor under El Centro Earthquake Motion (PGA= 0.55 g).....	95
Figure 4.29. The Displacement Improvement Graphs in Accordance with Story and Reinforcement Layers for (a) 1st Floor, (b) 5th Floor under El Centro Earthquake Motion (PGA= 0.55 g).....	96
Figure 4.30. Improvement Ratios considering (a) Story Drifts and (b) Arias Intensity under ElCentro Earthquake Motion (PGA= 0.55 g).....	98
Figure 4.31. Acceleration Measurements and FAS of 1st and 5th Floors under El Centro Earthquake Motion (PGA= 0.89 g).....	100
Figure 4.32. Displacement Measurements and FAS of 1st and 5th Floors under El Centro Earthquake Motion (PGA= 0.89 g).....	101

- Figure 4.33. The Acceleration Improvement Graphs in Accordance with Story and Reinforcement Layers for (a) Foundation, (b) 1st Floor, (c) 5th Floor under El Centro Earthquake Motion (PGA= 0.89 g).....102
- Figure 4.34. The Displacement Improvement Graphs in Accordance with Story and Reinforcement Layers for (a) 1st Floor, (b) 5th Floor under El Centro Earthquake Motion (PGA= 0.89 g).....103
- Figure 4.35. Improvement Ratios considering (a) Story Drifts and (b) Arias Intensity under El Centro Earthquake Motion (PGA= 0.55 g).....105
- Figure 4.36. Acceleration Measurements and FAS of 1st and 3rd Floors under Kobe Earthquake Motion (PGA= 0.74 g).....107
- Figure 4.37. Displacement Measurements and FAS of 1st and 3rd Floors under Kobe Earthquake Motion (PGA= 0.74 g).....108
- Figure 4.38. The Acceleration Improvement Graphs in Accordance with Story and Reinforcement Layers for (a) Foundation, (b) 1st Floor, (c) 3rd Floor under Kobe Earthquake Motion (PGA= 0.74 g).....109
- Figure 4.39. The Displacement Improvement Graphs in Accordance with Story and Reinforcement Layers for (a) 1st Floor, (b) 3rd Floor under Kobe Earthquake Motion (PGA= 0.74 g).....110
- Figure 4.40. Improvement Ratios considering (a) Story Drifts and (b) Arias Intensity under Kobe Earthquake Motion (PGA= 0.74 g).....112
- Figure 4.41. Acceleration Measurements and FAS of 1st and 3rd Floors under Kobe Earthquake Motion (PGA= 0.89 g).....114
- Figure 4.42. Displacement Measurements and FAS of 1st and 3rd Floors under Kobe Earthquake Motion (PGA= 0.89 g).....115

Figure 4.43. The Acceleration Improvement Graphs in Accordance with Story and Reinforcement Layers for (a) Foundation, (b) 1st Floor, (c) 3rd Floor under Kobe Earthquake Motion (PGA= 0.89 g).....	116
Figure 4.44. The Displacement Improvement Graphs in Accordance with Story and Reinforcement Layers for (a) 1st Floor, (b) 3rd Floor under Kobe Earthquake Motion (PGA= 0.89 g).....	117
Figure 4.45. Improvement Ratios considering (a) Story Drifts and (b) Arias Intensity under Kobe Earthquake Motion (PGA= 0.89 g).....	119
Figure 4.46. Acceleration Measurements and FAS of 1st and 3rd Floors under Kocaeli Earthquake Motion (PGA= 0.21 g).....	121
Figure 4.47. Displacement Measurements and FAS of 1st and 3rd Floors under Kocaeli Earthquake Motion (PGA= 0.21 g).....	122
Figure 4.48. The Acceleration Improvement Graphs in Accordance with Story and Reinforcement Layers for (a) Foundation, (b) 1st Floor, (c) 3rd Floor under Kocaeli Earthquake Motion (PGA= 0.21 g).....	123
Figure 4.49. The Displacement Improvement Graphs in Accordance with Story and Reinforcement Layers for (a) 1st Floor, (b) 3rd Floor under Kocaeli Earthquake Motion (PGA= 0.21 g).....	124
Figure 4.50. Improvement Ratios considering (a) Story Drifts and (b) Arias Intensity under Kocaeli Earthquake Motion (PGA= 0.21 g).....	126
Figure 4.51. Acceleration Measurements and FAS of 1st and 3rd Floors under Kocaeli Earthquake Motion (PGA= 0.51 g).....	128
Figure 4.52. Displacement Measurements and FAS of 1st and 3rd Floors under Kocaeli Earthquake Motion (PGA= 0.51 g).....	129

Figure 4.53. The Acceleration Improvement Graphs in Accordance with Story and Reinforcement Layers for (a) Foundation, (b) 1st Floor, (c) 3rd Floor under Kocaeli Earthquake Motion (PGA= 0.51 g).....	130
Figure 4.54. The Displacement Improvement Graphs in Accordance with Story and Reinforcement Layers for (a) 1st Floor, (b) 3rd Floor under Kocaeli Earthquake Motion (PGA= 0.51 g).....	131
Figure 4.55. Improvement Ratios considering (a) Story Drifts and (b) Arias Intensity under Kocaeli Earthquake Motion (PGA= 0.51 g).....	133
Figure 4.56. Acceleration Measurements and FAS of 1st and 3rd Floors under El Centro Earthquake Motion (PGA= 0.35 g).....	135
Figure 4.57. Displacement Measurements and FAS of 1st and 3rd Floors under El Centro Earthquake Motion (PGA= 0.35 g).....	136
Figure 4.58. The Acceleration Improvement Graphs in Accordance with Story and Reinforcement Layers for (a) Foundation, (b) 1st Floor, (c) 3rd Floor El Centro Earthquake Motion (PGA= 0.35 g).....	137
Figure 4.59. The Displacement Improvement Graphs in Accordance with Story and Reinforcement Layers for (a) 1st Floor, (b) 3rd Floor under El Centro Earthquake Motion (PGA= 0.35 g).....	138
Figure 4.60. Improvement Ratios considering (a) Story Drifts and (b) Arias Intensity El Centro Earthquake Motion (PGA= 0.35 g).....	140
Figure 4.61. Acceleration Measurements and FAS of 1st and 3rd Floors under El Centro Earthquake Motion (PGA= 0.55 g).....	142
Figure 4.62. Displacement Measurements and FAS of 1st and 3rd Floors under El Centro Earthquake Motion (PGA= 0.55 g).....	143

Figure 4.63. The Acceleration Improvement Graphs in Accordance with Story and Reinforcement Layers for (a) Foundation, (b) 1st Floor, (c) 3rd Floor El Centro Earthquake Motion (PGA= 0.55 g).....	144
Figure 4.64. The Displacement Improvement Graphs in Accordance with Story and Reinforcement Layers for (a) 1st Floor, (b) 3rd Floor under El Centro Earthquake Motion (PGA= 0.55 g).....	145
Figure 4.65. Improvement Ratios considering (a) Story Drifts and (b) Arias Intensity El Centro Earthquake Motion (PGA= 0.55 g).....	147
Figure 4.66. Acceleration Measurements and FAS of 1st and 3rd Floors under El Centro Earthquake Motion (PGA= 0.89 g).....	149
Figure 4.67. Displacement Measurements and FAS of 1st and 3rd Floors under El Centro Earthquake Motion (PGA= 0.89 g).....	150
Figure 4.68. The Acceleration Improvement Graphs in Accordance with Story and Reinforcement Layers for (a) Foundation, (b) 1st Floor, (c) 3rd Floor El Centro Earthquake Motion (PGA= 0.89 g).....	151
Figure 4.69. The Displacement Improvement Graphs in Accordance with Story and Reinforcement Layers for (a) 1st Floor, (b) 3rd Floor under El Centro Earthquake Motion (PGA= 0.89 g).....	152
Figure 4.70. Improvement Ratios considering (a) Story Drifts and (b) Arias Intensity El Centro Earthquake Motion (PGA= 0.89 g).....	154
Figure 4.71. Acceleration Measurements and FAS of Soil(A12) under Kobe Earthquake Motion (PGA= 0.89 g).....	156
Figure 4.72. The Acceleration Improvement Graphs in Soil(A12) under Kobe Earthquake Motion (PGA= 0.89 g).....	156

Figure 4.73. Improvement Ratios considering Arias Intensity under Kobe Earthquake Motion (PGA= 0.89 g).....	157
Figure 4.74. Acceleration Measurements and FAS of Soil(A8) under Kobe Earthquake Motion (PGA= 0.99 g).....	159
Figure 4.75. The Acceleration Improvement Graphs in Soil(A8) under Kobe Earthquake Motion (PGA= 0.99 g).....	159
Figure 4.76. Improvement Ratios considering Arias Intensity under Kobe Earthquake Motion (PGA= 0.99 g).....	160
Figure 4.77. Acceleration Measurements and FAS of Soil(A12) under Kocaeli Earthquake Motion (PGA= 0.16 g).....	162
Figure 4.78. The Acceleration Improvement Graphs in Soil(A12) under Kocaeli Earthquake Motion (PGA= 0.16 g).....	162
Figure 4.79. Improvement Ratios considering Arias Intensity under Kocaeli Earthquake Motion (PGA= 0.16 g).....	163
Figure 4.80. Acceleration Measurements and FAS of Soil(A12) under Kocaeli Earthquake Motion (PGA= 0.25 g).....	165
Figure 4.81. The Acceleration Improvement Graphs in Soil(A12) under Kocaeli Earthquake Motion (PGA= 0.25 g).....	165
Figure 4.82. Improvement Ratios considering Arias Intensity under Kocaeli Earthquake Motion (PGA= 0.25 g).....	166
Figure 4.83. Acceleration Measurements and FAS of Soil(A12) under El Centro Earthquake Motion (PGA= 0.35 g).....	168

Figure 4.84. The Acceleration Improvement Graphs in Soil(A12) under El Centro Earthquake Motion (PGA= 0.35 g).....	168
Figure 4.85. Improvement Ratios considering Arias Intensity under El Centro Earthquake Motion (PGA= 0.35 g).....	169
Figure 4.86. Acceleration Measurements and FAS of 1st and 5th Floors under 8.85 Hz - 0.35g.	172
Figure 4.87. Displacement Measurements and FAS of 1st and 5th Floors under 8.58 Hz - 0.35g.	173
Figure 4.88. The Acceleration Improvement Graphs in Accordance with Story and Reinforcement Layers for (a) Foundation, (b) 1st Floor, (c) 5th Floor under 8.58 Hz - 0.35g.	174
Figure 4.89. The Displacement Improvement Graphs in Accordance with Story and Reinforcement Layers for (a) 1st Floor, (b) 5th Floor under 8.58 Hz-0.35g.....	175
Figure 4.90. Improvement Ratios considering (a) Intensity and (b) Story Drifts under 8.58 Hz - 0.35g.....	177
Figure 4.91. Acceleration Measurements and FAS of 1st and 3rd Floors under 12.46 Hz- 0.4g.....	179
Figure 4.92. Displacement Measurements and FAS of 1st and 3rd Floors under 12.46 Hz- 0.4g.....	180
Figure 4.93. The Acceleration Improvement Graphs in Accordance with Story and Reinforcement Layers for (a) Foundation, (b) 1st Floor, (c) 3rd Floor under 12.46 Hz-0.4g..	181

Figure 4.94. The Displacement Improvement Graphs in Accordance with Story and Reinforcement Layers for (a) 1st Floor, (b) 3rd Floor under 12.46 Hz–0.4g.....	181
Figure 4.95. Improvement Ratios considering (a) Intensity and (b) Story Drifts under 12.46 Hz-0.35g.....	183
Figure 5.1. Reduction of Top Floor Acceleration under Input Motions for 5-Storey Model.....	186
Figure 5.2. Reduction of First Floor Acceleration under Input Motions for 5-Storey Model.....	187
Figure 5.3. Reduction of Top Floor Displacement under Input Motions for 5-Storey Model.....	189
Figure 5.4. Reduction of First Floor Displacement under Input Motions for 5-Storey Model.....	190
Figure 5.5. Reduction of Foundation Acceleration under Input Motions for 5-Storey Model.....	192
Figure 5.6. Reduction of Soil Acceleration under Input Motions for 5-Storey Model...	193
Figure 5.7. Reduction of Top Floor Arias Intensity under Input Motions for 5-Storey Model.....	195
Figure 5.8. Reduction of Foundation Arias Intensity under Input Motions for 5-Storey Model.....	196
.	
Figure 5.9. Reduction of Top Floor Acceleration under Input Motions for 3-Storey Model.....	198

Figure 5.10. Reduction of First Floor Acceleration under Input Motions for 3-Storey Model.....	199
Figure 5.11. Reduction of Top Floor Displacement under Input Motions for 3-Storey Model.....	201
Figure 5.12. Reduction of First Floor Displacement under Input Motions for 3-Storey Model.....	202
Figure 5.13. Reduction of Foundation Acceleration under Input Motions for 3-Storey Model.....	204
Figure 5.14. Reduction of Soil Acceleration under Input Motions for 3-Storey Model.....	205
Figure 5.15. Reduction of Top Floor Arias Intensity under Input Motions for 3-Storey Model.....	207
Figure 5.16. Reduction of Foundation Arias Intensity under Input Motions for 3-Storey Model.....	208

LIST OF TABLES

Table 3.1. The Scaled Building Model Parameters (Sekman, 2016)	33
Table 3.2. The Physical Properties of UR-55.....	37
Table 3.3. The Data of El Centro, Kobe and Kocaeli Earthquake Motions.....	38
Table 3.4. The Models and Input Motions.....	48
Table 4.1. Experimental Program (The Case Numbers and Model).....	54
Table 4.2. Summary of All Tested Cases under Kobe Earthquake motion (PGA=0.74g)...	57
Table 4.3. Fundamental Period and Period Lengthening Ratios under Kobe Earthquake Motion (PGA = 0.74g)	62
Table 4.4. RMS and Arias Intensity Improvement Ratios under Kobe Earthquake Motion (PGA = 0.74g)	62
Table 4.5. Summary of All Tested Cases under Kobe Earthquake motion (PGA=0.89g)...	64
Table 4.6. Fundamental Period and Period Lengthening Ratios under Kobe Earthquake Motion (PGA = 0.89g).....	69
Table 4.7. RMS and Arias Intensity Improvement Ratios under Kobe Earthquake Motion (PGA = 0.89g).....	69

Table 4.8. Summary of all tested Cases for 5-Story Model under Kocaeli Earthquake motion (PGA=0.21g).....	71
Table 4.9. Fundamental Period and Period Lengthening Ratios under Kobe Earthquake Motion (PGA = 0.89g).....	76
Table 4.10. RMS and Arias Intensity Improvement Ratios under Kobe Earthquake Motion (PGA = 0.89g).....	76
Table 4.11. Summary of all tested Cases under Kocaeli Earthquake motion (PGA=0.51g).	78
Table 4.12. Fundamental Period and Period Lengthening Ratios under Kocaeli Earthquake Motion (PGA= 0.51 g).....	83
Table 4.13. RMS and Arias Intensity Improvement Ratios under Kocaeli Earthquake Motion (PGA= 0.51 g).....	83
Table 4.14. Summary of all tested Cases under El Centro Earthquake motion (PGA=0.35g).....	85
Table 4.15. Fundamental Period and Period Lengthening Ratios under El Centro Earthquake Motion (PGA= 0.35 g).....	89
Table 4.16. RMS and Arias Intensity Improvement Ratios under Kocaeli Earthquake Motion (PGA= 0.51 g).....	90
Table 4.17. Summary of all tested Cases under El Centro Earthquake motion (PGA=0.55g).....	92
Table 4.18. Fundamental Period and Period Lengthening Ratios under El Centro Earthquake Earthquake Motion (PGA= 0.55 g).....	97

Table 4.19. RMS and Arias Intensity Improvement Ratios under El Centro Earthquake Motion (PGA= 0.55 g).....	97
Table 4.20. Summary of all tested Cases under El Centro Earthquake motion (PGA=0.89g).....	99
Table 4.21. Fundamental Period and Period Lengthening Ratios under El Centro Earthquake Motion (PGA= 0.89 g).....	104
Table 4.22. RMS and Arias Intensity Improvement Ratios under El Centro Earthquake Motion (PGA= 0.89 g).....	104
Table 4.22. Summary of all tested Cases under Kobe Earthquake motion (PGA=0.74g).....	106
Table 4.23. Fundamental Period and Period Lengthening Ratios under Kobe Earthquake Motion (PGA= 0.74 g).....	111
Table 4.24. RMS and Arias Intensity Improvement Ratios under Kobe Earthquake Motion (PGA= 0.74 g).....	111
Table 4.25. Summary of all tested Cases under Kobe Earthquake motion (PGA=0.89g).....	113
Table 4.26. Fundamental Period and Period Lengthening Ratios under Kobe Earthquake Motion (PGA= 0.74 g).....	118
Table 4.27. RMS and Arias Intensity Improvement Ratios under Kobe Earthquake Motion (PGA= 0.74 g).....	118
Table 4.28. Summary of all tested Cases under Kocaeli Earthquake motion(PGA=0.21g).....	120

Table 4.29. Fundamental Period and Period Lengthening Ratios under Kocaeli Earthquake Motion (PGA= 0.21 g).....	124
Table 4.30. RMS and Arias Intensity Improvement Ratios under Kocaeli Earthquake Motion (PGA= 0.21 g).....	125
Table 4.31. Summary of all tested Cases under Kocaeli Earthquake motion (PGA=0.51g).	127
Table 4.32. Fundamental Period and Period Lengthening Ratios under Kocaeli Earthquake Motion (PGA= 0.51 g).....	132
Table 4.33. RMS and Arias Intensity Improvement Ratios under Kocaeli Earthquake Motion (PGA= 0.51 g).....	132
Table 4.34. Summary of all tested Cases under El Centro Earthquake motion (PGA=0.35g).	134
Table 4.35. Fundamental Period and Period Lengthening Ratios under El Centro Earthquake Motion (PGA= 0.35 g).....	139
Table 4.36. RMS and Arias Intensity Improvement Ratios under El Centro Earthquake Motion (PGA= 0.35 g).....	139
Table 4.37. Summary of all tested Cases under El Centro Earthquake motion (PGA=0.55g).	141
Table 4.38. Fundamental Period and Period Lengthening Ratios under El Centro Earthquake Motion (PGA= 0.55 g).....	146
Table 4.39. RMS and Arias Intensity Improvement Ratios under El Centro Earthquake Motion (PGA= 0.55 g).....	146

Table 4.40. Summary of all tested Cases under El Centro Earthquake motion (PGA=0.89g).....	148
Table 4.41. Fundamental Period and Period Lengthening Ratios under El Centro Earthquake Motion (PGA= 0.89 g).....	152
Table 4.42. RMS and Arias Intensity Improvement Ratios under El Centro Earthquake Motion (PGA= 0.89 g).....	153
Table 4.43. Summary of all tested Cases under Kobe Earthquake motion (PGA=0.89g)..	155
Table 4.44. Fundamental Period and Period Lengthening Ratios under Kobe Earthquake Motion (PGA= 0.89 g).....	157
Table 4.45. RMS and Arias Intensity Improvement Ratios under Kobe Earthquake Motion (PGA= 0.89 g).....	157
Table 4.46. Summary of all tested Cases under Kobe Earthquake motion (PGA=0.99)...	158
Table 4.47. Fundamental Period and Period Lengthening Ratios under Kobe Earthquake Motion (PGA= 0.99 g).....	160
Table 4.48. RMS and Arias Intensity Improvement Ratios under Kobe Earthquake Motion (PGA= 0.99 g).....	160
Table 4.49. Summary of all tested Cases under Kocaeli Earthquake motion (PGA=0.16g).	161
Table 4.50. Fundamental Period and Period Lengthening Ratios under Kocaeli Earthquake Motion (PGA= 0.16 g).....	163

Table 4.51. RMS and Arias Intensity Improvement Ratios under Kocaeli Earthquake Motion (PGA= 0.16 g).....	163
Table 4.52. Summary of all tested Cases under Kocaeli Earthquake motion (PGA=0.25g).	164
Table 4.53. Fundamental Period and Period Lengthening Ratios under Kocaeli Earthquake Motion (PGA= 0.25 g).....	166
Table 4.54. RMS and Arias Intensity Improvement Ratios under Kocaeli Earthquake Motion (PGA= 0.25 g).....	166
Table 4.55. Summary of all tested Cases under El Centro Earthquake motion (PGA=0.35g).....	167
Table 4.56. Fundamental Period and Period Lengthening Ratios under El Centro Earthquake Motion (PGA= 0.35 g).....	169
Table 4.57. RMS and Arias Intensity Improvement Ratios under El Centro Earthquake Motion (PGA= 0.35 g).....	169
Table 4.58. Summary of all tested Cases for 5-Story Model under 8.58 Hz-0.35g.....	171
Table 4.59. Fundamental Period and Period Lengthening Ratios under 8.58 Hz-0.35g...	176
Table 4.60. RMS and Arias Intensity Improvement Ratios under 8.58 Hz-0.35g.....	176
Table 4.61. Summary of all tested Cases for 5-Story Model under 12.46 Hz-0.4g.....	178
Table 4.62. Fundamental Period and Period Lengthening Ratios under 12.46 Hz-0.4g....	182

Table 4.63. RMS and Arias Intensity Improvement Ratios under 12.46 Hz-0.4g.....	183
---	-----

LIST OF SYMBOLS

SP	Graded Sand
Cu	The Coefficient of Curvature
Cc	The Coefficient of Uniformity
Φ	The Internal Friction Angle
g	Gravitational Acceleration
G	Gravitational Constant
Gs	Specific Gravity
Dr	Unit Weight

LIST OF ACRONYMS/ABBREVIATIONS

GSR	Geosynthetic Reinforced Soil
FEA	Finite Element Analysis
FEM	Finite Element Model
A	Accelerometer
D	Displacement meter
N	Number of Geogrid Layer
B	One Side Length of Square Foundation
b	One Side Length Geogrid
h	Distances between Geogrid Layers
u	Distance between Bottom of Foundation and First Layer of Geogrid
d	Distance between Bottom of Foundation and Last Geogrid Layer
WR	Cases Without Geogrid Reinforcement
R	Cases with Geogrid Reinforcement
RSM	Root Mean Square
FAS	Fourier Amplitude Spectrum
PGA	Peak Ground Acceleration
PGV	Peak Ground Velocity
PGD	Peak Ground Displacement

1. INTRODUCTION

1.1. General

In recent decades, the way of construction of new structures has changed in many aspects. In that context, specifications have changed and been improved in the whole world.

The new engineering methods have induced new systems about preventing damages of the buildings from severe earthquakes. The new concept of protecting building from damaging effects provides the safety for buildings. In order to ensure this, by new methods, the internal forces and displacement were controlled. The widest method for protecting the structure is to reduce the seismic energy by the structural elements. The level of damage of the structural system directly connected the method how structure dissipates the input seismic energy. In conventional, it has provided through material ductility. Because of the fact that this method does not guarantee the required damage control, the new methods have started to be preferred.

All buildings should be designed to minimize the effects of severe earthquakes. The important studies show that increasing resistance capacity of the structures against to earthquakes through additional shear walls braced frames, and moment resisting frames can be effective ways to reduce the effect of earthquakes however, in some cases, it may be concluded with too high accelerations or large inter story drifts. Because of this, some structures have potential to be observed serious damage after severe earthquakes.

Accordingly, as an alternative method seismic protection concept has been emerged to protect buildings from the severe effects of earthquakes and reduce accelerations and inter story drifts. Main goal of it is to minimize the earthquake forces that are subjected to horizontal load carrying elements of the structure.

In the last decade soil reinforcement is one of the most popular seismic protection techniques against severe seismic events for civil engineering structures.

In the sake of being used for new protection techniques in engineering, geosynthetics have been so popular material and they have served to many features of the geotechnical engineering process. The use of geosynthetics in many cases can significantly improve performance, increase safety, and reduce costs compared to a conventional design methods.

The geosynthetics that are often used in construction are geofoam, geotextile, geomembrane, geogrid, geonet, geocomposites and geocell. Geosynthetics have been successfully used in several areas of civil engineering including railroads, roadways, airports, retaining structures, nowadays geosynthetics are being used for many methods not only in the geotechnical engineering. A number of research studies have been done to investigate the behaviour of reinforced soil foundations in the decades. All these works indicated that the use of reinforcements can significantly increase the bearing capacity and reduce the settlement of soil foundations. In this thesis, the experimental studies were conducted to determine the seismic performance of low-to medium rise buildings on geogrid reinforced soil under different dynamic loadings.

1.2.Objectives And Problem Statement

Before this experimental study, lots of numerical and experimental studies have been conducted to advance on seismic reinforcement with geogrids. However, most of them on the similar subject have not encompass the effect of it on both the foundation soil and structure in the same experimental model, so these studies have not considered the behavior of building models and the ground response all together.

In this study, it is significant to observe the seismic behavior of the foundation soil and superstructure together. In other words, the aim of this study, which is decisive point, to evaluate and investigate the effectiveness of geogrid reinforcement system on seismic behavior of low-rise and mid-rise buildings through shaking table experiments.

Due to the fact that the more realistic experimental researches are needed to verify the effectiveness and reliability of the proposed system, this study has been done. To

evaluate the validity of the proposed system and it can be important point to see the seismic behavior of the foundation soil and structure altogether. The main goal of this thesis to obtain preliminary results is to fulfill the needs in the literature and to be able to constitute a guidance model to help for further studies about geogrid reinforcement.

2. LITERATURE REVIEW

2.1. What is Soil Reinforcement

In essence, soil reinforcement is commonly used to change the strength of soil generally by utilizing geoen지니어ing methods. This allows the soil to resist more load. Many years ago, natural fiber were applied to reinforce soils, however this outdated technique did not produce a high yield and required too much time for the soil to recover.

In geotechnical engineering, reinforcement of soil is important in lands where the risk of erosion is high. Soil reinforcement techniques is commonly used in area with soft soil as because soft soil does not provide sufficient support to any construction. These types of soil may have many different problems like poor shear strength, high compressibility and temperature changes.

Soil is reinforced by placing tensile elements, such as geosynthetic, the soil to improve its natural strength and stability. This is accomplished by comprising reinforcement elements. When pressure is applied on the soil mass, it causes a strain on the reinforcement, and it may result in creating a tensile load. By doing this, soil is reinforced and provides much greater shear strength. In Figure 2.1. and Figure 2.2, examples of the slope stability and soil reinforcement with geosynthetic are given.



Figure 2.1. The slope stability with Geosynthetic (Geosyntheticsmagazine, 2019).



Figure 2.2. Soil Reinforcement with Geosynthetic (Geosyntheticsmagazine, 2019).

2.2. Types Of Soil Reinforcement

Commonly 3 main types of materials are used in reinforcement soil.

2.2.1. Soil-Fill Matrix

This method has a potential to reduce the shear of soil can be increased by this method. The well graded cohesionless soil is selected generally. However, the main disadvantage of this method is the cost.

2.2.2. Reinforcement or Anchor System

Many materials like glass, concrete, wood, rubber is proper to be utilized as materials of reinforcement. These reinforcements are kind of structural forms of planks.

2.2.3. Geosynthetics

Geosynthetics generally are known as resilient yield. These materials are made of synthetic polymers mainly and also can be comprised of natural materials. These are important in the engineering field because they can be used as filters, drains, reinforcements, erosion control applications. Engineering field can be benefited from geosynthetics to increase the soil strength, stability and to prevent erosion.

Geogrids is a geosynthetic material with a mesh. It has specific openings accordance with type of it. Following parts, the types of them will be explained.

Geonets have some similarities to geogrids however they have tinner member sand angular apertures, and instead of having square or rectangular openings they consist of parallelograms.

Geomembranes is evaluated a very low permeability and made of synthetic material.

Geosynthetic clay liners are manufactured from hydraulic barriers consisting of a layer of bentonite or other very low permeability material supported by geotextiles and/or geomembranes.

Geocells are common for protection and stabilization. They are used to increase the performance of standard construction materials and control erosion.



Figure 2.3. Overview of Geosynthetic Categories (Koerner, 2012).

2.3. Techniques of Soil Reinforcement

Soil reinforcement techniques can be categorized as two major groups in-situ soil reinforcement and constructed soil reinforcement.

2.3.1. In-situ Reinforcement

In situ reinforcement is a technique where reinforcements are placed in undistributed soil to form a reinforced soil structure. This includes the technique of soil nailing and soil dowelling.

2.3.1.1. Soil Nailing. Soil nailing is a technique commonly used to reinforce and strengthen the ground adjacent to an excavation by installing closely spaced steel bars or nails. Metal plates and other panels may also be utilized. Soil nails are installed at 20-to-25-degree inclinations horizontally to the ground, this is to avoid intercepting underground utilities. Soil nailing is an effective and economical method of constructing retaining wall for excavation support, bridge abutments, highways etc. The nails are subjected to tension compression, shear and bending moment.

2.3.1.1. Soil Dowelling. The technique of soil dowelling is used for fixing shallow, unstable slopes. In most cases of soil dowelling reinforcement is placed and it paves the way for maximum benefit from the reinforcement shear force. By driving or drilling installation of the reinforcement can be applied. And it has relationship with the type of soil and reinforcement. Generally, two or three rows of dowels should be long enough to pass through the creeping zone of soil.

2.3.2. Constructed Soil Reinforcement Technique

This technique encompasses reinforced soil structures with vertical side. The facings usually consist of concrete or steel panels. The soil is used as backfill in cases where the soil is granular with less than 15% fines in the sake of allowing the development of large friction between the soil and reinforcement. Because of their large tensile strength, steel strips are most common reinforcement.

This method describes the technique where the reinforcement is placed at the same time as an imported and remolded soil. These techniques are commonly known as ‘bottom up process’ as they involve the placement of a fill and reinforcement simultaneously, these

involve structures such as bridge abutments and soil embankments. The reinforcement required to carry out form of strips, grid or mats.

There are a number of application areas of soil reinforcement methods, where using geosynthetics or one of another techniques. These consist of some of them, but it can not be limited with these and can be reproduced.

- Embankments on weak foundations
- Retaining walls
- Subgrade stabilizing
- Reinforcing base course
- Slope failure repairs
- Slope cutting repairs
- Steep slopes embankments and bunds
- Bridge abutments and wing walls
- Road and Railway embankments

2.4. Geosynthetics in Soil Reinforcement

Geosynthetic Reinforced Soil (GRS) technology consists of closely spaced layers of geosynthetic reinforcement and compacted granular fill material. The principle of geosynthetic reinforced soil method briefly is to deploy horizontal layers of closely spaced tensile inclusion in the fill material to achieve stability of a soil mass. It can be regarded as adaptable to different environmental conditions, more economical, and offer high performance in a wide range. This method has been actively used for a variety of earthwork applications since the in the 1970s.

Geosynthetics are synthetic products used to stabilize terrain. They are generally polymeric products and includes eight main product categories: geotextiles, geogrids, geonets, geomembranes, geosynthetic clay liners, geo-foam, geocells and geo-composites. They have been an alternative product to be used in many different construction areas in recent decades. Main goals of utilization are separation, reinforcement, filtration, drainage, and containment applications.

However, with new studies in past decades about geosynthetics, it has been started to be used as a reinforcement material more commonly. Over the years, many studies about geosynthetic materials have been conducted and through all these studies the features of geosynthetic have been exhibited widely and the working principle in different ways of geosynthetic has been explained. Besides in these studies, several parameters such as depth, geometry, and geosynthetics type has been changed to understand the effect of them on working principle. Some of these studies are summarized below.

2.4.1. Geogrid Reinforcement

A geogrid is a geosynthetic material including polymeric substance. Geogrids are created by weaving ribs with proper openness. Geogrid may be proper material for reinforcement applications. It allows soil to hit with the help of open grids and another detail is that the two materials clamp together to exhibit composite behavior. There is a rising attention for geogrids in construction because of their good tension and increased ability to distribute loads across a large area.

A few different types of geogrids are used commonly due to their different which specific functions for the application. Briefly, three different types of geogrids can be mentioned uniaxial, biaxial, and triaxial. Each one has different tensile strength because of their dissimilar geometry so is preferred for different construction applications.

The main of uniaxial geogrids are to tolerate stress just for one single direction. They are created by stretching the ribs in a longitude direction. They may be useful for wall and slope applications like retaining walls, embankments constructed on soft soils. Also, another important point is that for this study as geogrid material, uniaxial geogrids was selected.

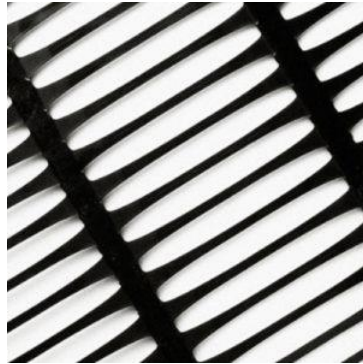


Figure 2.4. General View of Uniaxial Geogrid (<https://mainlinematerials.com>).

Biaxial geogrids have an equal balance of tensile strength in both machine and cross directions, with the help of this design method, they easily distribute loads in a wider area, and it makes useful in base stabilization such as foundations for runways, railroads, unpaved roads.



Figure 2.5. General View of Biaxial Geogrid (<https://indiamart.com>).

Triaxial geogrids consist of from perforated polypropylene sheets diverted with multiple directions to create triangular apertures. This smooths the way more powerful product transferring stress.

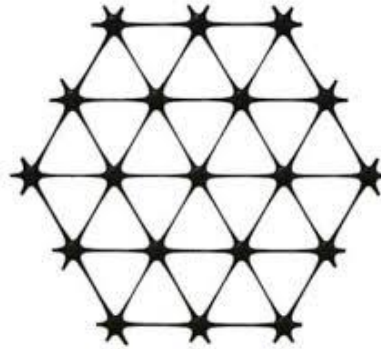


Figure 2.6. General View of Triaxial Geogrid (<https://indiamart.com>).

The use of geogrids for soil reinforcement purposes can significantly and effectively increase the stability of the foundation soil by providing an additional tensile strength to the soil mass and unique energy absorption properties.

In the past decades, to understand the effect of geogrid soil reinforcement on the seismic performance, many researches performed with geogrids. From lots of different viewpoints and changing different critical parameters such as spacing between the reinforcement layers, the depth of reinforcement, the width and length of geogrid layers, geogrid stiffness, several papers and studies have been published as related to the beneficial effects of soil reinforcement with geogrids.

In the following part, some of these studies and papers were examined and summarized.

2.5. Literature Review

2.5.1. Experimental Studies

Omar & Das (1993) conducted a significant study on ultimate bearing capacity of shallow foundations on geogrid reinforced sand. The purpose of this study is to compare the results of laboratory model tests with square and strip foundations on sand reinforced by of geogrids. For the model tests, a square foundation was used and in the soil geogrid

layers were located at determined distances. The distances between foundation and the first geogrid layer and the distance between geogrid layers were determined according to previous studies in literature. Totally four different test series were applied with square and strip foundation with and without geogrid reinforcement.

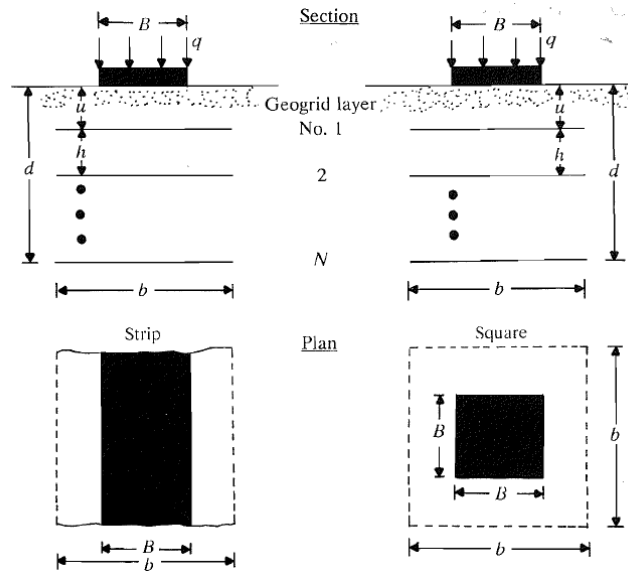


Figure 2.7. Sketches of Strip and Square Foundations used in the study (Omar & Das, 1993).

As a result, the following conclusions were obtained about the ultimate bearing capacity of strip and square foundations supported by sand, 2 times length of one side of foundation (B) and $1.4B$ were ideal depths for development of maximum bearing capacity for strip and square foundations. Maximum bearing-capacity ratio was $8B$ for strip foundations and $4.5B$ for square foundations. The maximum depth of placement of the first layer of geogrid had to be less than about B to obtain desired results.

Another study about geogrid reinforcement was conducted by Yetimoglu & Saglamer (1994). It was related to the bearing capacity of rectangular footings on geogrid reinforced sand by performing laboratory model tests with finite-element analyses. Main goal of this study was to investigate and indicate the effects of the depth to the first layer of reinforcement, vertical spacing of reinforcement layers, number of reinforcement layers and the size of reinforcement sheet on the bearing capacity.

With five different scenarios, the study was constituted, which were Effect of Depth to First Reinforcement Level, Effect of Vertical Spacing of Reinforcement Layers, Effect of Number of Reinforcement Layers, Effect of Reinforcement Size, Effect of Reinforcement Stiffness. This important study presented the results obtained from laboratory tests and finite-element analyses, and a comparison of these results.

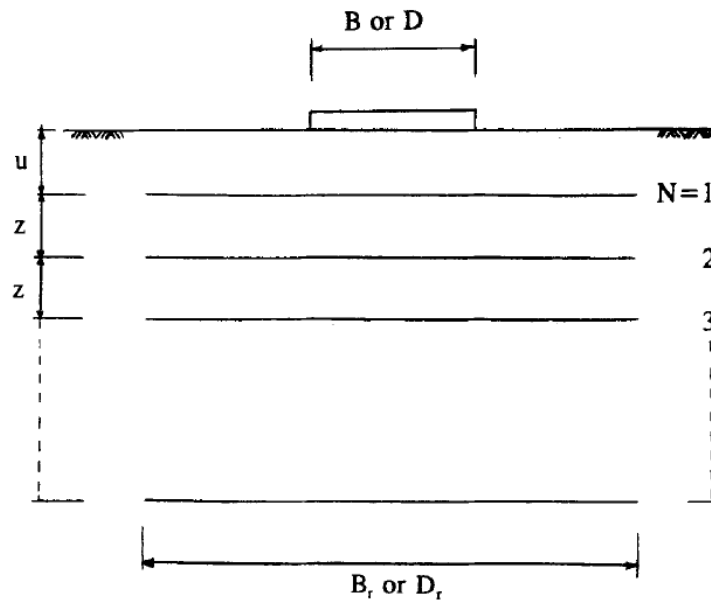


Figure 2.8. Geometric Parameters of Reinforced Foundation (Yetimoglu & Saglam, 1994).

Both the experimental and analytical studies indicated that there was an optimum reinforcement embedment depth at which the bearing capacity was the highest when single layer reinforcement was used. Also, there appeared to be an optimum reinforcement spacing for multilayer reinforced sand. The bearing capacity of reinforced sand was also found to increase with reinforcement layer number and reinforcement size when the reinforcement was placed within a certain effective zone. In addition, the analysis indicated that increasing reinforcement stiffness beyond a certain value would not bring about further increase in the bearing capacity. Besides, according to the reinforcement configuration the depth to the first layer of reinforcement, the vertical spacing of reinforcement layers, the size of reinforcement sheet and especially the number of reinforcement layers can have a very significant effect on the bearing capacity of the reinforced foundation. For single layer reinforced sand, there was an optimum embedment

depth for the first reinforcement layer at which the bearing capacity was the highest. Also, the model tests showed that the optimum embedment depth was approximately 0.3 of the footing widths. The analyses represented the optimum depth would be larger for settlement ratios greater than 6%. For multilayer reinforced sand, the highest bearing capacity happened at an embedment depth of approximately 0.25B. For multilayer reinforced sand there was an optimum vertical spacing of reinforcement layers. The ideal spacing for the reinforced sand were observed between 0.2B and 0.4B. The bearing capacity of reinforced sand increased significantly with reinforcement size and reinforcement layer number within a certain effective zone. Increasing reinforcement stiffness result in ineffective increases in the bearing capacity of reinforced sand.

Another study about geogrid reinforcement was conducted by Shin et al. (2000), which was regarding bearing capacity of strip foundation on reinforced sand with geogrid. The study aimed to observe the ultimate bearing capacity of a strip foundation with multiple layers of proposed geogrid reinforcement. During the test just monotype geogrid was used, relative density was not changed, and the embedment ratio of the foundation was varied from zero to 0.6.

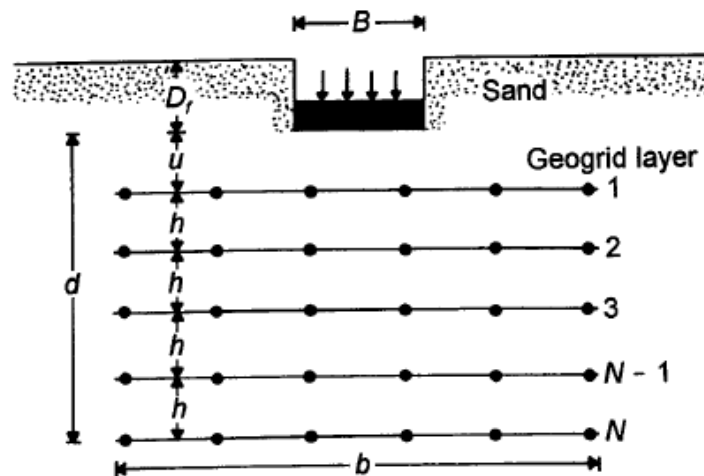


Figure 2.9. The general View of Strip Foundation on Geogrid-Reinforced Sand (Shin et al., 2000).

According to Figure 2.9. the ratios of b/B , h/B , u/B , and d/B were determined based on previous studies conducted on this subject in the literature. As a result, the ratios were

specified as $u/B = 0.4$, $h/B = 0.4$, $b/B = 6$. With the help of a metal box, having 1000-millimeter (mm) length, 174 mm width and 600 mm height, tests were conducted. And the strip model foundation put in metal box made of wood. According to the results of laboratory model tests, the obtained main conclusions were that the bearing capacity ratio was smaller than the value at ultimate load for limited levels of settlement and also it was found that, for a reinforcement depth ratio, the bearing capacity ratio in accordance with ultimate load increases with embedment. The critical reinforcement-depth ratio below the bottom of the foundation. For (d/B) ratio in order to obtain the maximum advantage from reinforcement was 2. For a given reinforcement-depth ratio, u/B , h/B , and b/B , the bearing capacity ratio with respect to the ultimate load (BCR_u) increases with the embedment ratio of the foundation.

One of the important studies about geogrid reinforcement is bearing capacity of embedded strip foundation on geogrid-reinforced sand conducted by Patra et al. (2000). The results of ultimate bearing capacity of a strip foundation supported by multi-layered geogrid-reinforced sand were investigated through laboratory model test and the ultimate aim of this study was to examine and report these laboratory model test result. During the tests, the depth of embedment of the model foundation was varied from zero to width of foundation. As geogrid material solely one type was used, and relative density of sand was not changed. As a result, the ultimate bearing capacity obtained from the model test program was compared with the wide-slab theory developed by Huang and Menq.

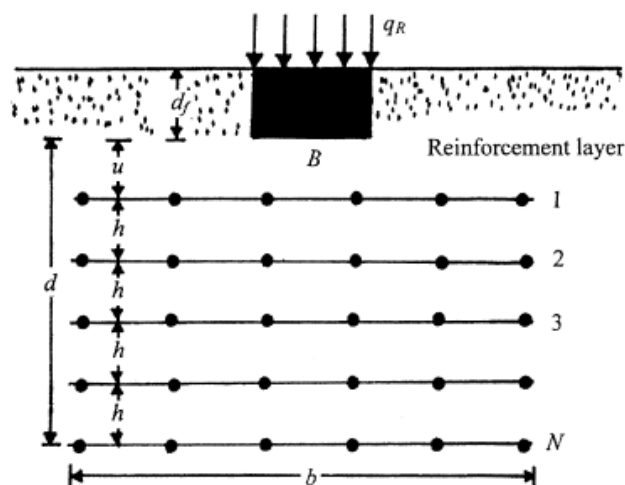


Figure 2.10. A General View of Shallow Strip Foundation on Geogrid Reinforced Sand for Model Test (Patra et al., 2000).

As a conclusion, laboratory model results for an embedded strip foundation supported by geogrid reinforced sand were submitted and the ultimate bearing capacities obtained from these tests were compared with Huang and Menq's theory and with reference to this the following conclusions were seen ; unless the soil, geogrid and its configuration changed, the ultimate bearing capacity(BCR) and BCR increases with the increase in embedment ratio and it was observed that the theory provided a consistent prediction of the ultimate bearing capacity.

Another experimental study about soil reinforcement is settlement and bearing capacity of geogrid-reinforced sand over collapsible soil published by Alawaji et al. (2000). The study was conducted to investigate the benefits of geogrid reinforced sand over collapsible soil to control wetting induced collapse settlement. As a material Tensar SS2 geogrids and a circular plate of 100mm diameter were selected. Then laboratory model load tests were applied with a circular foundation supported by geogrid reinforced sand layer underlined by collapsible soil. During the tests both the stress level and the loading conditions were considered and also the width and depth of the geogrid were changed in order to specify the effects of these parameters on the collapse settlement, deformation modulus and bearing capacity ratios. Figure 2.11. shows general view of test model.

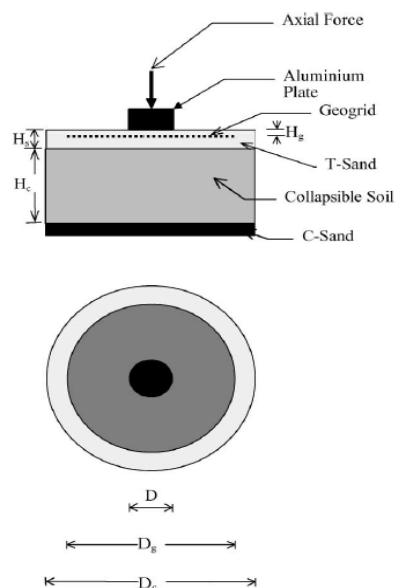


Figure 2.11. General View of Model Plate supported by Geogrid Reinforced over Collapsible Soil (Alawaji et al., 2000).

According to the results, it clearly showed the inclusion of geogrids increases the load-carrying capacity and decreases the wetting induced collapse settlement of sand over weak and collapsible soil. There was an important alteration in the structural contribution of the tested geogrid, it ranged from 95% reduction in settlement, to 2000% increase in elastic modulus and 320% increase in bearing capacity. It was observed that the effect of geogrid system increased with increasing geogrid width and decreasing geogrid depth. It was recommended that geogrid width of four times the diameter of loaded area (D) and depth of $0.1D$ could be proper ratios for efficient and economical reinforcement of sand over collapsible soil.

Another important study regarding geogrid reinforcement is geogrid reinforced subgrades under simulated earthquake loading, which was conducted by Santhakumar et al. (1999). This study conducted to understand the performance of the structures under dynamic cyclic loading, the dynamic loads of frequencies were applied as 0.2 Hz, 0.6 Hz and 1 Hz. And then the settlements of the footing and the matching dynamic loads were recorded. As a geosynthetic material, geogrid was preferred, and the soil was soft sand during the tests.

Based on the results of study, the obtained conclusions were that; there was no impact of frequency of dynamic loadings on the dynamic bearing capacity regardless of unreinforced and reinforced case. The number of reinforcements, spacing of the reinforcement, the size of the reinforcement caused significant impact on the dynamic bearing capacity of the subgrades. the coefficient of elastic uniform compression decreased up to 40% with respect to number of reinforcement so the natural frequency of subgrade with reinforcement reduced compared to unreinforced ones.

Another significant study was conducted and published by Kadim (2016), which was effective length of geogrid reinforcement layers under circular footing resting on sand. Main goal of the study was to investigate and obtain findings about of the effect of relative density of the sand, the depth of the footing on the effective length of geogrid reinforcement layer and the effect of the variation in the length of reinforcement layers on the ultimate bearing capacity. In the study a small experimental model were used for this purpose.

According to results, it was emerged that, the ultimate bearing pressure raised with increasing length of reinforcement layer ratio (up to a certain value. After this value, it did not change for any value of depth ratio and relative density. The relative density of sand influenced the effective length of reinforcement ratio, which was 2.25 for 60% relative density and 1.75 for 80% relative density and also the effective length of reinforcement layer was not affected by depth ratio of circular footing. Using two layers of geogrid reinforcement resulted in increase in the bearing capacity.

Another study about soil reinforcement was conducted by Yabu & Tripathi (2013), which is effect of the length of geogrid layers in the bearing capacity ratio of geogrid reinforced granular fill-soft subgrade soil system. In this paper, the effect of the length of geogrid in granulated blast furnace slag overlay on soft subgrade soil was investigated. The study was conducted in laboratory conditions with a small-scale model test. During the test bearing capacity ratio and reduction factor were evaluated. The aim was to observe the effect of various lengths of geogrid layers with optimal thickness on bearing capacity ratio. In Figure 2.12. a view of model setup can be seen.



Figure 2.12. A General View of the Model Test Setup. (Yabu & Tripathi, 2013)

According to the experimental test results, the following conclusions were obtained, reinforced granulated blast furnace slag (GBS) advanced bearing capacity and diminish settlement of the soft subgrade soil bed, also with b/B ratio of 4, a significant improvement was observed in bearing capacity ratio and beyond b/B ratio of 4 bearing capacity ratio did not exhibit important improvement. And improvement in load bearing capacity was detected up to 390% in reinforced soil with b/B ratio of 4 compared unreinforced soil. Settlement reduction ratio was increased up to 84% with geogrid reinforced GBS of b/B ratio 2 but a substantial improvement was not observed beyond b/B of 2 in settlement reduction ratio. Also, considerable development was not seen in improvement factor for the alteration of b/B .

2.5.2. Numerical Studies

One of important numerical studies about effect of geotextile arrangement on seismic performance of mid-rise buildings was conducted by Ruoshi & Behzad (2018). In this study a mid rise buildings sitting on shallow foundations was investigated in unfavorable soil conditions with the help of FLAC3D and a numerical study was constituted. During the test main goal of study was to exhibit the effect of geotextile arrangement on the seismic performance of mid-rise buildings under earthquake motions. The 1994 Northridge and the 1999 Chichi earthquakes were used as earthquake motions and the effects of stiffness, length, number, and spacing of geotextile layers were analyzed and investigated in a parametric study.

The created building model had fifteen story with an equal height of 3 meter(m). Structural analysis was performed with the help of SAP2000. Figure 2.13. and Figure 2.14. shows details of the structural sections of this building.

According to the results of numerical study, the structural shear forces rose with an increase in the length and number of geotextile layers also with stiffness. Besides, the structural shear forces increased with a reduce in the spacing of geotextile layers, which was through energy dissipation and thanks to the geotextile layers. On the other hand, when the geotextile layers were approached to the foundation edges, this resulted in the stresses because of foundation rocking. And an alternative solution, it was observed; with

the increase in the stiffness, length, number and spacing of geotextile layers, the rocking induced problems could be lessened for building.

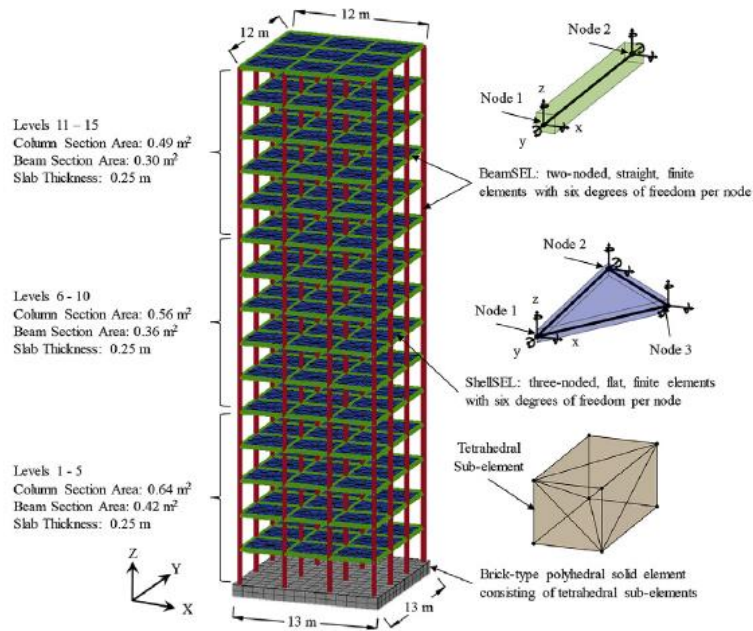


Figure 2.13. A general View of Building Model and Sections (Ruoshi & Behzad, 2018).

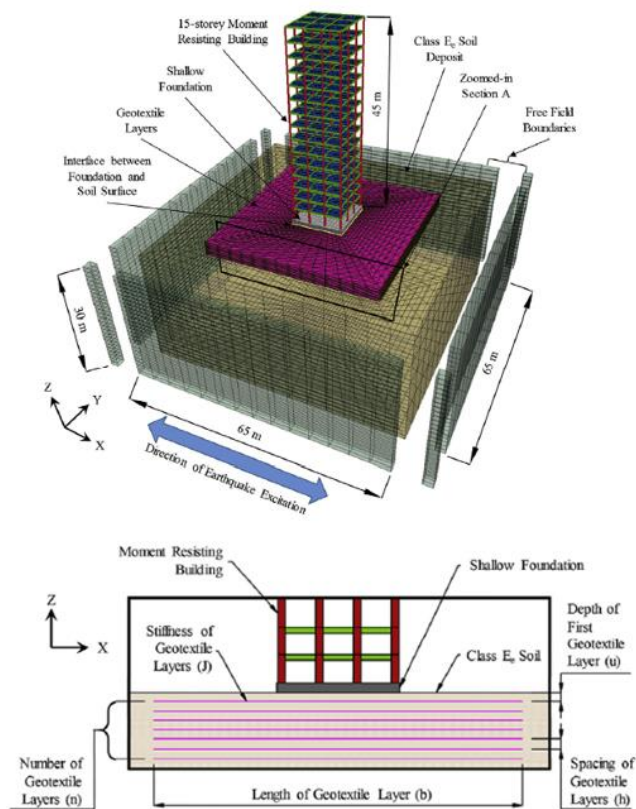


Figure 2.14. Adopted Soil-Structure System with Layers (Ruoshi & Behzad, 2018).

Consequently, the results of study show that the arrangement of geotextiles has substantial influence on seismic performance for mid-rise building. In order to ensure seismic protection of buildings, the geotextile reinforced systems certainly can be used by considering geotextile arrangements encompassing stiffness, length, number, and spacing of geotextile layers. These parameters will help find more effective condition for both cost and seismic protection.

Another important study about geogrid reinforcement was presented by Edinçliler et al. (2017). It was a Parametric study on seismic performance of low and mid-rise buildings on geogrid reinforced sand.

In this study, as 3 story and 5 story two buildings model were used and foundation soil was reinforced with 12 layers of geogrids with the help of finite element modelling (FEM) program, which is Plaxis. This study is based on the numerical results obtained from a series of FEM analyses of 3-storey and 5-storey buildings which are soil-geogrid reinforced and obtained results are compared with the unreinforced ones. Dimensions of the buildings were determined as; width of the building = 8 m, height of each story = 3 m and width of the footing = 10 m. The first layer of reinforcement was placed 3 m under the footing and the vertical distance between two consecutive reinforcement layers is 2 m. Figure 2.15. shows finite element model of study.

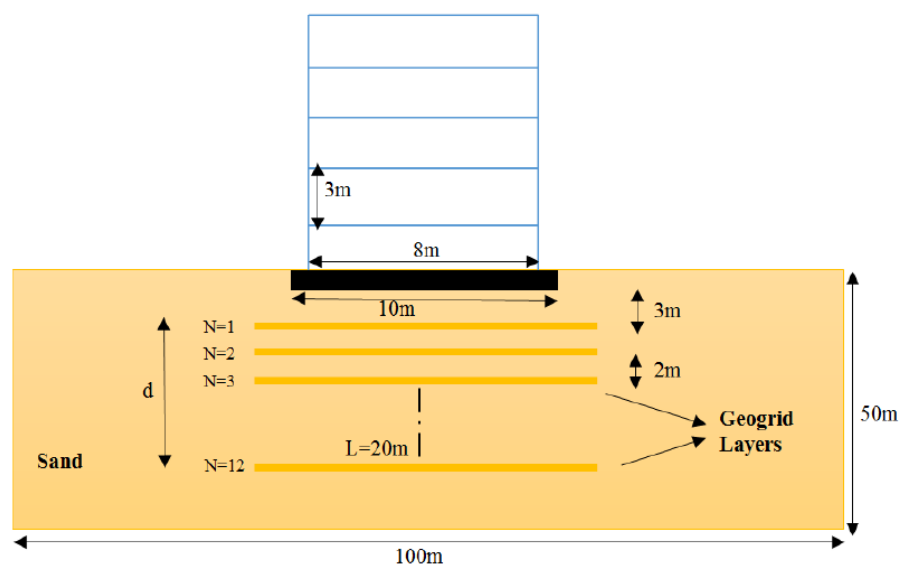


Figure 2.15. Finite Element Modelling for 5 Story Model (Edinçliler et al., 2017).

As geogrids material to reinforcement uniaxial type was selected and length of each geogrid layer was determined as 20 m. As a dynamic input, the real earthquake records of the Kobe Earthquake (PGA = 0.68 g) and Kocaeli Earthquake (PGA = 0.23 g) were functioned. For each and every model and dynamic motion, total displacements, transmitted accelerations, axial and shear forces and bending moments were investigated through the numerical.

According to the results, total displacement of the structure was decreased up to 90% for the 3-storey models and 66% for 5-storey models. Proposed reinforcement system functioned better at stronger dynamic inputs. Also, axial forces were dropped up to 17% in 3-storey model and 23% for 5-storey model in Kobe earthquake motion but the decrease ratio was 17 in 3 story model and 10% in 5-storey model under Kocaeli Earthquake motions. The obtained shear stresses exhibited similar manner. On the other hand, it was observed that the proposed geogrid reinforcement system worked better at low-rise structures. And, in conclusion, for this study it was clear that the utilization of geosynthetics for soil reinforcement was valid method.

One of the other significant numerical study is numerical analysis of shallow foundations on geogrid reinforced soil conducted by Tahmaz et al. (2017). This study investigated profoundly interaction between soil and geogrid through numerical study and during the tests, the effect of critical parameters which affect the overall behavior of geogrid reinforced such as the width and length of geogrid layers, spacing between the reinforcement layers, and the depth of reinforcement soil were discussed. Besides, this paper provided a general view of the important results of the existing studies on the load-bearing capacity of shallow foundations on geogrid-reinforced soil. These results regarding the ultimate and allowable bearing capacities of shallow foundations on geogrid reinforced soil can be examined in this paper. In Figure a general view of test model can be seen.

For the numerical study, a series of two-dimensional finite element analysis (FEA) of footing resting on geogrid reinforced soil was performed to examine behavior of foundation with geogrid reinforcement soil. The analysis was applied with the help of finite element program Plaxis software package. The scale of numerical model was assumed to be 10 times the laboratory model of Omer's study, which was mentioned in the

part of experimental studies of literature. The footing width and thickness was accepted 0.76 m and 0.2 m respectively and soil height was assumed 10 times 0.76 m.

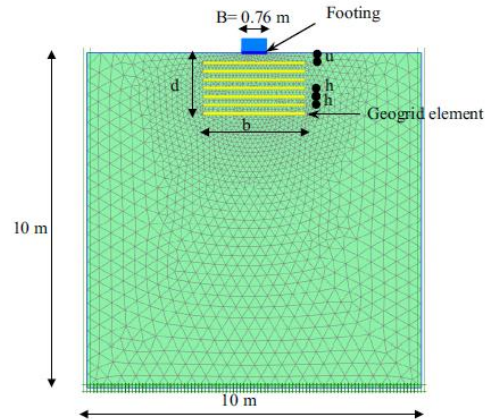


Figure 2.16. A general View of The Footing Model, generated Mesh and Boundary Conditions. (Tahmaz et al., 2017).

In conclusion, according to the results obtained from numerical study about the bearing capacity behavior of strip footing on geogrid reinforced soil, both for experimental and numerical study, a substantial increase in soil bearing capacity was observed, the numerical model did not detect the behavior of the geogrid-reinforced soil at low settlement. Based on the results of experimental and numerical studies of critical parameters on the geogrid-reinforced soil bearing capacity, for all cases of bearing capacity ratios calculated from the numerical analysis appeared to be smaller than calculated from the experimental results.

Another study about soil reinforcement with geosynthetic is bearing capacity of square footings on geosynthetic reinforced sand, which was conducted by Latha & Somwanshi (2008). Additionally, another importance of this study is that it encompasses both numerical and experimental study together. Results from laboratory model tests and numerical simulations on square footing supported by sand bed with and without geosynthetic reinforcement were investigated. Main goal of this study was to observe the influence of different reinforcement parameters, on the overall performance improvement of the footing and to evaluate the performance of geosynthetic layers in improving the bearing capacity of the square footings. During the tests, the width of reinforcing layers, spacing of geosynthetic layers, the type and tensile strength of the reinforcement, number

of geosynthetic layers and depth of reinforced zone were taken into account as parameters. And the effect of all these changing parameters were compared with the test on unreinforced sand. For the experimental study, a steel tank, which has 900x900x600 mm dimensions, also four types of grids, which were strong biaxial geogrid, weak biaxial geogrid, uniaxial geogrid and a geonet, each with different tensile strength, were used in the tests and for the numerical study, the computer program FLAC3D was used for modeling the behavior of soil.

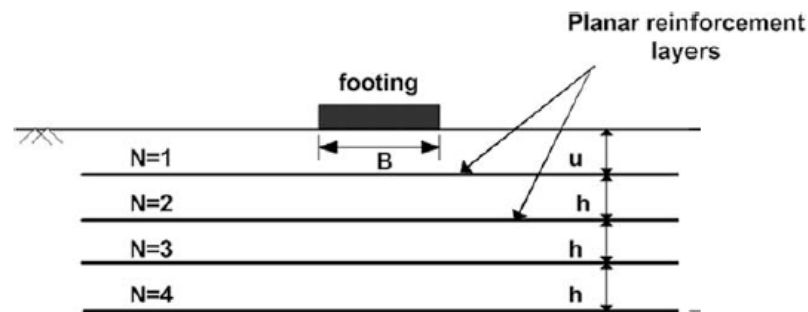


Figure 2.17. A general View of Geosynthetic Layers in The Model Tests (Latha & Somwanshi, 2008).

According to results, the experimental and numerical studies had supported each other. Results clearly showed that the layout and configuration of reinforcement had a significant importance in bearing capacity rather than the tensile strength of the geosynthetic material. And also, the following conclusions were obtained from the study; within the effective reinforcement zone, the optimum spacing of reinforcing layers was 0.4 times the width of the footing, the effective depth of reinforcement was twice the width of the footing, and the inclusion of reinforcing layers did not provide significant improvement in the bearing capacity of the footing. Besides, flexibility of geosynthetic material were significant parameters to be considered in the designs.

Another important study is load bearing characteristics of square footing on geogrid-reinforced sand subjected to repeated loading conducted by Liang et al. (2020). In this study, a series of dynamic model tests were applied on a geogrid-reinforced square footing. The dynamic (sinusoidal) loading was performed by using a mechanical testing and simulation (MTS) electro-hydraulic servo loading system. During the tests, three different

reinforcement depths were compared to an unreinforced foundation to observe the response of the footing and the effect of the depth of the first reinforcement layer was evaluated on the bearing capacity, foundation settlement, soil acceleration, earth pressure distribution, geogrid strain. In the light of the obtained results, for the optimal depth of the reinforcement layer and the effective reinforcement depth, specific values were recommended. For all the tests, the frequency of loading was 2 Hz, and the amplitude of loading was ± 160 kPa.

On condition that each with a single layer of reinforcement, the three different reinforcement layer depths were $0.3B$, $0.6B$ and $0.9B$, where B represents the width of footing. And as conclusion, $0.6B$ was determined as the optimal depth of reinforcement.

According to results, in comparison with the unreinforced footing, the bearing capacity ratio of reinforced foundation factors were found as 1.1, 1.4 and 1.2 for three reinforcement depths under dynamic loading. The reinforced foundation with single layer of geogrid had an influential reinforcement depth of the $1.7B$ below the footing base. Because of the fact that the dynamic load influenced the load transfer system, the punching shear failure happened for unreinforced foundation case. Also, the sensitivity of static loading is lower than dynamic loading.

Another noteworthy study was published by Noor et al., (2020). The importance of this study is that it was conducted by considering numerical and analytical study together. Its main goal was to specify the effect of using geogrid on the bearing capacity and settlement of strip footing for different types of soils in Iraq. During the study, by changing the width and the number of the geogrid layers, different tests were applied.

According to results, it can be clearly said that the geogrid could boost the footing's bearing capacity and decrease settlement. The ideal geogrid width was five times the footing width and based on results the optimum geogrid number wasn't obtained. Then the analytical results were compared with the numerical results of bearing capacity, it was revealed that there was a decent accord for two of them. And another important indication was that although the geogrid reinforcement had a potential to trigger improvement to the soil foundation, it was not dependent to the width and number of the geogrid. Besides, the

alteration of soil features and footing dimensions contribute to the bearing capacity ratio and settlement reduction ratio.

Another study about geotechnical design is a research on the effect of the reinforcement geometry on the soil bearing capacity under the strip footing loads, which was conducted and published by Majedi et al. (2018). In this study, main goal was to observe the effect of the reinforcement geometry on the soil bearing capacity and to find the optimum depth of reinforcement.

In conventional methods, geogrids for reinforcement of foundation soils are located horizontally in soil improvement to increase soil strength. However, in this study, a different approach was applied, a geotextile layer with wraparound ends was constituted on the granular soils. With help of PLAXIS (2D) finite element analysis software, a model with the new designs of reinforcement was created and analyzed with two-dimensional plane strain finite element analyses. Besides, apart from numerical studies, an experimental model was conducted to compare results each other.

The results of classical reinforced condition, unreinforced condition, and wraparound reinforcement condition showed the results of the numerical and experimental tests exhibited compliance, when the relative density of the soil was increased. Also, the wraparound reinforcement compared to unreinforced condition and classic reinforcement method indicated a better compliance, at the relative densities of 50%, 70%, 90% and led to reduce the settlement. It may be new idea for the usage of reinforcements. On the other hand, the ratio of the depth of insertion was fixed to 0.3, it paved the way for a significant reduction in the settlements compared to the other two conditions.

3. MATERIALS AND METHODS

3.1. Experimental Model Properties

Experimental model properties are mainly consisting of four parts, which are information on the shaking table, the measuring instruments, the laminar box and the scaled building models. This chapter will exhibit the details and features of all these properties.

3.1.1. Shaking Table

The shaking table test set-up used in this study is located in the Boğaziçi University Kandilli Observatory Soil Mechanics Laboratory. Shaking table is specified as uniaxial hydraulic shaking table. It can apply uniaxial horizontal vibration driven by a servo-hydraulic actuator. The dimension of shaking table is 3 m x 3 m. Besides, it is capable of carrying and shaking a maximum 10-ton payload with 2G. The shaking table is suited for seismic applications because the hydraulic actuator can produce a stroke of +/- 12 cm, which means it is able to waggle 24 cm total stroke. It has a digital outer loop control system and is controlled by the newly modified computer-based software system. General view of shaking table was shown in Figure 3.1.



Figure 3.1. A General View of Shaking Table and Laminar Box.

3.1.2. Measuring Instruments

As measuring instruments, Leuze ODSL 96B M/V6.XL-1200-S12 optical distance sensors (ODS) with 150 - 1200 mm measurement range and 2% absolute measurement accuracy were selected for measuring displacements. Besides, (+/-)3g capacity accelerometers and (+/-)20g capacity accelerometers were used in the experiments to measure the acceleration. The sample rate for cyclic sinusoidal motions was taken as 1000 sample / second (sec) and for earthquake motions, the sample rate was taken as 500 sample / sec. In Figure 3.2., an accelerometer example and displacement meter were indicated.

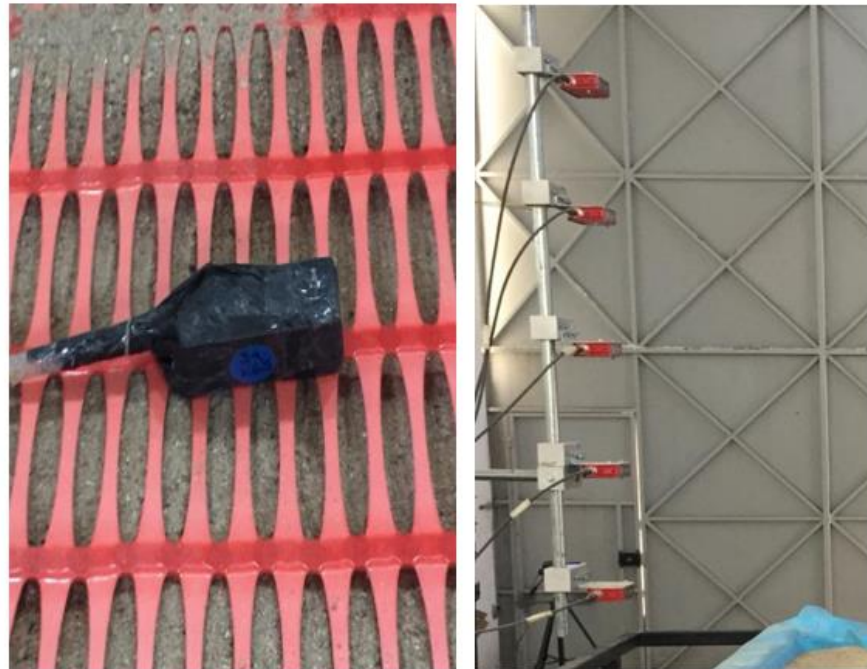


Figure 3.2. Accelerometer and Displacement sensor.

3.1.3. Laminar Box

To be able to apply test model a soil container is needed, placed on shaking table. Due to the requirement of confinement in the soil, the experimental model can not be directly put on shaking table. Soil has to be placed in a container. As a container, a laminar box was used in this study. Laminar boxes generally consist of a stack of laminates supported individually by bearings and a steel guide connected to an external frame. Rectangular laminar boxes are the most preferred ones in the literature. The basic design

principle of a laminar box is to destroy the lateral stiffness of the container to provide that the soil leads the response of the soil box system.

In this study, the laminar box used for the experiment was constructed and tested by Sekman (2016). It was previously used for another experimental study about seismic isolation with the help of geosynthetics. The laminar box that was benefited in this research was designed as 1.5 meters towards the direction of shaking by 1.3 meters with 1 meter depth and a square geometry.

Laminar box consists of eighteen sliding layers that were made by steel I-beam were composed of the walls of the laminar box. It was sliding and stopping the mechanism of the laminates with the help of roller bearings and rubber stoppers. Friction forces between laminates were reduced by using six sets roller bearings per laminate. Each set includes three roller bearings placed side by side. In total, 324 roller bearings provide the sliding to the laminates.

Additional inertial effects that could be caused by stroking the roller bearings to rubber strips at the end of the bearing houses were restricted by using shock absorption feature of rubber. The lowest layer was fixed on a steel base, that was fixed to shaking table. The side guides were made of steel tube sections to take precaution against unexpected accident. The membrane was attached to inner surface of the laminar box to prevent soil leakage that occurs in the box towards the gaps between two laminates. Additionally, between membrane and sidewalls of the box was greased to avoid additional friction forces. (Sekman 2016)

Over the years due to the fact that laminar box had been in laboratory condition, before experimental study, laminar box was elaborately cleaned, oiled and all performance tests was carried out. Also, friction and membrane effects were inspected and controlled. Profile view of laminar box was shown in Figure 3.3.



Figure 3.3. A Profile View of Laminar Box.

- Friction Effect

With the help of steelyard with 60 kg load measurement capacity, static pullout tests were applied to determine friction forces of the roller bearings that are required to initiate motion of the laminate so through these tests the friction effect on the performance of the

box was tested. It was started the bottom layer and continued toward above layer, and it was performed for each layer. During the test, the total weight of it increased from top to bottom because of joining weights of the upper laminate together. The measured friction forces are exhibited in the Figure 3.4.

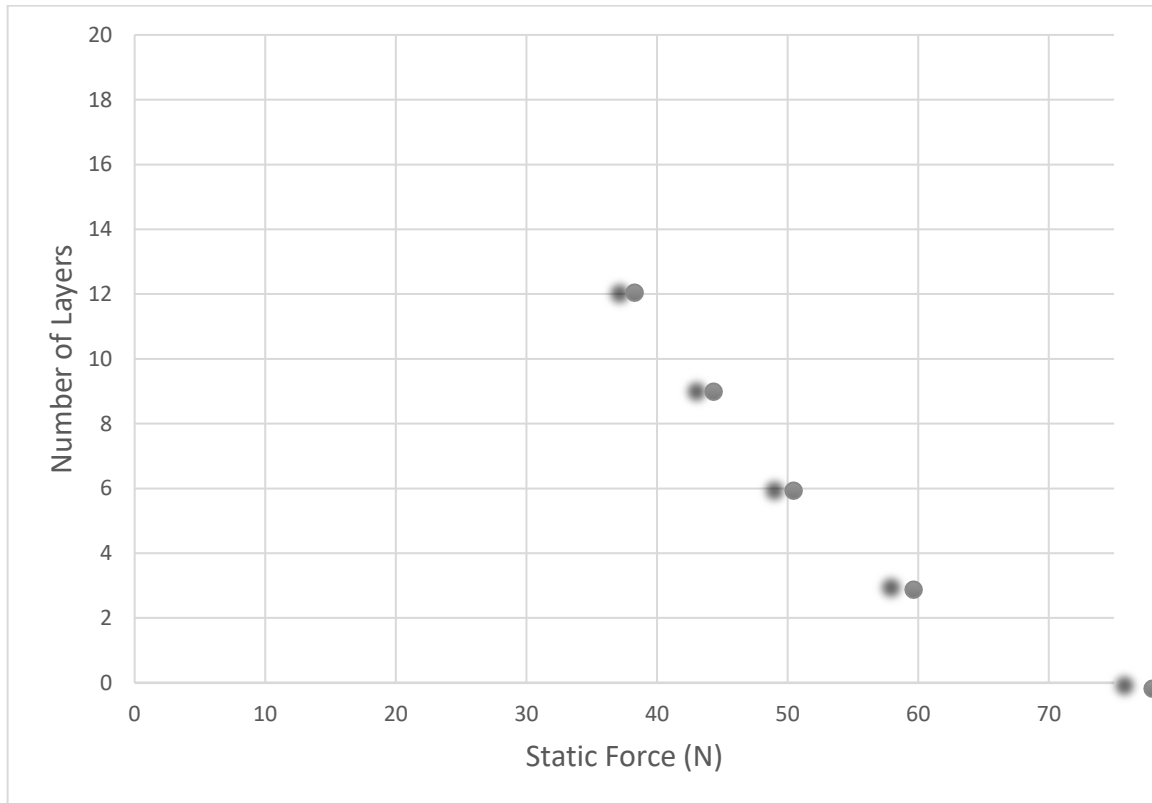


Figure 3.4. The Friction Forces of Laminar Box.

The maximum force to start motion from bottom layer was 68 Newton. The average friction force was 33.4 N. In addition to this, the average coefficient of friction was computed as 0.07 so static friction force can be neglected.

- Membrane Effect

As membrane, 1.0 mm thick rubber membrane was used in the experiment. The stiffness of the membrane was small compared to contained soil. Besides, according to free vibration test with and without membrane it was clearly see that the membrane would not induce the performance of contained soil, so the effect of the membrane was negligible.

3.1.4. Scaled Building Models

During the tests the proposed geogrid reinforcement system was applied to low-mid rise buildings and in-situ soil. 5-story and 3-story buildings model prototypes were selected as low-mid rise. For buildings model, 1:10 scale factor was implemented.

In this study, because of the fact that proposed geogrid reinforcement system and its effectiveness is the most important point, the prototype and all parameters was scaled oriented according to base pressure and soil structure behavior and the scale factors for these parameters exhibited in Table 3.1.

Table 3.1. The Scaled Building Model Parameters. (Sekman, 2016)

Parameter	1:10 Scale Model/ Prototype	
Length	L	1/10
Time	\sqrt{L}	$1/\sqrt{10}$
Mass	L^2	1/ 100
Displacement	L	1/10
Acceleration	1	1/1
Stress	1	1/1
Strain	1	1/1
Force	L^2	1/100

The columns of the scaled building model were manufactured with steel slim high carbon steel columns and just one row column was used at each corner of building model. In this way, the rigidity of model was reduced relatively and increase the reliability of the measurement and to observe the response of the buildings expressly.

Briefly, the properties of the buildings is that floors of the building models were made of St 42 steel with a dimension of 30 centimeter (cm) x 30 cm x 1 cm also, the weight blocks of the floors were made of St 42 with a dimension of 30 cm x 30 cm x 2 cm,

high carbon steel columns whose dimension was 26.5 cm x 5 cm x 0.5 cm were tied with metric eight bolts to floors, four flanges were welded on every floor as connection apparatus for attaching the columns. Foundation was made of St 42 steel with a dimension of 35 cm x 35 cm x 2 cm. The story weight blocks, and foundation blocks were manufactured as piecewise for the ease of carrying and reconstruction. The final height of the 5-story building was 135 cm without foundation, and the final height 3-story building was 81 cm without foundation. In Figure 3.5. and Figure 3.6., the profile of scaled building models can be seen.

Also, it has to be specified that this building model was manufactured and used by Sekman (2016) for the study about geotechnical seismic isolation.



Figure 3.5. The Profile View of 5 Storey Scaled Building Model.

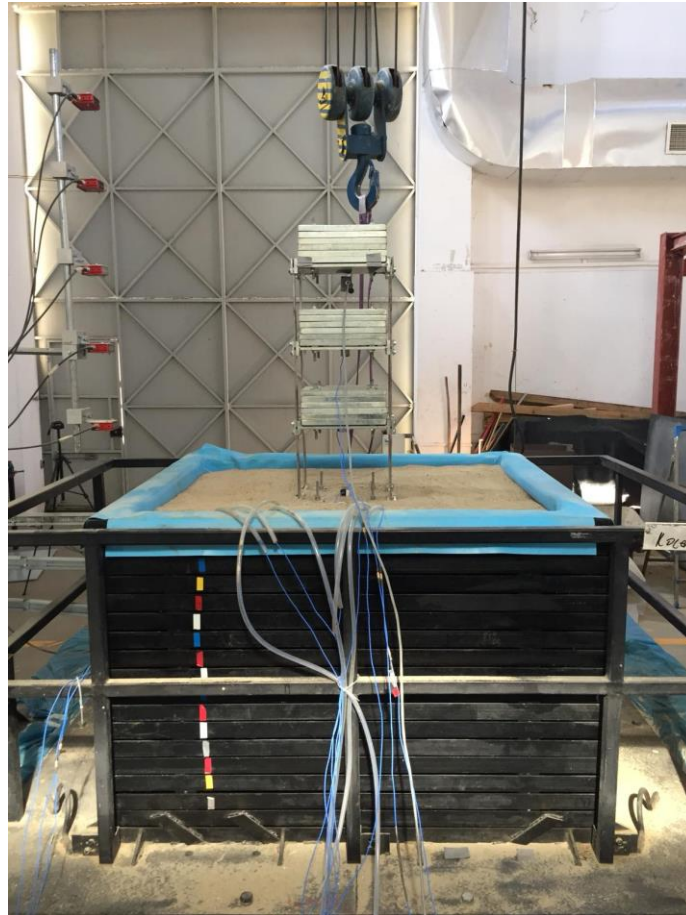


Figure 3.6. The Profile View of 3 Storey Scaled Building Model.

3.2. Materials

3.2.1. Soil Material

The soil material used in the experiments was Silivri Sand. Silivri is one of district of Istanbul and it was provided around Istanbul region. Because of its properties, Silivri Sand was preferred. Essential properties were determined according to the American Standard Test Method. The sand material is classified as poorly graded sand (SP) with the coefficient of curvature as $C_u = 2.29$ and the coefficient of uniformity as $C_c = 1.1$. The internal friction angle as $\Phi = 41.48^\circ$. Specific gravity of sand was obtained as $G_s = 2.67$ and bulk unit weight as 16.5 kN/m^3 . The maximum and minimum void ratios of the sand were obtained as 0.73 and 0.37, respectively. Grain-size distribution is shown in Figure 3.7.

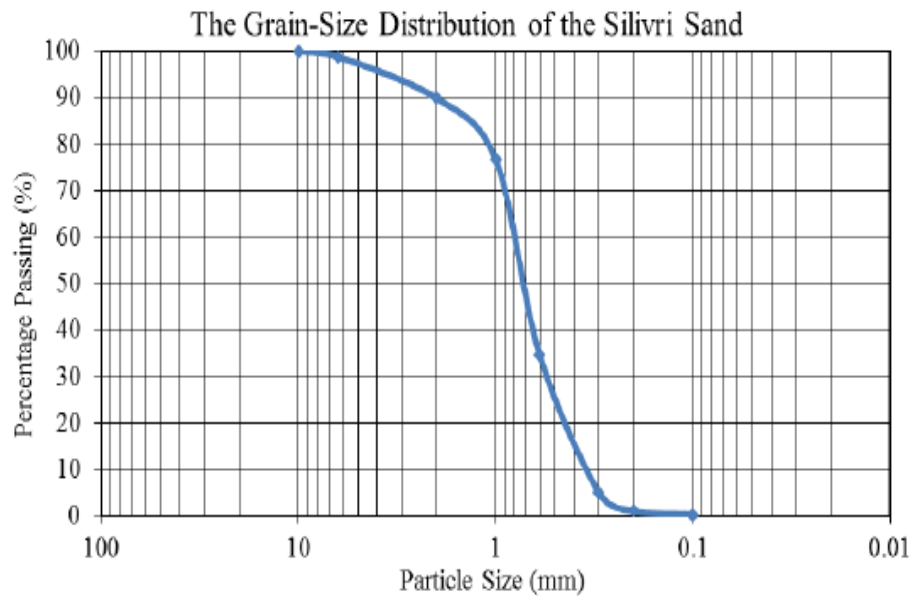


Figure 3.7. The Grain-Size Distribution of Silivri Sand.

3.2.2. Geogrid Material

As mentioned before in the second part elaborately, geogrids are geosynthetic material made from polymers such as polypropylene, polyethylene or polyester and are used widely in Civil Engineering applications. The main reason of using them for reinforcement is that they provide tensile reinforcement of soil through open grids so that soil can strike through the apertures.

The properties of geogrid used in this study was obtained from a company in Istanbul by examining literature and similar studies about geogrid reinforcement. After physical properties of available geogrids was examined, a geogrid with a peak tensile strength of 55 kN/m was ordered. As a result, UR-55 was selected as geogrid material. All mechanical properties of geogrid can be observed in Table 3.2. which was taken from brand catalog and a sample of geogrid material was shown in Figure 3.8.

Table 3.2. The Physical Properties of UR-55.

Name of The Product	Tensile Strength (kN/m)		Strain Failure(%)	
	Longitudinally	Transverse	Longitudinally	Transverse
UR-55	55	12	11	13



Figure 3.8. A Sample Piece of Geogrid Material (80 cm x 80 cm).

3.3. Input Seismic Motions

As input seismic motions three different severe earthquake motions were selected for the shaking table tests. These are the 1940 El Centro, 1995 Kobe and 1999 Kocaeli. Due to the uniaxial shaking table in the laboratory, the horizontal component of the earthquakes was selected. The main criteria of selection of earthquakes were frequency content and applicability to the shaking table. In addition to earthquake motions, also cyclic sinusoidal motions were applied with different frequencies. Frequencies of the cyclic sinusoidal motions were determined according to free vibration tests for each shaking table model.

The data of earthquakes can be observed with peak ground acceleration (PGA), peak ground velocity (PGV) and peak ground displacement (PGD) of earthquake motions in Table 3.3. Also, time-acceleration graphs of earthquake motions can be seen in Figure 3.9.

Table 3.3. The Data of El Centro, Kobe and Kocaeli Earthquake Motions.

Earthquake Name	Date	Station Name	Earthquake Magnitude	Component	High Pass Filter (Hz)	Low Pass Filter (Hz)	PGA (g)	PGV (cm/sec)	PGD (cm)
Imperial Valley-02	19.08.1940 4:37:00	El Centro Array #9	6.95	N-S	0.20	15	0.32	31.74	18.01
Kobe, Japan	16.01.1995 20:46:00	KJMA	6.90	N-S	0.05		0.82	77.83	18.87
Kocaeli, Turkey	17/8/1999	Izmit	7.51	E-W	0.10	30	0.22	27.02	14.61

All earthquakes' data were obtained from PEER Ground Motion Database.

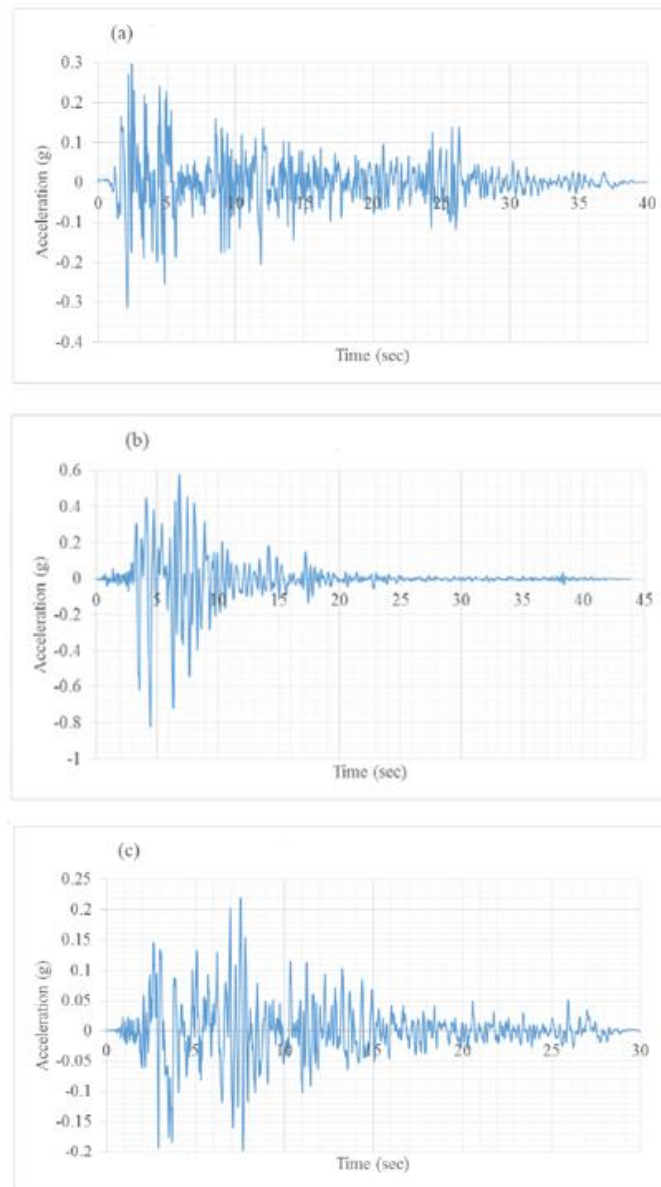


Figure 3.9. Time-Acceleration Records of (a) El Centro, (b) Kobe and (c) Kocaeli Earthquakes.

3.4. Determination of the Number and Location of Geogrid Layers

As mentioned in previous chapter, the main aim was to test the effectiveness and reliability of geogrid reinforcement system under earthquake loadings. Because of this, the experimental parameters, encompassing the number and depth of geogrids layers, the distance between the first geogrid layer and foundation and the location of sensors had to be determined precisely before the shaking table experiments.

3.4.1. The Number and Location of Geogrid Layers

First of all, the number of geogrid layers had to be determined to start establishing the experimental setup. By working on and examining studies and papers related to geogrid reinforcement located at under foundation, the number of geogrid layers was specified. According to previously the studies, it is clear that although it can be observed that there is significant increase in the bearing capacity and reduction in displacement and acceleration values up to four geogrid layers, there is no dramatic alteration after four layers. In Figure 3.10 and Figure 3.11, variation of load per unit area and bearing capacity ratio according to number of geogrid reinforcement layer can be observed for studies conducted by Omar et al. (1993) and Yetimoğlu et al. (1994).

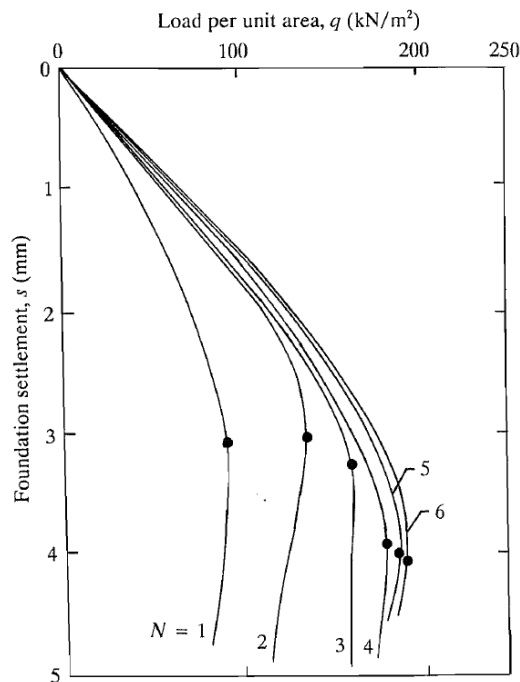


Figure 3.10. Variation with Number of Geogrid Reinforcement Layers (Omar et al., 1993).

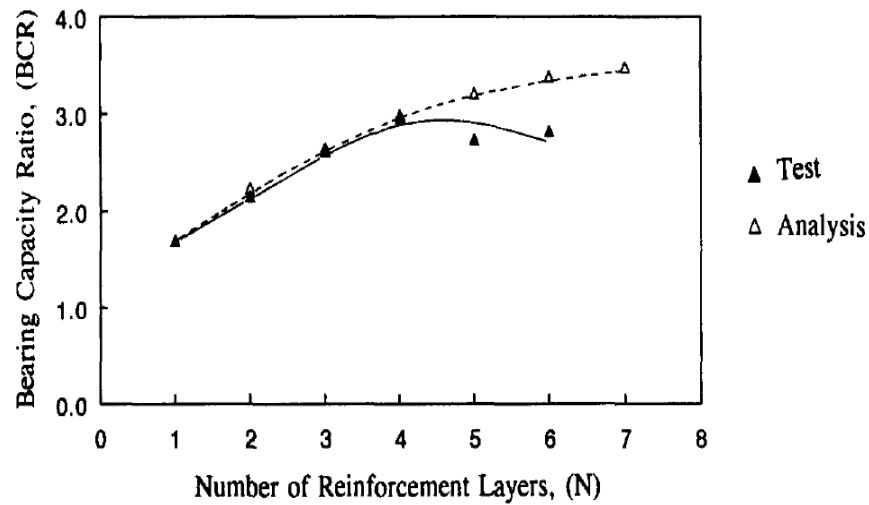


Figure 3.11. Variation with Number of Geogrid Reinforcement Layers (Yetimoglu et al., 1994).

In the light of all this investigation process, the number of geogrid layer (N) was determined as 4.

After the number of geogrid reinforcement layers was determined another point needed to be determined were the distance between the first geogrid layer and surface, and the distances between geogrid layers. In the literature, like the number of geogrid layers, there are lots of studies focusing on the optimal distances between layers. In order to decide the distances, these studies were examined and used as the criteria, principally Patra et al. (2005) and Omar et al. (1993). By considering the boundary condition of soil container and previous studies, in the experimental model the distance between the bottom of foundation and the first layer of geogrid (u), the distances between geogrid layers (h), the distance between the bottom of foundation and the last geogrid layer (d), the one side length of square foundation (B) and the one side length geogrid component (b) were determined as 12 cm, 12 cm, 48 cm, 35 cm and 80 cm respectively. A general view of experimental model can be observed in Figure 3.12.

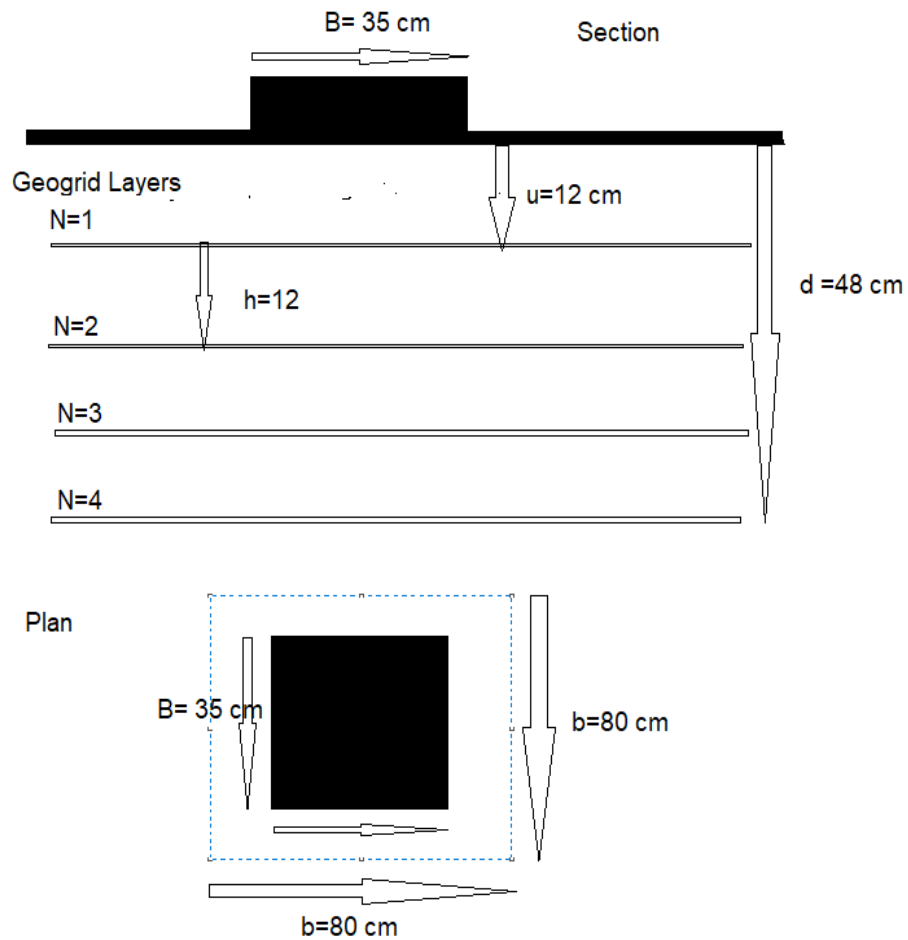


Figure 3.12. A General View of Experimental Model.

3.4.2. The Location of Sensors on Scaled Building Model and in Soil

Afterwards the details of model were determined, the location of sensors was regulated. First of all, the location of sensors in the soil was assigned. To be able to observe clearly the effectiveness of geogrid reinforcement system and see to what extent geogrid layers help reduce transmitted acceleration, all sensors in the soil were located proportional to geogrid layers. For the soil, just an accelerometer was preferred. After the sensors in the soil were placed, the scaled building model's sensors was located. For the middle of each story, an accelerometer was put in and for each story a laser displacement meter was placed consecutively. In order to analyze elaborately the effect of the geogrid reinforcement system on story drifts. In Figure 3.13, the locations of sensors in the soil are

exhibited and Figure 3.14 and 3.15 show general view of scaled building models of with sensors. Because this proposed geogrid reinforcement system is valid for low to medium rise structures. Scaled building model was selected as 3-story and 5-storey in experiments. Also, in Figure 3.16. the projection of displacement sensors on 5-storey building model can be seen.

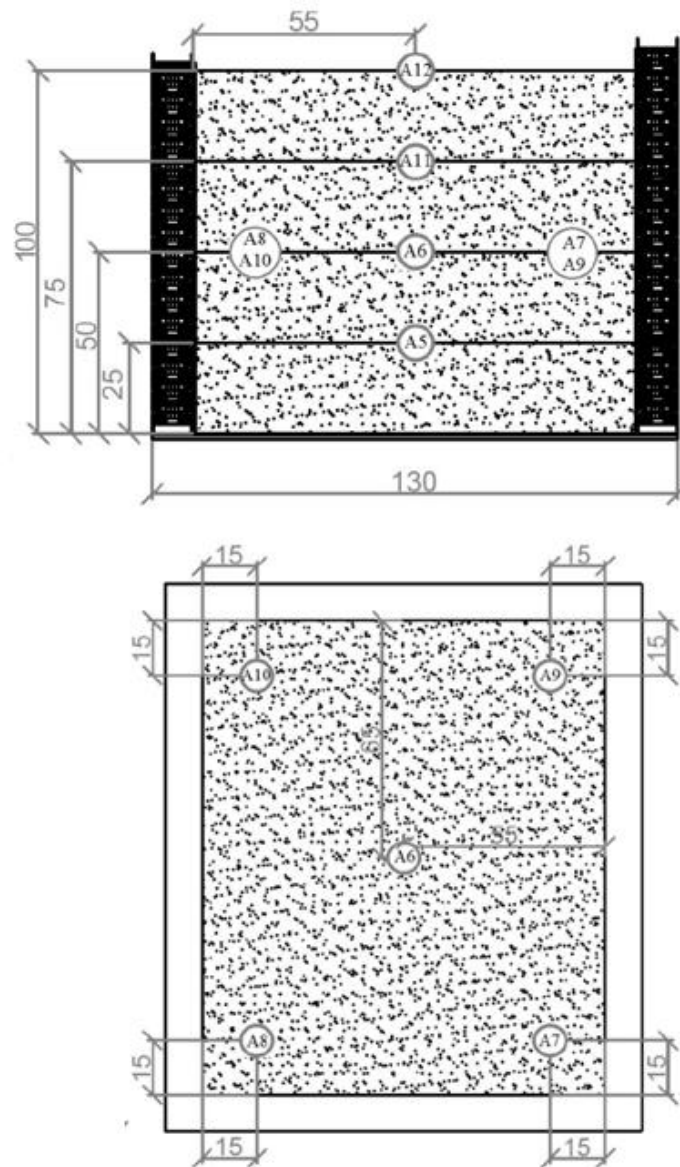


Figure 3.13. General View of Accelerometer's Locations in Soil. (Sekman, 2016)

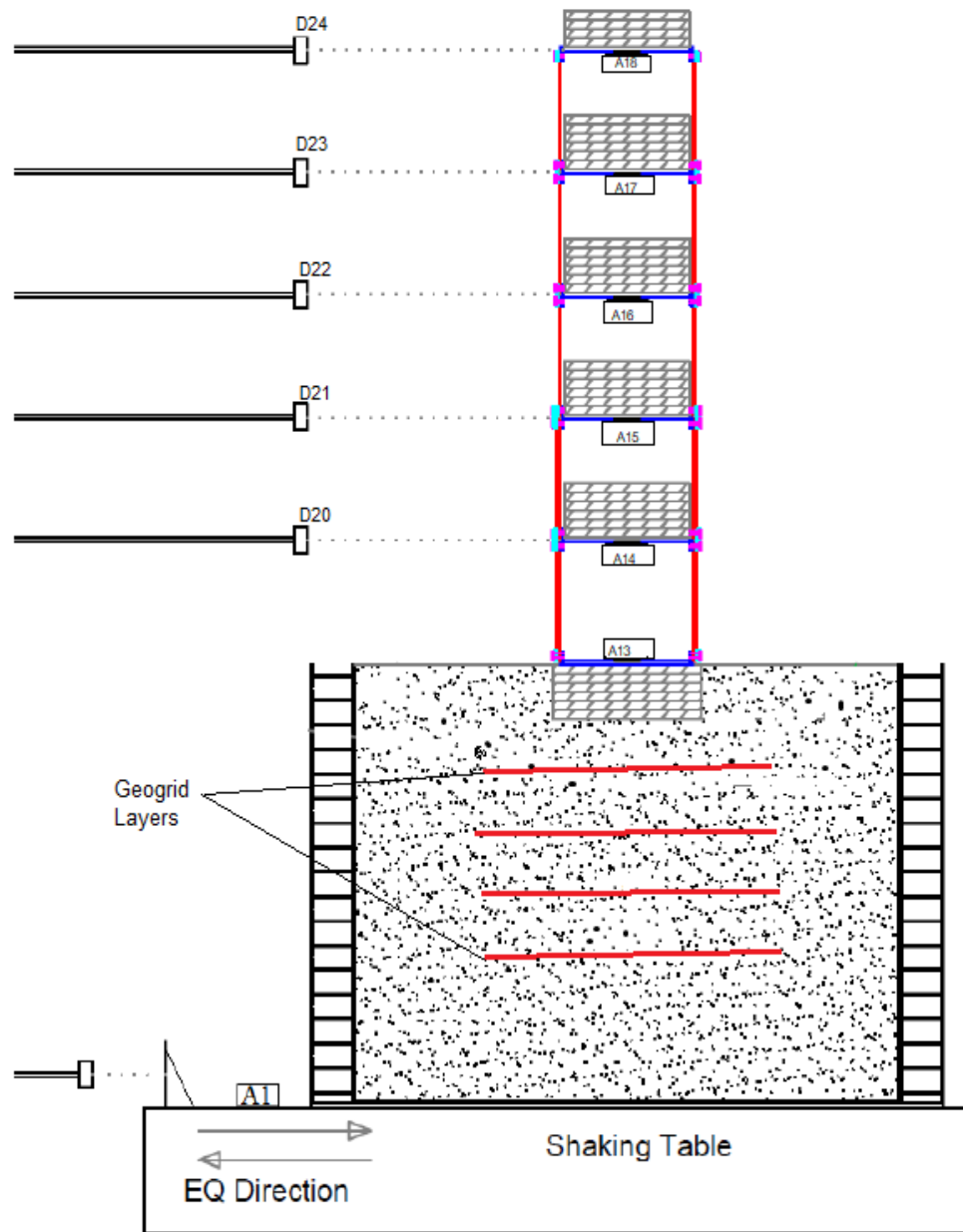


Figure 3.14. The Sketch of Scaled Building Model and Sensors for 5-Storey Building Model.

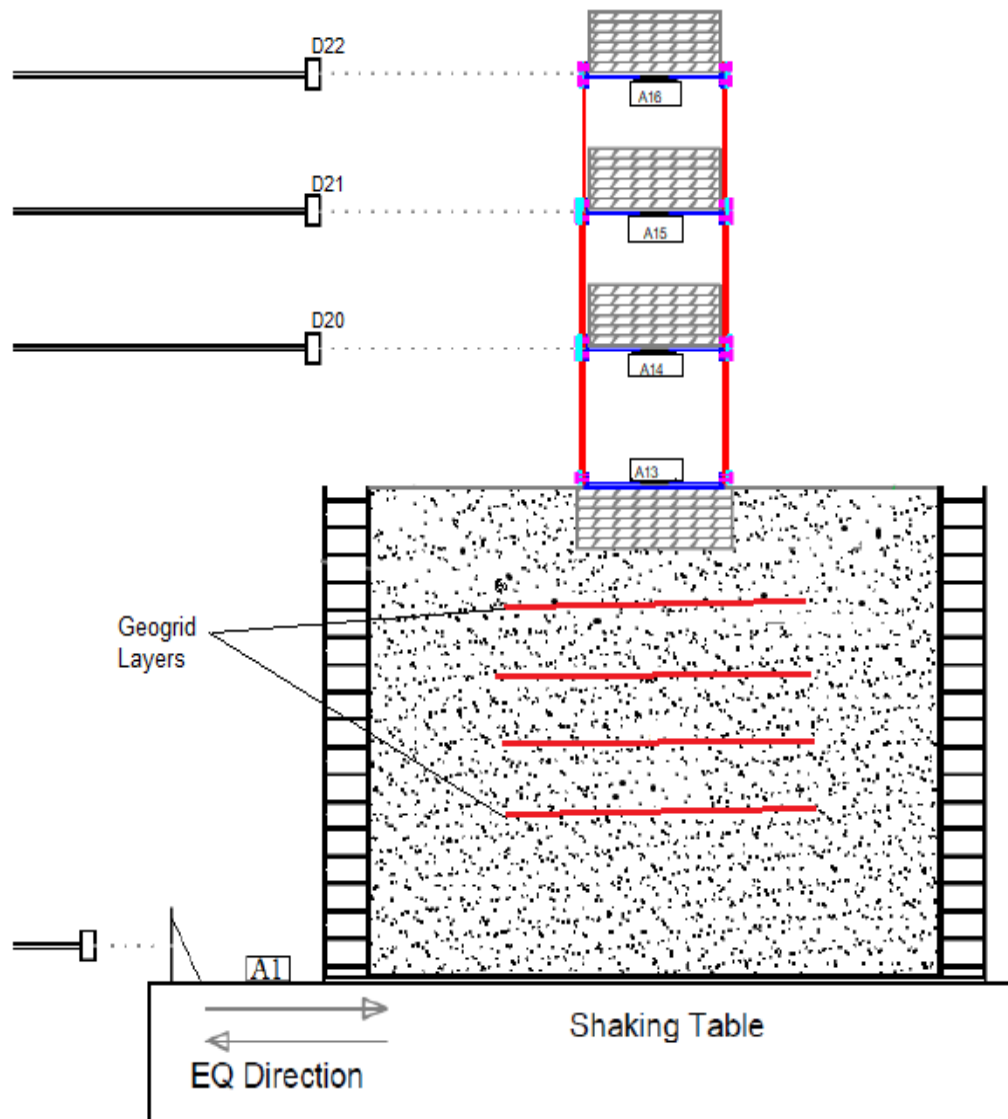


Figure 3.15. The Sketch of Scaled Building Model and Sensors For 3-Storey Building Model.



Figure 3.16. A View of the Scaled Building Model with Projection of Sensors.

3.4.3. The Scaled Input Motions

As mentioned in Chapter 3, input motions of the shaking table that were applied for proposed geogrid reinforcement system, experiments were divided into two categories that were cyclic sinusoidal and earthquake motions. Frequencies of the cyclic sinusoidal motions were decided regarding dominant frequencies of the building that were determined from the free vibration test. According to free vibration tests, cyclic sinusoidal motion frequencies of the 5-story building model were obtained 2.33 Hz, 8.58 Hz, 13.34 Hz, 17.52 Hz, 19.90 Hz and cyclic sinusoidal motion frequencies of the 3-story building model were measured 3.93 Hz, 12.46 Hz, and 18.35 Hz. And 0.5 Hz-0.1g, 1 Hz-0.3g, 2 Hz-0.5g, 3 Hz-0.6g, 4Hz-0.7g, 5Hz-0.8g for free surface.

In order to apply the earthquake records, which are Kocaeli (1999), Kobe (1995) and El Centro (1940) to the building models on geogrid reinforced foundation system, duration of the earthquake input data were scaled 1:10 by multiplying duration with a scaling factor of $\sqrt{10}$. It was applied to protect to dynamic assimilation in the system. Each earthquake record was compressed in time by a factor of $\sqrt{10}$. Time history, fourier amplitude spectrum, and response spectrum graphs of the scaled earthquake motions are shown in the Figure 4 ,respectively.

In addition to time scaling, the acceleration amplitudes of the earthquake records were scaled also to clearly observe effectiveness and robustness of the proposed geogrid reinforcement system under various amplitudes. Peak ground acceleration (PGA) of earthquake motions was scaled and after scaling PGA of the earthquakes, 9 earthquake motions with various peak accelerations were obtained. Besides, the acceleration amplitudes of the cyclic sinusoidal motions were determined according to the response of the building models. Acceleration amplitudes of the cyclic sinusoidal motions of the 5-story building model were 0.25g for 2.33 Hz, 0.35g for 8.58 Hz, 0.4g for 13.34 Hz, 0.5g for 17.52 Hz, 0.6g for 19.90 Hz and the 3-story building model were 0.3g for 3.93 Hz, 0.4g for 12.46 Hz, and 0.5g for 18.35 Hz. All motions applied to system and all cases are shown in Table 3.4.

With 3 different models and 5 different number of layers, in total 14 case was planned and applied.

Table 3.4. The Models and Input Motions.

	Sinusoidal Motions	Earthquake Motions		
		Kocaeli Eq.	El Centro Eq.	Kobe Eq.
FreeSurface	0.5 Hz-0.1g	0.21 g-0.51 g	0.35 g-0.55g-0.89 g	0.74 g-0.89 g
	1 Hz-0.3g			
	2 Hz-0.5g			
	3 Hz-0.6g			
	4 Hz-0.7g			
	5 Hz-0.8g			
5 Storey	2.33 Hz-0.25g	0.21 g-0.51 g	0.35 g-0.55g-0.89 g	0.74 g-0.89 g
	8.58 Hz-0.35g			
	13.34 Hz-0.4g			
	17.52 Hz-0.5g			
	19.90 Hz-0.6g			
3 Storey	3.93 Hz-0.3g	0.21 g-0.51 g	0.35 g-0.55g-0.89 g	0.74 g-0.89 g
	12.46 Hz-0.4g			
	18.35 Hz -0.5g			

3.4.4. Sample Preparation

By considering the total capacity of laminar box, an approximately 3 tons of Silivri sand were supplied. The unit weight of the compacted Silivri sand is 18.4 kN/m^3 ($D_r = 85\%$).

The dry sand was placed and compacted as manually layer by layer. While the sand was installing and compacting to protect sensors and geogrid materials from disturbing, this process was done carefully and lightly. During all this process, great importance was given to the locations of geogrids and sensors and the determined measurements of u , h , d , b was protected precisely. The installation of sand was continued up to 3 cm below from the top of laminar box and finally, the laminar box was filled with sand completely and the sand was again compacted manually.

For each scenario, which are $N=0$, $N=1$, $N=2$, $N=3$, $N=4$, to be able to prepare setup, laminar box was discharged and filled up with sand again. Apart from accelerometers in

the soil, 3 accelerometers were placed outside of laminar box at 9, 12, and 16 layers, which are A2, A3 and A4 to make sure that laminar box properly worked. Besides, the first accelerometer, that is A1 was placed at shaking table to control it. As a result, accelerometers A5 through A12 were placed in the soil and those between A13 and A18 were placed on the scaled building model.

There are some photos below on the experimental setup process. They were shown briefly the process of preparing experimental setup. Figure 3.17, Figure 3.18 and Figure 3.19 show preparation process of model test set-up with and without geogrid reinforcement. Also Figure 3.20 show 3-storey and 5-storey building models.



Figure 3.17. Soil Preparation Process of Experimental Model (a) Without Geogrid Reinforcement, (b) With Geogrid Reinforcement.



Figure 3.18. Soil Preparation Process of Model.

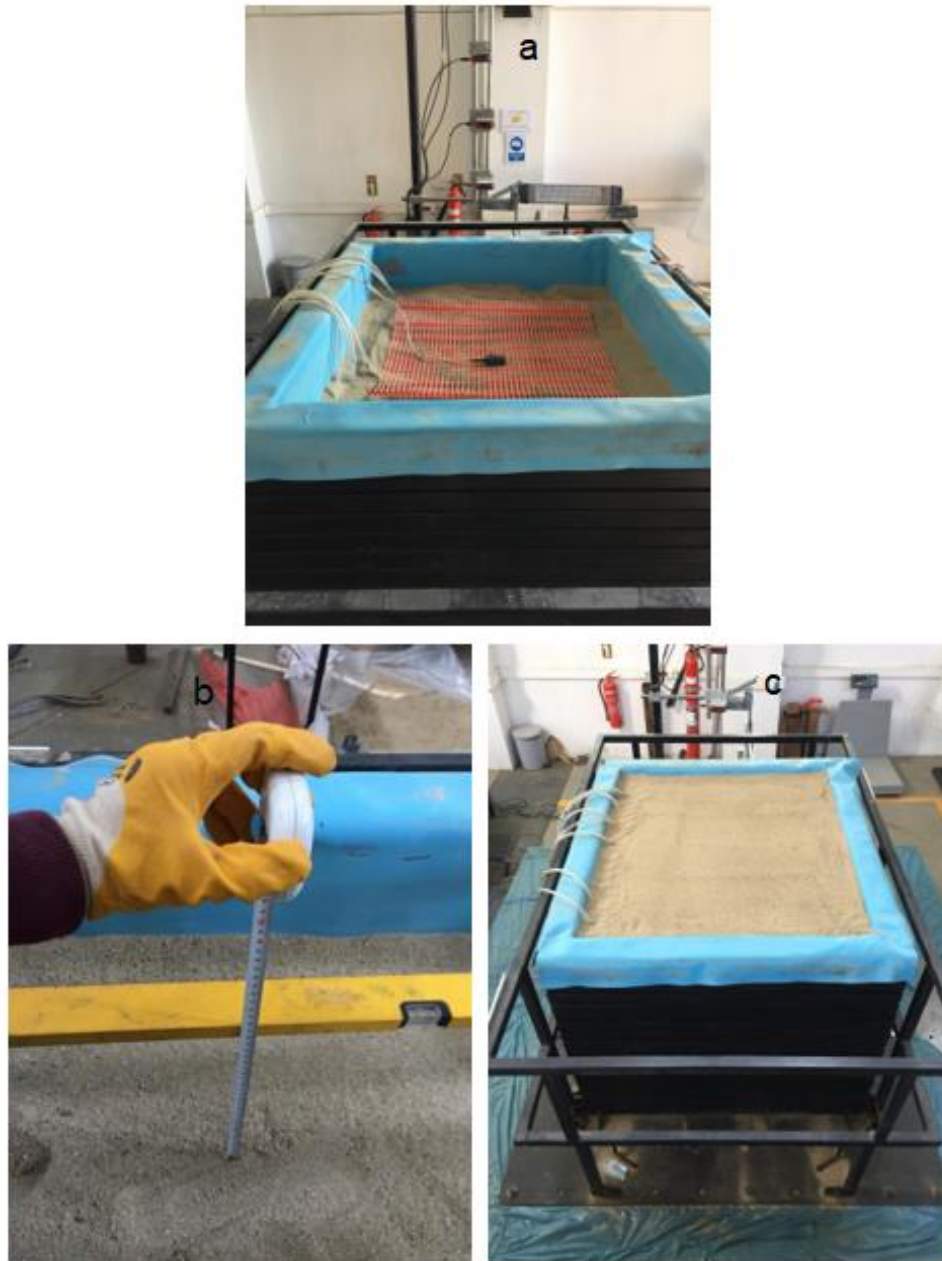


Figure 3.19. Soil Preparation Process of Model (a) Placement of Accelerometers and Geogrid Reinforcement in Soil, (b) Measurement of Soil Level, (c) Completed Soil Preparation.

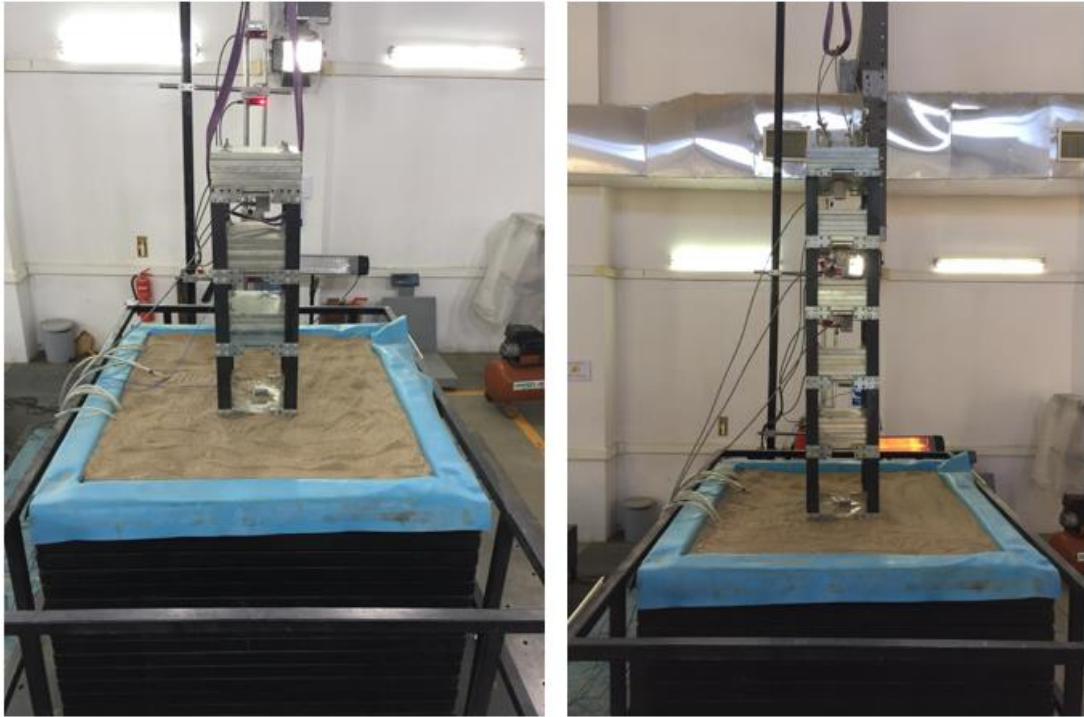


Figure 3.20. 5-Storey and 3-Storey Scaled Building Models.

4. RESULTS OF SHAKING TABLE TESTS

4.1. Experimental Program

In the experimental studies, the effects of the number of Geogrids (N), the number of floors of the buildings, earthquake motions in their own amplitudes and increased amplitudes on the seismic performance of low and medium buildings were evaluated. There are many experimental studies carried out under static loadings showing that the ratio of Geogrid length (L) to building foundation width (B) affects the experimental results. In the previous studies, the most effective L/B ratios were investigated by taking the L/B ratio between 1-10. In this study, the L/B ratio was taken as 2.3. This value is the highest possible L/B ratio due to limitations in the experimental setup. According to some literature studies, this value is within the limits of the most effective L/B ratio. This study, unlike the literature, was first carried out under earthquake loads. In the literature, there is no effective L/B defined under seismic loads.

The results of this study aim to determine to what extent the seismic performance of low and medium-rise buildings can be improved when $L/B=2.3$.

The results of all shaking table test series were evaluated to investigate the effectiveness and applicability of proposed geogrid reinforcement system in this part. In results, low-rise, mid-rise building models and in situ soil are exhibited separately.

As mentioned in part three briefly, during the model tests 3-storey and 5-storey building models with and without geogrid reinforcement were tested. Besides, without model the effectiveness of proposed geogrid reinforcement was tested to investigate soil response elaborately. Hence, the results were investigated and showed in the 3 main headings as free-surface, 3-storey, and 5-storey building models. With the changing number of geogrid layers, in total 14 different cases were examined. Information on cases can be seen below.

For the cases shown in Table 4.1. three different destructive earthquake motions, which are Kobe (1995), El Centro (1940), Kocaeli (1999) earthquake motions were

applied with their own amplitudes and increased amplitudes as input motions in shaking table experiments.

Table 4.1. Experimental Program (The Case Numbers and Model).

Case Number	Model	Number of Layers
CASE 1	FREE SURFACE	0
CASE 2	FREE SURFACE	1
CASE 3	FREE SURFACE	2
CASE 4	FREE SURFACE	3
CASE 5	5 STOREY	0
CASE 6	5 STOREY	1
CASE 7	5 STOREY	2
CASE 8	5 STOREY	3
CASE 9	5 STOREY	4
CASE 10	3 STOREY	0
CASE 11	3 STOREY	1
CASE 12	3 STOREY	2
CASE 13	3 STOREY	3
CASE 14	3 STOREY	4

All cases were repeated at least two times to verify and advance the reliability of the experimental results. And they were compared to each other.

The cases which were not used geogrid layer (N=0) was accepted as reference to observe the effectiveness of geogrid reinforcement system and was named as “without reinforcement (WR)” in the results. The cases used geogrid layer (N=1,2,3,4) was compared to the cases without geogrid layer (N=0).

Case 1 for Free Surface, Case 5 for 5-Storey and Case 10 for 3-Storey was the cases without reinforcement ($N=0$). And based on these cases, the improvement of the cases with the number of geogrid layers was observed and analyzed under same input motions.

Every improvement in the sensors for each case was detected and expressed as numerical and also specified as a percentage value (%) in tables. In the tables, “A” represents accelerometers and “D” represents displacement meters, also the numbers next them specify the sensor numbers, the locations of which was remarked previous chapter.

As performance indicators, horizontal acceleration responses, horizontal drifts and their peak values were presented with root-mean square (RSM) for the soil and each story. Besides, due to the fact that it gives the maximum horizontal acceleration response of the structure, the top floor and it is generally considered as the location where earthquake input ground motion is applied, the foundation (foun.) was chosen and improvements in there was displayed in graphs. Also in the same way, the first was displayed in graphs, especially because the first floor represent the main reason of soft story mechanism. Except these parameters, by benefiting horizontal drifts story drifts were shown.

As additional performance indicator parameters, arias intensity was chosen to see strength of earthquake on reinforcement and unreinforced systems. Also, in order to observe whether the natural period is shifting or not for geogrid reinforcement system, for all sensors fourier amplitude spectrum (FAS) was displayed and natural period shifting ratios were presented.

Below, the test results under Kocaeli earthquake, El Centro earthquake and Kobe earthquake motions were illustrated both graphical and tabular for 5-Storey, 3-Storey and Free-Surface separately.

If the improvements for all sensors was exhibited in the results, because it would occupy too much space, all of them were not put in result chapter. Including the first and top floor just four graphs for $N=4$ was exhibited in the result for each earthquake. The graphs belonging to sensor are encompassing horizontal acceleration response, horizontal displacement for story and their fourier transforms.

4.2. 5-Story Building Model on Geogrid Reinforced Soil

This part includes the results of 5-Story model with and without geogrid reinforcement and comparison of the results under the applied input (earthquake) motions with their original amplitude and increased amplitudes. As mentioned before, the case without geogrid reinforcement was Case 5 for 5-Storey model and it was defined as WR (without reinforcement), the cases with geogrid reinforcement were defined as R (reinforcement) in all tables and comparisons were made according to the mentioned experimental program in previous section.

4.2.1. Seismic Response of 5-Story Model under Kobe Earthquake Motion (PGA=0.74 g)

Table 4.2 show the reduced acceleration and displacement values through all sensors comparing to unreinforced system for 5-Storey model under Kobe Earthquake motion. The results of Cases 6,7,8 and 9, which were the cases with 5 story model with geogrid reinforcement from N=1 to N=4 can be seen. In the soil, peak accelerations are 0.9g in the underside and midpoint, and 0.89g in the upper side. The reduction of acceleration in underside is %5, %7, %18 and %20, the reduction of acceleration in midpoint is 7%, 7%, 20% and 20%, the reduction of acceleration in upper side is 3%, 4%, 14% and 25% for N=1, N=2, N=3 and N=4, respectively. The maximum acceleration improvement in the soil is 25%.

Table 4.2. Summary of All Tested Cases under Kobe Earthquake Motion (PGA=0.74g).

		N=4			N=3			N=2			N=1		
		WR	R	IMP. (%)	WR	R	IMP. (%)	WR	R	IMP. (%)	WR	R	IMP. (%)
In Soil	A5	0.9	0.75	20.000	0.9	0.76	18.421	0.9	0.84	7.143	0.9	0.85	5.882
	A6	0.9	0.75	20.000	0.9	0.75	20.000	0.9	0.84	7.143	0.9	0.84	7.143
	A7	0.84	0.73	15.068	0.84	0.73	15.068	0.84	0.81	3.704	0.84	0.82	2.439
	A8	0.86	0.7	22.857	0.86	0.78	10.256	0.86	0.85	1.176	0.86	0.84	2.381
	A9	0.87	0.76	14.474	0.87	0.79	10.127	0.87	0.81	7.407	0.87	0.8	8.750
	A10	0.88	0.73	20.548	0.88	0.76	15.789	0.88	0.81	8.642	0.88	0.84	4.762
	A11	0.87	0.71	22.535	0.87	0.73	19.178	0.87	0.84	3.571	0.87	0.86	1.163
	A12	0.89	0.71	25.352	0.89	0.78	14.103	0.89	0.85	4.706	0.89	0.86	3.488
Foun.(g)	A13	0.82	0.69	18.841	0.82	0.71	15.493	0.82	0.76	7.895	0.82	0.77	6.494
5 Storey Model	A14	1.25	1.05	19.048	1.25	1.08	15.741	1.25	1.16	7.759	1.25	1.24	0.806
	A15	1.18	1.08	9.259	1.18	1.11	6.306	1.18	1.14	3.509	1.18	1.19	-0.84
	A16	1.01	0.79	27.848	1.01	0.91	10.989	1.01	0.95	6.316	1.01	1.03	-1.942
	A17	0.75	0.56	33.929	0.75	0.63	19.048	0.75	0.65	15.385	0.75	0.67	11.940
	A18	1.43	1.04	37.500	1.43	1.28	11.719	1.43	1.3	10.000	1.43	1.33	7.519
	D20	2.67	2.22	20.270	2.67	2.39	11.715	2.67	2.42	10.331	2.67	2.43	9.877
	D21	2.86	2.66	7.519	2.86	2.69	6.320	2.86	2.73	4.762	2.86	2.76	3.623
	D22	3.51	3.06	14.706	3.51	3.13	12.141	3.51	3.21	9.346	3.51	3.21	9.346
	D23	3.95	3.62	9.116	3.95	3.71	6.469	3.95	3.75	5.333	3.95	3.77	4.775
	D24	4.74	4.37	8.467	4.74	4.42	7.240	4.74	4.66	1.717	4.74	4.66	1.717

The sensors showing acceleration, displacement measurement and fourier amplitude spectrum in Figure 5.1 and 5.2 were selected between unreinforced system and N=4 and through these figures the maximum improvement can be seen at these points. For the first floor, N=1 slightly effects the reduction of acceleration, it is 0.8%. However, with the increase in the geogrid layers it becomes 7%, 15% and 19% for N=2, N=3, N=4, respectively. For the third floor and the fifth floor, the acceleration reduction values become up to approximately 27% and 37% comparing to unreinforced system.

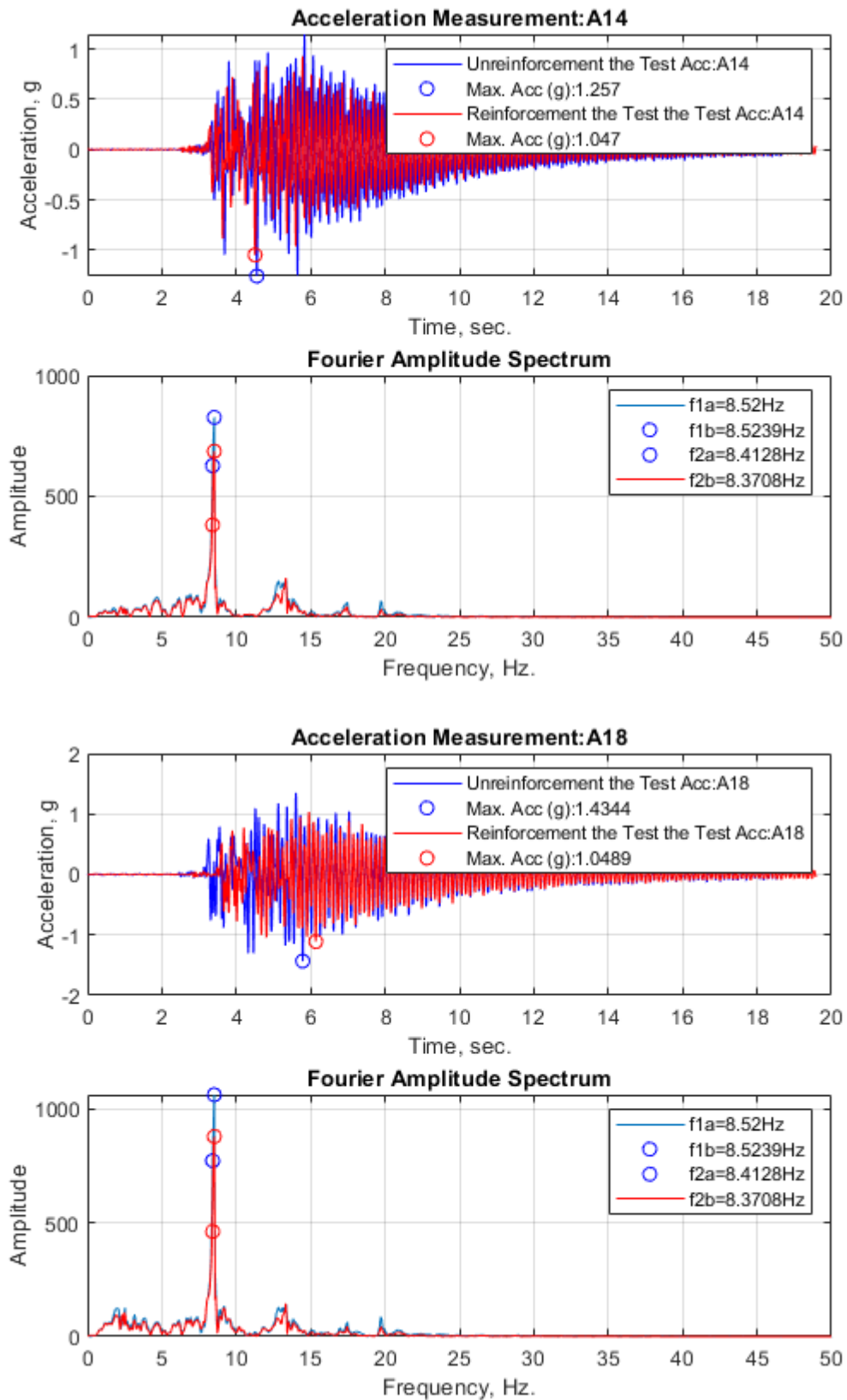


Figure 4.1. Acceleration Measurements and FAS of 1st and 5th Floors under Kobe Earthquake Motion (PGA= 0.74 g).

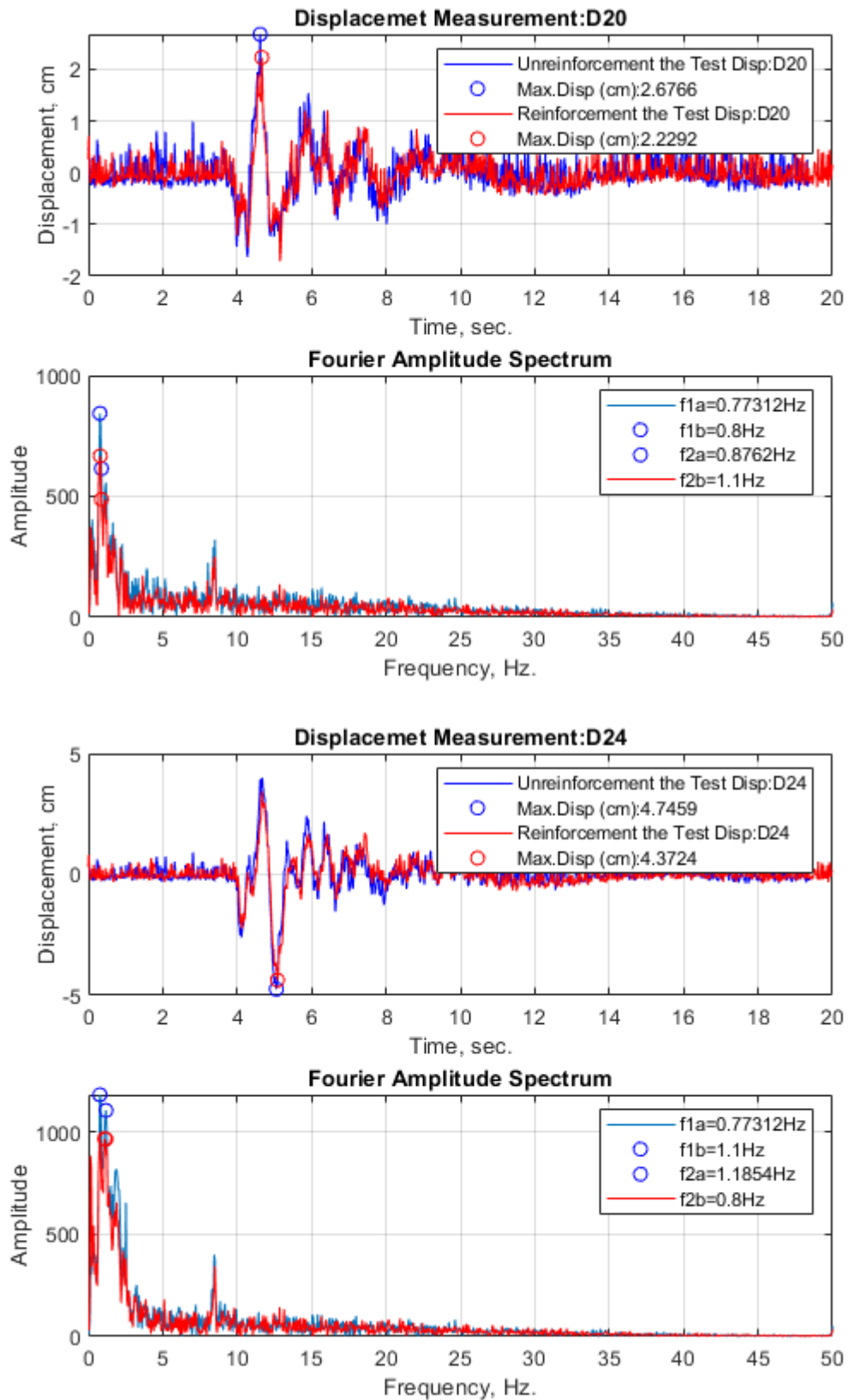


Figure 4.2. Displacement Measurements and FAS of 1st and 5th Floors under Kobe Earthquake Motion (PGA= 0.74 g).

Based on the results of all tested cases under Kobe Earthquake motion, the changing acceleration and displacement values in accordance with story and reinforcement layers were given in Figure 5.4 and Figure 5.5. Through the graphs the improvements compared unreinforced system can be seen easily for foundation, first and fifth story for each N values.

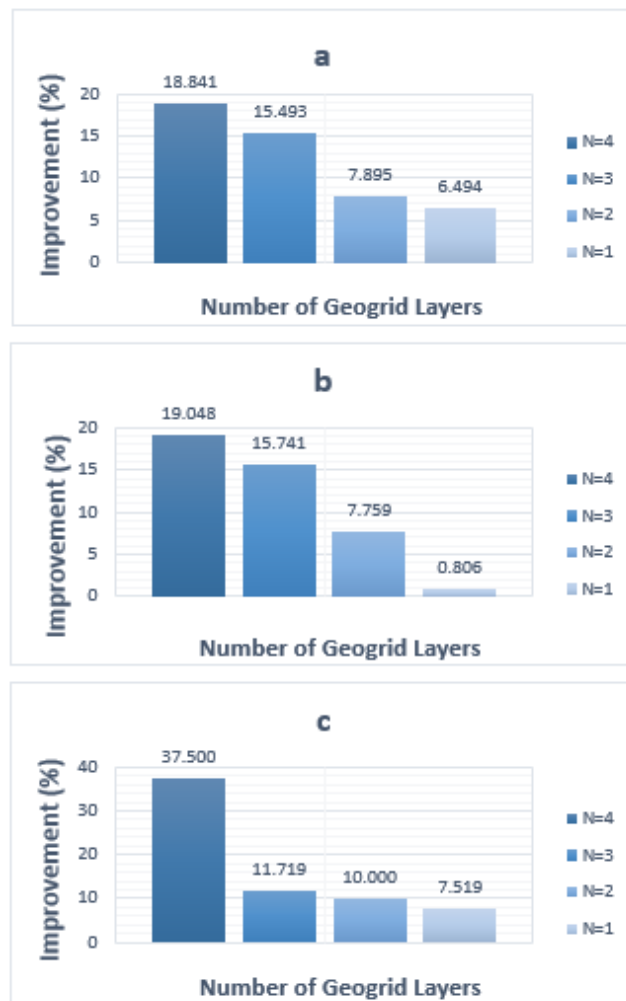


Figure 4.3. The Acceleration Improvement Graphs in Accordance with Story and Reinforcement Layers for (a) Foundation, (b) 1st Floor, (c) 5th Floor under Kobe Earthquake Motion (PGA= 0.74 g).

In the first, third and fifth floor, the maximum decrease of story's displacement is 20%, 14% and 8% respectively. In fifth floor, there is no considerable reduction. For N=1 and N=2, it is just 1% but for N=3 it reaches up to 7%.

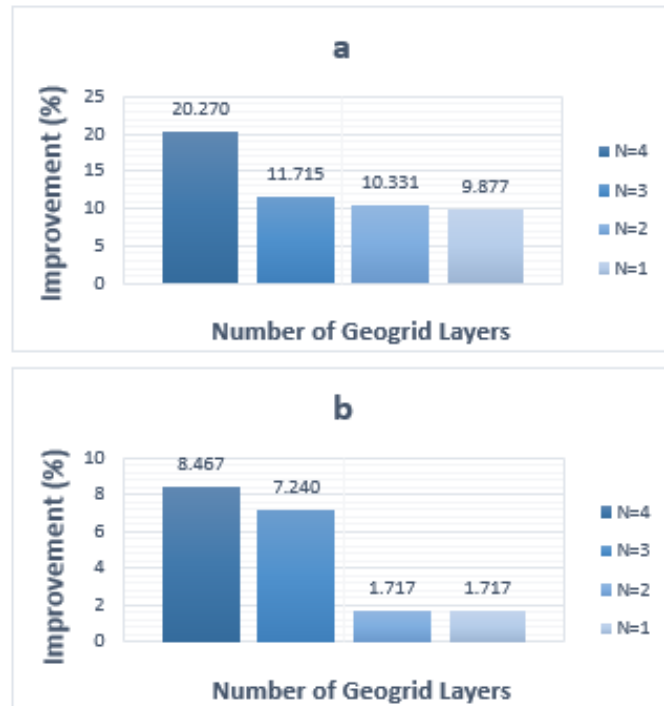


Figure 4.4. The Displacement Improvement Graphs in Accordance with Story and Reinforcement Layers for (a) 1st Floor, (b) 5th Floor under Kobe Earthquake Motion (PGA= 0.74 g).

In Table 4.3 and Table 4, fundamental periods were exhibited and with the help of the fundamental period of all N values under dynamic loads for soil, foundations, floors, the period lengthening ratios were shown, and also RMS of peak values and arias intensity values were exhibited.

Table 4.3. Fundamental Period and Period Lengthening Ratios under Kobe Earthquake Motion (PGA = 0.74g).

	Fundamental Period (Hz)					Period Lengthening Ratio			
	N=4	N=3	N=2	N=1	N=0	N=4	N=3	N=2	N=1
In-Soil	4.65	4.65	4.65	4.68	4.66	1.00	1.00	1.00	1.00
Foundation	4.65	4.65	4.67	4.68	4.65	1.00	1.00	1.00	0.99
1st Floor	0.8	0.8	0.77	0.79	0.77	0.96	0.96	1.00	0.97
2nd Floor	0.8	0.8	0.77	0.79	0.77	0.96	0.96	1.00	0.97
3rd Floor	0.8	0.8	0.77	0.79	0.77	0.96	0.96	1.00	0.97
4th Floor	0.8	0.8	0.77	0.79	0.77	0.96	0.96	1.00	0.97
5th Floor	0.8	0.8	0.77	0.79	0.77	0.96	0.96	1.00	0.97

As can be seen, arias intensity values for soil region are approximately 30% and it reduce up to 43% for floors. RMS improvement values for soil, foundation and floors are 12%, 11%, 10%, 4%, 9%, 19% and 15%, respectively. Also, there is no change in the natural period of model. The period lengthening ratio fluctuates up to 3%. In Figure 4.5, arias intensity improvement chart and story drifts can be seen.

Table 4.4. RMS and Arias Intensity Improvement Ratios under Kobe Earthquake Motion (PGA = 0.74g).

Root Mean Square (RSM)					
Horizontal Acceleration(g)	Peak	RSM-Rein.	RSM Imp (%)		Arias Intensity Imp(%)
In-Soil	0.9	0.8	12.32	In-Soil	30.68
Foundation	0.82	0.73	11.83	Foundation	22.04
1st Floor	1.25	1.13	10.14	1st Floor	21.14
2nd Floor	1.18	1.13	4.36	2nd Floor	11.02
3rd Floor	1.01	0.92	9.3	3rd Floor	33.14
4th Floor	0.75	0.63	19.26	4th Floor	36.3
5th Floor	1.43	1.24	15.06	5th Floor	43.13

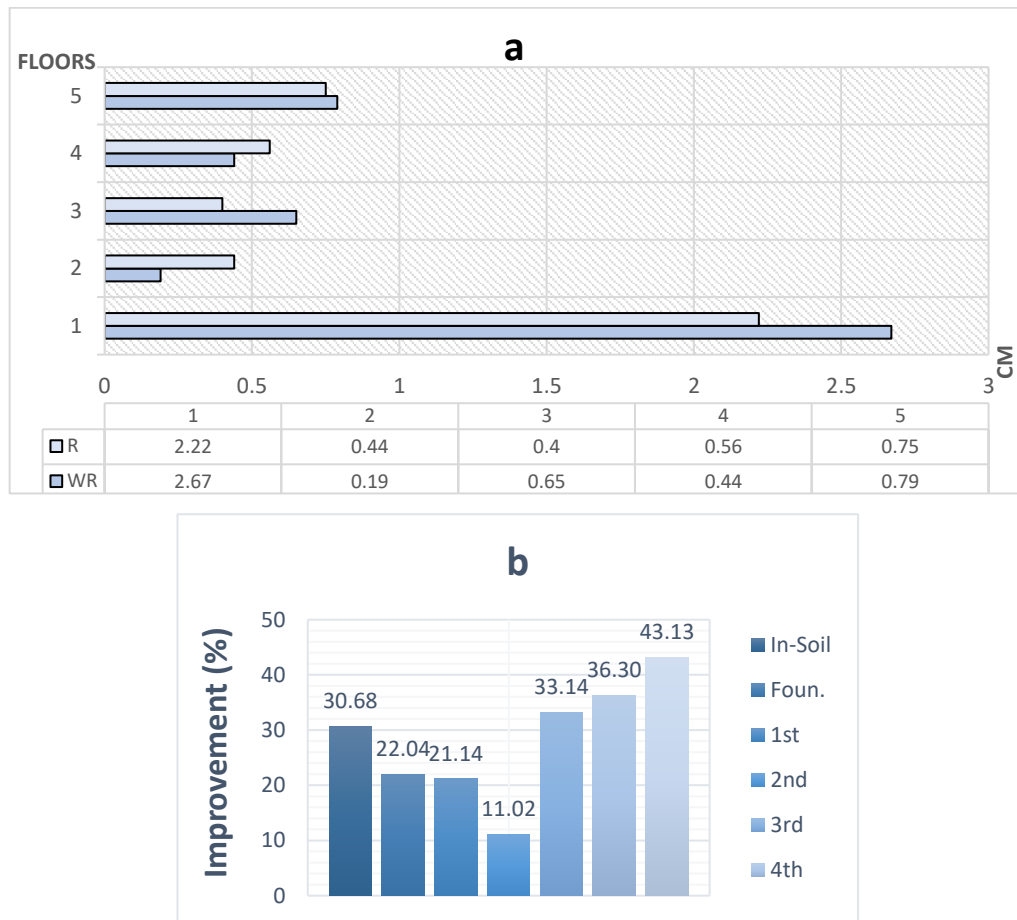


Figure 4.5. Improvement Ratios considering (a) Story Drifts and (b) Arias Intensity under Kobe Earthquake Motion (PGA= 0.74 g).

4.2.2. Seismic Response of 5-Story Model under Kobe Earthquake Motion (PGA= 0.89 g)

Table 4.5 shows the reduced acceleration and displacement values through all sensors comparing to unreinforced system for 5-Storey model under Kobe Earthquake (0.89g). In the soil, peak accelerations are 1.12g in the underside and 1.05g in the midpoint, and 0.96g in the upper side. The maximum improvement of acceleration in the underside, midpoint upper side is 20%, 16% and 15%, respectively. The results of Cases 6, 7, 8 and 9, which were the cases with 5 story model with geogrid reinforcement from N=1 to N=4 can be seen.

Table 4.5. Summary of All Tested Cases under Kobe Earthquake Motion (PGA=0.89g).

		N=4			N=3			N=2			N=1		
		WR	R	IMP. (%)	WR	R	IMP. (%)	WR	R	IMP. (%)	WR	R	IMP. (%)
In Soil (g)	A5	1.12	0.93	20.430	1.12	0.97	15.464	1.12	1.01	10.891	1.12	1.04	7.692
	A6	1.1	0.93	18.280	1.1	0.98	12.245	1.1	1.02	7.843	1.1	1.05	4.762
	A7	1.03	0.9	14.444	1.03	0.93	10.753	1.03	0.98	5.102	1.03	1	3.000
	A8	1.05	0.9	16.667	1.05	0.94	11.702	1.05	0.99	6.061	1.05	1.04	0.962
	A9	1.04	0.94	10.638	1.04	0.95	9.474	1.04	0.97	7.216	1.04	1	4.000
	A10	1.03	0.95	8.421	1.03	0.95	8.421	1.03	0.97	6.186	1.03	1	3.000
	A11	1.01	0.88	14.773	1.01	0.89	13.483	1.01	0.96	5.208	1.01	0.99	2.020
	A12	0.96	0.83	15.663	0.96	0.87	10.345	0.96	0.92	4.348	0.96	0.95	1.053
Foun.(g)	A13	0.89	0.78	14.103	0.89	0.81	9.877	0.89	0.84	5.952	0.89	0.87	2.299
5 Storey Model (cm)	A14	1.33	1.25	6.400	1.33	1.28	3.906	1.33	1.29	3.101	1.33	1.33	0
	A15	1.2	1.12	7.143	1.2	1.17	2.564	1.2	1.17	2.564	1.2	1.2	0
	A16	1.21	1.04	16.346	1.21	1.08	12.037	1.21	1.12	8.036	1.21	1.15	5.217
	A17	1.06	0.85	24.706	1.06	0.89	19.101	1.06	0.91	16.484	1.06	0.95	11.579
	A18	1.61	1.42	13.380	1.61	1.46	10.274	1.61	1.49	8.054	1.61	1.56	3.205
	D20	2.79	2.46	13.415	2.79	2.61	6.897	2.79	2.62	6.489	2.79	2.74	1.825
	D21	3.25	2.64	23.106	3.25	3.1	4.839	3.25	3.17	2.524	3.25	3.23	0.619
	D22	4.17	3.37	23.739	4.17	3.52	18.466	4.17	3.85	8.312	4.17	3.97	5.038
	D23	4.93	3.72	32.527	4.93	4.17	18.225	4.93	4.24	16.274	4.93	4.45	10.787
	D24	5.36	4.07	31.695	5.36	4.3	24.651	5.36	4.89	9.611	5.36	5.14	4.280

Figure 4.6 and 4.7 shows displacement and acceleration measurements and fourier amplitude spectrum of 1st and 5th Floors. Despite the fact that the first floor is decreased up to 30% in acceleration value, the maximum reduction of fifth floor is 8%. The third floor's improvement is 17%. Besides, for N=1, the second floor's improvement become negative, which is -1.5% and for N=4 it reaches up to 16%. The sensors showing acceleration, displacement measurement and fourier amplitude spectrum in Figure 4.6 and 4.7 was selected between unreinforced system and N=4 and through these figures, the maximum improvement can be seen at these points.

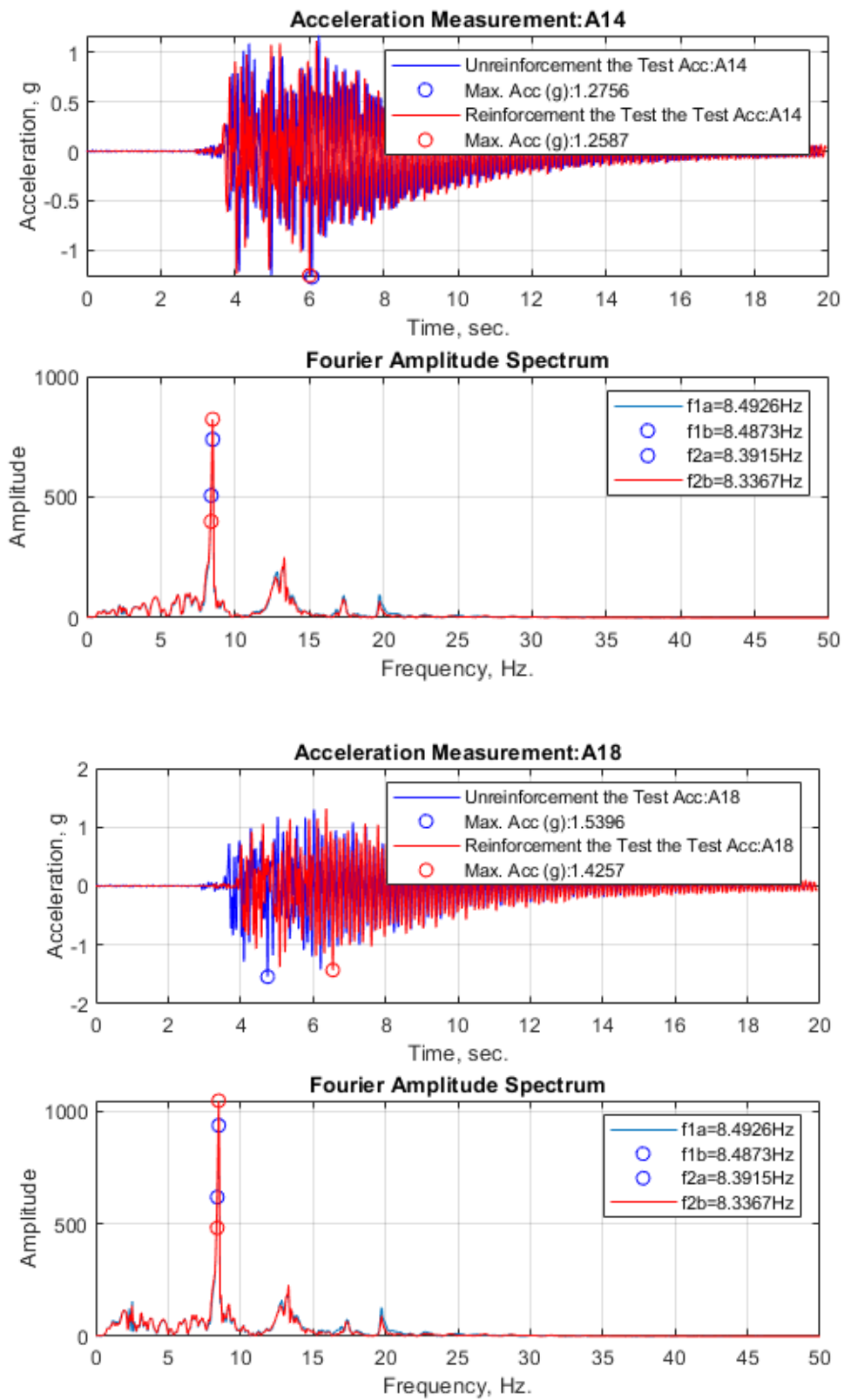


Figure 4.6. Acceleration Measurements and FAS of 1st and 5th Floors under Kobe Earthquake Motion (PGA= 0.89 g).

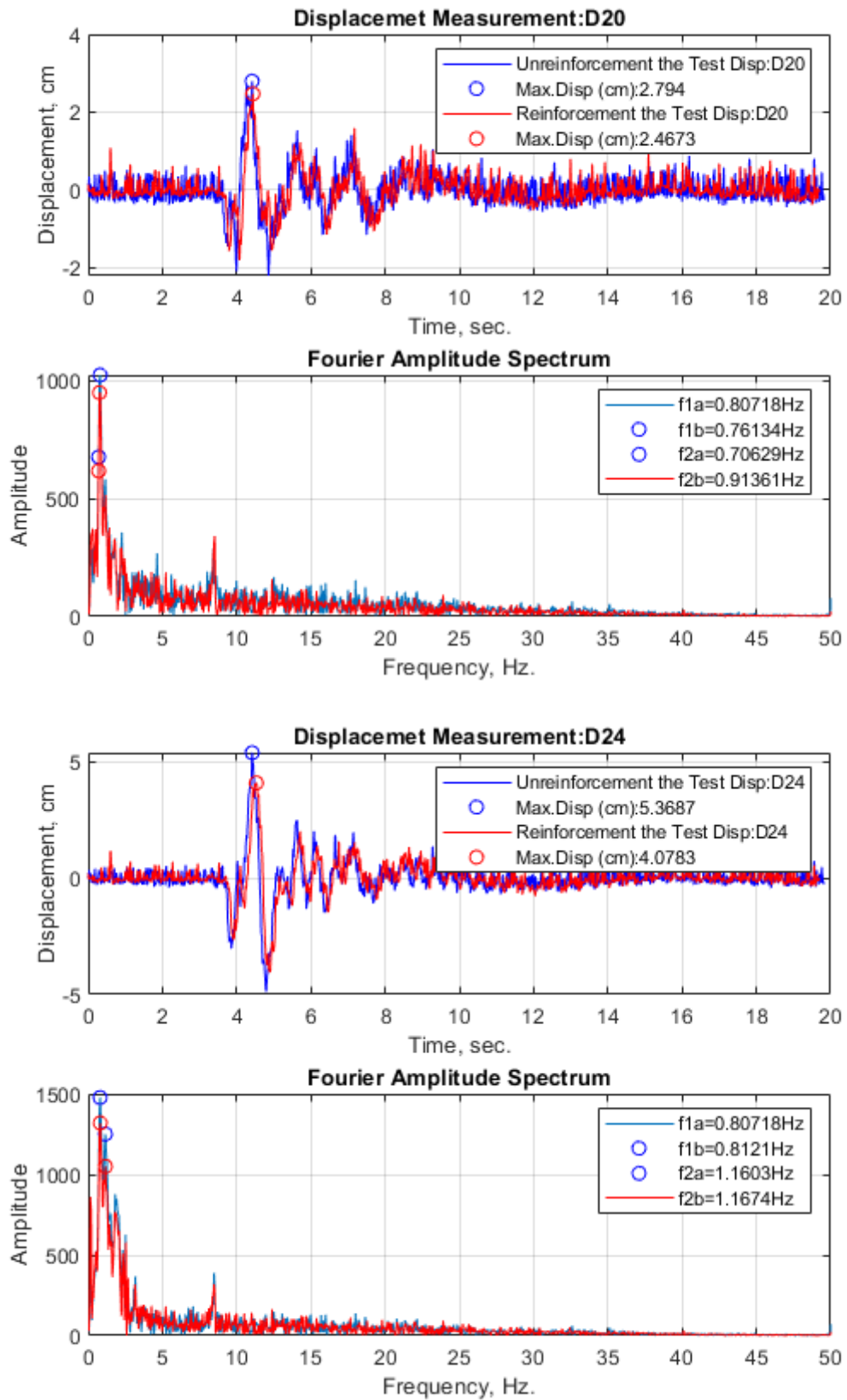


Figure 4.7. Displacement Measurements and FAS of 1st and 5th Floors under Kobe Earthquake Motion (PGA= 0.89 g).

The reduction of foundation acceleration is roughly 2%, 5%, 9% and 14% for N=1, N=2, N=3 and N=4 respectively.

Based on the results of all tested cases under Kobe Earthquake 0.89g, the changing acceleration values and the changing displacement values in accordance with story and reinforcement layers were given in Figure 4.8. and Figure 4.9., which show the comparisons of N=1, N=2, N=3 and N=4 for foundation, first and fifth story for each N values.

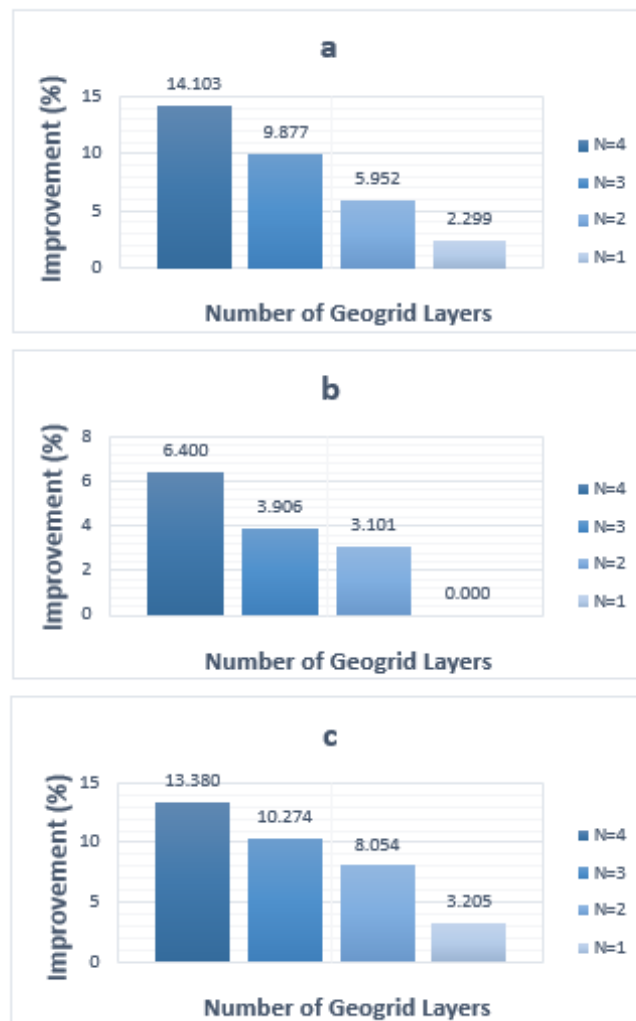


Figure 4.8. The Acceleration Improvement Graphs in Accordance with Story and Reinforcement Layers for (a) Foundation, (b) 1st Floor, (c) 5th Floor under Kobe Earthquake Motion (PGA= 0.89 g).

For the first floor, for N=1 there is no reduction in acceleration value. However, with the increase in the geogrid layers it becomes nearly 3%, 4% and 6% for N=2, N=3, N=4. On the third floor and the fifth floor, the acceleration reduction values become up to 16% and 13% comparing to unreinforced system.

For the first, third and fifth floor, the maximum decrease of story's displacement values is 13%, 23%, 31% respectively. All of them obtain in N=4. Except the fourth story, for all stories there is no significant improvement for N=1.

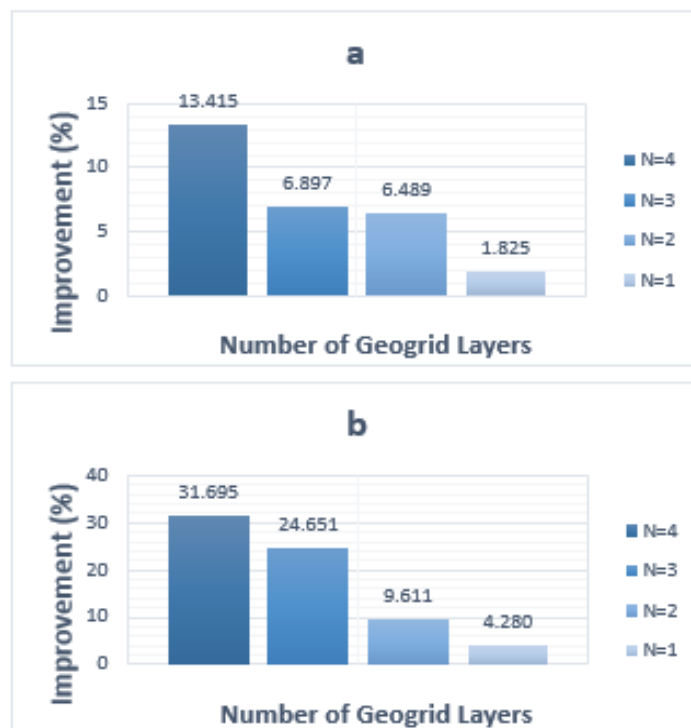


Figure 4.9. The Displacement Improvement Graphs in Accordance with Story and Reinforcement Layers for (a) 1st Floor, (b) 5th Floor under Kobe Earthquake Motion (PGA= 0.89 g).

In Table 4.6 and Table 4.7 arias intensity improvements were exhibited as well as with the help of the fundamental period of all N values under dynamic loads for soil, foundations, floors, the period lengthening ratios were given, and RMS of peak values were shown.

Table 4.6. Fundamental Period and Period Lengthening Ratios under Kobe Earthquake Motion (PGA = 0.89g).

	Fundamental Period (Hz)					Period Lengthening Ratio			
	N=4	N=3	N=2	N=1	N=0	N=4	N=3	N=2	N=1
In-Soil	4.57	4.65	4.65	4.68	4.57	1	0.98	0.98	0.98
Foundation	4.67	4.65	4.67	4.68	4.68	1	1.01	1	1
1st Floor	0.8	0.8	0.77	0.79	0.8	1	1	1.04	1.01
2nd Floor	0.8	0.8	0.77	0.79	0.8	1	1	1.04	1.01
3rd Floor	0.8	0.8	0.77	0.79	0.8	1	1	1.04	1.01
4th Floor	0.8	0.8	0.81	0.79	0.8	1	1	0.99	1.01
5th Floor	0.8	0.8	0.81	0.81	0.8	1	1	0.99	0.99

Table 4.7. RMS and Arias Intensity Improvement Ratios under Kobe Earthquake Motion (PGA = 0.89g).

Root Mean Square (RSM)					
Horizontal Acceleration(g)	Peak	RSM-Rein.	RSM Imp (%)		Arias Intensity Imp (%)
In-Soil	1.12	0.99	13.32	In-Soil	18.95
Foundation	0.89	0.83	7.79	Foundation	16.5
1st Floor	1.33	1.29	3.28	1st Floor	7.1
2nd Floor	1.2	1.17	2.97	2nd Floor	8.5
3rd Floor	1.21	1.1	10.17	3rd Floor	19.45
4th Floor	1.06	0.9	17.68	4th Floor	26.44
5th Floor	1.61	1.48	8.54	5th Floor	15.39

As can be seen in Table 4.6 and Table 4.7, arias intensity values are reduced up to 5%, 4% and 8% for soil region, foundation, and floors in order of. Reduction of RMS ascend at soil and foundation to 13%, 7% and at floors to 6%, 5%, 5%, 4% and 7% respectively. Also, there is no change the natural period of model. The period lengthening ratio fluctuates up to %4. Also, in Figure 4.10, arias intensity improvement chart and story drifts can be observed.

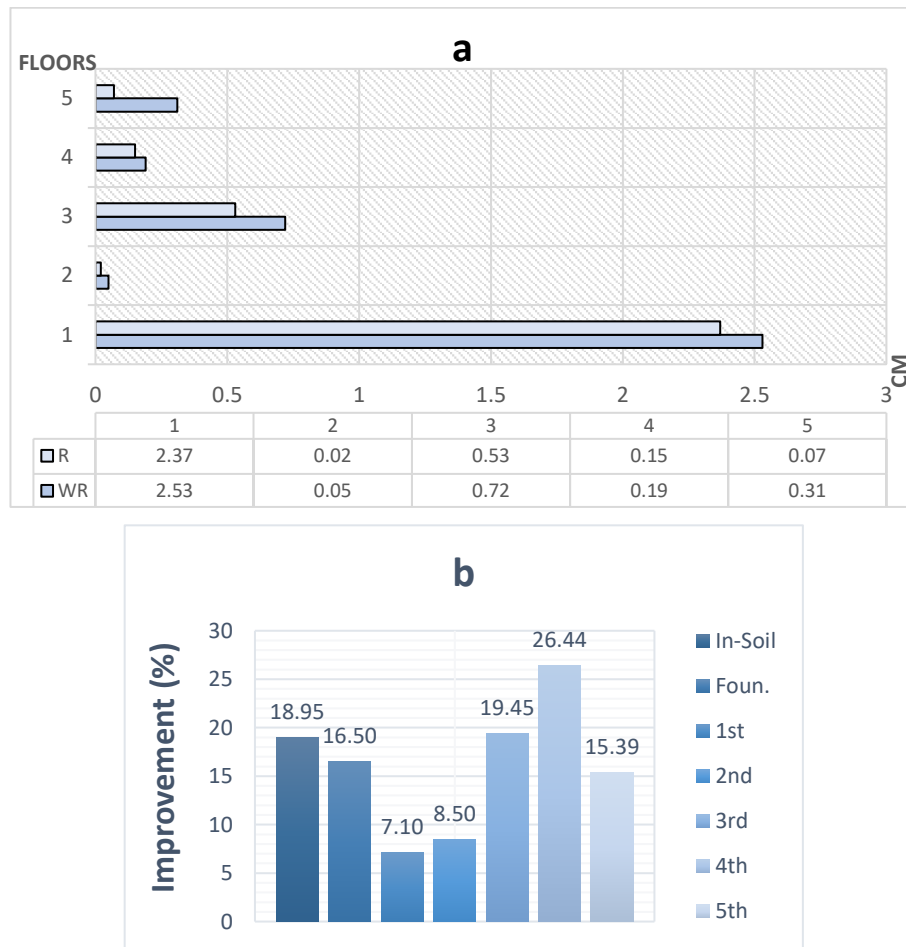


Figure 4.10. Improvement Ratios considering (a) Story Drifts and (b) Arias Intensity under Kobe Earthquake Motion (PGA= 0.89 g).

4.2.3. Seismic Response of 5-Story Model under Kocaeli Earthquake Motion (PGA= 0.21 g)

In Table 4.8, the results of Cases 6, 7, 8 and 9 for 5-Storey model under the Kocaeli earthquake motion (PGA=0.21g) are summarized. The reduced acceleration and displacement values through all sensor points comparing to unreinforced system can be seen easily. In the soils, peak accelerations are 0.19g in the underside, 0.28g in the midpoint, and 0.32g in the upper side. The maximum improvement ratio of acceleration in the underside, midpoint and upper side is 35%, 27% and 14%, respectively. For N=1, nearly all location in the soil the reduction in acceleration is approximately 4-5%.

Table 4.8. Summary of all tested Cases for 5-Story Model under Kocaeli Earthquake Motion (PGA=0.21g).

		N=4			N=3			N=2			N=1		
		WR	R	IMP. (%)	WR	R	IMP. (%)	WR	R	IMP. (%)	WR	R	IMP. (%)
In Soil (g)	A5	0.19	0.14	35.714	0.19	0.16	18.750	0.19	0.17	11.765	0.19	0.18	5.556
	A6	0.22	0.18	22.222	0.22	0.2	10.000	0.22	0.22	0	0.22	0.23	-4.348
	A7	0.21	0.18	16.667	0.21	0.2	5.000	0.21	0.21	0	0.21	0.21	0
	A8	0.22	0.18	22.222	0.22	0.2	10.000	0.22	0.21	4.762	0.22	0.21	4.762
	A9	0.24	0.19	26.316	0.24	0.22	9.091	0.24	0.23	4.348	0.24	0.23	4.348
	A10	0.24	0.18	33.333	0.24	0.2	20.000	0.24	0.23	4.348	0.24	0.23	4.348
	A11	0.28	0.22	27.273	0.28	0.22	27.273	0.28	0.28	0	0.28	0.28	0
	A12	0.32	0.28	14.286	0.32	0.3	6.667	0.32	0.31	3.226	0.32	0.34	-5.882
Foun.(g)	A13	0.33	0.26	26.923	0.33	0.3	10.000	0.33	0.31	6.452	0.33	0.33	0
5 Storey Model (cm)	A14	0.52	0.4	30.000	0.52	0.44	18.182	0.52	0.47	10.638	0.52	0.48	8.333
	A15	0.65	0.56	16.071	0.65	0.61	6.557	0.65	0.64	1.563	0.65	0.66	-1.515
	A16	0.55	0.47	17.021	0.55	0.49	12.245	0.55	0.51	7.843	0.55	0.54	1.852
	A17	0.39	0.3	30.000	0.39	0.31	25.806	0.39	0.35	11.429	0.39	0.38	2.632
	A18	0.8	0.74	8.108	0.8	0.77	3.896	0.8	0.78	2.564	0.8	0.78	2.564
	D20	2.53	2.37	6.751	2.53	2.4	5.417	2.53	2.46	2.846	2.53	2.51	0.797
	D21	2.58	2.39	7.950	2.58	2.45	5.306	2.58	2.54	1.575	2.58	2.59	-0.386
	D22	3.3	2.92	13.014	3.3	3.1	6.452	3.3	3.19	3.448	3.3	3.28	0.61
	D23	3.49	3.07	13.681	3.49	3.24	7.716	3.49	3.43	1.749	3.49	3.5	-0.286
	D24	3.8	3.14	21.019	3.8	3.4	11.765	3.8	3.72	2.151	3.8	3.79	0.264

Figure 4.11 and 4.12 shows displacement and acceleration measurements and fourier amplitude spectrum of 1st and 5th Floors. Despite the fact that the first floor is decreased up to 30% in acceleration value, the maximum reduction of fifth floor is 8%. The third floor' improvement is 17%. Besides, for N=1, the second floor's improvement become negative, which is -1.5% and for N=4 it reaches up to 16%.

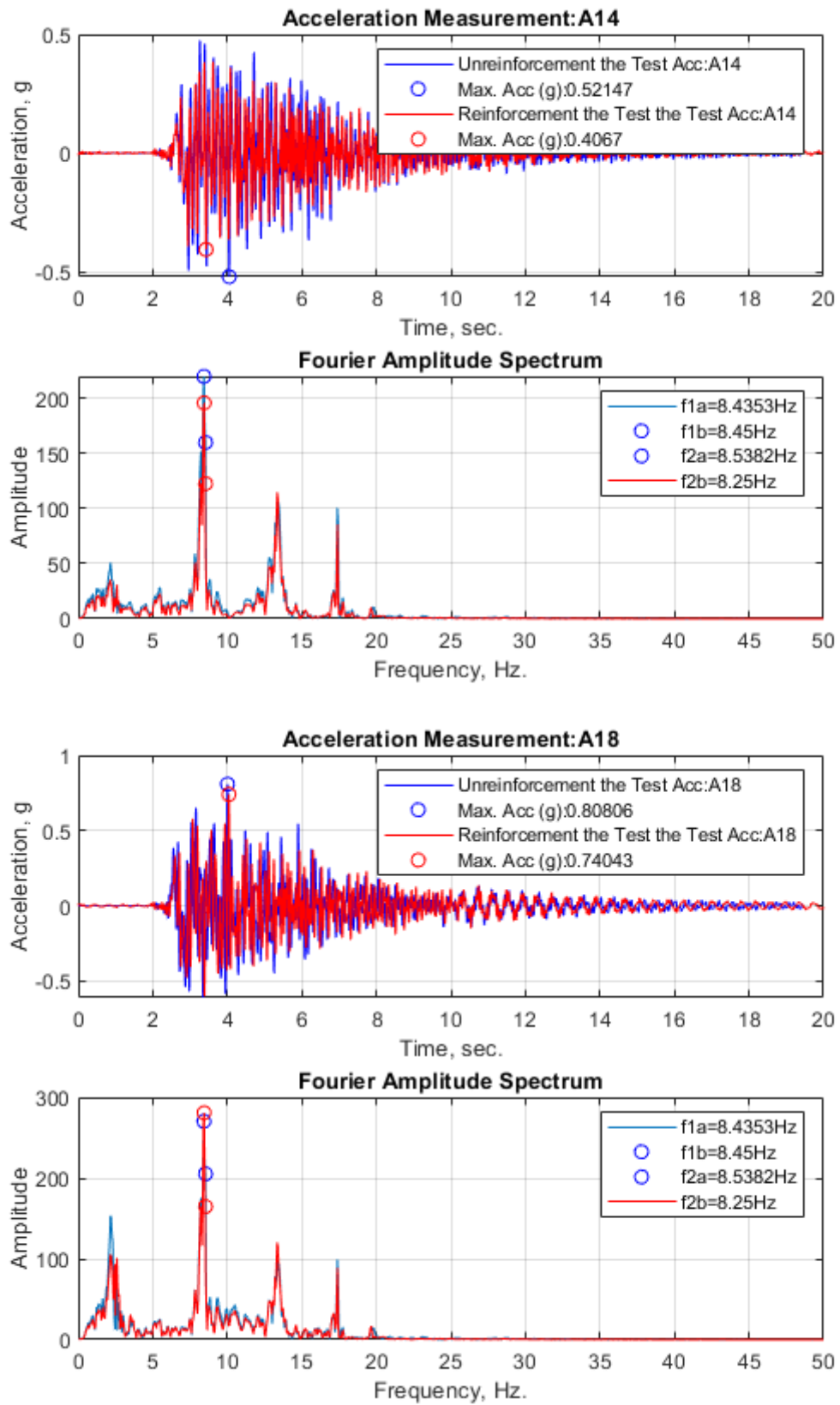


Figure 4.11. Acceleration Measurements and FAS of 1st and 5th Floors under Kocaeli Earthquake Motion (PGA= 0.21 g).

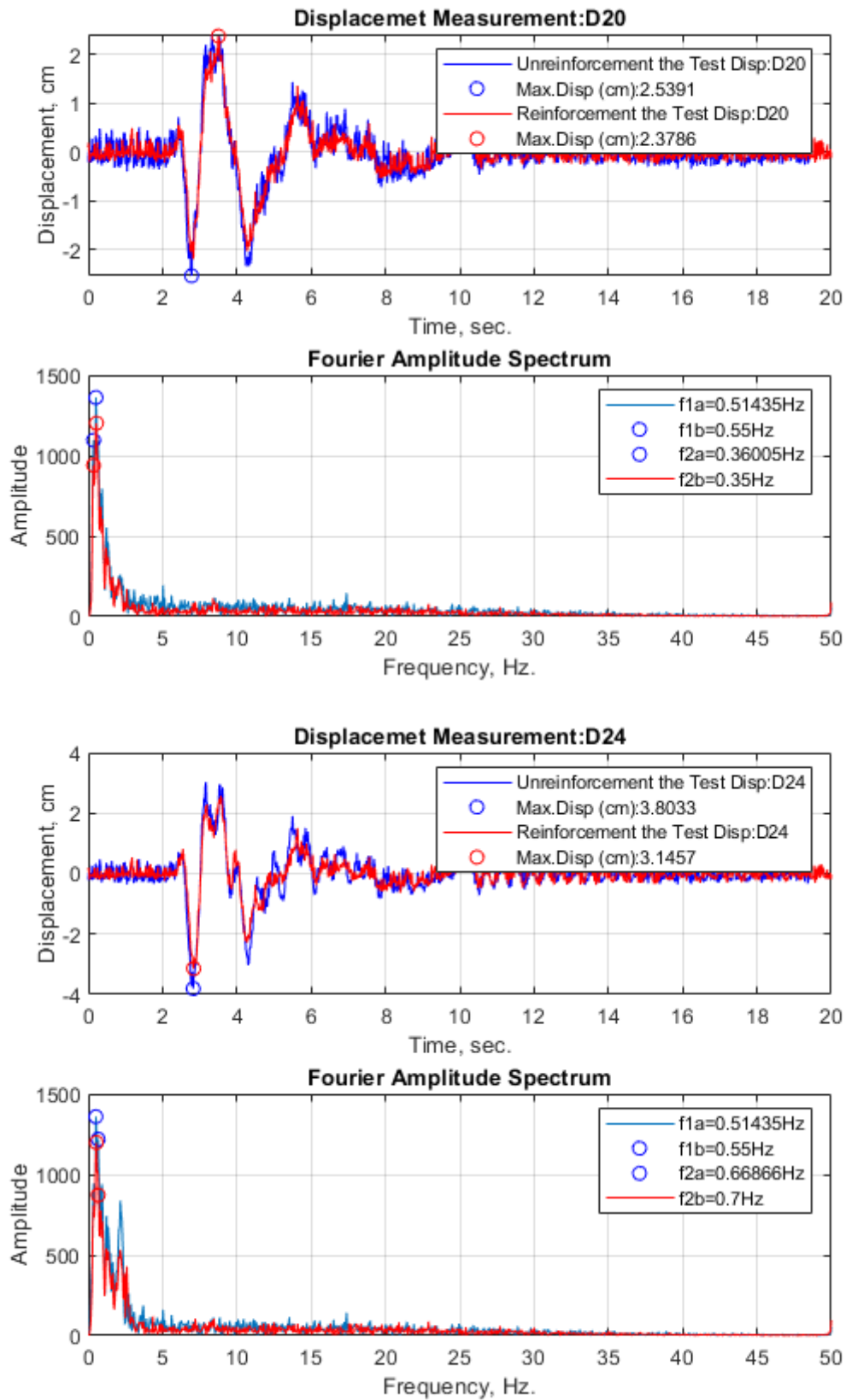


Figure 4.12. Displacement Measurements and FAS of 1st and 5th Floors under Kocaeli Earthquake Motion (PGA= 0.21 g).

According to Figure 4.13., which illustrates the comparisons of N=1, N=2, N=3 and N=4, the reduction of foundation, acceleration is 0%, 6%, 10% and 26% and top floor decrease is 2%, 2%, 3% and 8%. for N=1, N=2, N=3 and N=4 respectively, also there is no improvement for N=1 in foundation.

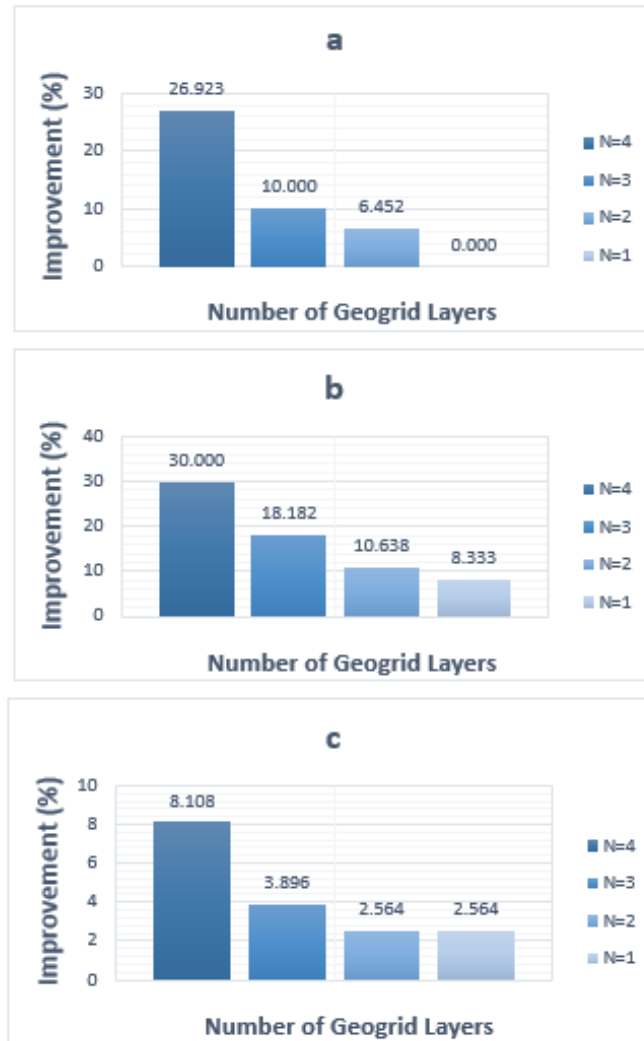


Figure 4.13. The Acceleration Improvement Graphs in Accordance with Story and Reinforcement Layers for (a) Foundation, (b) 1st Floor, (c) 5th Floor under Kocaeli Earthquake Motion (PGA= 0.21 g).

As it can be seen in Figure 4.14. for the first, and fifth floor, the maximum decrease of story's displacement is 6%, 13%, 21% respectively. The improvement of displacement of second and fourth floor for N=1 become negative because they are almost same value.

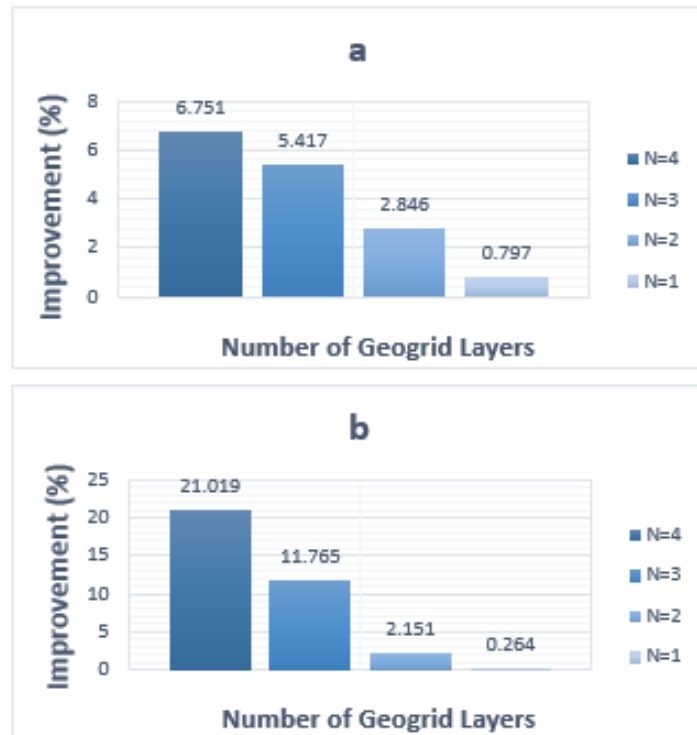


Figure 4.14. The Displacement Improvement Graphs in Accordance with Story and Reinforcement Layers for (a) 1st Floor, (b) 5th Floor under Kocaeli Earthquake Motion (PGA= 0.89 g).

In Table 5.6. and Table 5.7, arias intensity improvements were shown. Besides, with the help of the fundamental period of all N values under dynamic loads for soil, foundations, floors, by comparing fundamental periods, the period lengthening ratios were given, and also RMS of peak values were shown.

Table 4.9. Fundamental Period and Period Lengthening Ratios under Kobe Earthquake Motion (PGA = 0.89g).

	Fundamental Period (Hz)					Period Lengthening Ratio			
	N=4	N=3	N=2	N=1	N=0	N=4	N=3	N=2	N=1
In-Soil	4.57	4.65	4.65	4.68	4.57	1.00	0.98	0.98	0.98
Foundation	4.67	4.65	4.67	4.68	4.68	1.00	1.01	1.00	1.00
1st Floor	0.8	0.8	0.77	0.79	0.8	1.00	1.00	1.04	1.01
2nd Floor	0.8	0.8	0.77	0.79	0.8	1.00	1.00	1.04	1.01
3rd Floor	0.8	0.8	0.77	0.79	0.8	1.00	1.00	1.04	1.01
4th Floor	0.8	0.8	0.81	0.79	0.8	1.00	1.00	0.99	1.01
5th Floor	0.8	0.8	0.81	0.81	0.8	1.00	1.00	0.99	0.99

Table 4.10. RMS and Arias Intensity Improvement Ratios under Kobe Earthquake Motion (PGA = 0.89g).

Root Mean Square (RSM)				Arias Intensity	
Horizontal Acceleration(g)	Peak	RSM-Rein.	RSM Imp (%)		Arias Intensity Imp (%)
In-Soil	0.32	0.24	25	In-Soil	17.29
Foundation	0.33	0.3	9.6	Foundation	31.5
1st Floor	0.52	0.45	15.92	1st Floor	33.3
2nd Floor	0.65	0.62	5.07	2nd Floor	19.13
3rd Floor	0.55	0.5	9.31	3rd Floor	20.26
4th Floor	0.39	0.34	15.89	4th Floor	32.1
5th Floor	0.8	0.77	4.21	5th Floor	9.32

As it is shown in Table 4.9 and Table 4.10, arias intensity values are decreased almost 1%, 2% and 4% for soil, foundation and floors. The reduction of RMS is 25% for soil, 9% for foundation, 15%, 5%, 9%, 15%, and %4 for floors roughly. Also, there is no change the natural period of model. The period lengthening ratio fluctuates up to %4. In Figure 4.15, improvement ratios considering, Arias Intensity and Story Drifts are given.

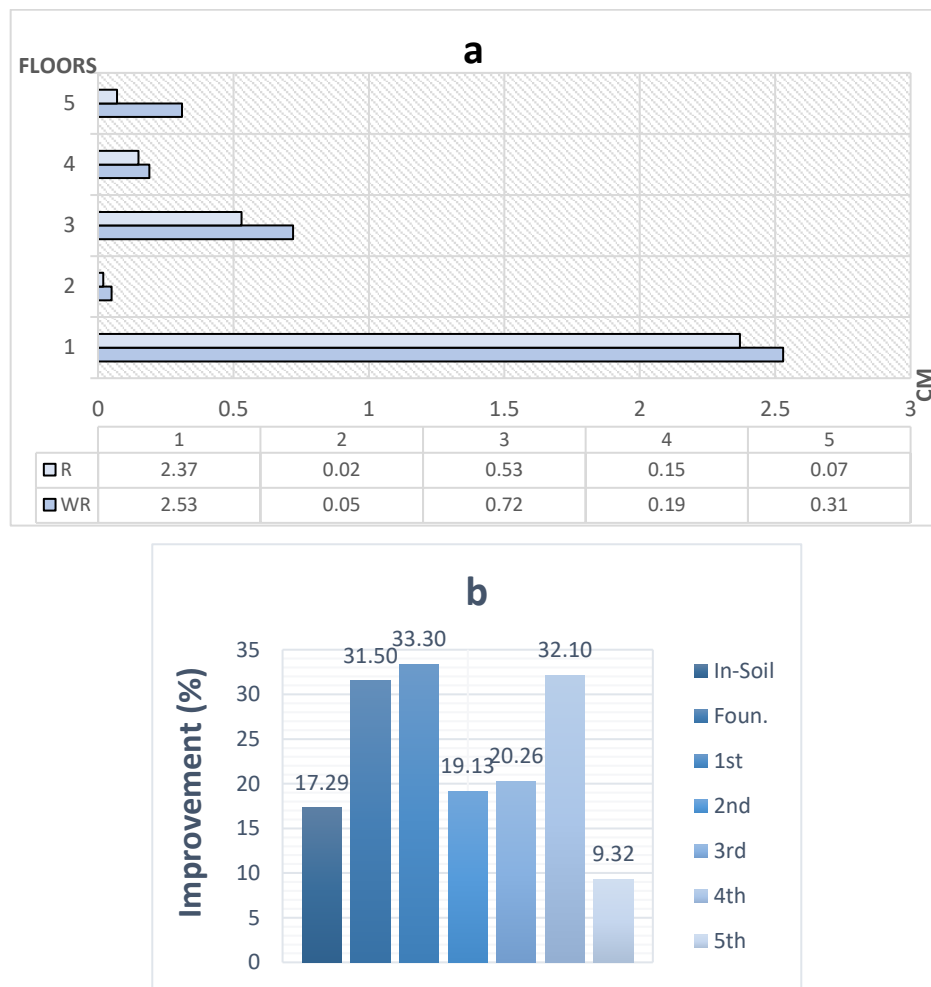


Figure 4.15. Improvement Ratios considering (a) Story Drifts and (b) Arias Intensity under Kocaeli Earthquake Motion (PGA= 0.21 g).

4.2.4. Seismic Response of 5-Story Model under Kocaeli Earthquake Motion (PGA= 0.51 g)

Table 4.11 shows the reduced acceleration and displacement values through all sensors comparing to unreinforced system for 5-Storey model under Kocaeli Earthquake (0.51g). In the soil, peak accelerations are 0.45g in the underside, 0.49g midpoint, and 0.52g in the upper side. The reduction of acceleration in underside is 2%, 4%, 18% and 25%, the reduction of acceleration in midpoint is 6%, 13%, 28% and 36%, the reduction of acceleration in upper side is 1%, 15%, 26% and 30% roughly for N=1, N=2, N=3 and N=4, respectively. The maximum acceleration improvement in the soil is 38%. It is significant value for soil.

Table 4.11. Summary of all tested Cases under Kocaeli Earthquake motion (PGA=0.51g)

		N=4			N=3			N=2			N=1		
		WR	R	IMP. (%)	WR	R	IMP. (%)	WR	R	IMP. (%)	WR	R	IMP. (%)
In Soil (g)	A5	0.45	0.36	25.000	0.45	0.38	18.421	0.45	0.43	4.651	0.45	0.44	2.273
	A6	0.47	0.36	30.556	0.47	0.39	20.513	0.47	0.45	4.444	0.47	0.47	0
	A7	0.44	0.37	18.919	0.44	0.39	12.821	0.44	0.45	-2.222	0.44	0.46	-4.348
	A8	0.45	0.33	36.364	0.45	0.4	12.500	0.45	0.45	0	0.45	0.46	-2.174
	A9	0.47	0.39	20.513	0.47	0.4	17.500	0.47	0.46	2.174	0.47	0.48	-2.083
	A10	0.47	0.34	38.235	0.47	0.39	20.513	0.47	0.44	6.818	0.47	0.47	0
	A11	0.49	0.36	36.111	0.49	0.38	28.947	0.49	0.43	13.953	0.49	0.46	6.522
	A12	0.52	0.4	30.000	0.52	0.41	26.829	0.52	0.45	15.556	0.52	0.51	1.961
Foun.(g)	A13	0.6	0.43	39.535	0.6	0.49	22.449	0.6	0.54	11.111	0.6	0.58	3.448
5 Storey Model (cm)	A14	1.08	0.78	42.105	1.08	0.78	38.462	1.08	0.89	21.348	1.08	0.97	11.340
	A15	1.35	1.04	29.808	1.35	1.06	27.358	1.35	1.17	15.385	1.35	1.21	11.570
	A16	0.98	0.74	32.432	0.98	0.76	28.947	0.98	0.91	7.692	0.98	0.94	4.255
	A17	0.61	0.51	19.608	0.61	0.52	17.308	0.61	0.57	7.018	0.61	0.59	3.390
	A18	1.45	1.27	14.173	1.45	1.29	12.403	1.45	1.36	6.618	1.45	1.46	-0.685
	D20	5.14	4.21	22.090	5.14	4.76	7.983	5.14	5.01	2.595	5.14	5.12	0.391
	D21	5.74	4.73	21.353	5.74	5.22	9.962	5.74	5.5	4.364	5.74	5.69	0.879
	D22	8.05	6.7	20.149	8.05	7.08	13.701	8.05	7.45	8.054	8.05	7.85	2.548
	D23	9.98	8.28	20.531	9.98	8.38	19.093	9.98	8.82	13.152	9.98	9.03	10.520
	D24	11.78	9.88	19.231	11.78	9.93	18.630	11.78	10.45	12.727	11.78	10.9	8.073

The sensors showing acceleration, displacement measurement and fourier amplitude spectrum in Figure 4.16 And 4.17 were selected between unreinforced system and N=4 and through these figures the maximum improvement can be seen at these points.

The decrease of foundation acceleration is 3%, 11%, 22% and 39% for N=1, N=2, N=3 and N=4, respectively.

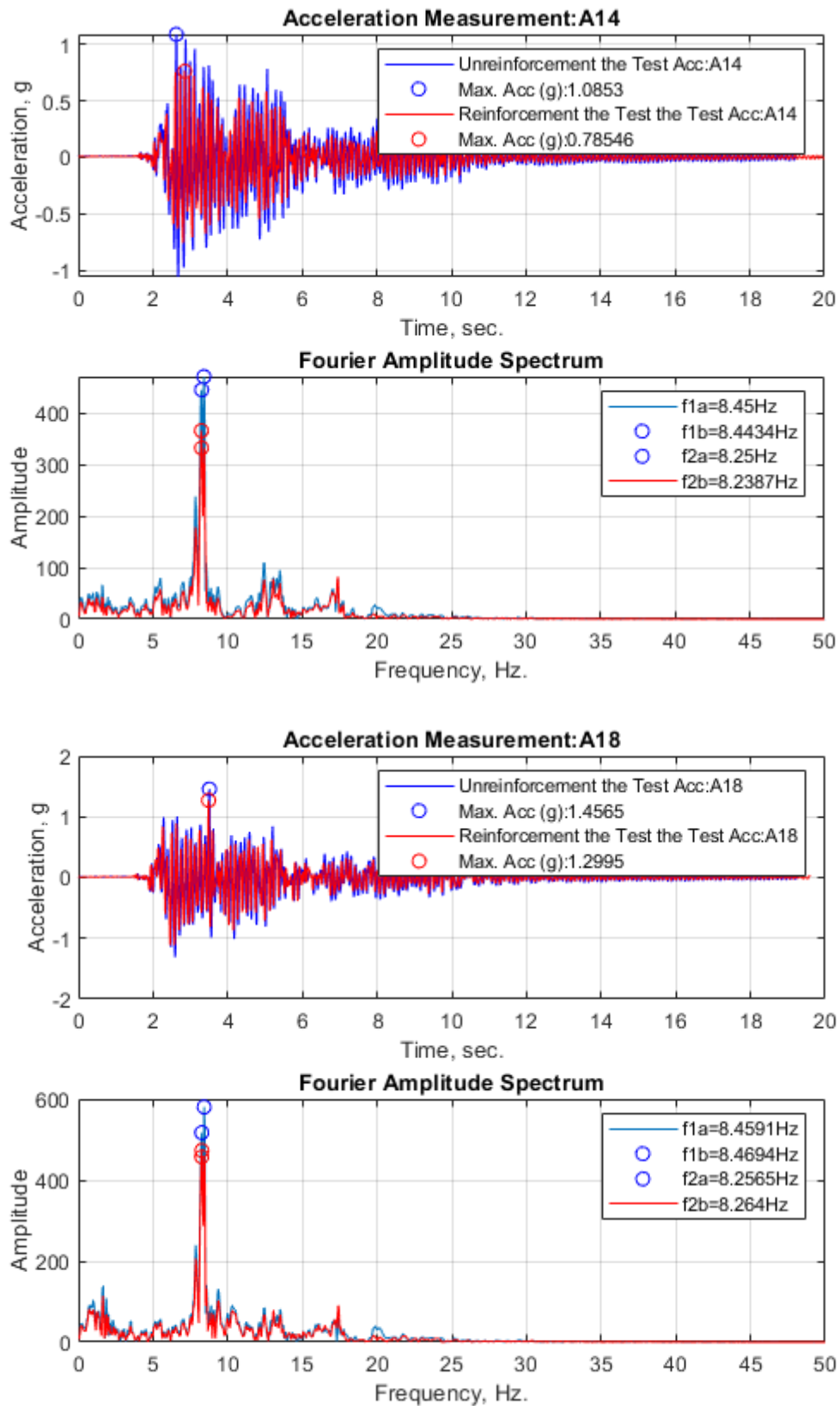


Figure 4.16. Acceleration Measurements and FAS of 1st and 5th Floors under Kocaeli Earthquake Motion (PGA= 0.51 g).

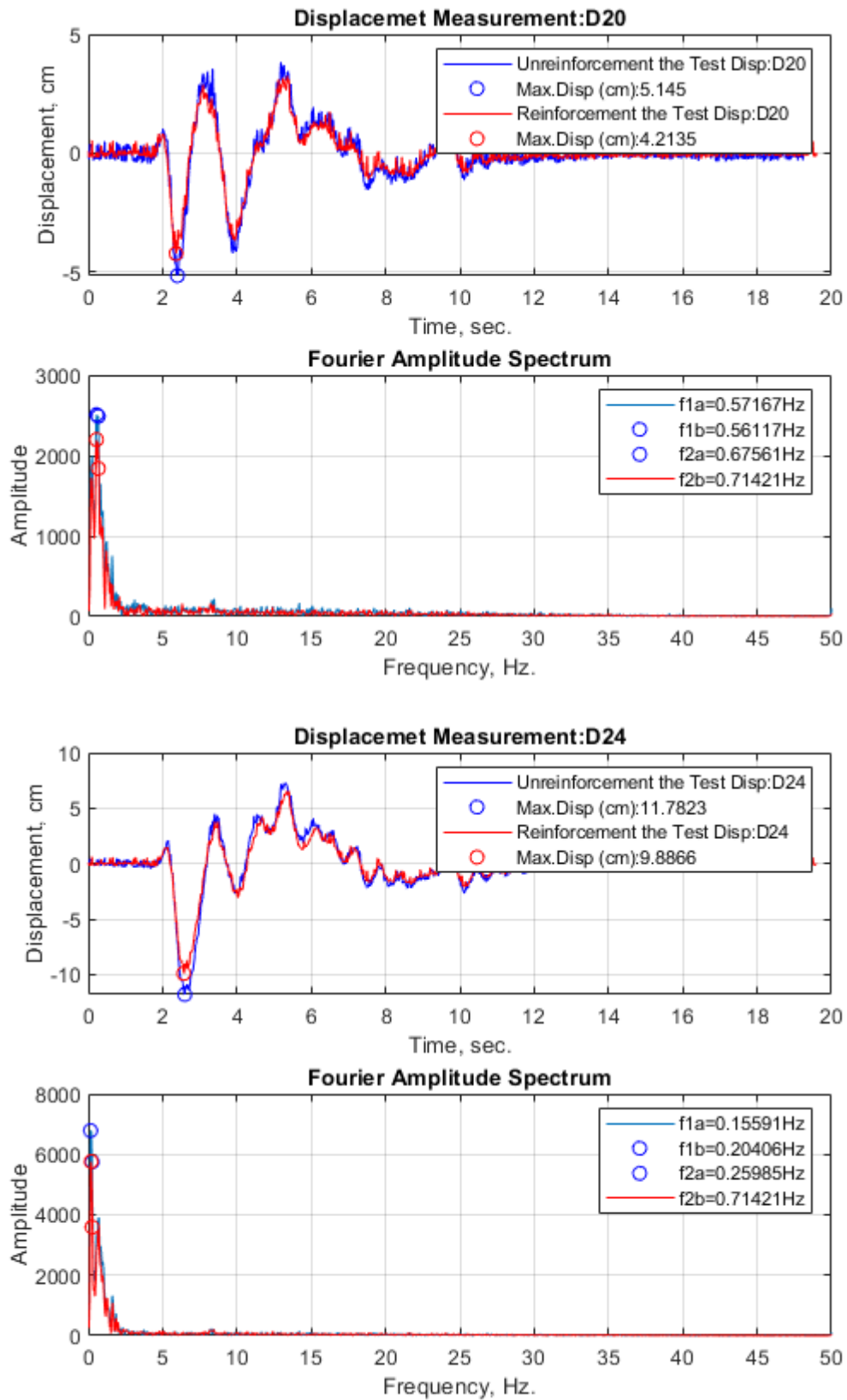


Figure 4.17. Displacement Measurements and FAS of 1st and 5th Floors under Kocaeli Earthquake Motion (PGA= 0.51 g).

The effect of one layer geogrid reinforcement is remarkably high on model for Kocaeli Earthquake. The improvements in acceleration start with nearly 11%. With the increase in the geogrid layer, it becomes 21%, 38%, 42% for the first floor and 15%, 27%, 29% for N=2, N=3, N=4 respectively. For the third floor and the fifth floor, the acceleration reduction values are reduced approximately 14% and 32% comparing to unreinforced system. The changing acceleration values and the changing displacement values in accordance with story and reinforcement layers were given in Figure 4.18. and Figure 4.19. Through the graphs the improvements compared unreinforced system can be seen easily for foundation, first and fifth story for each N values.

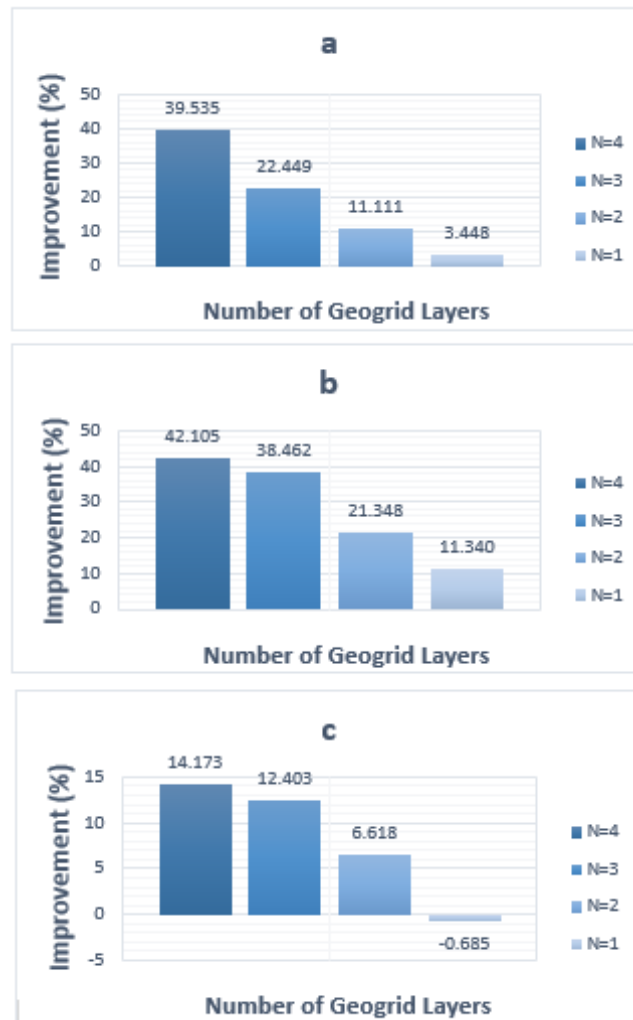


Figure 4.18. The Acceleration Improvement Graphs in Accordance with Story and Reinforcement Layers for (a) Foundation, (b) 1st Floor, (c) 5th Floor under Kocaeli Earthquake Motion (PGA= 0.51 g).

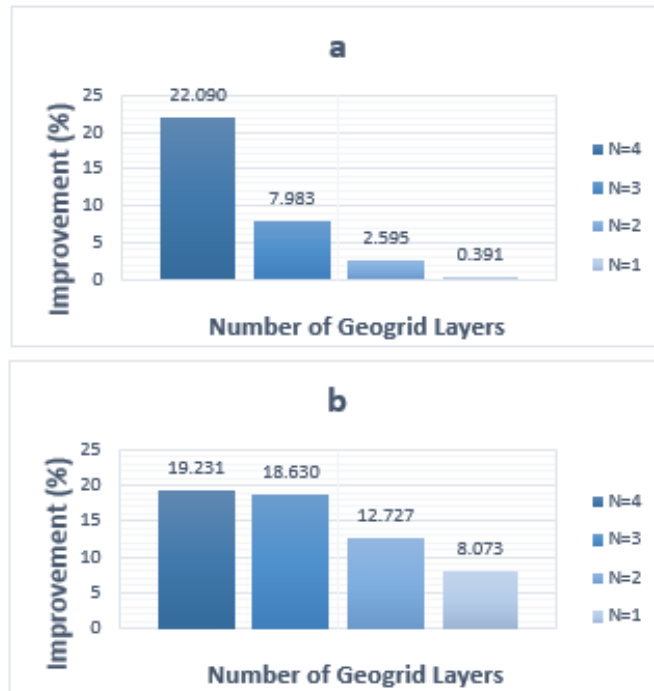


Figure 4.19. The Displacement Improvement Graphs in Accordance with Story and Reinforcement Layers for (a) 1st Floor, (b) 5th Floor under Kocaeli Earthquake Motion (PGA= 0.51 g).

In the first, third and fifth floor, the maximum decrease of story's displacement is 22%, 20%, 19%, respectively. There is no considerable reduction, it is just 1% but for N=3 it reaches up to 7%.

In Table 4.12 and Table 4.13, arias intensity improvements were illustrated also with the help of the fundamental period of all N values, the period lengthening ratios were given, and also RMS of peak values were exhibited.

Table 4.12. Fundamental Period and Period Lengthening Ratios under Kocaeli Earthquake Motion (PGA= 0.51 g).

	Fundamental Period (Hz)					Period Lengthening Ratio			
	N=4	N=3	N=2	N=1	N=0	N=4	N=3	N=2	N=1
In-Soil	10.5	10.5	10.5	10.5	10.49	1.00	1.00	1.00	1.00
Foundation	10.49	10.49	10.5	10.5	10.5	1.00	1.00	1.00	1.00
1st Floor	0.56	0.56	0.56	0.56	0.57	1.02	1.02	1.02	1.02
2nd Floor	0.2	0.2	0.2	0.2	0.2	1.00	1.00	1.00	1.00
3rd Floor	0.2	0.2	0.2	0.2	0.2	1.00	1.00	1.00	1.00
4th Floor	0.2	0.2	0.2	0.2	0.18	0.9	0.9	0.9	0.9
5th Floor	0.25	0.2	0.2	0.2	0.2	0.8	1.00	1.00	1.00

Table 4.13. RMS and Arias Intensity Improvement Ratios under Kocaeli Earthquake Motion (PGA= 0.51 g).

Root Mean Square (RSM)				Arias Intensity	
Horizontal Acceleration(g)	Peak	RSM-Rein.	RSM Imp (%)		Arias Intensity Imp (%)
In-Soil	0.52	0.4	28.75	In-Soil	36.3
Foundation	0.6	0.51	16.94	Foundation	46.26
1st Floor	1.08	0.85	26.43	1st Floor	46.74
2nd Floor	1.35	1.12	20.29	2nd Floor	35.47
3rd Floor	0.98	0.84	16.37	3rd Floor	38.59
4th Floor	0.61	0.55	11.21	4th Floor	20.98
5th Floor	1.45	1.35	7.64	5th Floor	16.3

Arias intensity values for soil region and foundation are nearly 3% and it reduce up to 7% for floors. RMS improvement values for soil, foundation and floors are 28%, 16%, 26% 20%, 7%, 11% and 16%, respectively. Also, there is no change in the natural period of model. The period lengthening ratio fluctuates up to %2. In Figure 4.20, improvement ratios considering, Arias Intensity and Story Drifts can be observed.

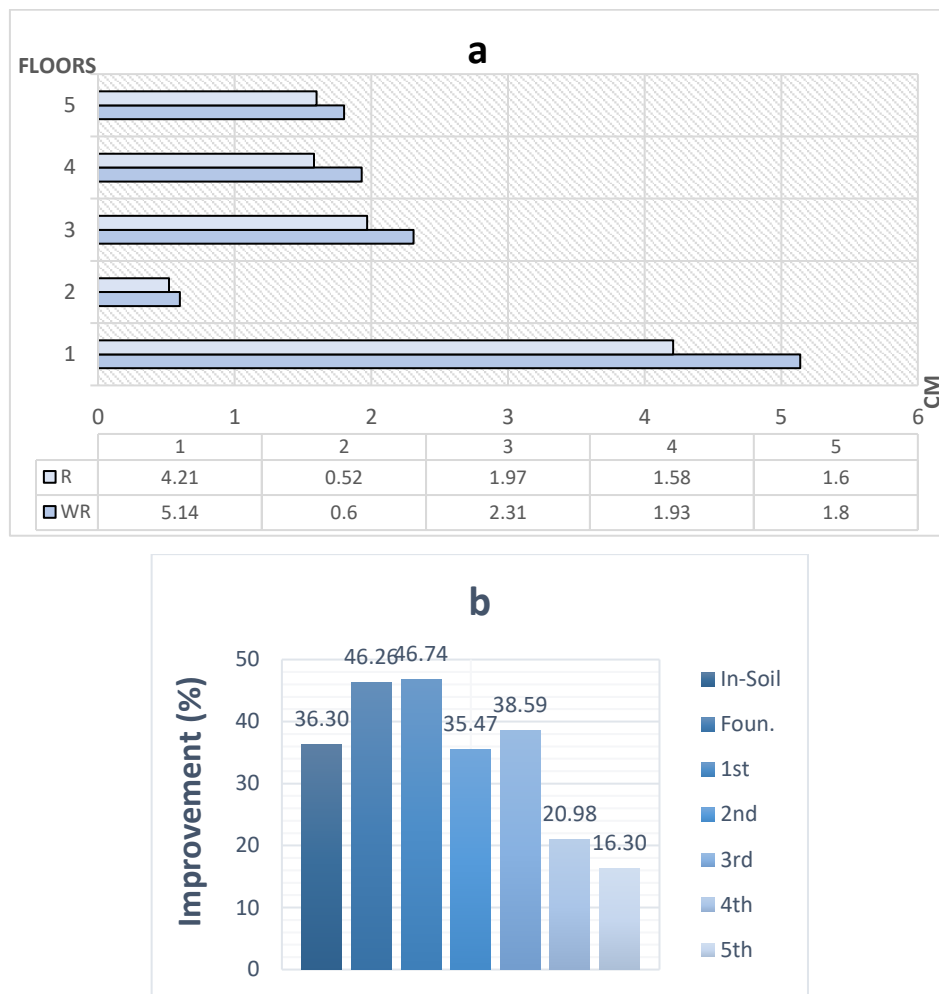


Figure 4.20. Improvement Ratios considering (a) Story Drifts and (b) Arias Intensity under Kocaeli Earthquake Motion (PGA= 0.51 g).

4.2.5. Seismic Response of 5-Story Model under El Centro Earthquake Motion (PGA =0.35 g)

Table 4.14 shows the reduced acceleration and displacement values through all sensors comparing to unreinforced system for 5-Storey model under El Centro Earthquake (0.35g). In the soil, peak accelerations are 0.34g in the underside and 0.45g in the midpoint, and upper side. The maximum improvement of acceleration in the underside, midpoint upper side is 21%, 21% and 15%, respectively. Also, in the soil for N=1 almost there is no reduction in accelerations. In lots of point, the improvement in acceleration is 0% or negative.

The sensors showing acceleration, displacement measurement and fourier amplitude spectrum in Figure 4.21 and 4.22 were selected between unreinforced system and N=4 For the first and top floor, the maximum improvements are 20% and 30% in acceleration respectively. The reduction of foundation acceleration is roughly 4%, 9%, 17% and 20% for N=1, N=2, N=3 and N=4, respectively.

Table 4.14. Summary of all tested Cases under El Centro Earthquake motion (PGA=0.35g).

		N=4			N=3			N=2			N=1		
		WR	R	IMP. (%)	WR	R	IMP. (%)	WR	R	IMP. (%)	WR	R	IMP. (%)
In Soil (g)	A5	0.34	0.28	21.429	0.34	0.29	17.241	0.34	0.31	9.677	0.34	0.32	6.250
	A6	0.36	0.28	28.571	0.36	0.31	16.129	0.36	0.33	9.091	0.36	0.34	5.882
	A7	0.36	0.29	24.138	0.36	0.31	16.129	0.36	0.34	5.882	0.36	0.35	2.857
	A8	0.34	0.25	36.000	0.34	0.31	9.677	0.34	0.34	0	0.34	0.34	0
	A9	0.36	0.31	16.129	0.36	0.32	12.500	0.36	0.34	5.882	0.36	0.37	-2.703
	A10	0.36	0.31	16.129	0.36	0.32	12.500	0.36	0.34	5.882	0.36	0.36	0
	A11	0.45	0.37	21.622	0.45	0.38	18.421	0.45	0.43	4.651	0.45	0.45	0
	A12	0.45	0.39	15.385	0.45	0.39	15.385	0.45	0.43	4.651	0.45	0.45	0
Foun.(g)	A13	0.48	0.4	20.000	0.48	0.41	17.073	0.48	0.44	9.091	0.48	0.46	4.348
5 Storey Model (cm)	A14	0.89	0.74	20.270	0.89	0.79	12.658	0.89	0.8	11.250	0.89	0.85	4.706
	A15	0.97	0.85	14.118	0.97	0.9	7.778	0.97	0.93	4.301	0.97	0.96	1.042
	A16	0.62	0.54	14.815	0.62	0.6	3.333	0.62	0.61	1.639	0.62	0.64	-3.125
	A17	0.56	0.44	27.273	0.56	0.44	27.273	0.56	0.5	12.000	0.56	0.55	1.818
	A18	1.25	0.96	30.208	1.25	1.01	23.762	1.25	1.13	10.619	1.25	1.2	4.167
	D20	2.91	2.32	25.431	2.91	2.51	15.936	2.91	2.6	11.923	2.91	2.89	0.692
	D21	2.86	2.38	20.168	2.86	2.6	10.000	2.86	2.65	7.925	2.86	2.81	1.779
	D22	3.29	2.65	24.151	3.29	2.98	10.403	3.29	3.09	6.472	3.29	3.12	5.449
	D23	3.7	2.92	26.712	3.7	3.02	22.517	3.7	3.44	7.558	3.7	3.46	6.936
	D24	3.78	3.01	25.581	3.78	3.19	18.495	3.78	3.62	4.420	3.78	3.66	3.279

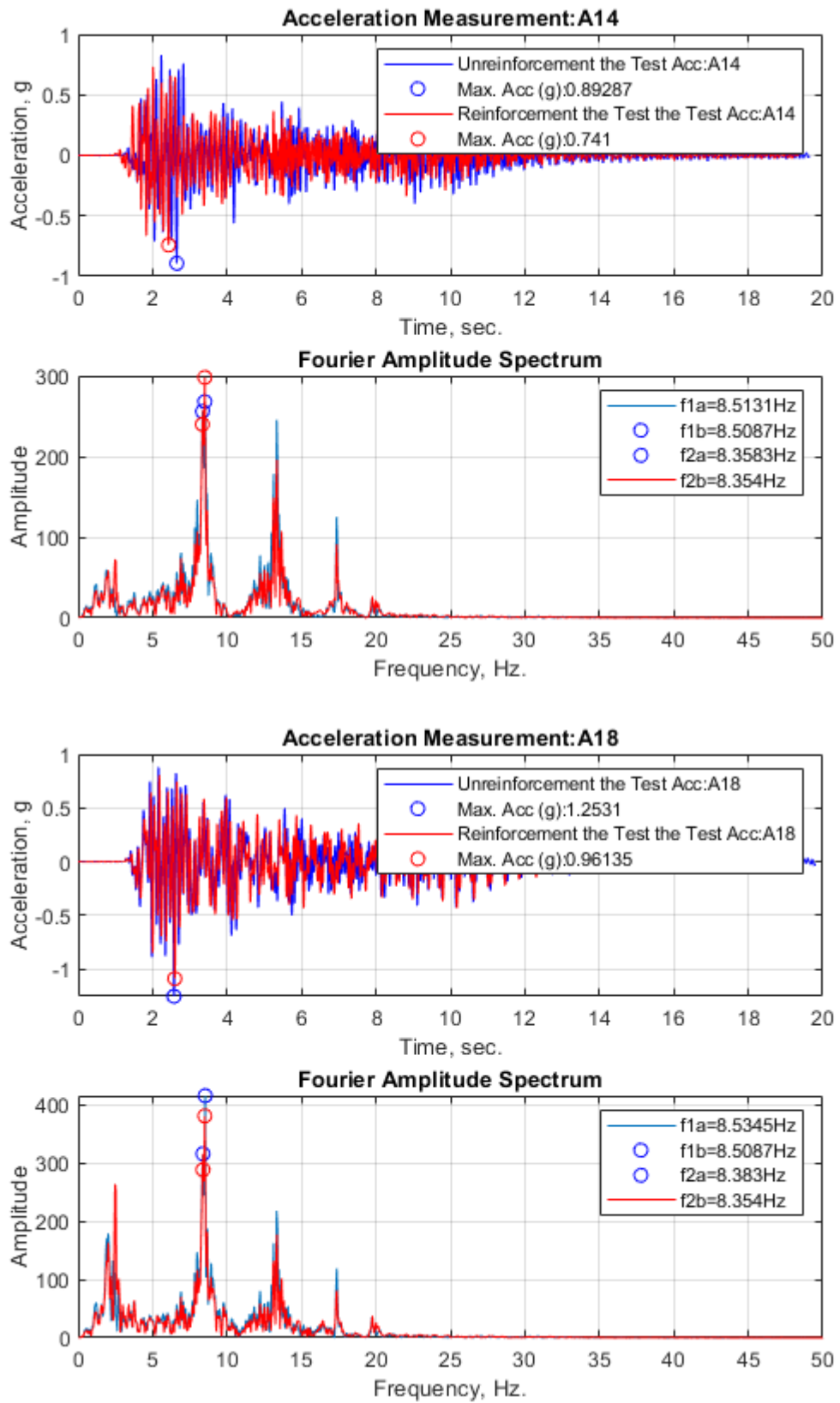


Figure 4.21. Acceleration Measurements and FAS of 1st and 5th Floors under El Centro Earthquake Motion (PGA= 0.35 g).

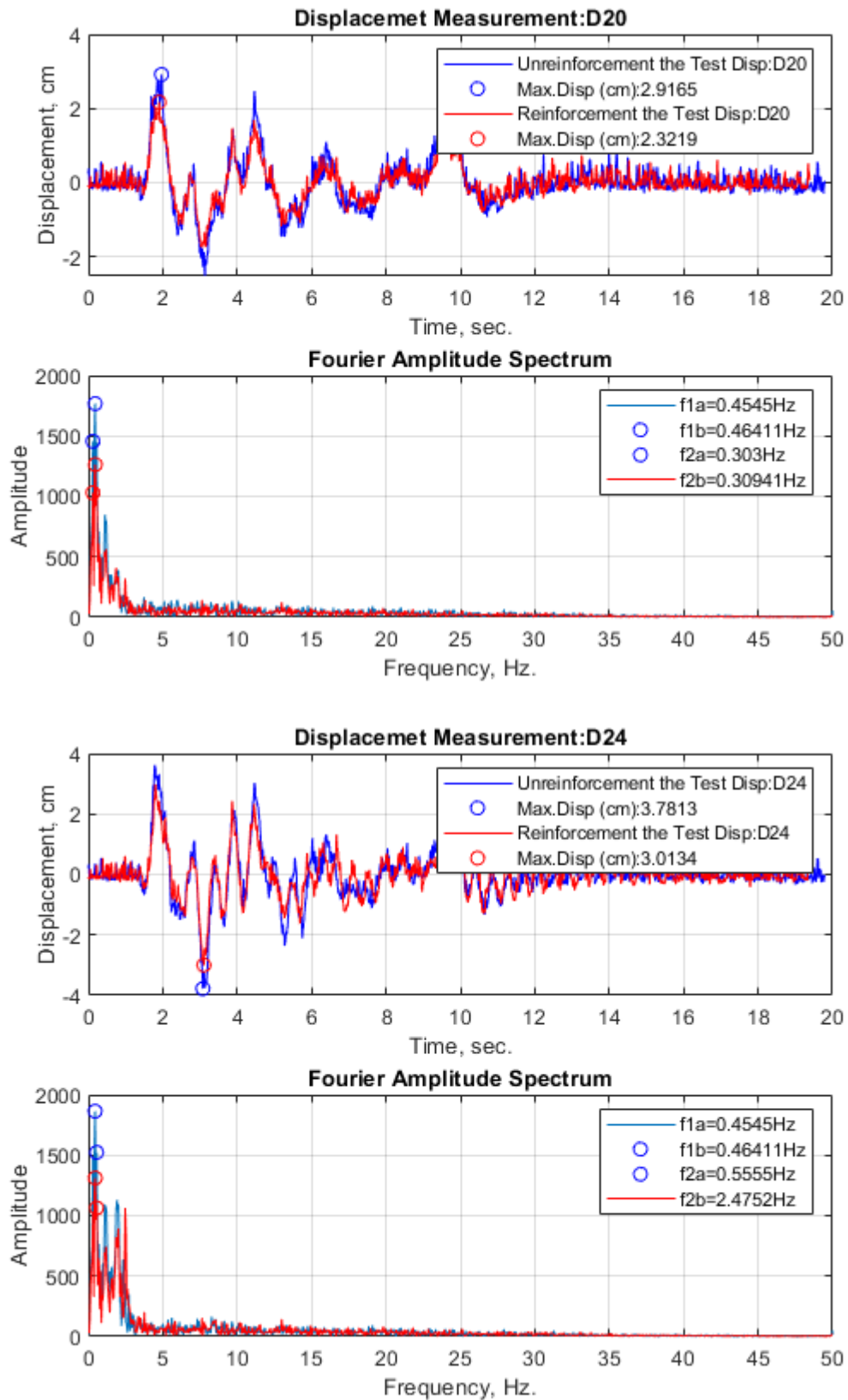


Figure 4.22. Displacement Measurements and FAS of 1st and 5th Floors under El Centro Earthquake Motion (PGA= 0.35 g).

For the third floor, for N=1 the improvement in acceleration value become negative. Besides, this floor's improvement is not remarkable value for N=2 and N=3. They are %1 and %3 nor N=2 and N=3. Acceleration reductions ascend at floor to 20%, 14%, 14%, 27% and 30% in peak comparing to unreinforced system. The changing acceleration values and the changing displacement values in accordance with story and reinforcement layers can be seen in Figure 4.23. and Figure 4.24.

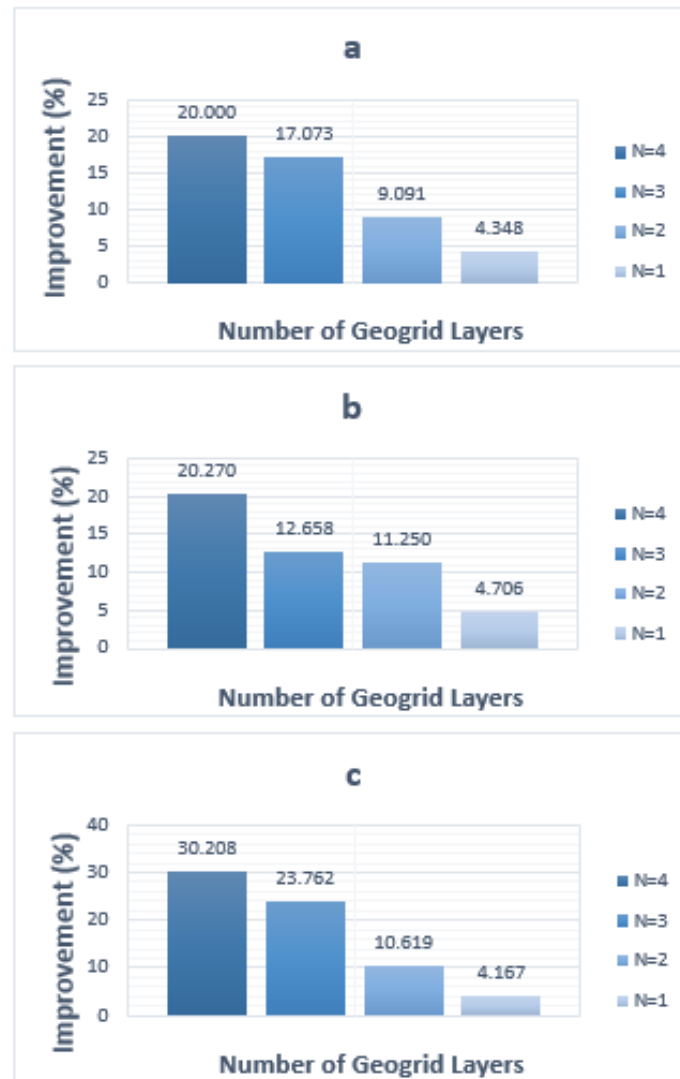


Figure 4.23. The Acceleration Improvement Graphs in Accordance with Story and Reinforcement Layers for (a) Foundation, (b) 1st Floor, (c) 5th Floor under El Centro Earthquake Motion (PGA= 0.35 g).

For the first, and fifth floor, the maximum decrease of story's displacement values is 25% and 25% respectively. For the fourth and third floors, in N=1 the improvements can be regard as significant value, which is nearly 6%.

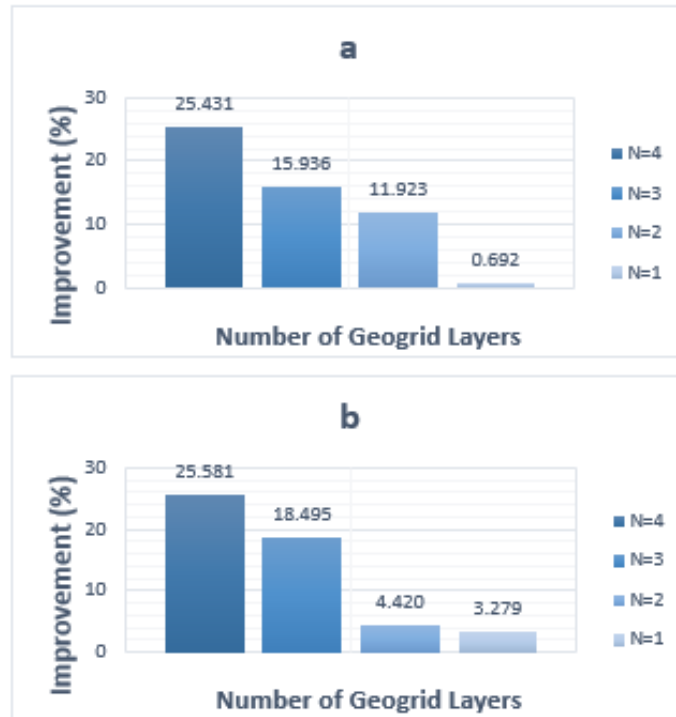


Figure 4.24. The Displacement Improvement Graphs in Accordance with Story and Reinforcement Layers for (a) 1st Floor, (b) 5th Floor under El Centro Earthquake Motion (PGA= 0.35 g).

Table 4.15. Fundamental Period and Period Lengthening Ratios under El Centro Earthquake Motion (PGA= 0.35 g).

	Fundamental Period (Hz)					Period Lengthening Ratio			
	N=4	N=3	N=2	N=1	N=0	N=4	N=3	N=2	N=1
In-Soil	6.91	6.91	6.91	6.91	6.91	1.00	1.00	1.00	1.00
Foundation	6.91	6.91	6.91	6.91	6.91	1.00	1.00	1.00	1.00
1st Floor	0.46	0.46	0.46	0.46	0.45	0.98	0.98	0.98	0.98
2nd Floor	0.45	0.46	0.45	0.45	0.45	1.00	0.98	1.00	1.00
3rd Floor	0.45	0.46	0.45	0.45	0.45	1.00	0.98	1.00	1.00
4th Floor	0.45	0.45	0.45	0.45	0.45	1.00	1.00	1.00	1.00
5th Floor	0.46	0.46	0.45	0.45	0.45	0.98	0.98	1.00	1.00

Table 4.16. RMS and Arias Intensity Improvement Ratios under Kocaeli Earthquake Motion (PGA= 0.51 g).

Root Mean Square (RSM)				Arias Intensity	
Horizontal Acceleration(g)	Peak	RSM-Rein.	RSM Imp (%)		Arias Intensity Imp (%)
In-Soil	0.45	0.3	49.79	In-Soil	18.62
Foundation	0.48	0.43	12.11	Foundation	23.4
1st Floor	0.89	0.8	11.81	1st Floor	22.5
2nd Floor	0.97	0.91	6.49	2nd Floor	16.8
3rd Floor	0.62	0.6	3.57	3rd Floor	17.63
4th Floor	0.56	0.48	15.54	4th Floor	29.18
5th Floor	1.25	1.08	15.83	5th Floor	34.74

As can be seen in Table 4.15 and Table 4.16, arias intensity values are approximately reduced up to 1%, 2% and 6% for soil region, foundation, and floors in order of. Reduction of RMS ascend at soil and foundation to 49%, 12% and at floors to 11%, 6%, 3%, 15% and 15% respectively. There is no change the natural period of model. The period lengthening ratio fluctuates up to %2. Also Figure 4.25. shows improvement ratios of Arias Intensity and Story Drifts.

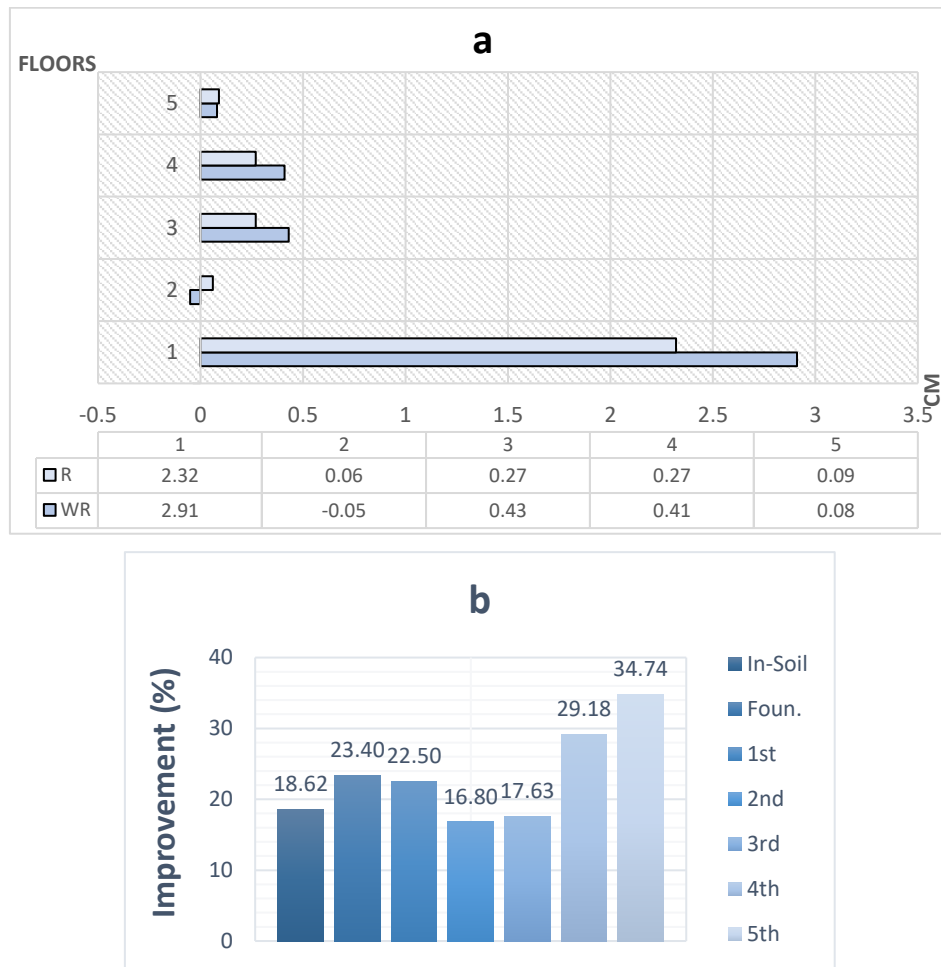


Figure 4.25. Improvement Ratios considering (a) Story Drifts and (b) Arias Intensity under El Centro Earthquake Motion (PGA= 0.35 g).

4.2.6. Seismic Response of 5-Story Model under El Centro Earthquake Motion (PGA =0.55 g)

Table 4.17 shows the reduced acceleration and displacement values through all sensors comparing to unreinforced system for 5-Storey model under El Centro Earthquake-0.55g. In the soil, peak accelerations are 0.57g in the underside, 0.55g in the midpoint, and 0.5g in the upper side. The maximum improvement of acceleration in the underside, midpoint and upper side is %29, %34 and %16, respectively.

Table 4.17. Summary of all tested Cases under El Centro Earthquake motion
(PGA=0.55g).

		N=4			N=3			N=2			N=1		
		WR	R	IMP. (%)	WR	R	IMP. (%)	WR	R	IMP. (%)	WR	R	IMP. (%)
In Soil	A5	0.57	0.44	29.545	0.57	0.46	23.913	0.57	0.5	14.000	0.57	0.54	5.556
	A6	0.55	0.41	34.146	0.55	0.44	25.000	0.55	0.5	10.000	0.55	0.54	1.852
	A7	0.53	0.4	32.500	0.53	0.43	23.256	0.53	0.49	8.163	0.53	0.52	1.923
	A8	0.53	0.43	23.256	0.53	0.48	10.417	0.53	0.52	1.923	0.53	0.53	0
	A9	0.54	0.41	31.707	0.54	0.43	25.581	0.54	0.5	8.000	0.54	0.53	1.887
	A10	0.5	0.43	16.279	0.5	0.45	11.111	0.5	0.49	2.041	0.5	0.5	0
	A11	0.51	0.45	13.333	0.51	0.46	10.870	0.51	0.49	4.082	0.51	0.5	2.000
	A12	0.5	0.43	16.279	0.5	0.47	6.383	0.5	0.49	2.041	0.5	0.5	0
Foun.(g)	A13	0.5	0.45	11.111	0.5	0.46	8.696	0.5	0.47	6.383	0.5	0.51	-1.961
5 Storey Model	A14	1.1	1	10.000	1.1	1.01	8.911	1.1	1.02	7.843	1.1	1.05	4.762
	A15	1.17	1.08	8.333	1.17	1.11	5.405	1.17	1.12	4.464	1.17	1.15	1.739
	A16	0.79	0.66	19.697	0.79	0.7	12.857	0.79	0.75	5.333	0.79	0.77	2.597
	A17	0.73	0.61	19.672	0.73	0.67	8.955	0.73	0.71	2.817	0.73	0.73	0
	A18	1.37	1.12	22.321	1.37	1.18	16.102	1.37	1.24	10.484	1.37	1.34	2.239
	D20	4.77	3.84	24.219	4.77	3.97	20.151	4.77	4.17	14.388	4.77	4.25	12.235
	D21	4.72	3.92	20.408	4.72	4.02	17.413	4.72	4.3	9.767	4.72	4.38	7.763
	D22	5.47	4.5	21.556	5.47	4.62	18.398	5.47	5.07	7.890	5.47	5.17	5.803
	D23	5.54	4.77	16.143	5.54	5.09	8.841	5.54	5.43	2.026	5.54	5.5	0.727
	D24	5.69	4.89	16.360	5.69	5.35	6.355	5.69	5.61	1.426	5.69	5.67	0.353

Figures 4.26 and 4.27 represent displacement and acceleration measurements and fourier amplitude spectrum of 1st and 5th Floors. Although the first floor is decreased up to 10% in acceleration value, the maximum reduction of fifth floor is %22. The third floor' improvement is %19. Besides, for N=1, the fourth floor's improvement become 0% and for N=4 it reaches up to %20. The foundation acceleration improvements are -1%, 6%, 8% and 11% for N=1, 2, 3, and 4, respectively.

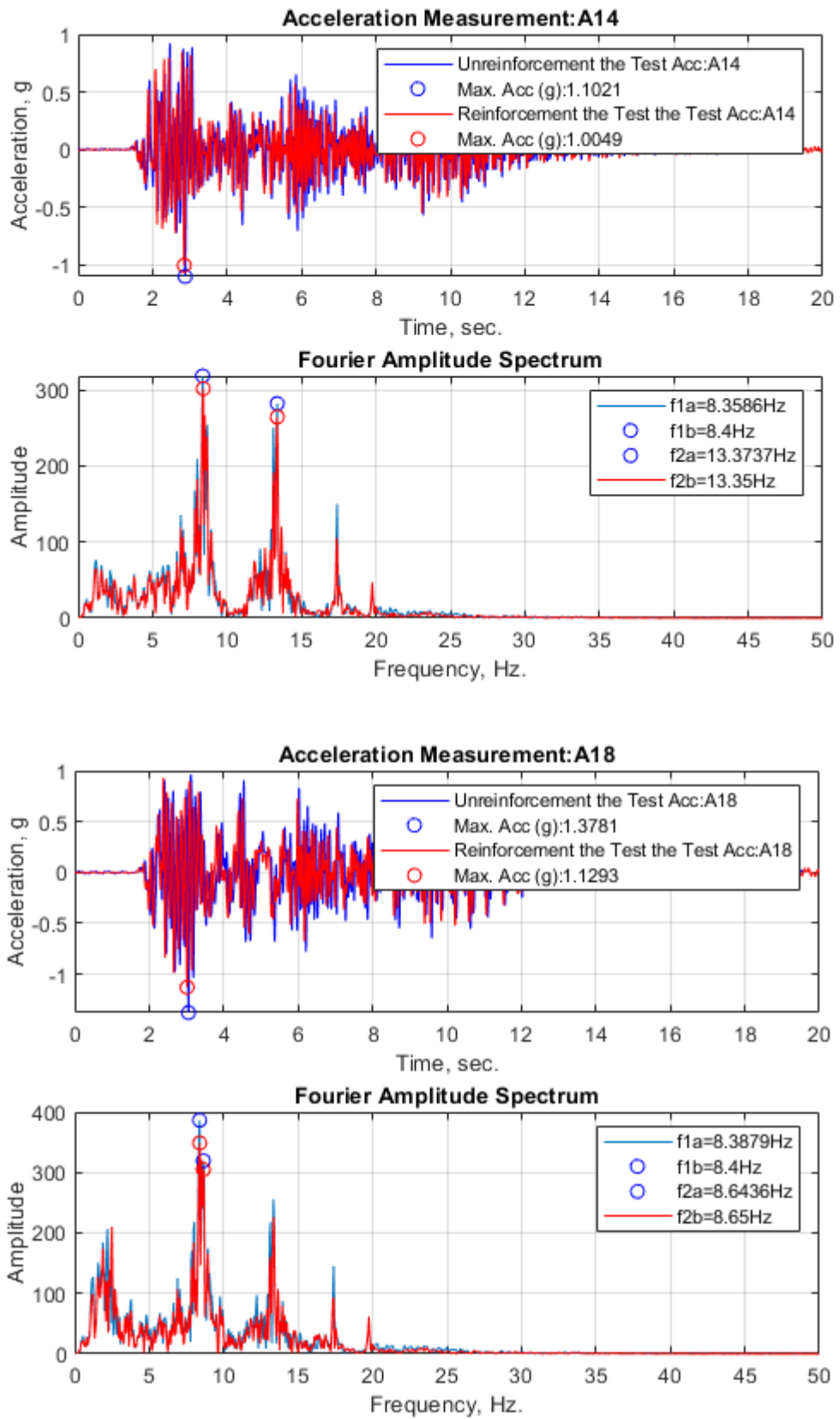


Figure 4.26. Acceleration Measurements and FAS of 1st and 5th Floors under El Centro Earthquake Motion (PGA= 0.55 g).

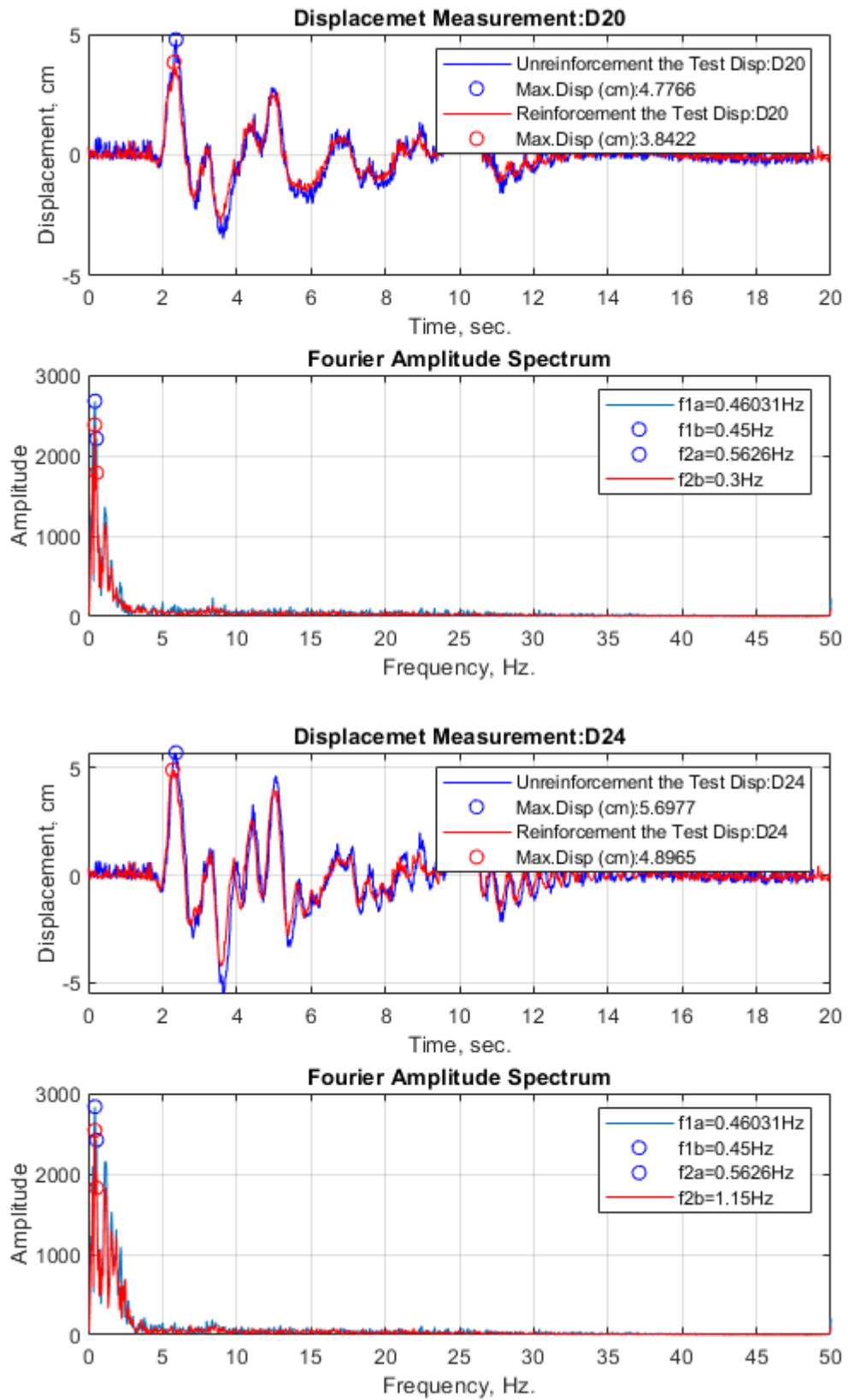


Figure 4.27. Displacement Measurements and FAS of 1st and 5th Floors under El Centro Earthquake Motion (PGA= 0.55 g).

The changing acceleration values and the changing displacement values in accordance with story and reinforcement layers were given in Figure 4.28. and Figure 4.29. With the help of graphs, the improvements compared unreinforced system can be observed for foundation, first and fifth story for each N values. The first floor is decreased up to 10% in acceleration value, the maximum reduction of fifth floor is 22%. The third floor's improvement is 19%. While for N=1, the third floor's improvement become 0%, other floors have slightly improvement in acceleration values for N=1.

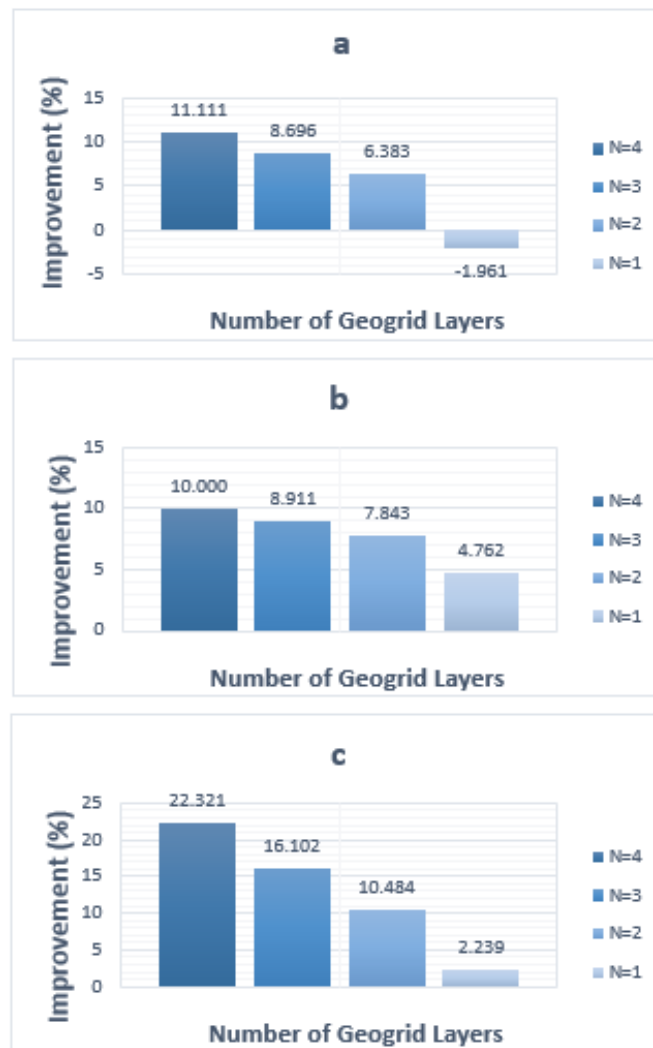


Figure 4.28. The Acceleration Improvement Graphs in Accordance with Story and Reinforcement Layers for (a) Foundation, (b) 1st Floor, (c) 5th Floor under El Centro Earthquake Motion (PGA= 0.55 g).

As it can be seen for the first, third and fifth floor, the maximum decrease of story's displacement is 24%, 21%, and 16% respectively. For N=1 the reduction of displacement of the first floor is a substantial value, it is nearly 12%.

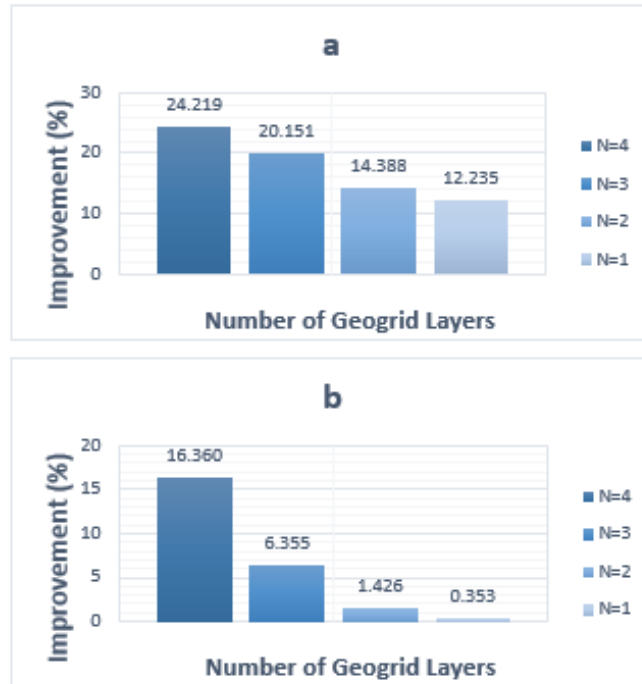


Figure 4.29. The Displacement Improvement Graphs in Accordance with Story and Reinforcement Layers for (a) 1st Floor, (b) 5th Floor under El Centro Earthquake Motion (PGA= 0.55 g).

Table 4.18. and Table 4.19. indicate arias intensity improvements and the period lengthening ratios and RMS of peak values were exhibited. As it is shown in Table 4.18. and Table 4.19. Arias intensity values are decreased almost 17%, 5% and 12% for soil, foundation and floors.

Table 4.18. Fundamental Period and Period Lengthening Ratios under El Centro Earthquake Motion (PGA= 0.55 g).

	Fundamental Period (Hz)					Period Lengthening Ratio			
	N=4	N=3	N=2	N=1	N=0	N=4	N=3	N=2	N=1
In-Soil	3.75	3.75	3.75	3.75	3.74	1.00	1.00	1.00	1.00
Foundation	6.91	6.91	6.91	6.91	6.91	1.00	1.00	1.00	1.00
1st Floor	0.45	0.45	0.45	0.45	0.46	1.02	1.02	1.02	1.02
2nd Floor	0.45	0.45	0.45	0.45	0.46	1.02	1.02	1.02	1.02
3rd Floor	0.45	0.45	0.45	0.45	0.46	1.02	1.02	1.02	1.02
4th Floor	0.45	0.45	0.45	0.45	0.46	1.02	1.02	1.02	1.02
5th Floor	0.45	0.45	0.45	0.45	0.46	1.02	1.02	1.02	1.02

Table 4.19. RMS and Arias Intensity Improvement Ratios under El Centro Earthquake Motion (PGA= 0.55 g).

Root Mean Square (RSM)				Arias Intensity	
Horizontal Acceleration(g)	Peak	RSM-Rein.	RSM Imp (%)		Arias Intensity Imp (%)
In-Soil	0.57	0.49	17.16	In-Soil	19.7
Foundation	0.5	0.47	5.7	Foundation	13
1st Floor	1.1	1.02	7.83	1st Floor	11.1
2nd Floor	1.17	1.12	4.91	2nd Floor	9.92
3rd Floor	0.79	0.72	9.53	3rd Floor	23.44
4th Floor	0.73	0.68	7.11	4th Floor	21.05
5th Floor	1.37	1.22	12.05	5th Floor	25.67

The reduction of RMS is 17% for soil, 5% for foundation, 7%, 4%, 9%, 7%, and 12% for floors roughly. Also, there is no change the natural period of model. The period lengthening ratio fluctuates up to %2 and in Figure 4.30. improvement ratios considering, Arias Intensity and Story Drifts can be observed.

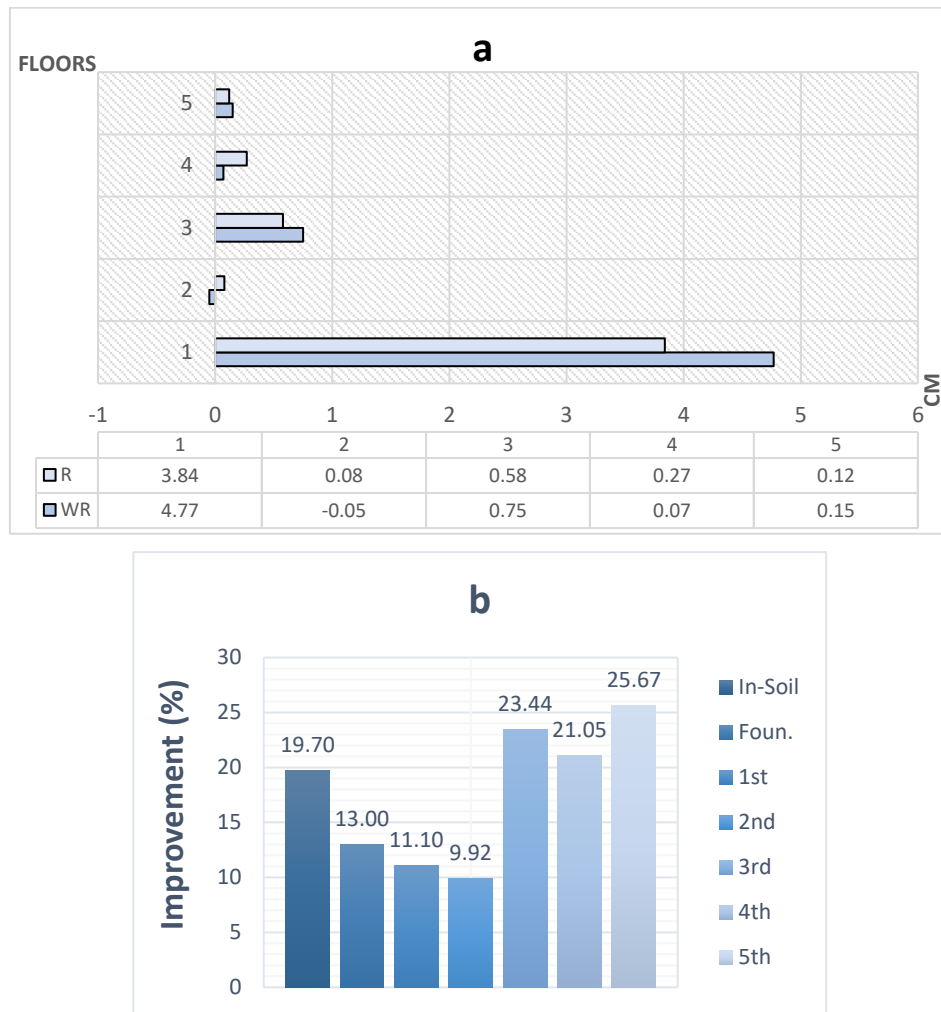


Figure 4.30. Improvement Ratios considering (a) Story Drifts and (b) Arias Intensity under El Centro Earthquake Motion (PGA= 0.55 g).

4.2.7. Seismic Response of 5-Story Model under El Centro Earthquake Motion (PGA =0.89 g)

Table 4.20. shows the reduced acceleration and displacement values through all sensors comparing to unreinforced system for 5-Storey model under El Centro Earthquake-0.89g. In the soil, peak accelerations are 1.44g in the underside, 1.39g midpoint, and 1.18g in the upper side. The reduction of acceleration in underside is 2%, 7%, 12% and 17%, the reduction of acceleration in midpoint is 7%, 13%, 25% and 29%, the reduction of acceleration in upper side is 11%, 16%, 25% and 29% roughly for N=1, N=2, N=3 and

N=4, respectively. The maximum acceleration improvement in midpoint and upper side is nearly 30% and 17% in underside for soil.

Table 4.20. Summary of all tested Cases under El Centro Earthquake motion (PGA=0.89g).

		N=4			N=3			N=2			N=1		
		WR	R	IMP. (%)	WR	R	IMP. (%)	WR	R	IMP. (%)	WR	R	IMP. (%)
In Soil	A5	1.44	1.23	17.073	1.44	1.28	12.501	1.44	1.34	7.463	1.44	1.41	2.128
	A6	1.34	1.12	19.643	1.34	1.15	16.522	1.34	1.21	10.744	1.34	1.3	3.077
	A7	1.39	1.07	29.906	1.39	1.11	25.225	1.39	1.23	13.008	1.39	1.29	7.752
	A8	1.24	1.14	8.772	1.24	1.2	3.333	1.24	1.21	2.479	1.24	1.25	-0.8
	A9	1.31	1.08	21.296	1.31	1.16	12.931	1.31	1.21	8.264	1.31	1.31	0
	A10	1.31	1.11	18.018	1.31	1.2	9.167	1.31	1.24	5.645	1.31	1.3	0.769
	A11	1.09	0.85	28.235	1.09	0.87	25.287	1.09	1	9.000	1.09	0.98	11.224
	A12	1.18	0.91	29.670	1.18	0.94	25.532	1.18	1.01	16.832	1.18	1.06	11.321
Foun.(g)	A13	1.1	0.98	12.245	1.1	1.05	4.762	1.1	1.05	4.762	1.1	1.07	2.804
5 Storey Model	A14	1.2	1.1	9.091	1.2	1.14	5.263	1.2	1.15	4.348	1.2	1.19	0.84
	A15	1.15	1.03	11.650	1.15	1.06	8.491	1.15	1.11	3.604	1.15	1.14	0.877
	A16	0.92	0.82	12.195	0.92	0.88	4.545	0.92	0.9	2.222	0.92	0.93	-1.075
	A17	0.78	0.63	23.810	0.78	0.7	11.429	0.78	0.74	5.405	0.78	0.79	-1.266
	A18	1.2	1.06	13.208	1.2	1.1	9.091	1.2	1.16	3.448	1.2	1.2	0
	D20	7.09	5.88	20.578	7.09	6.73	5.349	7.09	6.89	2.903	7.09	6.96	1.868
	D21	7.08	5.99	18.197	7.08	6.81	3.965	7.08	6.92	2.312	7.08	7	1.143
	D22	8.45	7.28	16.071	8.45	7.85	7.643	8.45	8.29	1.930	8.45	8.38	0.835
	D23	9.09	7.97	14.053	9.09	8.27	9.915	9.09	8.88	2.365	9.09	8.97	1.338
	D24	9.29	8.12	14.409	9.29	8.52	9.038	9.29	9.23	0.65	9.29	9.32	-0.322

The sensors shown in Figure 4.31 and 4.32. represent the first and fifth floor. The improvement of N=4 compared to unreinforced system can be seen from there under dynamic loads. The decrease of foundation acceleration is 2%, 4%, 4% and 12% for N=1, N=2, N=3 and N=4, respectively. For N=2 and N=3, there is no reduction for foundation level.

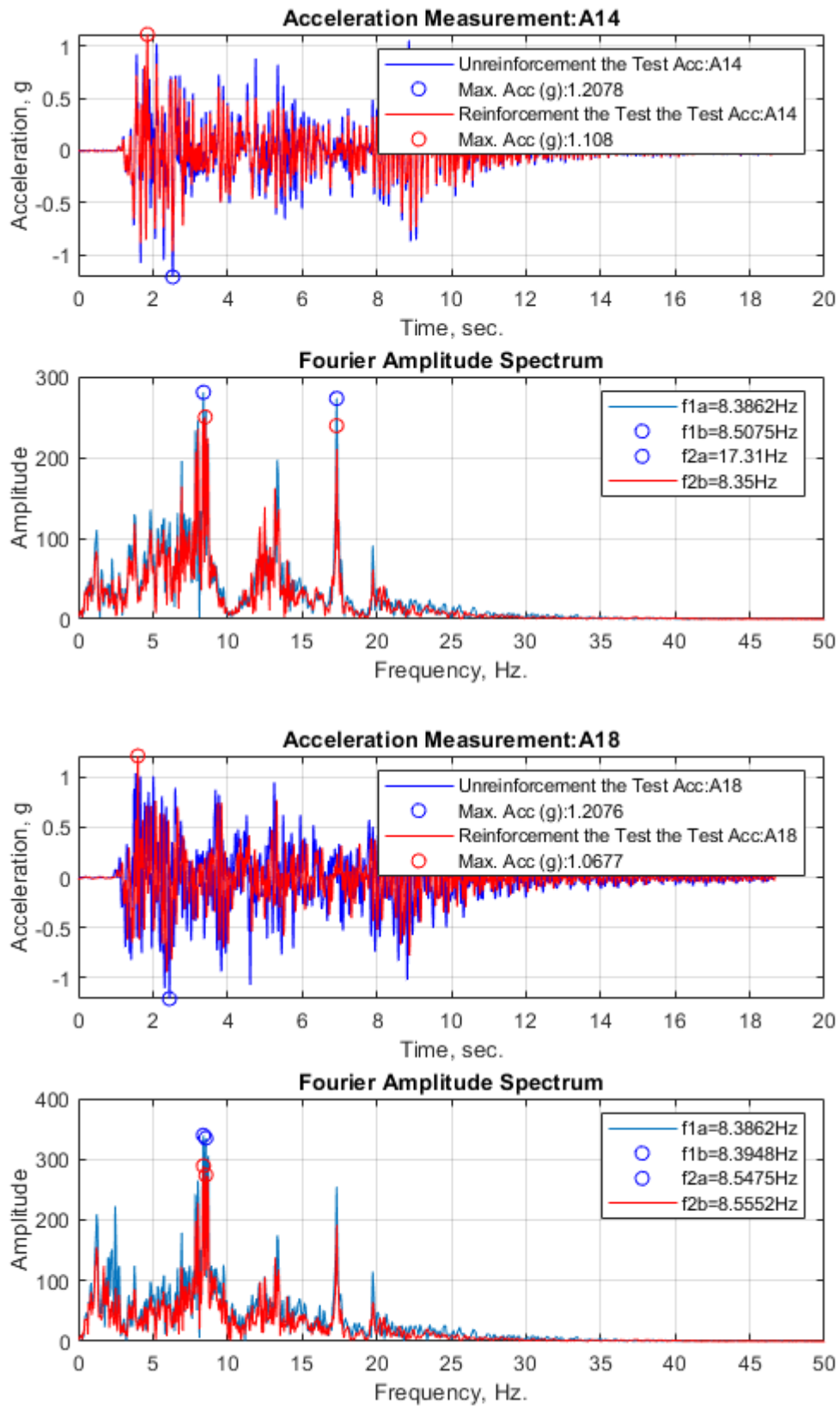


Figure 4.31. Acceleration Measurements and FAS of 1st and 5th Floors under El Centro Earthquake Motion (PGA= 0.89 g).

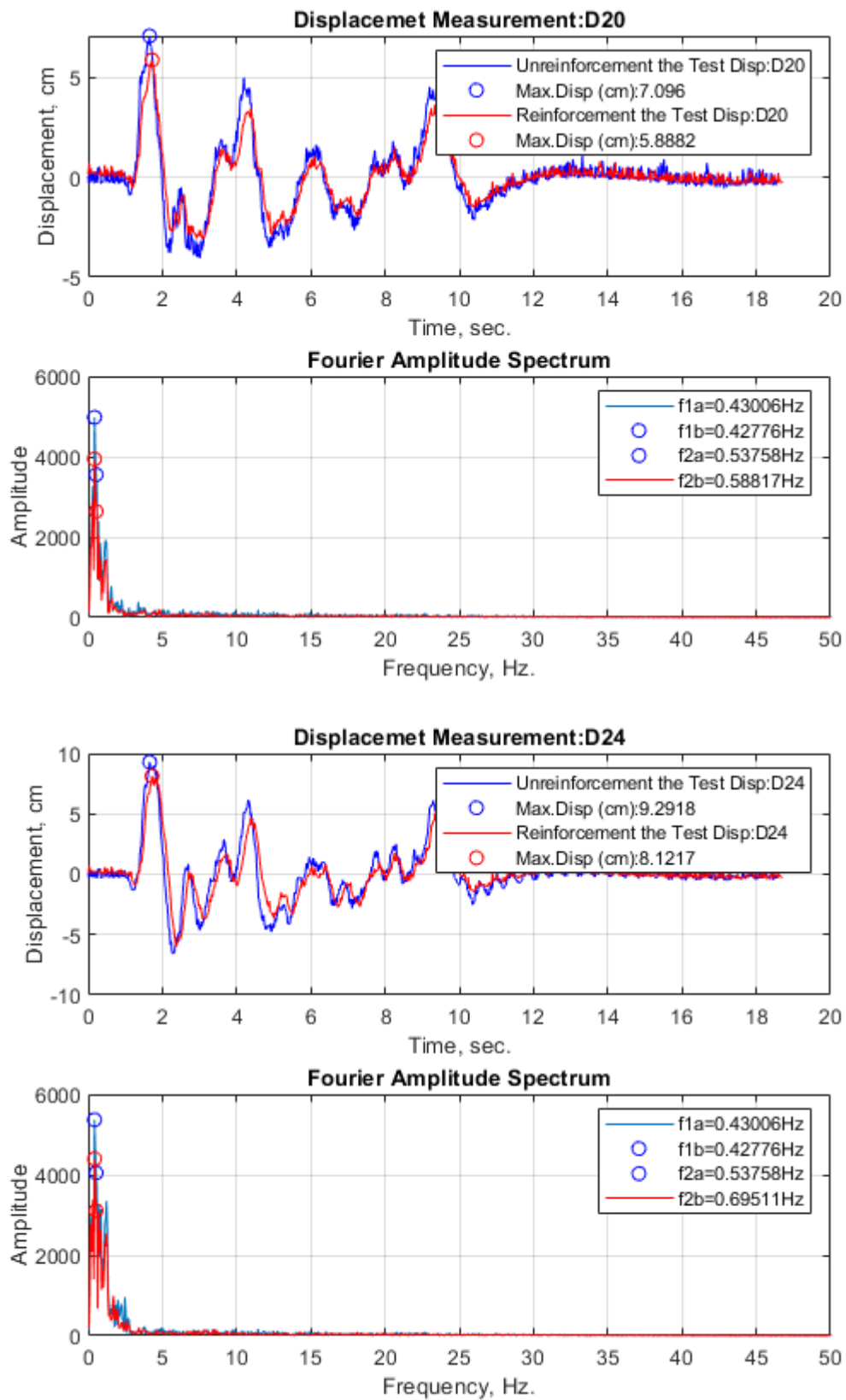


Figure 4.32. Displacement Measurements and FAS of 1st and 5th Floors under El Centro Earthquake Motion (PGA= 0.89 g).

The changing acceleration and the displacement values in accordance with story and reinforcement layers were given in Figure 4.33 and Figure 4.34. Graphs include the improvements compared unreinforced system for foundation, first and fifth floors for each N values.

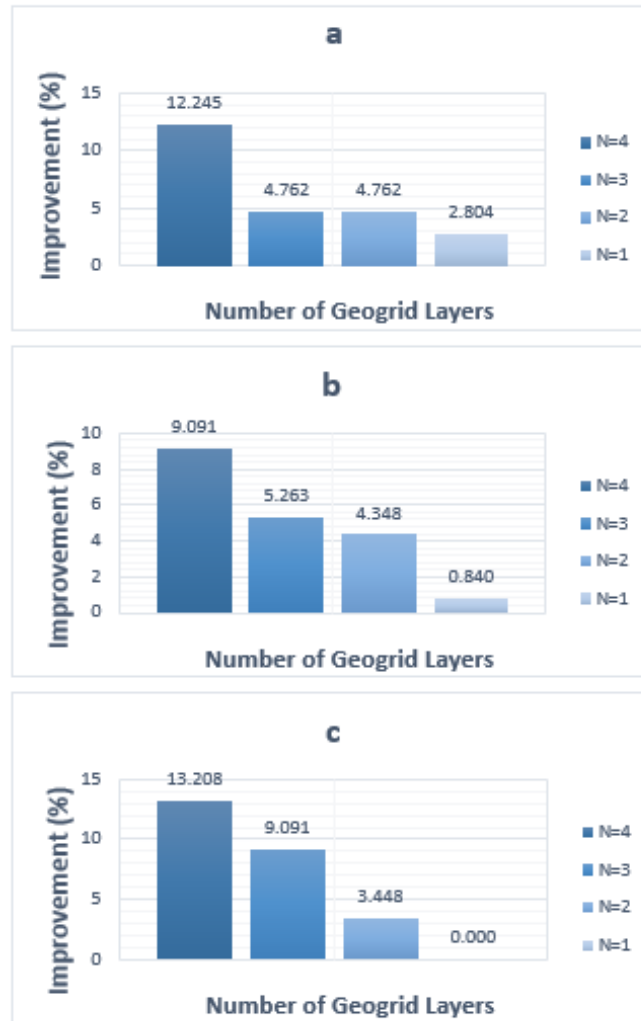


Figure 4.33. The Acceleration Improvement Graphs in Accordance with Story and Reinforcement Layers for (a) Foundation, (b) 1st Floor, (c) 5th Floor under El Centro Earthquake Motion (PGA= 0.89 g).

It can be said that for N=1 nearly there is no contribution to the reduction of acceleration on the model for El Centro Earthquake (0.89g). The improvements in acceleration values become negative or %0 in N=1. With the increase in the geogrid layers,

the reduction of acceleration becomes 4%, 5%, 9% for the first floor, 2%, 4%, 12% for the second floor and 3%, 9%, 13% for the third floor for N=2, N=3, N=4 ,respectively.

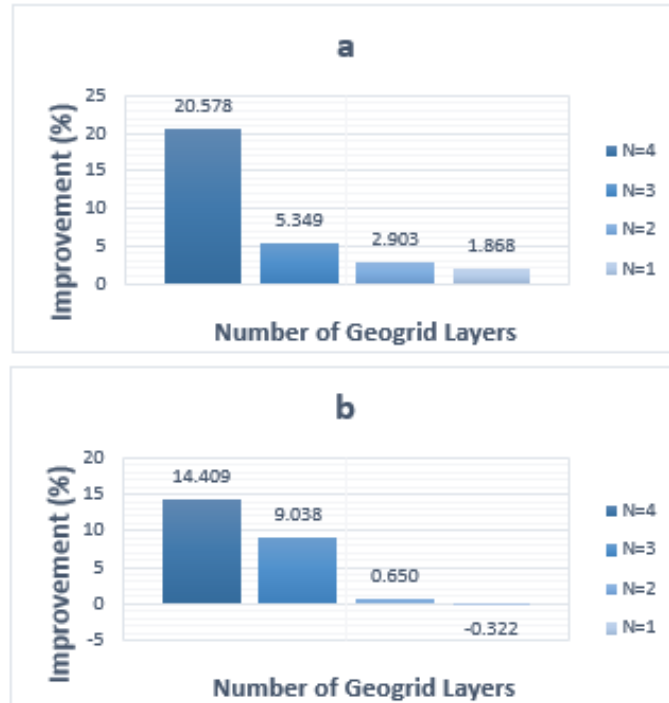


Figure 4.34. The Displacement Improvement Graphs in Accordance with Story and Reinforcement Layers for (a) 1st Floor, (b) 5th Floor under El Centro Earthquake Motion (PGA= 0.89 g).

In the first, third and fifth floor, the maximum decrease of story's displacement is 22%, 20%, 19%, respectively. For the first floor there is no considerable reduction, it is just 1% but for N=3 it reaches up to 5%.

Table 4.21. Fundamental Period and Period Lengthening Ratios under El Centro Earthquake Motion (PGA= 0.89 g).

	Fundamental Period (Hz)					Period Lengthening Ratio			
	N=4	N=3	N=2	N=1	N=0	N=4	N=3	N=2	N=1
In-Soil	3.78	3.78	3.78	3.78	3.76	0.99	0.99	0.99	0.99
Foundation	3.78	3.78	3.78	3.78	3.76	0.99	0.99	0.99	0.99
1st Floor	0.42	0.42	0.42	0.42	0.43	1.02	1.02	1.02	1.02
2nd Floor	0.42	0.42	0.42	0.42	0.43	1.02	1.02	1.02	1.02
3rd Floor	0.42	0.42	0.42	0.42	0.43	1.02	1.02	1.02	1.02
4th Floor	0.42	0.42	0.42	0.42	0.43	1.02	1.02	1.02	1.02
5th Floor	0.42	0.42	0.42	0.42	0.43	1.02	1.02	1.02	1.02

Table 4.22. RMS and Arias Intensity Improvement Ratios under El Centro Earthquake Motion (PGA= 0.89 g).

Root Mean Square (RSM)				Arias Intensity	
Horizontal Acceleration(g)	Peak	RSM-Rein.	RSM Imp (%)		Arias Intensity Imp (%)
In-Soil	1.44	1.34	7.73	In-Soil	35.9
Foundation	1.1	1.04	5.97	Foundation	14.33
1st Floor	1.2	1.15	4.76	1st Floor	10.09
2nd Floor	1.15	1.09	5.91	2nd Floor	13.86
3rd Floor	0.92	0.88	4.14	3rd Floor	14.51
4th Floor	0.78	0.72	8.73	4th Floor	25.48
5th Floor	1.2	1.13	6.07	5th Floor	15.19

As it is shown in Table 4.21 and Table 4.22, Arias intensity values are decreased for soil region and foundation nearly 7% and 5%. It reduces up to 6% for floors. RMS improvement values for soil, foundation and floors are 7%, 5%, 4%, 5%, 4%, 8%, and 6%, respectively. Also, there is no change the natural period of model. The period lengthening ratio fluctuates up to %2. Also Figure 4.35 shows improvement ratios of Arias Intensity and story drifts.

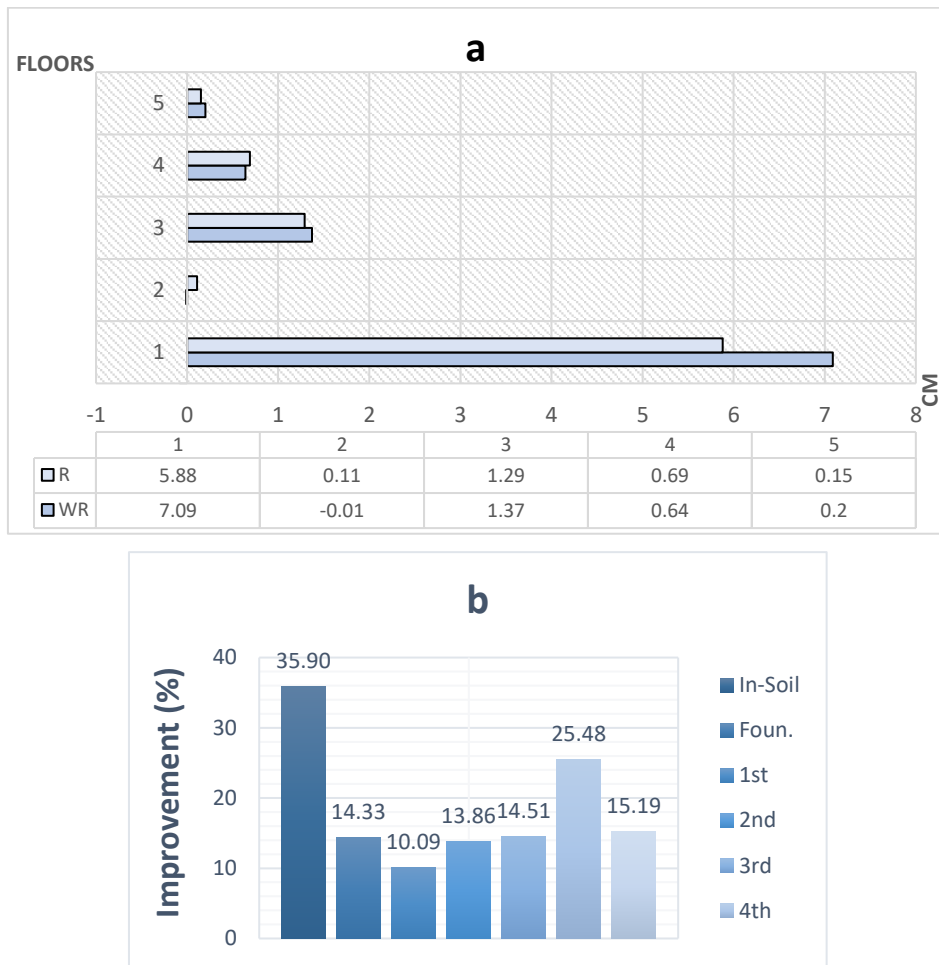


Figure 4.35. Improvement Ratios considering (a) Story Drifts and (b) Arias Intensity under El Centro Earthquake Motion (PGA= 0.89 g).

4.3. 3-Story Building Model on Geogrid Reinforced Soil

These parts include the results and comparison of 3-Story model with and without geogrid reinforcement for all earthquakes. As mentioned before, the case without geogrid reinforcement was Case 10 for 3-Storey model and it was defined as WR (without reinforcement), the cases with geogrid reinforcement were defined as R (reinforcement) in all tables and all comparisons was done according to this.

4.3.1. Seismic Response of 3-Story Model under Kobe Earthquake Motion (PGA= 0.74 g)

Table 4.22 shows the reduced acceleration and displacement values through all sensors comparing to unreinforced system for 3-Storey model under Kobe Earthquake (0.74g).

In the soil, peak accelerations are 0.65g in the underside, 0.81g in the midpoint, and 0.8g in the upper side. The reduction of acceleration in the underside is -2%, 0%, 6% and 10%, the reduction of acceleration in the midpoint is 2%, 5%, 14% and 20%, the reduction of acceleration in upper side is 3%, 6%, 21% and 35% for N=1, N=2, N=3 and N=4, respectively. The maximum improvement for acceleration in the soil is 35%. In the underside for N=1 and N=2 the reduction of acceleration becomes negative and 0%. The noteworthy improvement in acceleration starts with N=3.

Table 4.22. Summary of all tested Cases under Kobe Earthquake motion (PGA=0.74g).

		N=4			N=3			N=2			N=1		
		WR	R	IMP. (%)	WR	R	IMP. (%)	WR	R	IMP. (%)	WR	R	IMP. (%)
In Soil (g)	A5	0.65	0.59	10.169	0.65	0.61	6.557	0.65	0.65	0	0.65	0.66	-1.515
	A6	0.68	0.56	21.429	0.68	0.6	13.333	0.68	0.66	3.030	0.68	0.68	0
	A7	0.63	0.57	10.526	0.63	0.59	6.780	0.63	0.62	1.613	0.63	0.63	0
	A8	0.72	0.6	20.000	0.72	0.63	14.286	0.72	0.68	5.882	0.72	0.75	-4.000
	A9	0.66	0.56	17.857	0.66	0.59	11.864	0.66	0.63	4.762	0.66	0.63	4.762
	A10	0.66	0.58	13.793	0.66	0.6	10.000	0.66	0.61	8.197	0.66	0.64	3.125
	A11	0.81	0.67	20.896	0.81	0.71	14.085	0.81	0.77	5.195	0.81	0.79	2.532
	A12	0.8	0.59	35.593	0.8	0.66	21.212	0.8	0.75	6.667	0.8	0.77	3.896
Foun.(g)	A13	0.62	0.54	14.815	0.62	0.58	6.897	0.62	0.6	3.333	0.62	0.63	-1.587
3 Storey Model (cm)	A14	0.95	0.83	14.458	0.95	0.88	7.955	0.95	0.93	2.151	0.95	0.95	0
	A15	0.64	0.55	16.364	0.64	0.59	8.475	0.64	0.61	4.918	0.64	0.63	1.587
	A16	1.05	0.87	20.690	1.05	0.9	16.667	1.05	0.97	8.247	1.05	1.06	-0.943
	D20	2.58	2.06	25.243	2.58	2.11	22.275	2.58	2.28	13.158	2.58	2.34	10.256
	D21	2.73	2.33	17.167	2.73	2.41	13.278	2.73	2.61	4.598	2.73	2.68	1.866
	D22	3.46	2.85	21.404	3.46	2.96	16.892	3	3.26	6.135	3.46	3.35	3.284

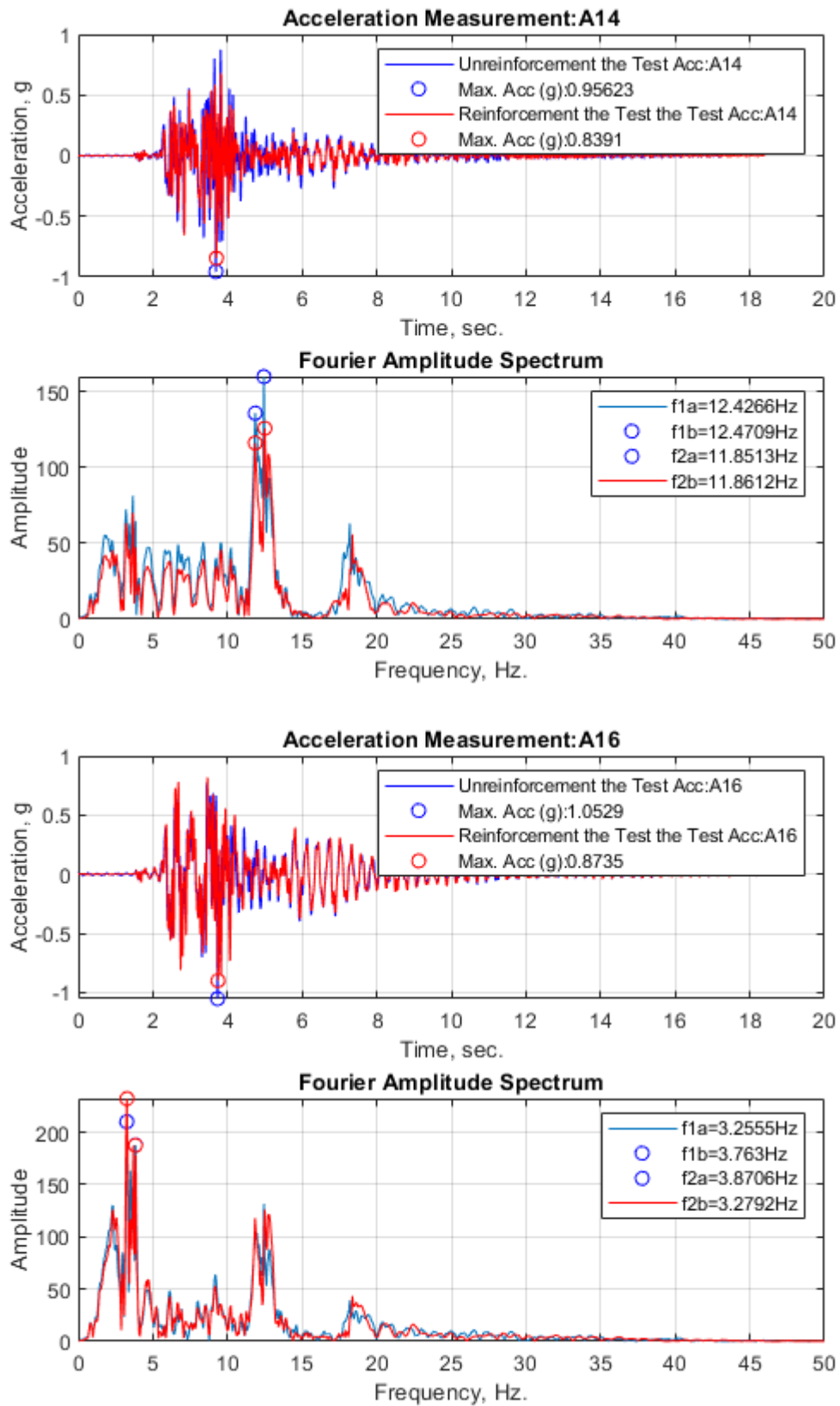


Figure 4.36. Acceleration Measurements and FAS of 1st and 3rd Floors under Kobe Earthquake Motion (PGA= 0.74 g).

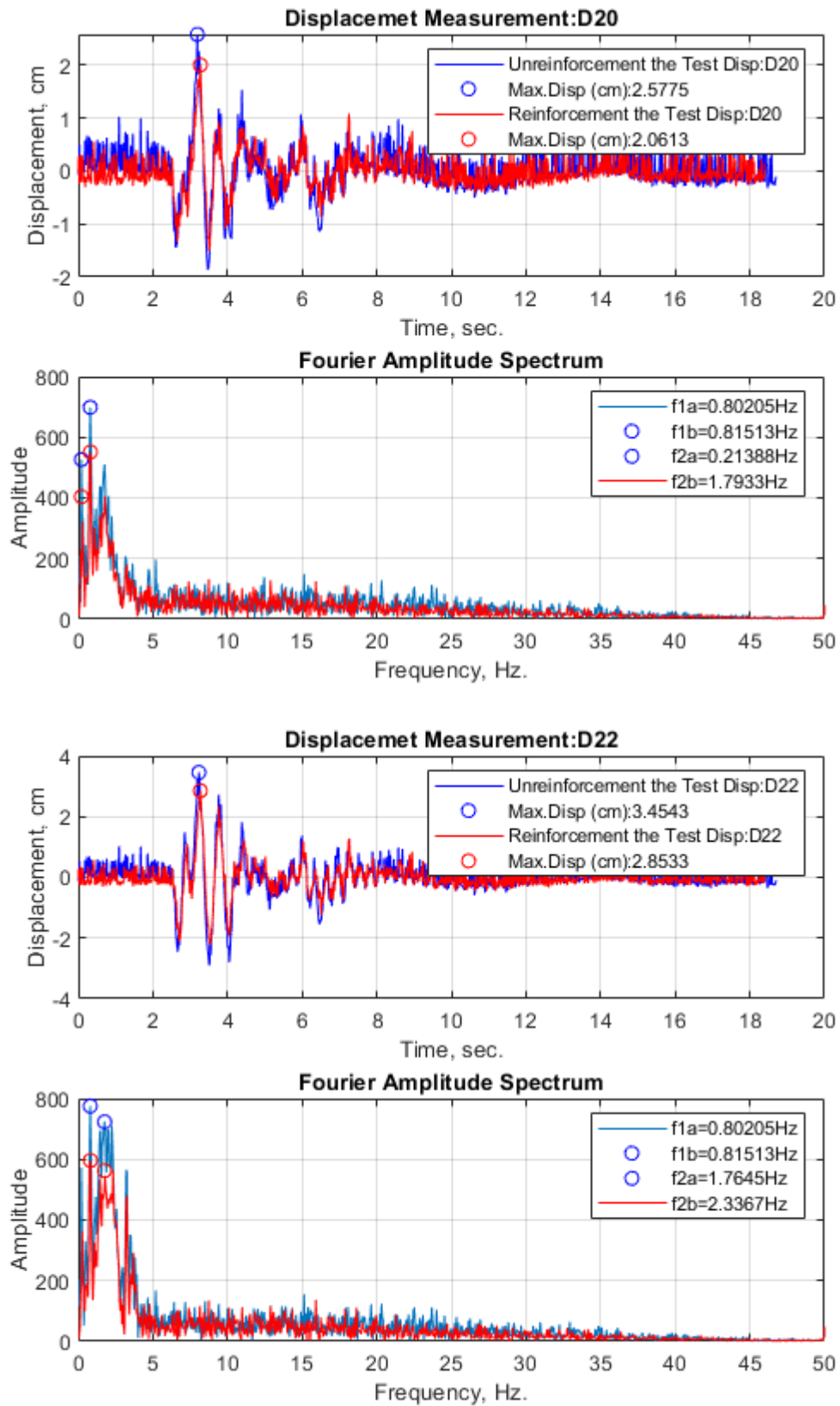


Figure 4.37. Displacement Measurements and FAS of 1st and 3rd Floors under Kobe Earthquake Motion (PGA= 0.74 g).

The sensors shown in Figure 4.36 and 4.37 represent the first and third floor. The improvement of N=4 compared to unreinforced system can be seen. The decrease of first floor acceleration is 0%, 2%, 7% and 14% for N=1, N=2, N=3 and N=4, respectively. For N=2 and N=3, there is no significant improvements.

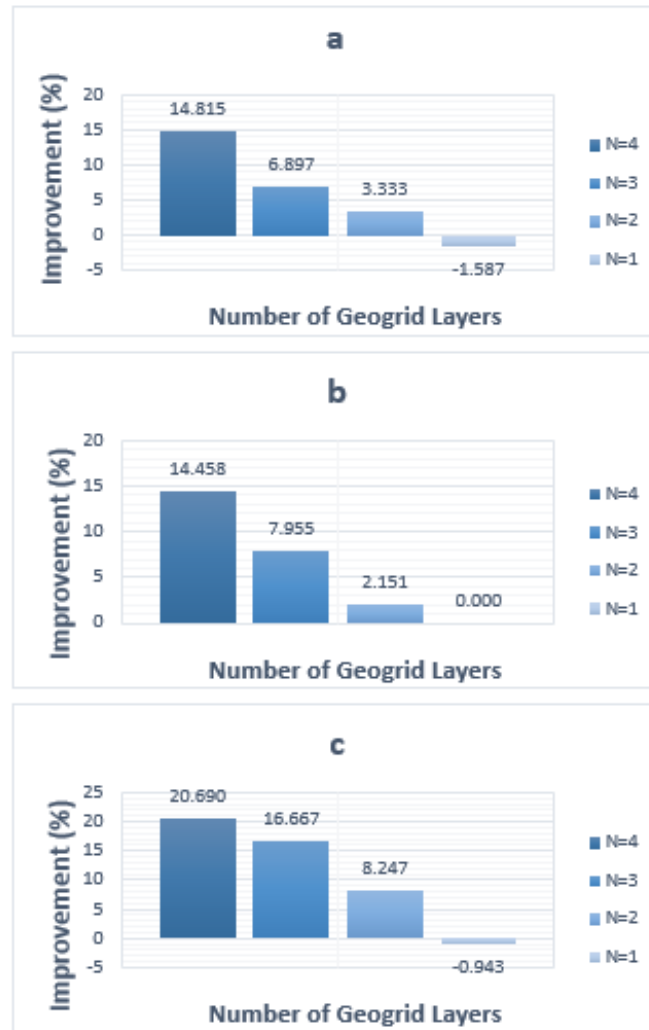


Figure 4.38. The Acceleration Improvement Graphs in Accordance with Story and Reinforcement Layers for (a) Foundation, (b) 1st Floor, (c) 3rd Floor under Kobe Earthquake Motion (PGA= 0.74 g).

The changing acceleration and the changing displacement values in accordance with story and reinforcement layers were given in Figure 4.38. and Figure 4.39. Graphs encompass the improvements compared unreinforced system for foundation, first and third floor for each N values.

The reduction of foundation acceleration is -2%, 3%, 6% and 14% for N=1, N=2, N=3 and N=4, respectively. For all floors, N=1 slightly effects or does not affect the reduction of acceleration, the reduction values of floors for N=1 are 0%, 2% and -1%, respectively. However, with the increase in the geogrid layers, especially for N=3, the significant improvement can be observed. It becomes 2%, 8%, 14% for the first floor and 8%, 16%, 20% for the third floor in N=2, N=3, N=4, respectively. The maximum acceleration reduction values become up to approximately 20% comparing to unreinforced system.

In the first and third floor, the maximum decrease of story's displacement is 25% and 21% respectively. Except the first floor there is no considerable reduction for N=1.

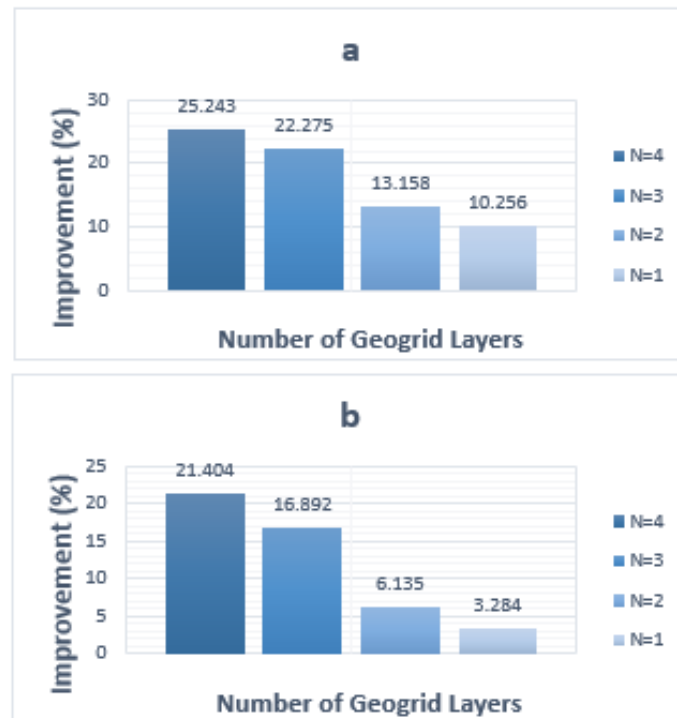


Figure 4.39. The Displacement Improvement Graphs in Accordance with Story and Reinforcement Layers for (a) 1st Floor, (b) 3rd Floor under Kobe Earthquake Motion (PGA= 0.74 g).

In Table 4.23 and Table 4.24., Arias intensity improvements were exhibited and with the help of the fundamental period of all N values under dynamic loads for soil,

foundations, floors, the period lengthening ratios were shown, and also RMS of peak values were exhibited.

Table 4.23. Fundamental Period and Period Lengthening Ratios under Kobe Earthquake Motion (PGA= 0.74 g).

	Fundamental Period (Hz)					Period Lengthening Ratio			
	N=4	N=3	N=2	N=1	N=0	N=4	N=3	N=2	N=1
In-Soil	4.67	4.67	4.67	4.67	4.7	1.01	1.01	1.01	1.01
Foundation	4.67	4.67	4.67	4.67	4.67	1.00	1.00	1.00	1.00
1st Floor	0.81	0.81	0.81	0.81	0.8	0.99	0.99	0.99	0.99
2nd Floor	0.81	0.81	0.81	0.81	0.8	0.99	0.99	0.99	0.99
3rd Floor	0.81	0.81	0.81	0.81	0.8	0.99	0.99	0.99	0.99

Table 4.24. RMS and Arias Intensity Improvement Ratios under Kobe Earthquake Motion (PGA= 0.74 g).

Root Mean Square (RSM)				Arias Intensity	
Horizontal Acceleration(g)	Peak	RSM-Rein.	RSM Imp (%)		Arias Intensity Imp (%)
In-Soil	0.81	0.63	28.95	In-Soil	43.07
Foundation	0.62	0.59	5.37	Foundation	17.33
1st Floor	0.95	0.9	5.71	1st Floor	16.05
2nd Floor	0.64	0.6	7.43	2nd Floor	19.47
3rd Floor	1.05	0.95	10.2	3rd Floor	24.62

As can be seen, Arias intensity values for soil region and foundation are decreased approximately 3% and it reduces up to 5% for floors. RMS improvement values for soil, foundation and floors are 28%, 5%, 5%, 7%, and 10%, respectively. Also, there is no change the natural period of model. The period lengthening ratio fluctuates up to %1 and in Figure 4.40, improvement ratios of Arias Intensity and Story Drifts can be observed.

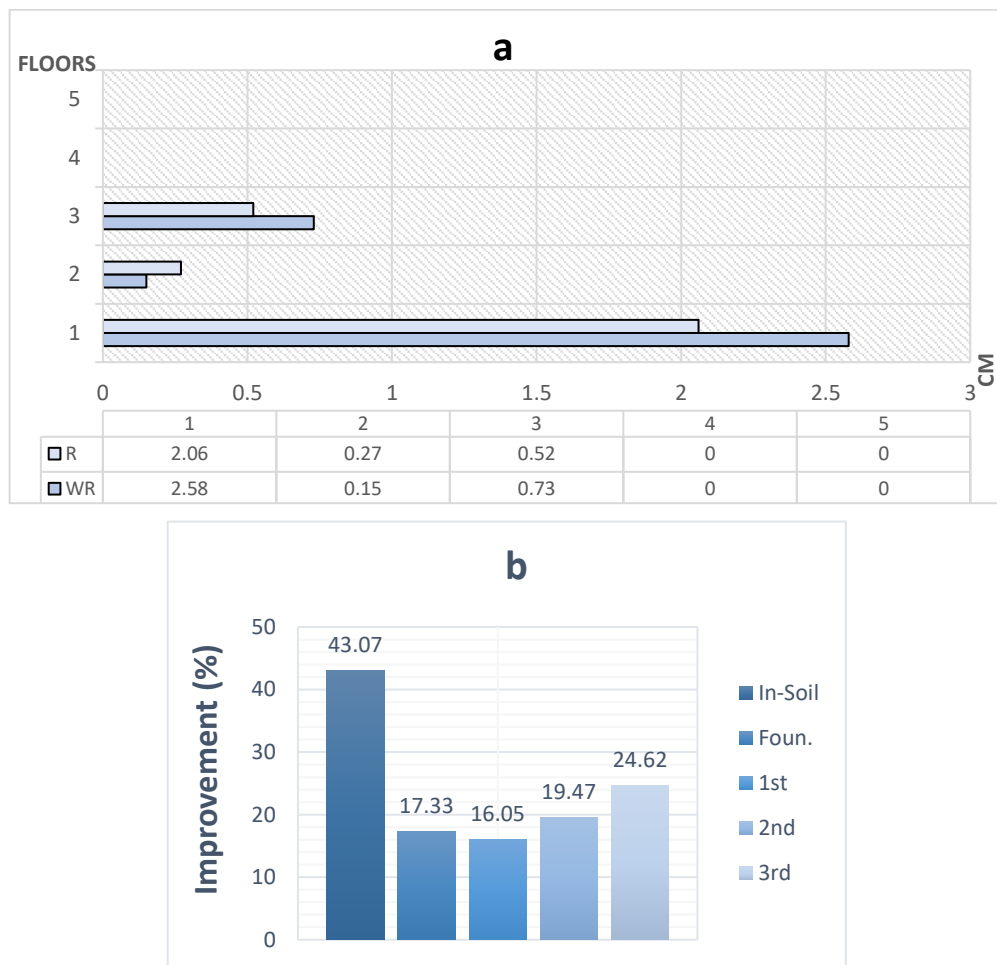


Figure 4.40. Improvement Ratios considering (a) Story Drifts and (b) Arias Intensity under under Kobe Earthquake Motion (PGA= 0.74 g).

4.3.2. Seismic Response of 3-Story Model under Kobe Earthquake Motion (PGA= 0.89 g)

Table 4.25 shows the reduced acceleration and displacement values through all sensors comparing to unreinforced system for 3-Storey model under Kobe Earthquake-0.89g. In the soil, peak accelerations are 0.97g in the underside and 0.98g in the midpoint, and 0.92g in the upper side. The maximum improvement of acceleration in the underside, midpoint upper side is %19, %27 and %24, respectively. For N=1, there is no considerable reduction in the soil, it becomes even negative value.

Table 4.25. Summary of all tested Cases under Kobe Earthquake motion (PGA=0.89g).

		N=4			N=3			N=2			N=1		
		WR	R	IMP. (%)	WR	R	IMP. (%)	WR	R	IMP. (%)	WR	R	IMP. (%)
In Soil (g)	A5	0.97	0.81	19.753	0.97	0.84	15.476	0.97	0.93	4.301	0.97	0.97	0
	A6	0.98	0.77	27.273	0.98	0.82	19.512	0.98	0.93	5.376	0.98	1	-2.000
	A7	0.93	0.77	20.779	0.93	0.79	17.722	0.93	0.89	4.494	0.93	0.92	1.087
	A8	1	0.81	23.457	1	0.86	16.279	1	0.96	4.167	1	1.07	-6.542
	A9	0.94	0.83	13.253	0.94	0.86	9.302	0.94	0.88	6.818	0.94	0.92	2.174
	A10	0.94	0.8	17.500	0.94	0.86	9.302	0.94	0.92	2.174	0.94	0.93	1.075
	A11	0.97	0.81	19.753	0.97	0.84	15.476	0.97	0.94	3.191	0.97	0.96	1.042
	A12	0.92	0.74	24.324	0.92	0.78	17.949	0.92	0.86	6.977	0.92	0.89	3.371
Foun.(g)	A13	0.8	0.61	31.148	0.8	0.67	19.403	0.8	0.75	6.667	0.8	0.78	2.564
3 Storey Model (cm)	A14	0.97	0.84	15.476	0.97	0.88	10.227	0.97	0.94	3.191	0.97	0.97	0
	A15	0.78	0.61	27.869	0.78	0.65	20.000	0.78	0.75	4.000	0.78	0.76	2.632
	A16	0.9	0.79	13.924	0.9	0.84	7.143	0.9	0.89	1.124	0.9	0.92	-2.174
	D20	3.49	2.55	36.863	3.49	2.72	28.309	3.49	3.25	7.385	3.49	3.32	5.120
	D21	3.61	2.93	23.208	3.61	3.01	19.934	3.61	3.27	10.398	3.61	3.4	6.176
	D22	3.96	3.31	19.637	3.95	3.48	13.506	3.95	3.61	9.418	3.95	3.81	3.675

The sensors shown in Figures 4.41 and 4.42 represent the soil, foundation, first and third floor. The improvement of N=4 compared to unreinforced system can be seen from there under dynamic loads. The maximum acceleration improvements for first and top floor are 15% and 13%.

The reduction of foundation acceleration is roughly 2%, 6%, 19% and 31% for N=1, N=2, N=3 and N=4, respectively.

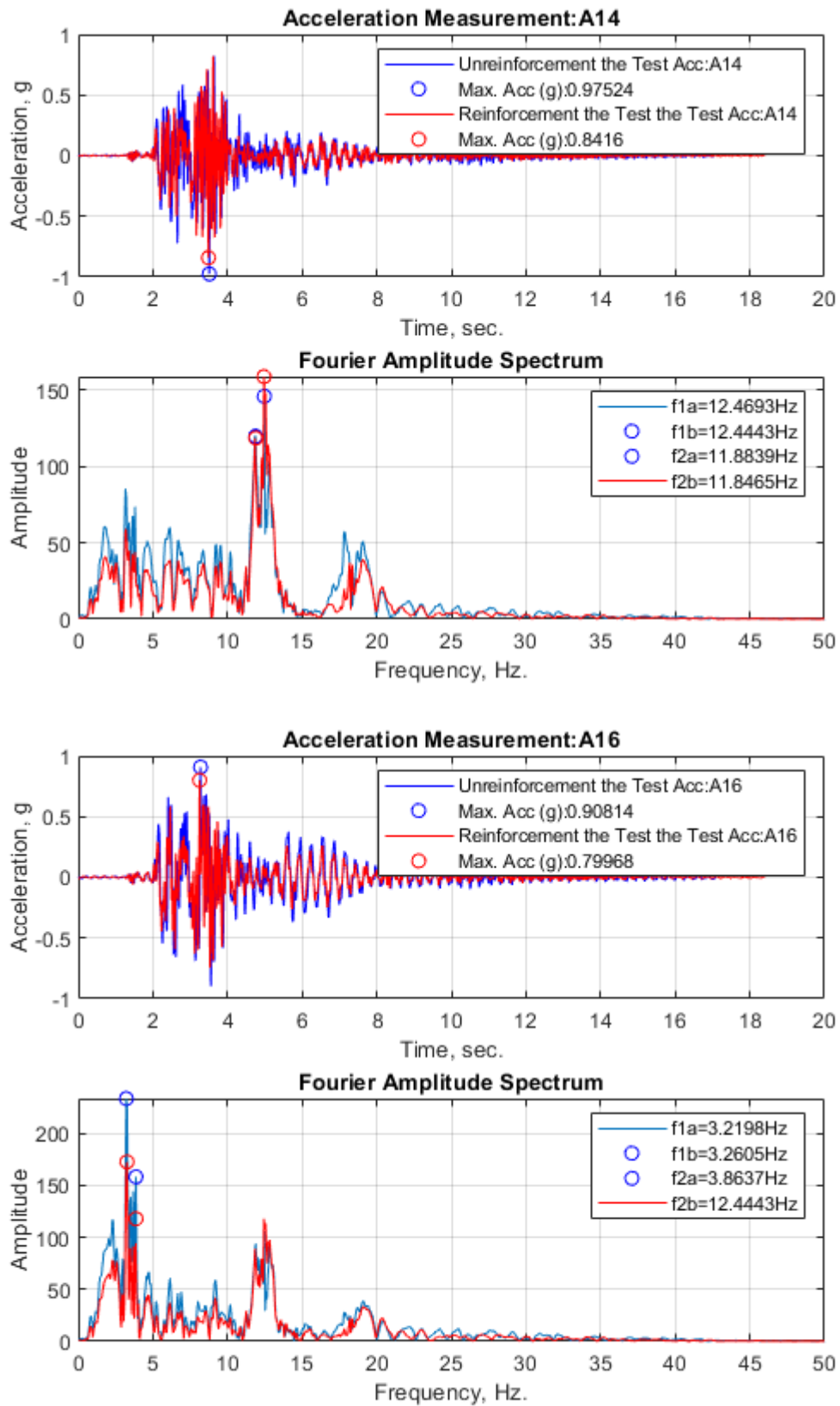


Figure 4.41. Acceleration Measurements and FAS of 1st and 3rd Floors under Kobe Earthquake Motion (PGA= 0.89 g).

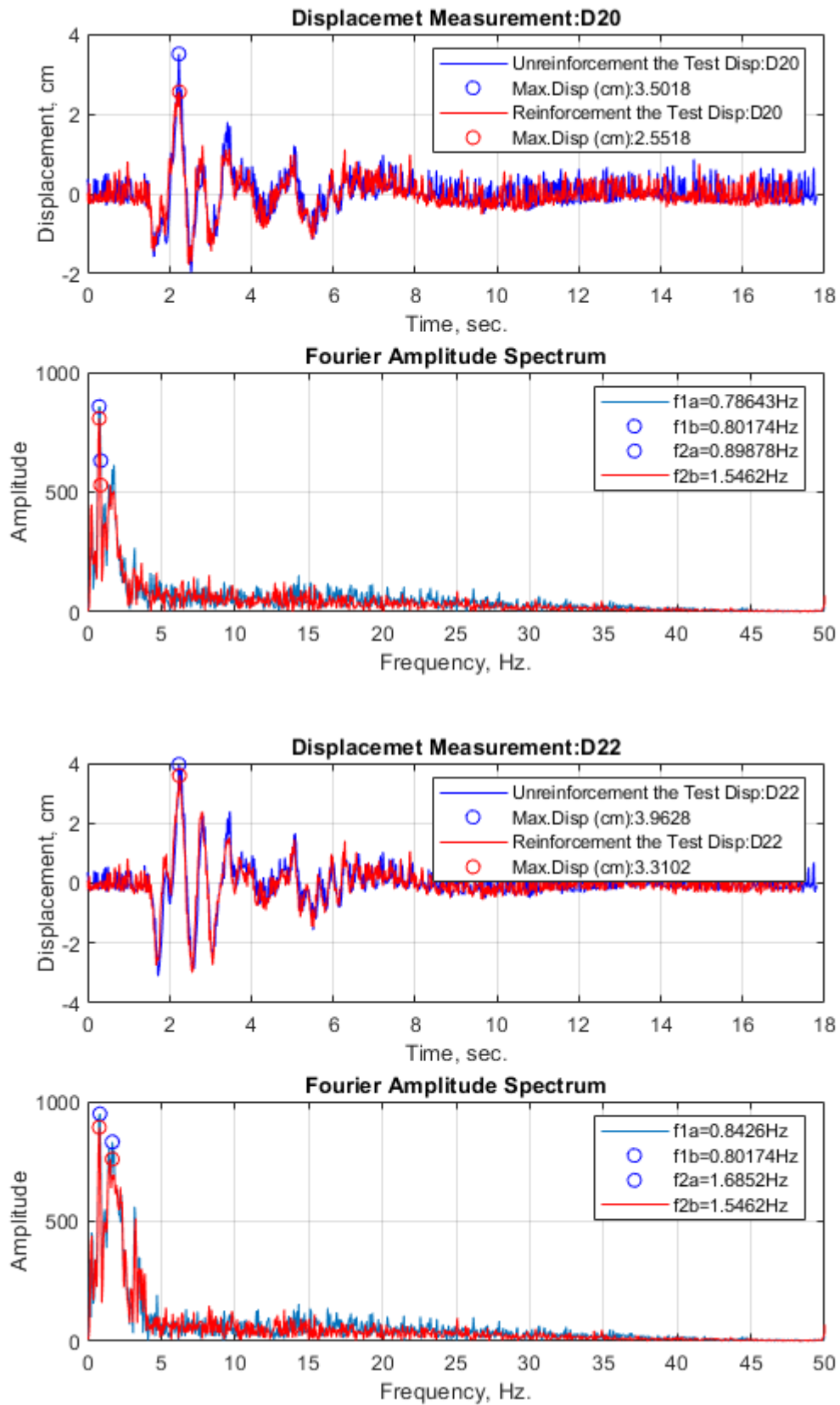


Figure 4.42. Displacement Measurements and FAS of 1st and 3rd Floors under Kobe Earthquake Motion (PGA= 0.89 g).

The changing acceleration values and the changing displacement values in accordance with story and reinforcement layers were given in Figure 4.43 and Figure 4.44. They show the comparisons of N=1, N=2, N=3 and N=4 for foundation, first, and third story for each N values.

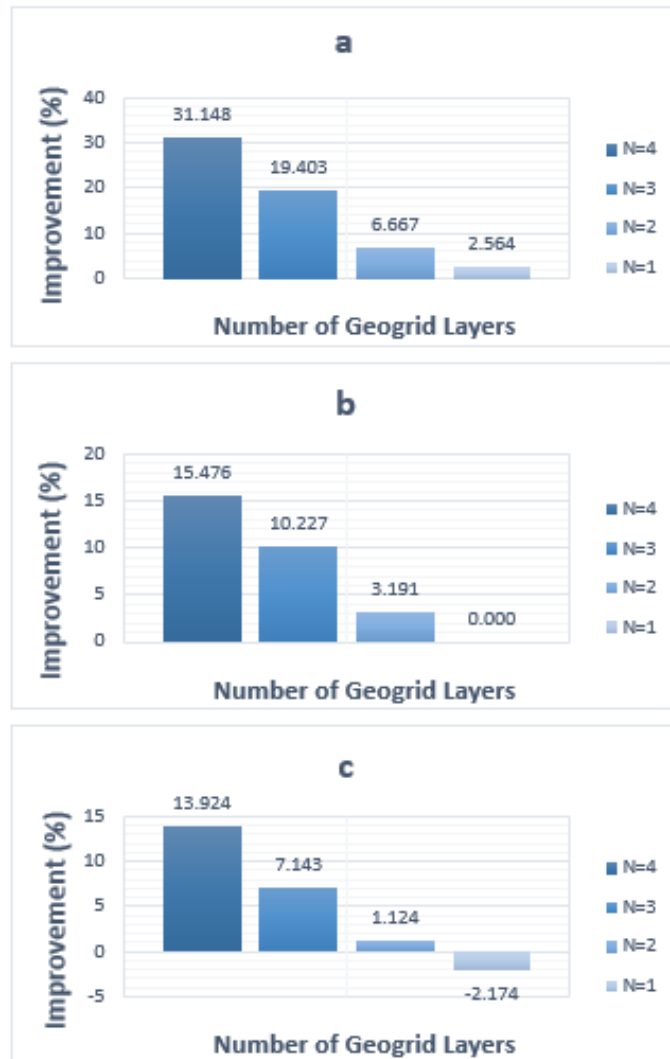


Figure 4.43. The Acceleration Improvement Graphs in Accordance with Story and Reinforcement Layers for (a) Foundation, (b) 1st Floor, (c) 3rd Floor under Kobe Earthquake Motion (PGA= 0.89 g).

For the first and third floor, for N=1 there is no reduction in acceleration value. However, with the increase in the geogrid layers, it decreases nearly 3%, 10%, and 15% for the first floor and 1%, 7%, and 13% for the third floor for N=2, N=3, N=4. The

maximum acceleration reduction values become up to 27% comparing to unreinforced system.

For the first and third floor, the maximum decrease of story's displacement values is 36% and 19%, respectively. They are obtained in N=4. Also, the first and second floor for N=1 have significant improvement, which is nearly 6%.

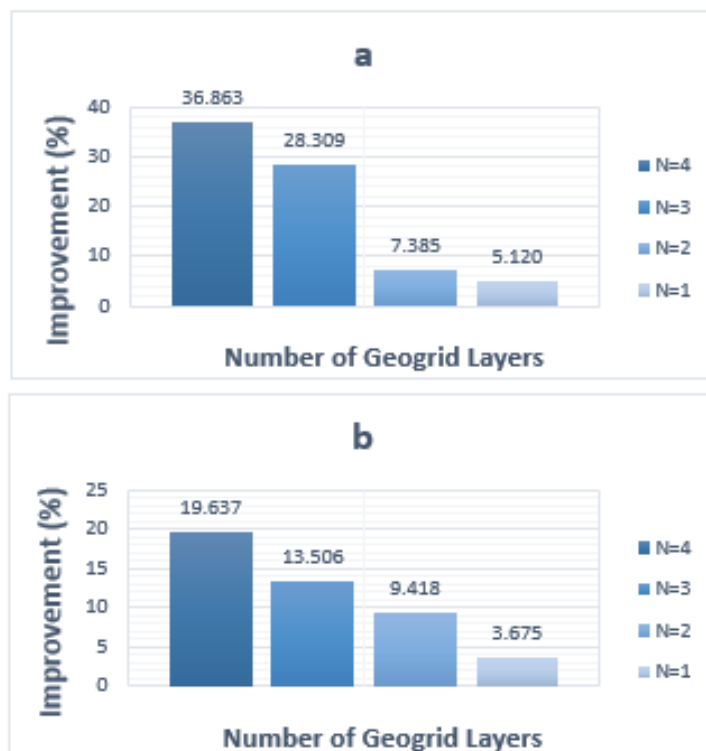


Figure 4.44. The Displacement Improvement Graphs in Accordance with Story and Reinforcement Layers for (a) 1st Floor, (b) 3rd Floor under Kobe Earthquake Motion (PGA= 0.89 g).

Table 4.26. Fundamental Period and Period Lengthening Ratios under Kobe Earthquake Motion (PGA= 0.74 g).

	Fundamental Period (Hz)					Period Lengthening Ratio			
	N=4	N=3	N=2	N=1	N=0	N=4	N=3	N=2	N=1
In-Soil	4.63	4.63	4.63	4.63	4.65	1.00	1.00	1.00	1.00
Foundation	4.67	4.67	4.67	4.67	4.68	1.00	1.00	1.00	1.00
1st Floor	0.81	0.81	0.81	0.81	0.78	0.96	0.96	0.96	0.96
2nd Floor	0.81	0.81	0.81	0.81	0.8	0.99	0.99	0.99	0.99
3rd Floor	0.8	0.81	0.8	0.81	0.84	1.05	1.04	1.05	1.04

Table 4.27. RMS and Arias Intensity Improvement Ratios under Kobe Earthquake Motion (PGA= 0.74 g).

Root Mean Square (RSM)				Arias Intensity	
Horizontal Acceleration(g)	Peak	RSM-Rein.	RSM Imp (%)		Arias Intensity Imp (%)
In-Soil	1.00	0.89	12.38	In-Soil	29.43
Foundation	0.80	0.71	13.37	Foundation	36.44
1st Floor	0.97	0.91	6.72	1st Floor	17.18
2nd Floor	0.78	0.70	12.15	2nd Floor	33.16
3rd Floor	0.90	0.86	4.48	3rd Floor	16.57

As can be seen in Table 4.26 and Table 4.27, Arias intensity values are reduced up to 3%, 4% and 4% for soil region, foundation and floors in order of. Reduction of RMS ascend at soil and foundation to 12%, 13% and at floors to 6%, 12% and 4%, respectively. There is no change in the natural period of model. The period lengthening ratio fluctuates up to %5. Also, in Figure 4.45, improvement ratios of Arias Intensity and Story Drifts were shown.

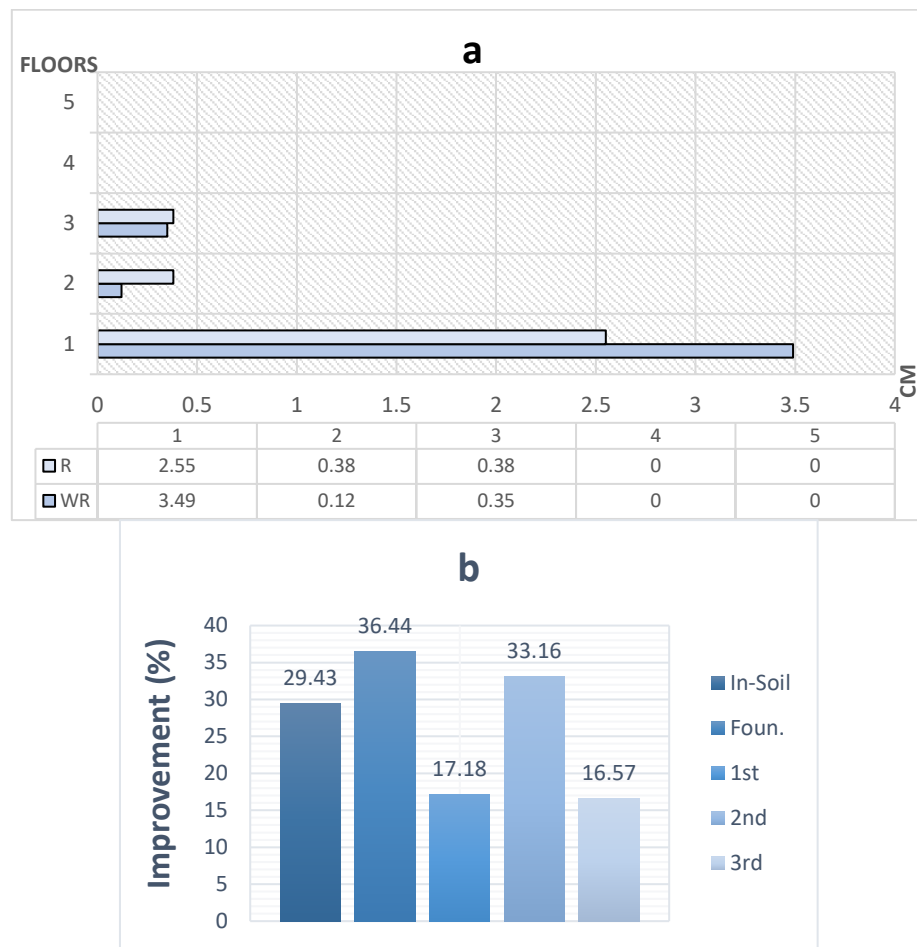


Figure 4.45. Improvement Ratios considering (a) Story Drifts and (b) Arias Intensity under Kobe Earthquake Motion (PGA= 0.89 g).

4.3.3. Seismic Response of 3-Story Model under Kocaeli Earthquake Motion (PGA= 0.21 g)

Table 4.28 shows the reduced acceleration and displacement values through all sensors comparing to unreinforced system for 3-Storey model under Kocaeli Earthquake (0.21g). In the soil, peak accelerations are 0.18g in the underside, 0.27g in the midpoint, and 0.30g in the upper side. The maximum improvement of acceleration in the underside, midpoint and upper side is 38%, 17% and 20%, respectively. For the most part of soil, the reduction of acceleration become negative or 0% for N=1. Especially there is a dramatic improvement in transition between N=2 and N=3.

Table 4.28. Summary of all tested Cases under Kocaeli Earthquake motion (PGA=0.21g).

		N=4			N=3			N=2			N=1		
		WR	R	IMP. (%)	WR	R	IMP. (%)	WR	R	IMP. (%)	WR	R	IMP. (%)
In Soil (g)	A5	0.18	0.13	38.462	0.18	0.15	20.000	0.18	0.16	12.500	0.18	0.17	5.882
	A6	0.19	0.15	26.667	0.19	0.16	18.750	0.19	0.18	5.556	0.19	0.18	5.556
	A7	0.19	0.16	18.750	0.19	0.16	18.750	0.19	0.18	5.556	0.19	0.2	-5.000
	A8	0.19	0.15	26.667	0.19	0.16	18.750	0.19	0.18	5.556	0.19	0.19	0
	A9	0.2	0.17	17.647	0.2	0.18	11.111	0.2	0.19	5.263	0.2	0.21	-4.762
	A10	0.21	0.15	40.000	0.21	0.17	23.529	0.21	0.19	10.526	0.21	0.21	0
	A11	0.27	0.23	17.391	0.27	0.23	17.391	0.27	0.26	3.846	0.27	0.27	0
	A12	0.3	0.25	20.000	0.3	0.27	11.111	0.3	0.28	7.143	0.3	0.32	-6.250
Foun.(g)	A13	0.3	0.26	15.385	0.3	0.28	7.143	0.3	0.3	0	0.3	0.31	-3.226
3 Storey Model (cm)	A14	0.71	0.52	36.538	0.71	0.65	9.231	0.71	0.66	7.576	0.71	0.68	4.412
	A15	0.56	0.46	21.739	0.56	0.49	14.286	0.56	0.5	12.000	0.56	0.53	5.660
	A16	0.68	0.54	25.926	0.68	0.58	17.241	0.68	0.64	6.250	0.68	0.69	-1.449
	D20	2.85	2.3	23.913	2.85	2.45	16.327	2.85	2.58	10.465	2.85	2.71	5.166
	D21	2.8	2.25	24.444	2.8	2.46	13.821	2.8	2.6	7.692	2.8	2.69	4.089
	D22	3.13	2.51	24.701	3.13	2.67	17.228	3.13	2.86	9.441	3.13	2.97	5.387

The sensors shown in Figures 4.46 and 4.47 represent the soil, foundation, first and third floor. The improvement of N=4 compared to unreinforced system can be seen in these figures. The maximum acceleration improvements of first and third floor are 36% and 25%. It can be observed that the reduction of foundation acceleration is -3%, 0%, 7% and 15% for N=1, N=2, N=3 and N=4, respectively. There is no improvement for N=1 and N=2 in foundation.

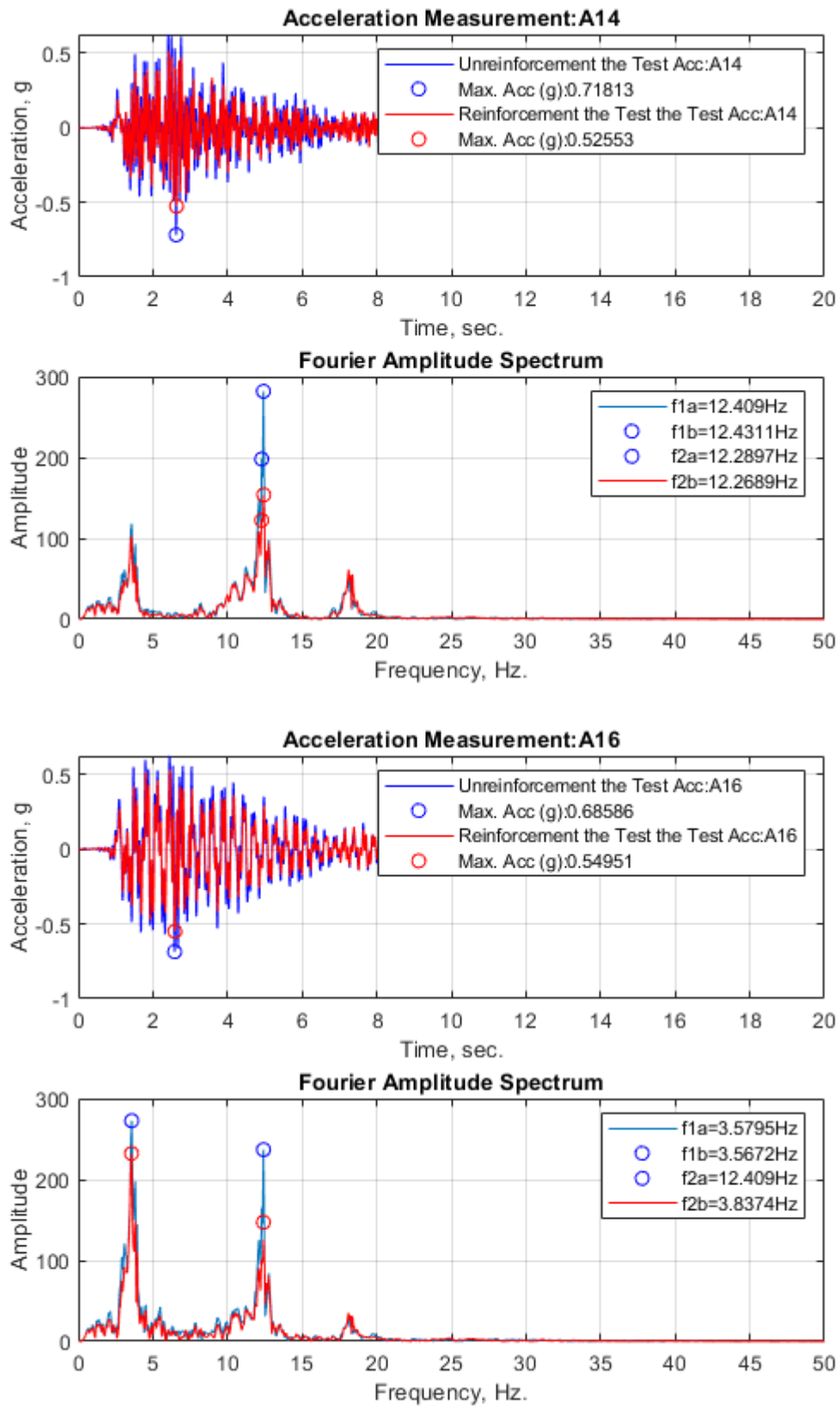


Figure 4.46. Acceleration Measurements and FAS of 1st and 3rd Floors under Kocaeli Earthquake Motion (PGA= 0.21 g).

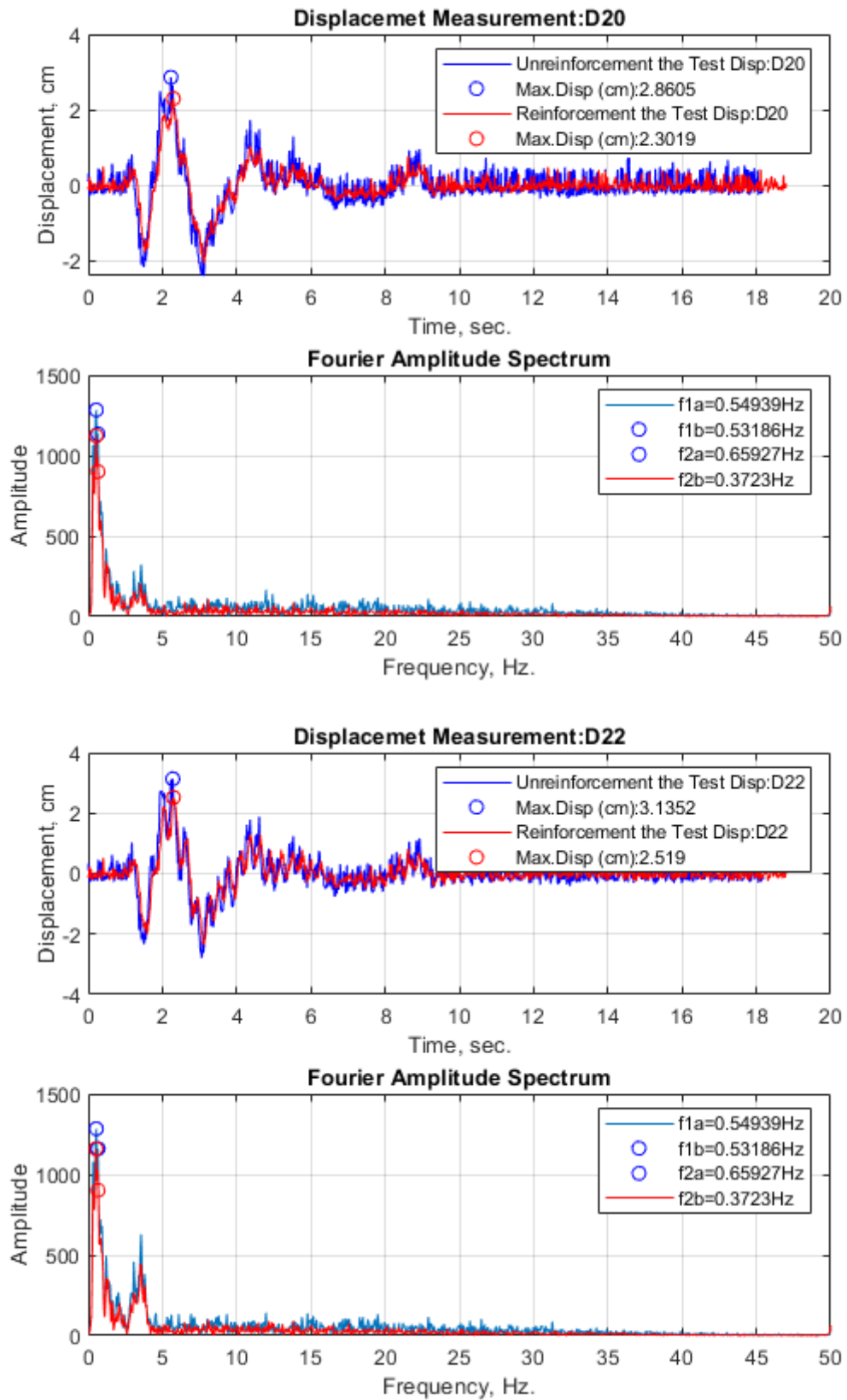


Figure 4.47. Displacement Measurements and FAS of 1st and 3rd Floors under Kocaeli Earthquake Motion (PGA= 0.21 g).

In Figure 4.48 and Figure 4.49., the changing acceleration values and the changing displacement values in accordance with story and reinforcement layers can be seen. The first floor is decreased up to 36% in acceleration value and the maximum reduction of third floor is 25%. Besides, for N=1, the third floor's improvement become negative, which is nearly 1.5%.

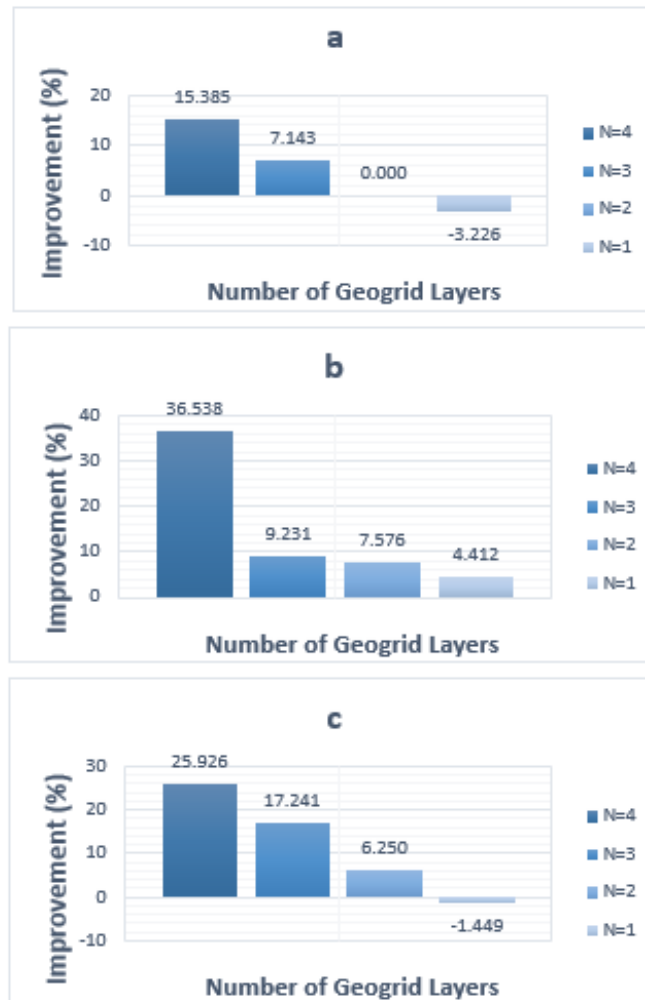


Figure 4.48. The Acceleration Improvement Graphs in Accordance with Story and Reinforcement Layers for (a) Foundation, (b) 1st Floor, (c) 3rd Floor under Kocaeli Earthquake Motion (PGA= 0.21 g).

As it can be seen for the first, second and third floor, the maximum decrease of story's displacement is approximately 24%.

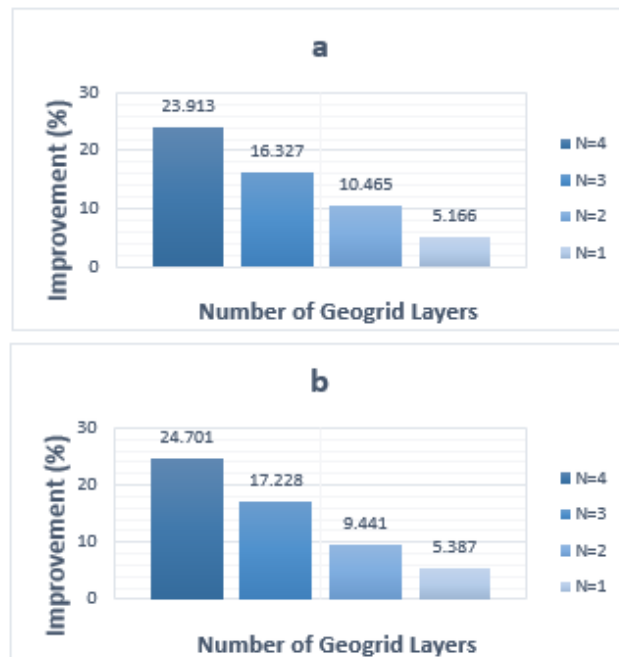


Figure 4.49. The Displacement Improvement Graphs in Accordance with Story and Reinforcement Layers for (a) 1st Floor, (b) 3rd Floor under Kocaeli Earthquake Motion (PGA= 0.21 g).

Arias intensity improvements, with the help of the fundamental period of all N values under dynamic loads for soil, foundations, floors, the period lengthening ratios and also RMS of peak values can be observed in Table 4.29 and Table 4.30.

Table 4.29. Fundamental Period and Period Lengthening Ratios under Kocaeli Earthquake Motion (PGA= 0.21 g).

	Fundamental Period (Hz)					Period Lengthening Ratio			
	N=4	N=3	N=2	N=1	N=0	N=4	N=3	N=2	N=1
In-Soil	10.48	10.32	10.32	10.32	10.32	0.98	1.00	1.00	1.00
Foundation	10.48	10.32	10.32	10.32	10.32	0.98	1.00	1.00	1.00
1st Floor	0.53	0.53	0.53	0.53	0.54	1.02	1.02	1.02	1.02
2nd Floor	0.53	0.53	0.53	0.53	0.54	1.02	1.02	1.02	1.02
3rd Floor	0.53	0.53	0.53	0.53	0.54	1.02	1.02	1.02	1.02

Table 4.30. RMS and Arias Intensity Improvement Ratios under Kocaeli Earthquake Motion (PGA= 0.21 g).

Root Mean Square (RSM)				Arias Intensity	
Horizontal Acceleration(g)	Peak	RSM-Rein.	RSM Imp (%)		Arias Intensity Imp (%)
In-Soil	0.3	0.26	13.33	In-Soil	24.2
Foundation	0.3	0.29	4.12	Foundation	18
1st Floor	0.71	0.63	12.58	1st Floor	40.56
2nd Floor	0.56	0.5	12.99	2nd Floor	25.87
3rd Floor	0.68	0.62	10.54	3rd Floor	30.85

Arias intensity values are decreased almost 1%, 1% and 3% for soil, foundation and floors. The reduction of RMS is 13% for soil, 4% for foundation, 12%, 12%, and 10%. Also, there is no change the natural period of model. The period lengthening ratio fluctuates up to %2. In Figure 4.50, improvement ratios of Arias Intensity and story drifts were exhibited.

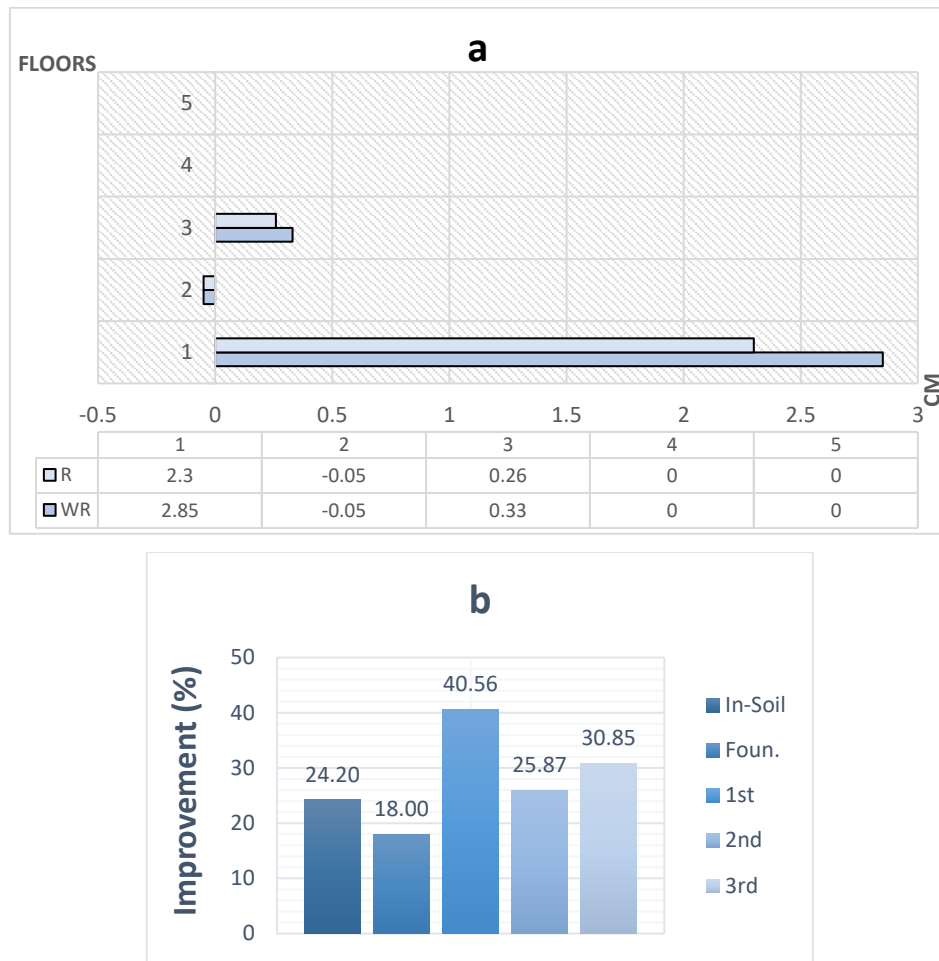


Figure 4.50. Improvement Ratios considering (a) Story Drifts and (b) Arias Intensity under Kocaeli Earthquake Motion (PGA= 0.21 g).

4.4.3. Seismic Response of 3-Story Model under Kocaeli Earthquake Motion (PGA= 0.51 g)

Table 4.31 shows the reduced acceleration and displacement values through all sensors comparing to unreinforced system for 3-Storey model under Kocaeli Earthquake (0.51g). In the soil, peak accelerations are 0.47g in the underside, 0.5g midpoint, and 0.51g in the upper side. The reduction of acceleration in underside is -2%, 4%, 17% and 20%, the reduction of acceleration in midpoint is 0%, 6%, 16% and 19%, the reduction of acceleration in upper side is -2%, 4%, 15% and 21% roughly for N=1, N=2, N=3 and N=4, respectively.

Table 4.31. Summary of all tested Cases under Kocaeli Earthquake motion (PGA=0.51g).

		N=4			N=3			N=2			N=1		
		WR	R	IMP. (%)	WR	R	IMP. (%)	WR	R	IMP. (%)	WR	R	IMP. (%)
In Soil (g)	A5	0.47	0.39	20.513	0.47	0.4	17.500	0.47	0.45	4.444	0.47	0.48	-2.083
	A6	0.48	0.39	23.077	0.48	0.41	17.073	0.48	0.45	6.667	0.48	0.47	2.128
	A7	0.48	0.39	23.077	0.48	0.41	17.073	0.48	0.45	6.667	0.48	0.47	2.128
	A8	0.5	0.4	25.000	0.5	0.42	19.048	0.5	0.47	6.383	0.5	0.49	2.041
	A9	0.49	0.39	25.641	0.49	0.41	19.512	0.49	0.46	6.522	0.49	0.49	0
	A10	0.49	0.4	22.500	0.49	0.42	16.667	0.49	0.46	6.522	0.49	0.5	-2.000
	A11	0.5	0.42	19.048	0.5	0.43	16.279	0.5	0.47	6.383	0.5	0.5	0
	A12	0.51	0.42	21.429	0.51	0.44	15.909	0.51	0.49	4.082	0.51	0.52	-1.923
Foun.(g)	A13	0.49	0.38	28.947	0.49	0.41	19.512	0.49	0.47	4.255	0.49	0.48	2.083
3 Storey Model (cm)	A14	1.01	0.91	10.989	1.01	0.93	8.602	1.01	0.98	3.061	1.01	1.02	-0.98
	A15	0.86	0.72	19.444	0.86	0.76	13.158	0.86	0.81	6.173	0.86	0.87	-1.149
	A16	1.06	0.89	19.101	1.06	0.96	10.417	1.06	1	6.000	1.06	1.1	-3.636
	D20	5.72	4.6	24.348	5.72	4.67	22.484	5.72	5.57	2.693	5.72	5.71	0.175
	D21	5.63	4.49	25.390	5.63	4.56	23.465	5.63	5.39	4.453	5.63	5.49	2.550
	D22	6.94	5.38	28.996	6.94	5.62	23.488	6.94	6.16	12.662	6.94	6.37	8.948

In Figure 4.51. and 4.52, The sensors showing acceleration, displacement measurement and fourier amplitude spectrum can be seen, two of them were selected between unreinforced system and N=4 and through these figures the maximum improvement can be observed at these points.

The decrease of foundation acceleration is 2%, 4%, 19% and 28% for N=1, N=2, N=3 and N=4, respectively.

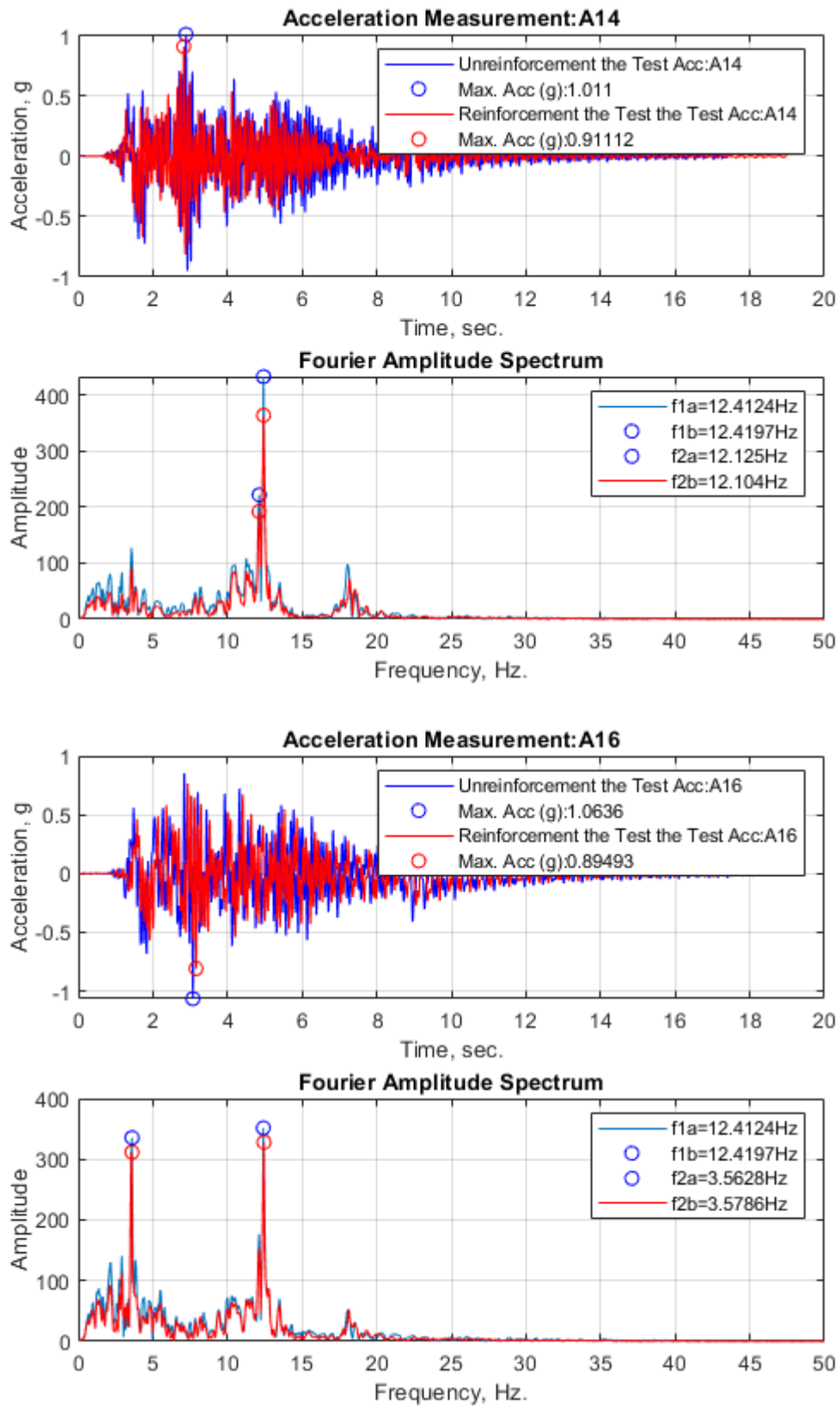


Figure 4.51. Acceleration Measurements and FAS of 1st and 3rd Floors under Kocaeli Earthquake Motion (PGA= 0.51 g).

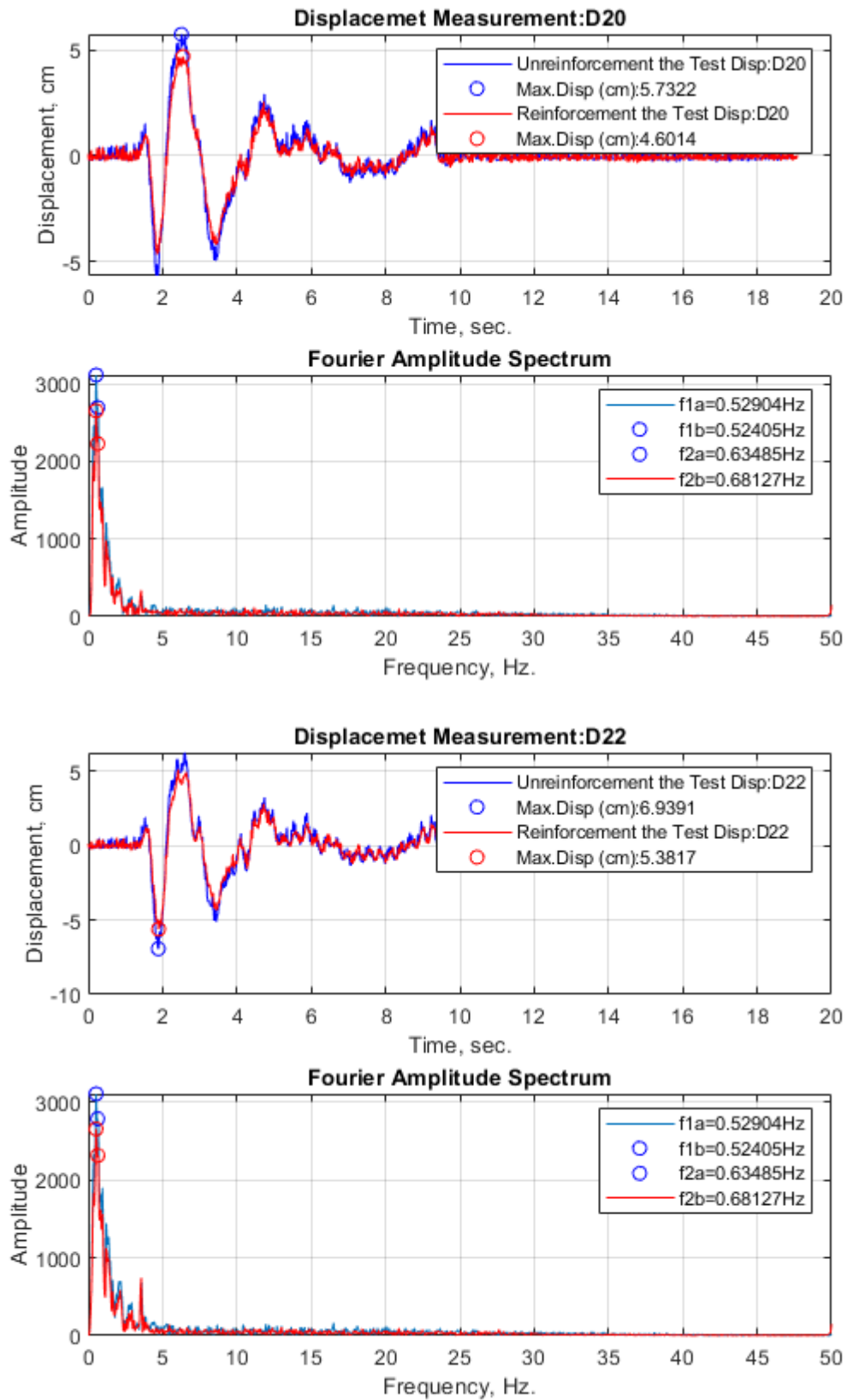


Figure 4.52. Displacement Measurements and FAS of 1st and 3rd Floors under Kocaeli Earthquake Motion (PGA= 0.51 g).

Figure 4.53 and Figure 4.54 represent the changing acceleration values and the changing displacement values in accordance with story and reinforcement layers. The graphs include the improvements compared unreinforced system for foundation, first and third floor for each N values.

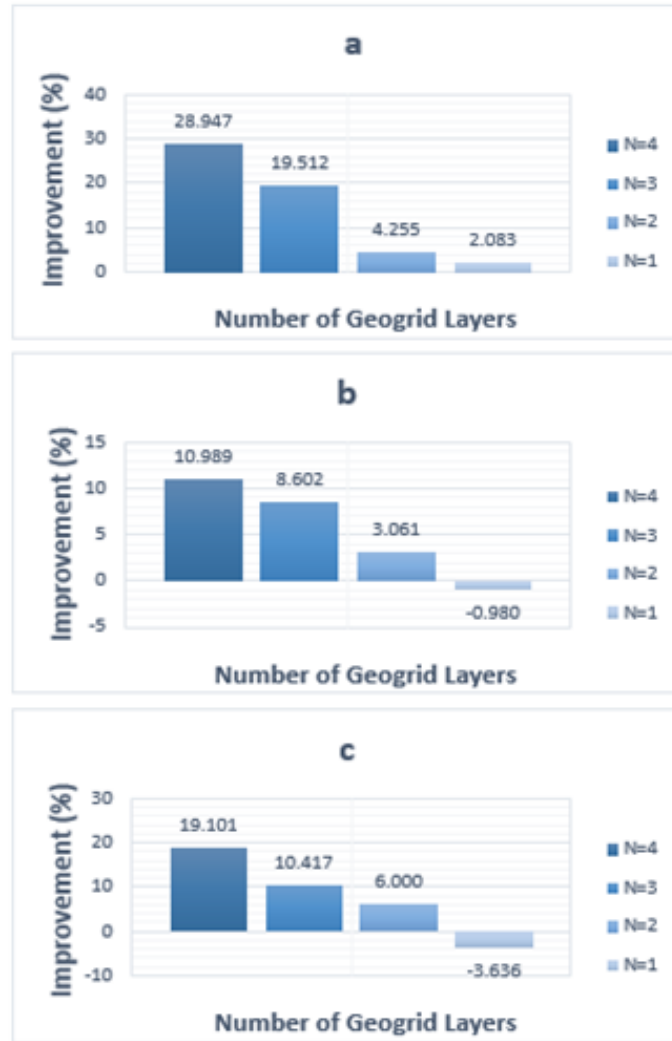


Figure 4.53. The Acceleration Improvement Graphs in Accordance with Story and Reinforcement Layers for (a) Foundation, (b) 1st Floor, (c) 3rd Floor under Kocaeli Earthquake Motion (PGA= 0.51 g).

The changing acceleration start with -1% for N=1, with the increase in the geogrid layers it becomes 3%, 8%, 10% on the first floor for N=2, N=3, N=4, respectively. For the third floor, the acceleration reduction values are reduced approximately -3% and 6%, 10%

and 19% comparing to unreinforced system. For all floors, the reduction of acceleration becomes negative in $N=1$.

For the first, and third floor, the maximum decrease of story's displacement is 24% and 28% respectively. Also, for the first floor there is no considerable reduction in $N=1$, but for $N=3$ it reaches up to 22%.

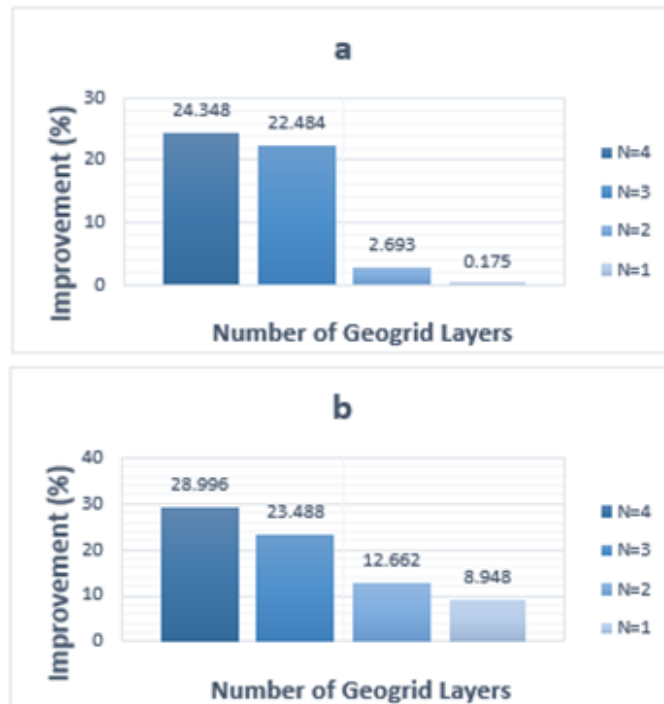


Figure 4.54. The Displacement Improvement Graphs in Accordance with Story and Reinforcement Layers for (a) 1st Floor, (b) 3rd Floor under Kocaeli Earthquake Motion (PGA= 0.51 g).

Arias intensity improvements the period lengthening ratios and for RMS of peak values soil, foundations and floors were shown in Table 4.32 and 4.33.

Table 4.32. Fundamental Period and Period Lengthening Ratios under Kocaeli Earthquake Motion (PGA= 0.51 g).

	Fundamental Period (Hz)					Period Lengthening Ratio			
	N=4	N=3	N=2	N=1	N=0	N=4	N=3	N=2	N=1
In-Soil	10.48	10.47	10.48	10.48	10.28	0.98	0.98	0.98	0.98
Foundation	10.47	10.47	10.47	10.47	10.31	0.98	0.98	0.98	0.98
1st Floor	0.52	0.52	0.52	0.52	0.52	1.00	1.00	1.00	1.00
2nd Floor	0.52	0.52	0.52	0.52	0.52	1.00	1.00	1.00	1.00
3rd Floor	0.52	0.52	0.52	0.52	0.52	1.00	1.00	1.00	1.00

Table 4.33. RMS and Arias Intensity Improvement Ratios under Kocaeli Earthquake Motion (PGA= 0.51 g).

Root Mean Square(RSM)				Arias Intensity	
Horizontal Acceleration(g)	Peak	RSM-Rein.	RSM Imp(%)		Arias Intensity Imp (%)
In-Soil	0.51	0.47	8.7	In-Soil	25.93
Foundation	0.49	0.44	12.13	Foundation	33.87
1st Floor	1.01	0.96	5.1	1st Floor	12.2
2nd Floor	0.86	0.79	8.59	2nd Floor	23.14
3rd Floor	1.06	0.99	7.03	3rd Floor	22.73

Arias intensity values for soil region and foundation are decreased nearly 8%, 12% and it reduces up to 8% for floors. RMS improvement values for soil, foundation and floors are 8% 12%, 5%, 8%, and 7%, respectively. Also, there is no change in the natural period of model. The period lengthening ratio fluctuates up to %2. Improvement ratios of Arias Intensity and Story Drifts can be seen in Figure 4.55.

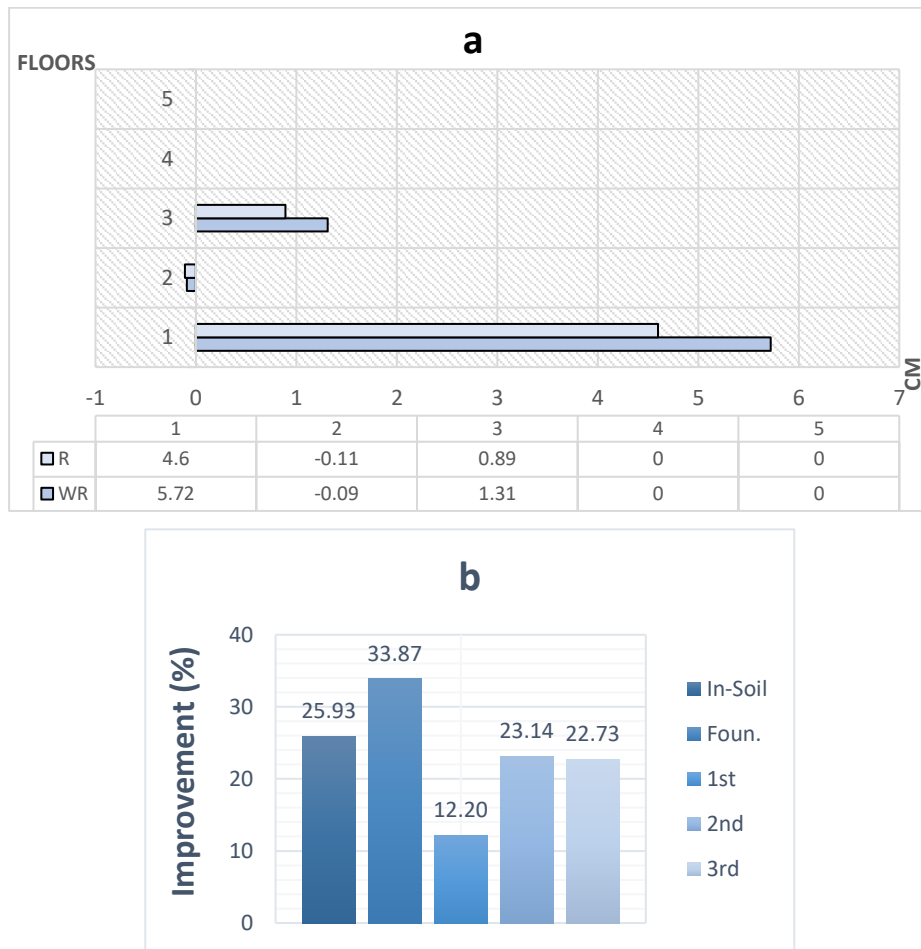


Figure 4.55. Improvement Ratios considering (a) Story Drifts and (b) Arias Intensity under Kocaeli Earthquake Motion (PGA= 0.51 g).

4.3.5. Seismic Response of 3-Story Model under El Centro Earthquake Motion (PGA =0.35 g)

Table 4.34 shows the reduced acceleration and displacement values through all sensors comparing to unreinforced system for 3-Storey model under El Centro Earthquake (0.35g). In the soil, peak accelerations are 0.35g in the underside, 0.45g in midpoint, and 0.49g in the upper side. The reduction of acceleration in underside is 6%, 6%, 9% and 25%, the reduction of acceleration in midpoint is -2%, 2%, 28% and 32%, the reduction of acceleration in upper side is 2%, 6%, 19% and 22% roughly for N=1, N=2, N=3 and N=4, respectively. The maximum acceleration improvement in the soil is nearly 32%. For this earthquake motion, the progression between N=2 and N=3 is quite effective for certain parts.

Table 4.34. Summary of all tested Cases under El Centro Earthquake motion
(PGA=0.35g).

		N=4			N=3			N=2			N=1		
		WR	R	IMP. (%)	WR	R	IMP. (%)	WR	R	IMP. (%)	WR	R	IMP. (%)
In Soil (g)	A5	0.35	0.28	25.000	0.35	0.32	9.375	0.35	0.33	6.061	0.35	0.33	6.061
	A6	0.36	0.3	20.000	0.36	0.33	9.091	0.36	0.33	9.091	0.36	0.34	5.882
	A7	0.36	0.31	16.129	0.36	0.33	9.091	0.36	0.35	2.857	0.36	0.36	0
	A8	0.37	0.31	19.355	0.37	0.34	8.824	0.37	0.34	8.824	0.37	0.34	8.824
	A9	0.37	0.3	23.333	0.37	0.34	8.824	0.37	0.36	2.778	0.37	0.37	0
	A10	0.37	0.31	19.355	0.37	0.32	15.625	0.37	0.35	5.714	0.37	0.36	2.778
	A11	0.45	0.34	32.353	0.45	0.35	28.571	0.45	0.44	2.273	0.45	0.46	-2.174
	A12	0.49	0.4	22.500	0.49	0.41	19.512	0.49	0.46	6.522	0.49	0.48	2.083
Foun.(g)	A13	0.45	0.4	12.500	0.45	0.4	12.500	0.45	0.43	4.651	0.45	0.45	0
3 Storey Model (cm)	A14	0.68	0.58	17.241	0.68	0.59	15.254	0.68	0.66	3.030	0.68	0.72	-5.556
	A15	0.62	0.55	12.727	0.62	0.57	8.772	0.62	0.59	5.085	0.62	0.62	0
	A16	0.79	0.71	11.268	0.79	0.71	11.268	0.79	0.73	8.219	0.79	0.76	3.947
	D20	2.92	2.28	28.070	2.92	2.5	16.800	2.92	2.6	12.308	2.92	2.68	8.955
	D21	2.81	2.46	14.228	2.81	2.4	17.083	2.81	2.62	7.252	2.81	2.73	2.930
	D22	3.19	2.9	10.000	3.19	2.96	7.770	3.19	3.03	5.281	3.19	3.12	2.244

The sensors shown in Figures 4.56 and 4.57 represent first and third floor improvements in displacement and acceleration. N=4 compared to unreinforced system was constituted. The decrease of foundation acceleration is 0%, 4%, 12% and 12% for N=1, N=2, N=3 and N=4, respectively. For N=3 and N=4, there is no reduction for acceleration values.

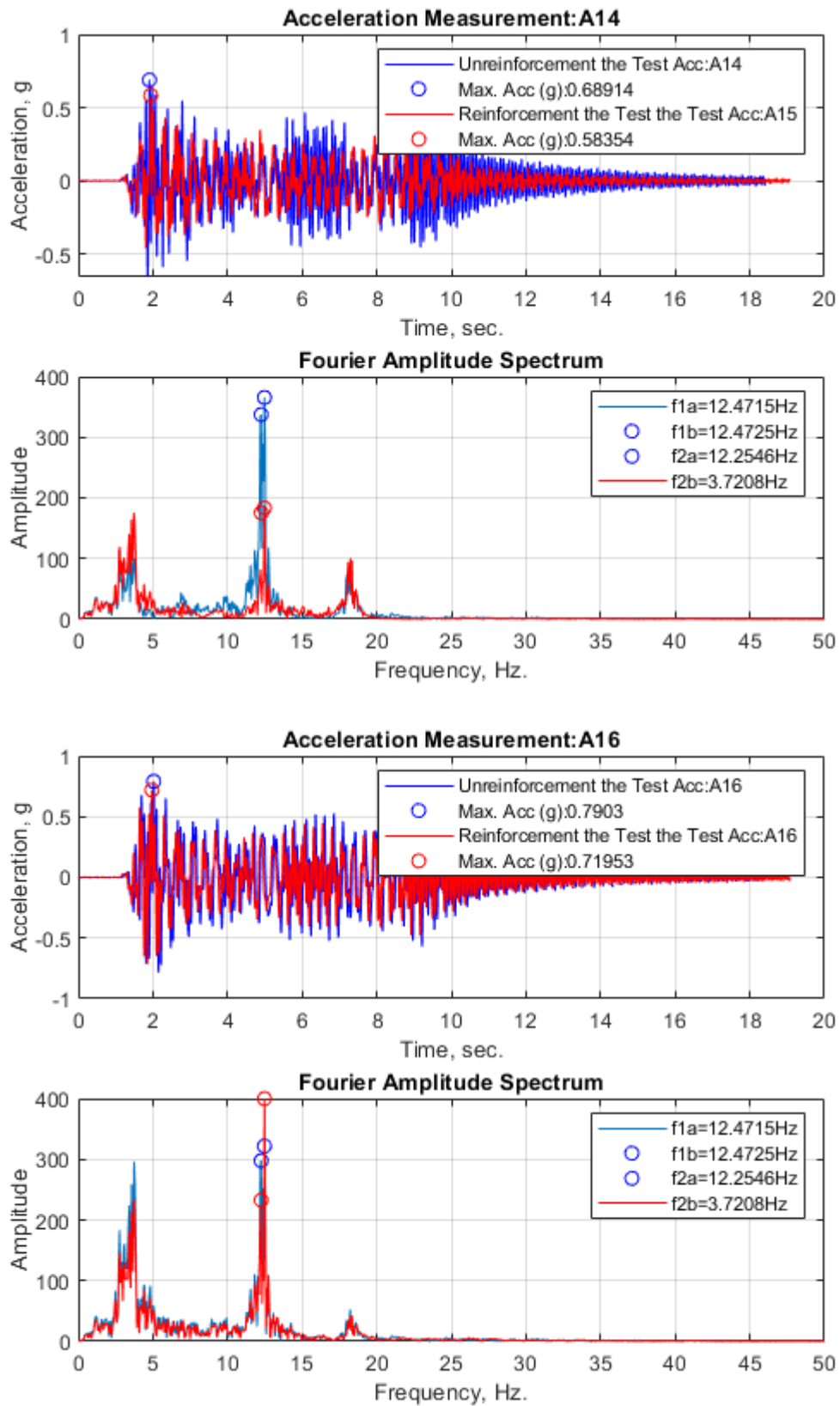


Figure 4.56. Acceleration Measurements and FAS of 1st and 3rd Floors under El Centro Earthquake Motion (PGA= 0.35 g).

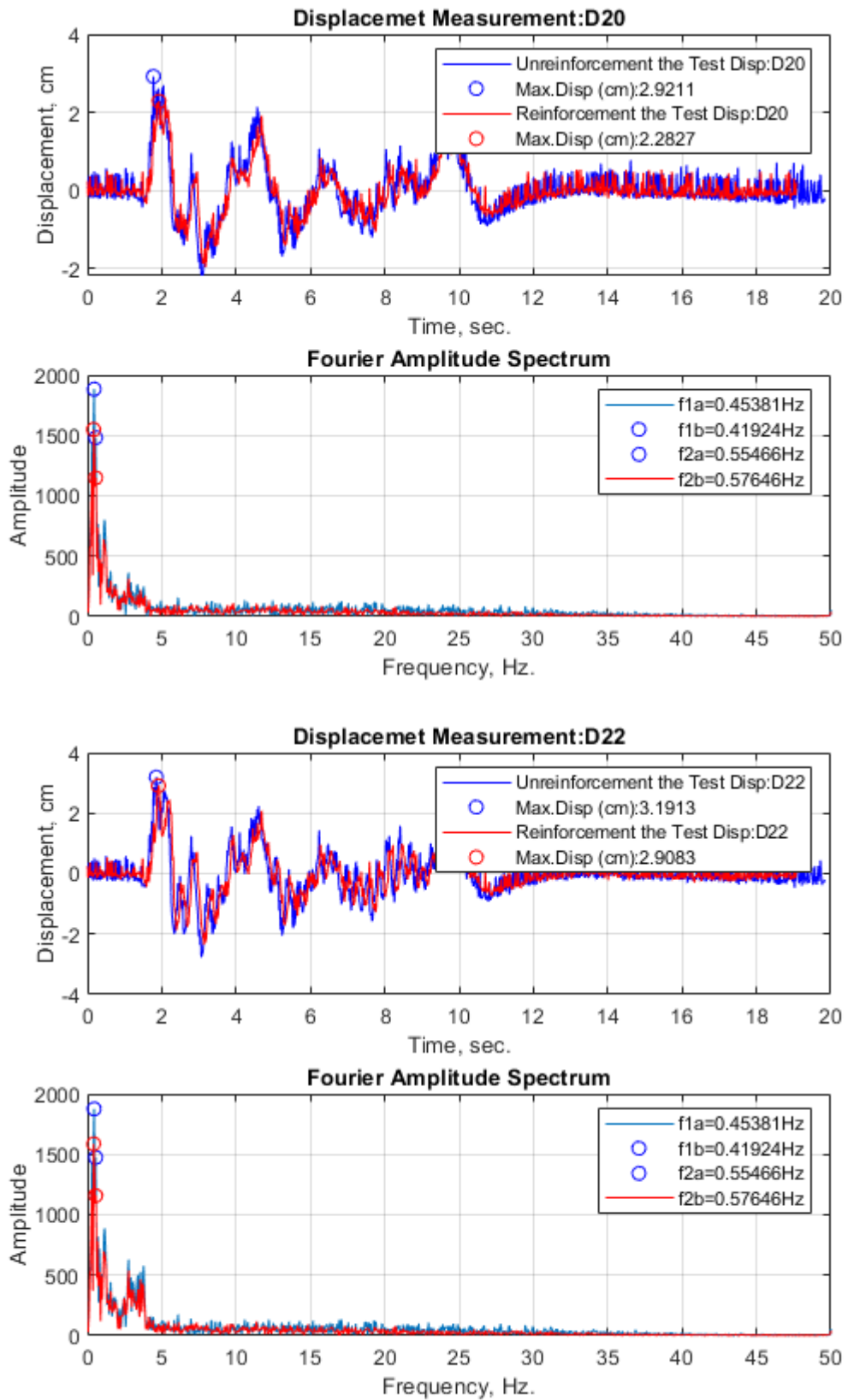


Figure 4.57. Displacement Measurements and FAS of 1st and 3rd Floors under El Centro Earthquake Motion (PGA= 0.35 g).

In Figure 4.58 and Figure 4.59, the changing acceleration values and the changing displacement values in accordance with story and reinforcement layers can be seen the improvements compared unreinforced system for foundation, first and third floor for each N values.

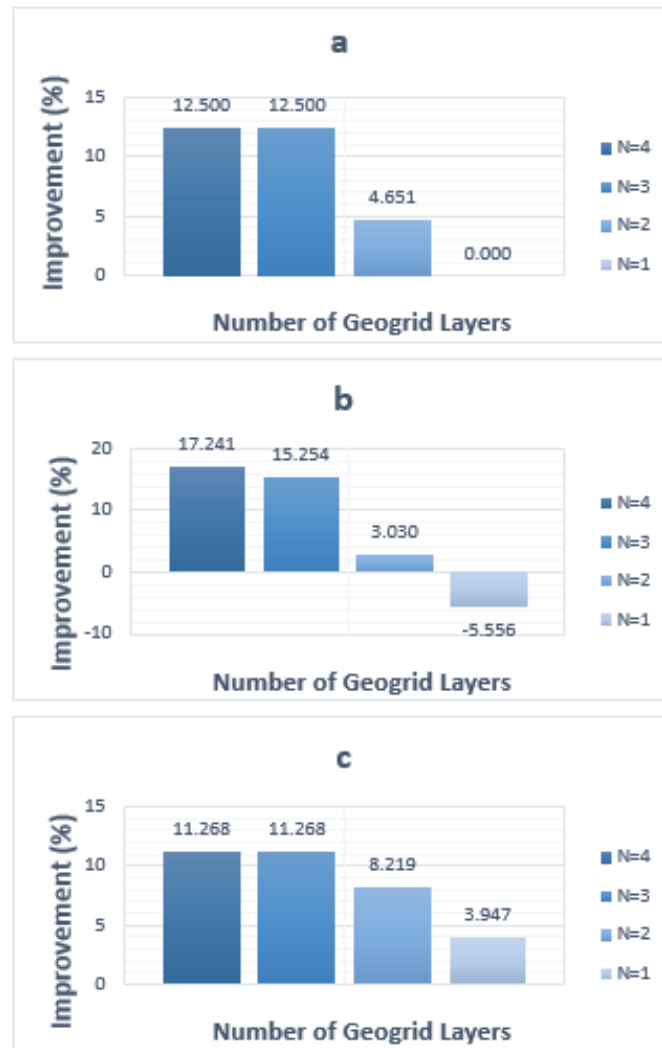


Figure 4.58. The Acceleration Improvement Graphs in Accordance with Story and Reinforcement Layers for (a) Foundation, (b) 1st Floor, (c) 3rd Floor El Centro Earthquake Motion (PGA= 0.35 g).

It can be observed that for N=1 nearly there is no contribution to the reduction of acceleration on the model except the third floor for El Centro Earthquake (0.35g). The improvements in acceleration values become negative or 0% for N=1. With the increase in

the geogrid layers, the reduction of acceleration becomes 3%, 15%, and 17% for the first floor 8%, 11%, and 11% for the third floor for N=2, N=3, and N=4, respectively.

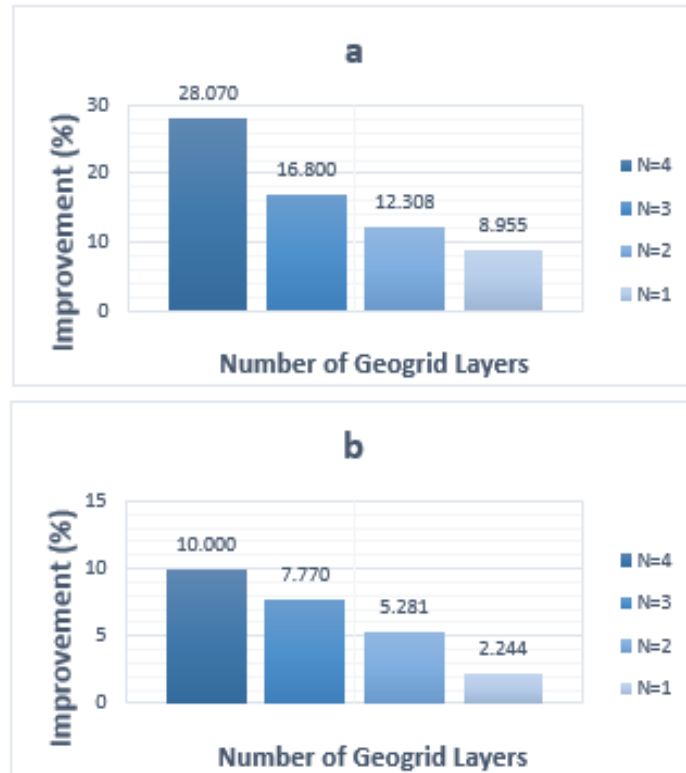


Figure 4.59. The Displacement Improvement Graphs in Accordance with Story and Reinforcement Layers for (a) 1st Floor, (b) 3rd Floor under El Centro Earthquake Motion (PGA= 0.35 g).

In the first, and third floor, the maximum decrease of story's displacement is 28% and 10%, respectively. For the second and third floors, there is no considerable reduction, it is just 2%.

Table 4.35. Fundamental Period and Period Lengthening Ratios under El Centro Earthquake Motion (PGA= 0.35 g).

	Fundamental Period (Hz)					Period Lengthening Ratio			
	N=4	N=3	N=2	N=1	N=0	N=4	N=3	N=2	N=1
In-Soil	6.91	6.91	6.91	6.91	6.88	1.00	1.00	1.00	1.00
Foundation	6.91	6.91	6.91	6.91	6.88	1.00	1.00	1.00	1.00
1st Floor	0.41	0.41	0.41	0.41	0.45	1.10	1.10	1.10	1.10
2nd Floor	0.41	0.41	0.41	0.41	0.45	1.10	1.10	1.10	1.10
3rd Floor	0.41	0.41	0.41	0.41	0.45	1.10	1.10	1.10	1.10

Table 4.36. RMS and Arias Intensity Improvement Ratios under El Centro Earthquake Motion (PGA= 0.35 g).

Root Mean Square (RSM)				Arias Intensity	
Horizontal Acceleration(g)	Peak	RSM-Rein.	RSM Imp (%)		Arias Intensity Imp (%)
In-Soil	0.49	0.44	11.67	In-Soil	27.23
Foundation	0.45	0.42	7.01	Foundation	14.63
1st Floor	0.68	0.64	6.25	1st Floor	19.14
2nd Floor	0.62	0.58	6.33	2nd Floor	15.15
3rd Floor	0.79	0.73	8.55	3rd Floor	13.41

As it is shown in Table 4.35 and Table 4.36, Arias intensity values are decreased for soil region and foundation nearly 1% and 2%. It reduces up to 3% for floors. RMS improvement values for soil, foundation and floors are 11%, 7%, 7%, 6% and 8%, respectively. The period lengthening ratio fluctuates up to %10. In Figure 4.60, Arias Intensity improvement graph and Story Drifts are given.

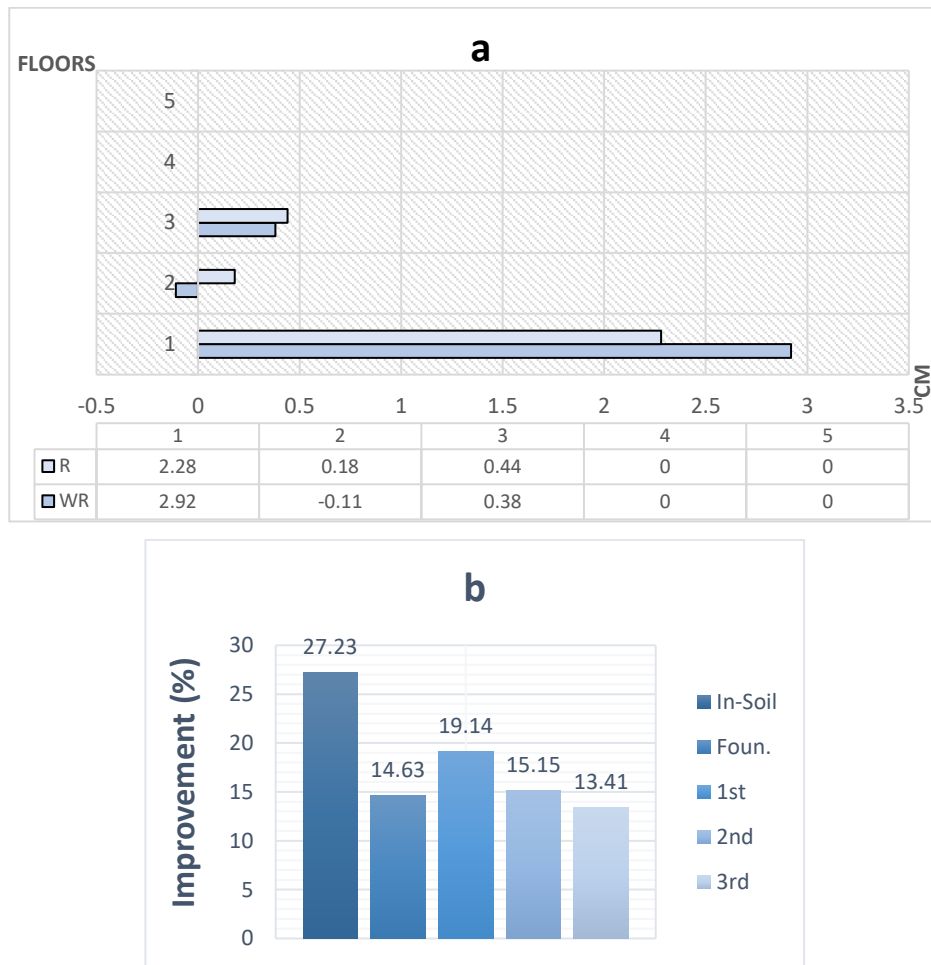


Figure 4.60. Improvement Ratios considering (a) Story Drifts and (b) Arias Intensity under El Centro Earthquake Motion (PGA= 0.35 g).

4.3.6. Seismic Response of 3-Story Model under El Centro Earthquake Motion (PGA =0.55 g)

Table 4.37.shows the reduced acceleration and displacement values through all sensors comparing to unreinforced system for 3-Storey model under El Centro Earthquake (0.55g). In the soil, peak accelerations are 0.54g in the underside, 0.58g in the midpoint, and 0.59g in the upper side. The maximum improvement of acceleration in the underside, midpoint and upper side is 17%, 34% and 22%, respectively. Also, some parts in the soil the reduction becomes negative.

Table 4.37. Summary of all tested Cases under El Centro Earthquake motion
(PGA=0.55g).

		N=4			N=3			N=2			N=1		
		WR	R	IMP. (%)	WR	R	IMP. (%)	WR	R	IMP. (%)	WR	R	IMP. (%)
In Soil (g)	A5	0.54	0.46	17.391	0.54	0.46	17.391	0.54	0.52	3.846	0.54	0.56	-3.571
	A6	0.56	0.45	24.444	0.56	0.45	24.444	0.56	0.5	12.000	0.56	0.52	7.692
	A7	0.54	0.45	20.000	0.54	0.45	20.000	0.54	0.49	10.204	0.54	0.55	-1.818
	A8	0.59	0.5	18.000	0.59	0.5	18.000	0.59	0.54	9.259	0.59	0.55	7.273
	A9	0.55	0.46	19.565	0.55	0.46	19.565	0.55	0.51	7.843	0.55	0.57	-3.509
	A10	0.56	0.46	21.739	0.56	0.46	21.739	0.56	0.52	7.692	0.56	0.54	3.704
	A11	0.58	0.43	34.884	0.58	0.43	34.884	0.58	0.54	7.407	0.58	0.59	-1.695
	A12	0.59	0.48	22.917	0.59	0.48	22.917	0.59	0.55	7.273	0.59	0.57	3.509
Foun.(g)	A13	0.47	0.41	14.634	0.47	0.41	14.634	0.47	0.46	2.174	0.47	0.48	-2.083
3 Storey Model (cm)	A14	0.72	0.61	18.033	0.72	0.61	18.033	0.72	0.68	5.882	0.72	0.7	2.857
	A15	0.83	0.66	25.758	0.83	0.66	25.758	0.83	0.77	7.792	0.83	0.86	-3.488
	A16	0.74	0.6	23.333	0.74	0.6	23.333	0.74	0.71	4.225	0.74	0.74	0
	D20	4.33	3.67	17.984	4.33	3.67	17.984	4.33	4.14	4.589	4.34	4.22	2.844
	D21	4.47	3.89	14.910	4.47	3.89	14.910	4.47	4.27	4.684	4.47	4.4	1.591
	D22	5.23	4.65	12.473	5.23	4.65	12.473	5.23	5	4.600	5.24	5.19	0.963

It can be observed that the reduction of foundation acceleration is -2%, 2%, 14% and 14% for N=1, N=2, N=3 and N=4, respectively. Despite the fact that the improvement in acceleration value become negative for N=1 in foundation, it becomes 14% with the increasing geogrid layers. However, there is no change for N=3 and N=4.

The sensors shown in Figures 4.61 and 4.62 represent the soil, foundation, first and third floor. The improvement of N=4 compared to unreinforced system can be observed with the help of them. The decrease of top floor acceleration is 0%, 4%, 23% and 23% for N=1, N=2, N=3 and N=4, respectively.

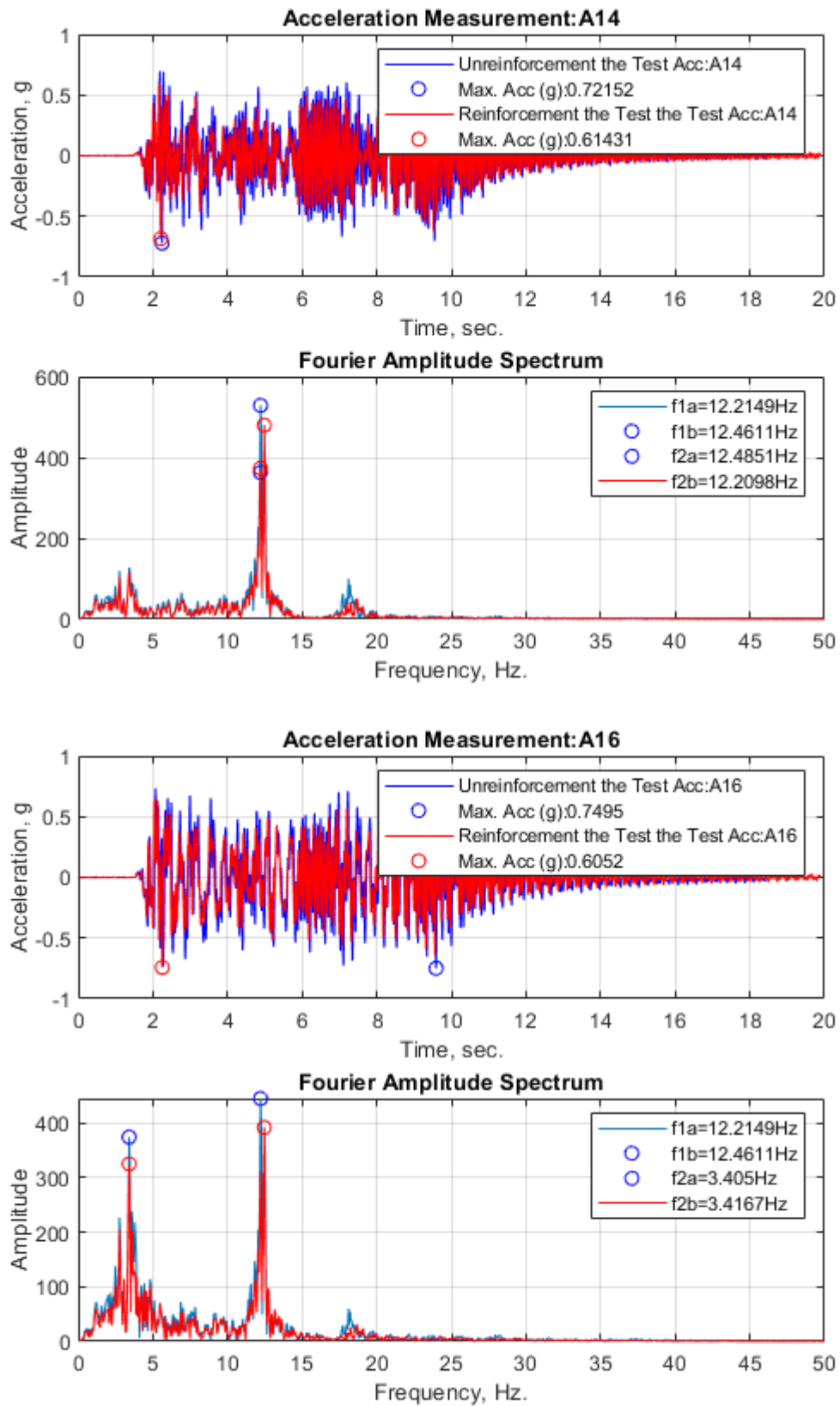


Figure 4.61. Acceleration Measurements and FAS of 1st and 3rd Floors under El Centro Earthquake Motion (PGA= 0.55 g).

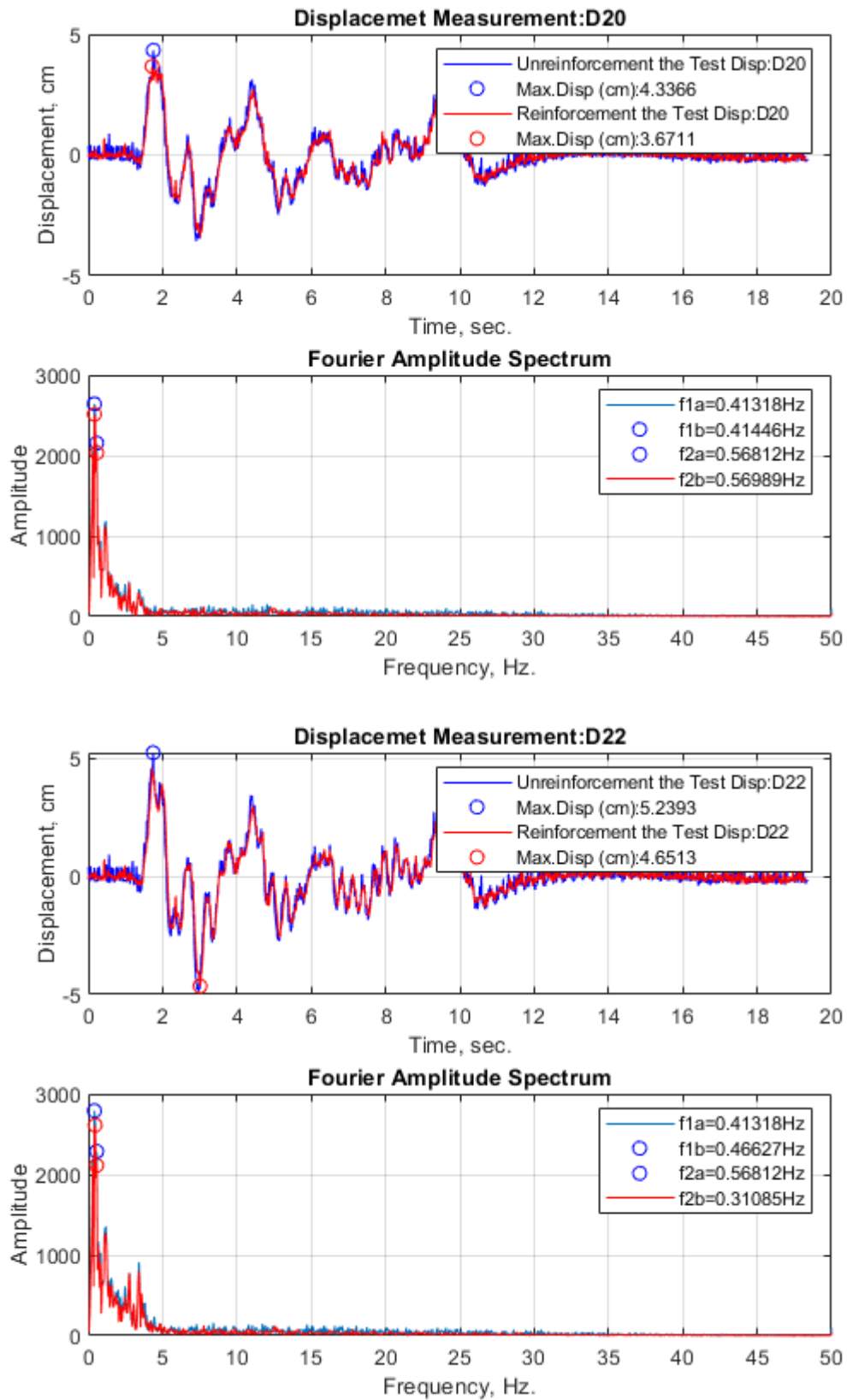


Figure 4.62. Displacement Measurements and FAS of 1st and 3rd Floors under El Centro Earthquake Motion (PGA= 0.55 g).

The changing acceleration values and the changing displacement values in accordance with story and reinforcement layers were shown in Figure 4.63. and Figure 4.64 for soil, foundation, first, and third floor for each N values.

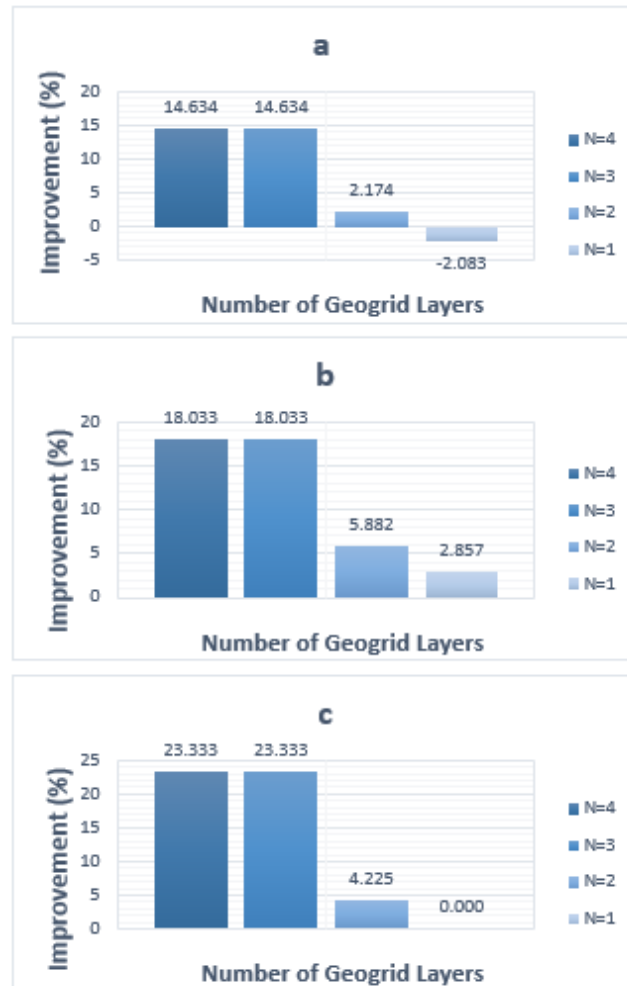


Figure 4.63. The Acceleration Improvement Graphs in Accordance with Story and Reinforcement Layers for (a) Foundation, (b) 1st Floor, (c) 3rd Floor El Centro Earthquake Motion (PGA= 0.55 g).

The first floor is decreased up to 18% in acceleration value, and the maximum reduction of third floor is 23%. For N=1, while the third floor's improvement become zero, the second floor's improvement becomes negative, and the first floor has slightly improvement in acceleration values for N=1. Also, another important point for the reduction of acceleration on model is that there is significant decrease in values for N=2 and N=3.

As it can be seen for the first, and third floors, the maximum decrease of story's displacement is 17% and 12%, respectively. The reduction of displacement becomes 0% for N=1 on the third floor.

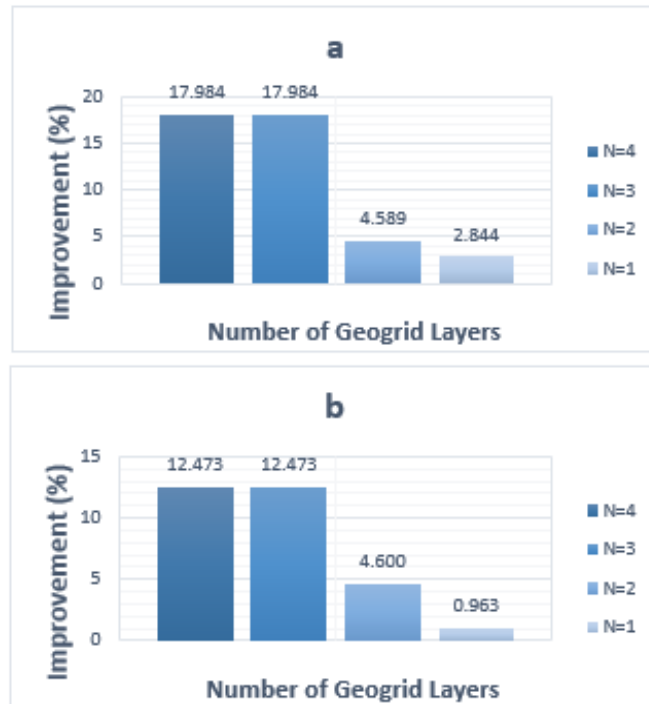


Figure 4.64. The Displacement Improvement Graphs in Accordance with Story and Reinforcement Layers for (a) 1st Floor, (b) 3rd Floor under El Centro Earthquake Motion (PGA= 0.55 g).

In Table 4.37 and Table 4.38, Arias intensity improvements were exhibited as well as with the help of the fundamental period of all N values for soil, foundations, floors, the period lengthening ratios were given and also RMS of peak values were shown.

Table 4.38. Fundamental Period and Period Lengthening Ratios under El Centro Earthquake Motion (PGA= 0.55 g).

	Fundamental Period (Hz)					Period Lengthening Ratio			
	N=4	N=3	N=2	N=1	N=0	N=4	N=3	N=2	N=1
In-Soil	6.91	6.91	6.91	6.91	6.88	1.00	1.00	1.00	1.00
Foundation	6.91	6.91	6.91	6.91	6.88	1.00	1.00	1.00	1.00
1st Floor	0.41	0.41	0.41	0.41	0.45	1.10	1.10	1.10	1.10
2nd Floor	0.41	0.41	0.41	0.41	0.45	1.10	1.10	1.10	1.10
3rd Floor	0.41	0.41	0.41	0.41	0.45	1.10	1.10	1.10	1.10

Table 4.39. RMS and Arias Intensity Improvement Ratios under El Centro Earthquake Motion (PGA= 0.55 g).

Root Mean Square (RSM)				Arias Intensity	
Horizontal Acceleration(g)	Peak	RSM-Rein.	RSM Imp (%)		Arias Intensity Imp (%)
In-Soil	0.59	0.52	13.12	In-Soil	27.73
Foundation	0.47	0.44	6.56	Foundation	17.12
1st Floor	0.72	0.65	10.55	1st Floor	20.02
2nd Floor	0.83	0.74	11.82	2nd Floor	30.65
3rd Floor	0.74	0.67	11.19	3rd Floor	27.77

As it is shown, arias intensity values are decreased almost 2%, 2% and 3% for soil, foundation, and floors. The reduction of RMS is 13% for soil, 6% for foundation, 10%, 11% and 11% for floors roughly. Also, there is no change the natural period of model. The period lengthening ratio fluctuates up to 10% for a few times. In Figure 4.65, Arias Intensity improvement graph and Story Drifts can be observed.

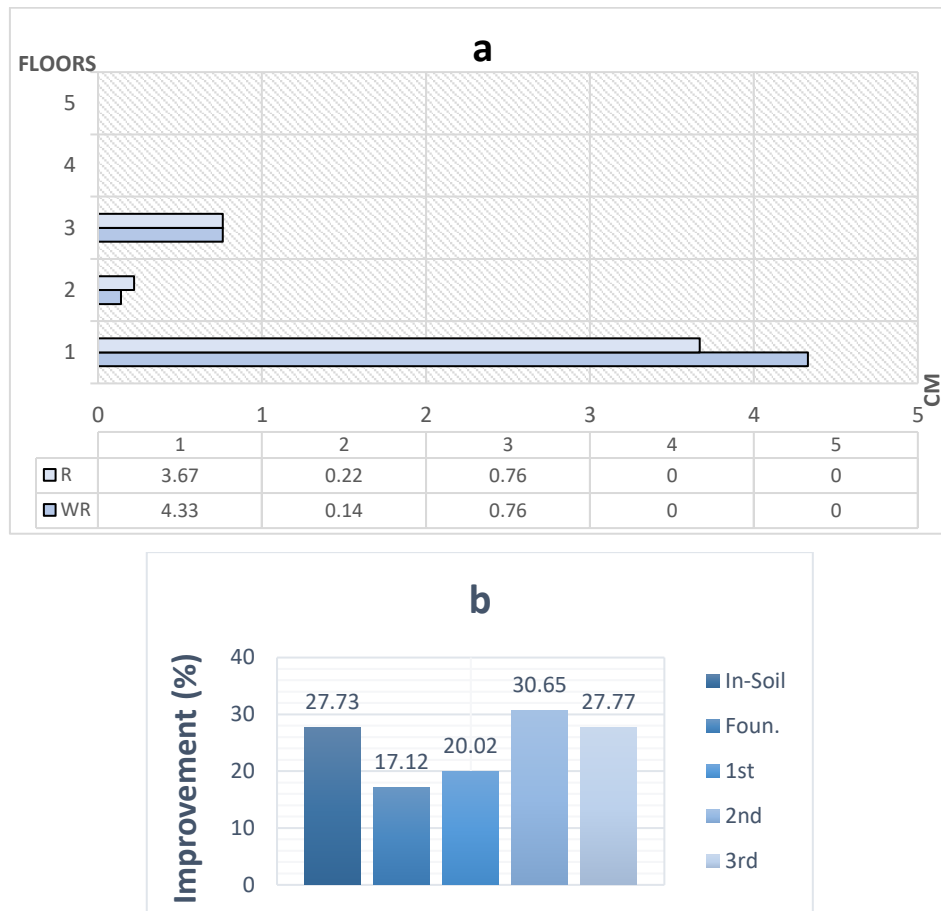


Figure 4.65. Improvement Ratios considering (a) Story Drifts and (b) Arias Intensity under El Centro Earthquake Motion (PGA= 0.55g).

4.3.7. Seismic Response of 3-Story Model under El Centro Earthquake Motion (PGA =0.89 g)

Table 4.40 shows the reduced acceleration and displacement values through all sensors comparing to unreinforced system for 3-Storey model under El Centro Earthquake (0.89g). In the soil, peak accelerations are 0.84g in the underside and 0.92g in the midpoint and 1.03g upper side. The maximum improvement of acceleration in the underside, midpoint upper side is 35%, 15% and 6%, respectively. Also, in the underside of soil for N=1 there is no reduction in accelerations.

Table 4.40. Summary of all tested Cases under El Centro Earthquake motion
(PGA=0.89g).

		N=4			N=3			N=2			N=1		
		WR	R	IMP. (%)	WR	R	IMP. (%)	WR	R	IMP. (%)	WR	R	IMP. (%)
In Soil (g)	A5	0.84	0.79	6.329	0.84	0.8	5.000	0.84	0.83	1.205	0.84	0.86	-2.326
	A6	0.83	0.74	12.162	0.83	0.76	9.211	0.83	0.78	6.410	0.83	0.8	3.750
	A7	0.79	0.69	14.493	0.79	0.72	9.722	0.79	0.74	6.757	0.79	0.74	6.757
	A8	0.86	0.76	13.158	0.86	0.8	7.500	0.86	0.84	2.381	0.86	0.88	-2.273
	A9	0.82	0.73	12.329	0.82	0.76	7.895	0.82	0.77	6.494	0.82	0.8	2.500
	A10	0.82	0.71	15.493	0.82	0.75	9.333	0.82	0.79	3.797	0.82	0.8	2.500
	A11	0.92	0.8	15.000	0.92	0.82	12.195	0.92	0.86	6.977	0.92	0.91	1.099
	A12	1.03	0.76	35.526	1.03	0.82	25.610	1.03	0.95	8.421	1.03	0.98	5.102
Foun.(g)	A13	0.82	0.71	15.493	0.82	0.75	9.333	0.82	0.79	3.797	0.82	0.82	0
3 Storey Model (cm)	A14	1.17	0.96	21.875	1.17	1.06	10.377	1.17	1.14	2.632	1.17	1.17	0
	A15	0.92	0.82	12.195	0.92	0.87	5.747	0.92	0.9	2.222	0.92	0.94	-2.128
	A16	0.92	0.77	19.481	0.92	0.8	15.000	0.92	0.86	6.977	0.92	0.89	3.371
	D20	8.24	6.83	20.644	8.24	7.09	16.220	8.24	7.63	7.995	8.24	7.71	6.874
	D21	8.14	6.99	16.452	8.14	7.33	11.050	8.14	7.6	7.105	8.14	7.88	3.299
	D22	9.94	8.56	16.121	9.94	8.98	10.690	9.94	9.07	9.592	9.94	9.3	6.882

The sensors shown in Figures 4.66 and 4.67 show the soil, foundation, first and third floor. The improvement of N=4 compared to unreinforced system can be observed with the help of them. The decrease of top and first floor acceleration is 3%, 6%, 15% and 19% and 0%, 2%, 10%, 21% for N=1, N=2, N=3 and N=4, respectively. Also, the reduction of foundation acceleration is roughly %0, %3, %9 and %15 for N=1, N=2, N=3 and N=4, respectively. There is no reduction for N=1 in foundation. It becomes %0.

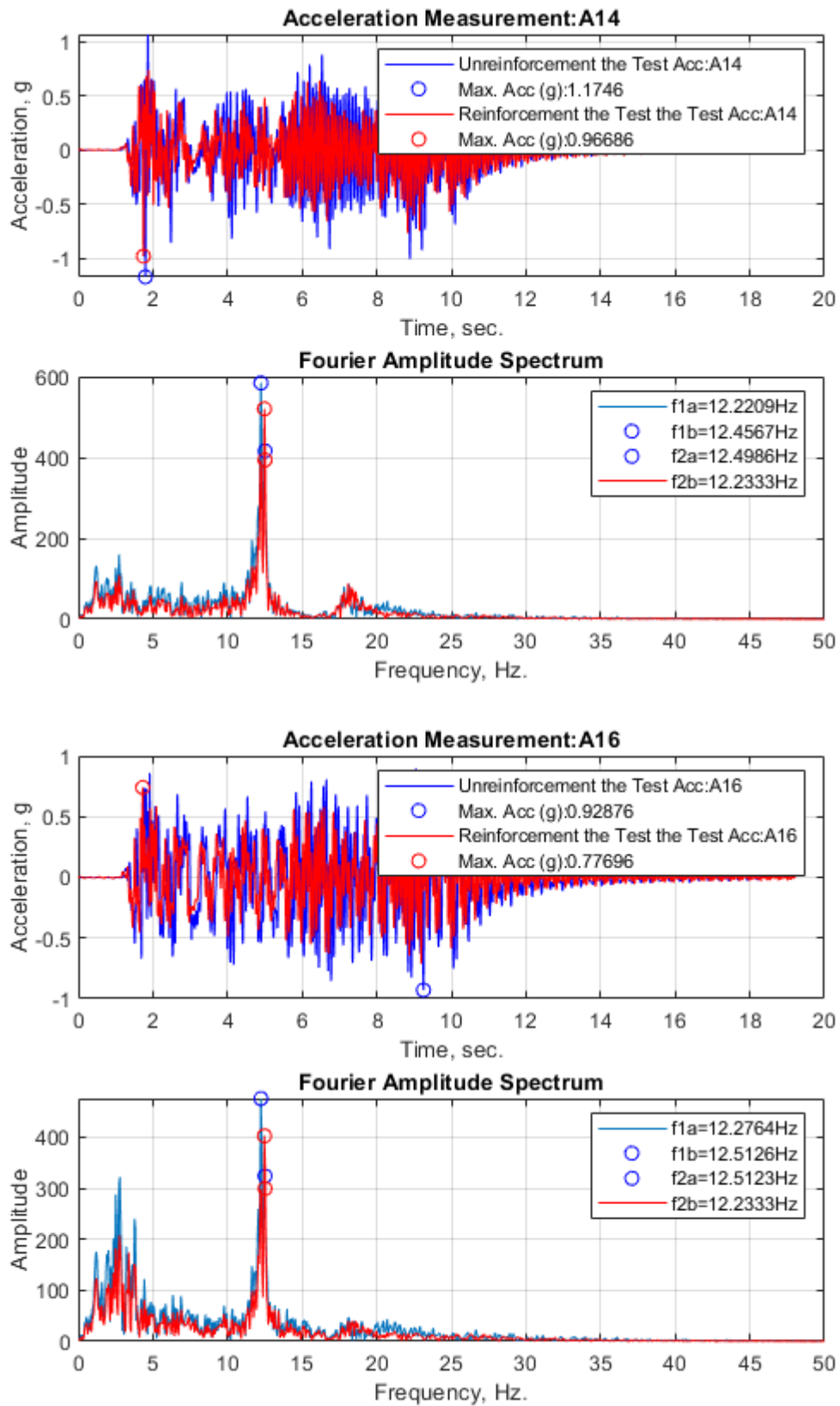


Figure 4.66. Acceleration Measurements and FAS of 1st and 3rd Floors under El Centro Earthquake Motion (PGA= 0.89 g).

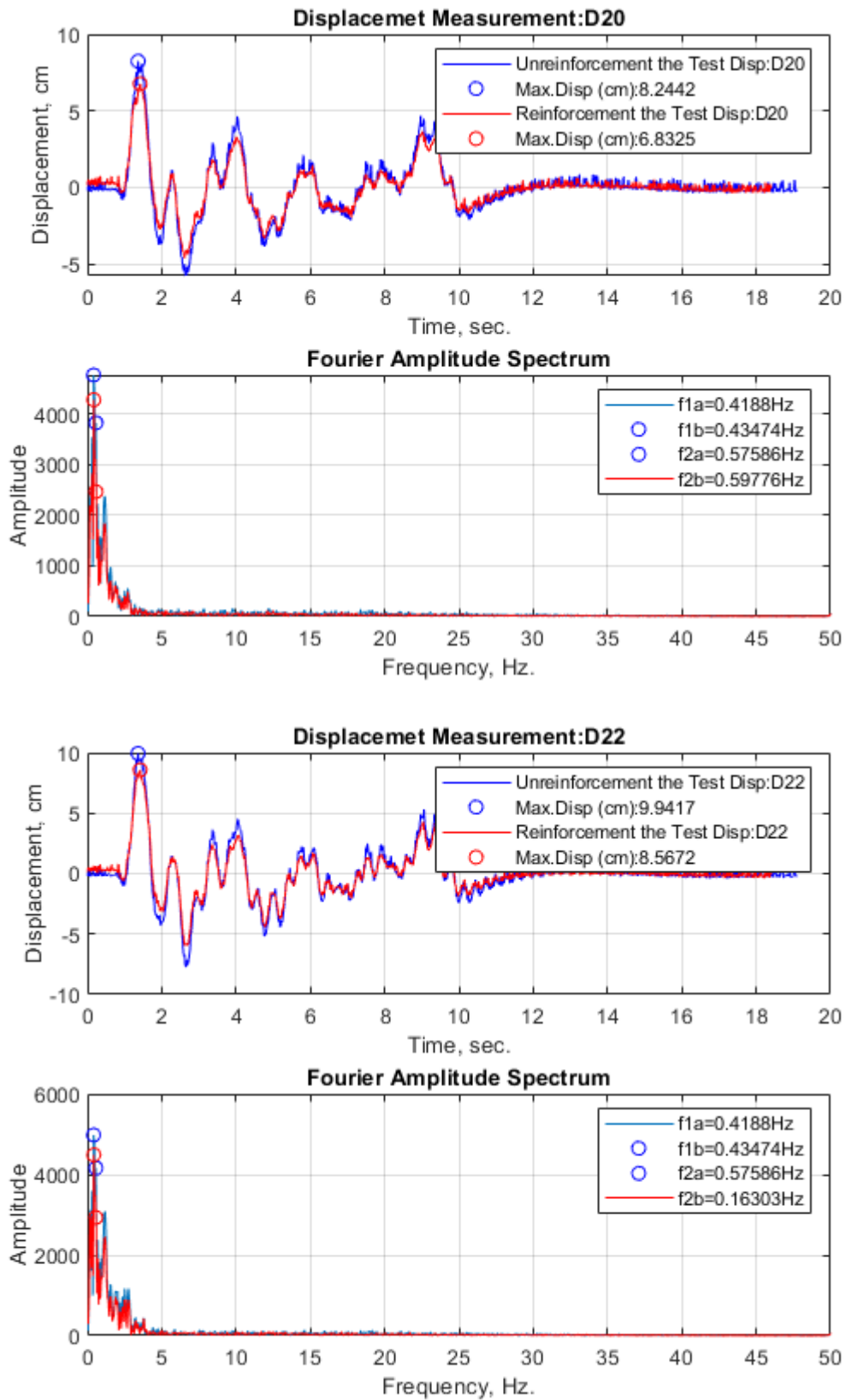


Figure 4.67. Displacement Measurements and FAS of 1st and 3rd Floors under El Centro Earthquake Motion (PGA= 0.89 g).

In Figure 4.68 and Figure 4.69, the changing acceleration values and the changing displacement values in accordance with story and reinforcement layers can be seen. For the first, for N=1 the improvement in acceleration value become 0% and with increase in the number of geogrid layers, it ascends to 2%, 10% and 21% for N=2, N=3 and N=4, respectively. The reduction of acceleration reduces up to 3%, 6%, 15% and 19%, respectively for the third floor. Besides, the improvement in acceleration value becomes negative for the second floor in N=1 comparing to unreinforced system.

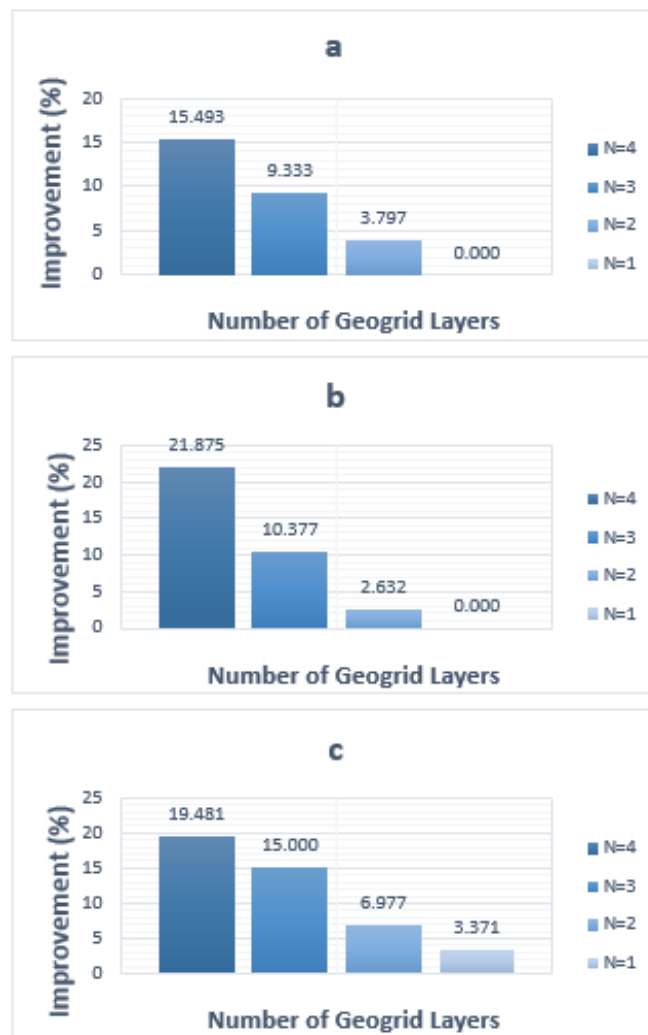


Figure 4.68. The Acceleration Improvement Graphs in Accordance with Story and Reinforcement Layers for (a) Foundation, (b) 1st Floor, (c) 3rd Floor El Centro Earthquake Motion (PGA= 0.89 g).

For the first and third floor, the maximum decrease of story's displacement values is 20% and 16%, respectively.

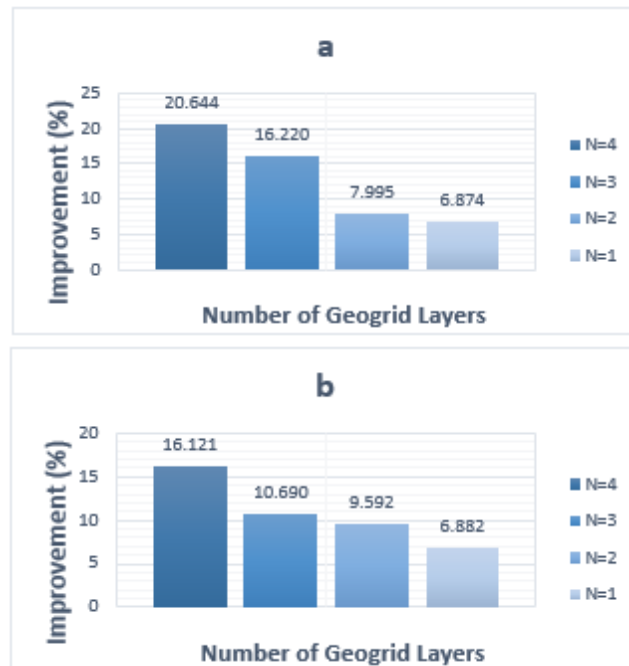


Figure 4.69. The Displacement Improvement Graphs in Accordance with Story and Reinforcement Layers for (a) 1st Floor, (b) 3rd Floor under El Centro Earthquake Motion (PGA= 0.89 g).

In Table 4.41 and Table 4.42, Arias intensity improvements were exhibited and with the help of the fundamental period of all N values for soil, foundations, floors, the period lengthening ratios were exhibited and also RMS of peak values were shown.

Table 4.41. Fundamental Period and Period Lengthening Ratios under El Centro Earthquake Motion (PGA= 0.89 g).

	Fundamental Period (Hz)					Period Lengthening Ratio			
	N=4	N=3	N=2	N=1	N=0	N=4	N=3	N=2	N=1
In-Soil	3.76	3.80	3.80	3.80	3.75	1.00	0.99	0.99	0.99
Foundation	6.88	3.80	3.80	3.80	3.75	0.55	0.99	0.99	0.99
1st Floor	0.41	0.43	0.41	0.41	0.41	1.00	0.95	1.00	1.00
2nd Floor	0.43	0.43	0.41	0.41	0.41	0.95	0.95	1.00	1.00
3rd Floor	0.43	0.43	0.41	0.41	0.41	0.95	0.95	1.00	1.00

Table 4.42. RMS and Arias Intensity Improvement Ratios under El Centro Earthquake Motion (PGA= 0.89 g).

Root Mean Square (RSM)				Arias Intensity	
Horizontal Acceleration(g)	Peak	RSM-Rein.	RSM Imp (%)		Arias Intensity Imp (%)
In-Soil	1.03	0.88	16.76	In-Soil	42.99
Foundation	0.82	0.77	6.68	Foundation	18.13
1st Floor	1.17	1.09	7.78	1st Floor	24.28
2nd Floor	0.92	0.88	4.12	2nd Floor	14.51
3rd Floor	0.92	0.83	10.66	3rd Floor	23.18

As can be observed in Arias intensity values are approximately reduced up to 4%, 3% and 5% for soil region, foundation and floors in order of reduction of RMS ascend at soil and foundation to 16%, 6% and at floors to 7%, 4%, and 10%, respectively. Also, there is no change in the natural period of model. The period lengthening ratio fluctuates up to 5%. Arias Intensity improvement graph and Story Drifts can be seen in Figure 4.70.

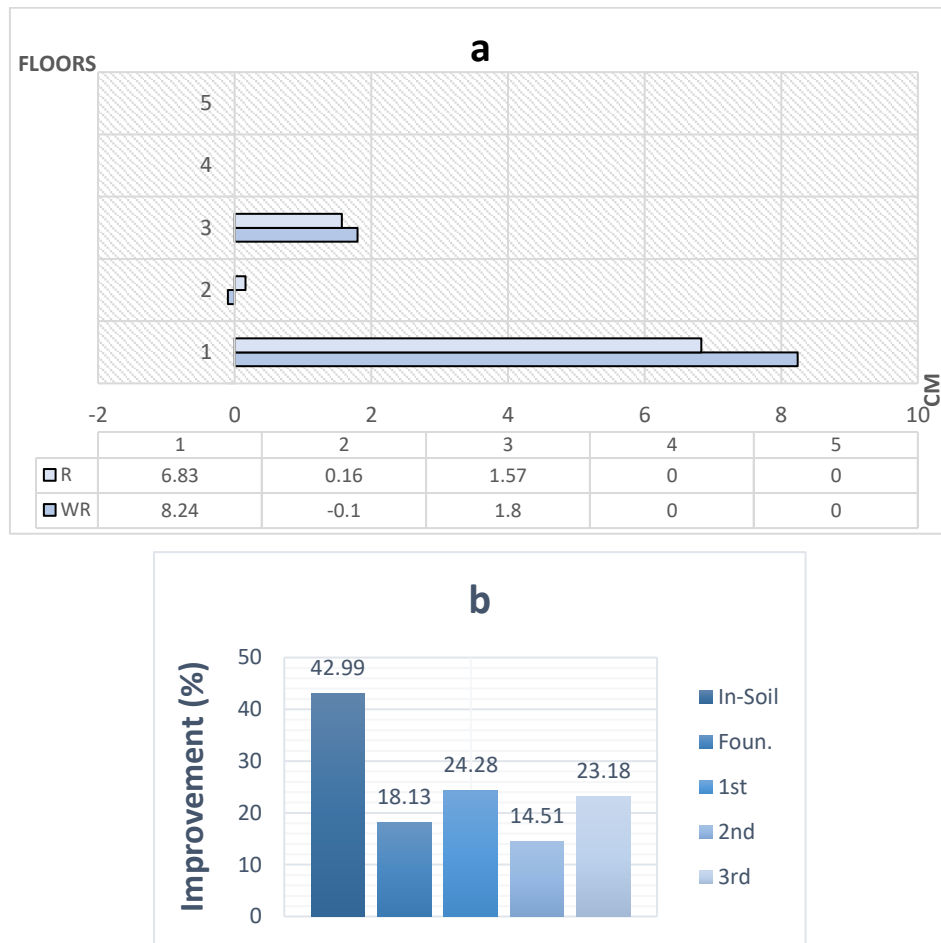


Figure 4.70. Improvement Ratios considering (a) Story Drifts and (b) Arias Intensity under El Centro Earthquake Motion (PGA= 0.89 g).

4.4. Free-Surface Tests for Geogrid Reinforced Soil

This part includes the results and comparison of Free-Surface with and without geogrid reinforcement for all earthquakes. Because there was no model in free surface, the results only encompassed in-situ soil. As mentioned before, the case without geogrid reinforcement was Case 1 for Free-Surface and it was defined as WR (without reinforcement), the cases with geogrid reinforcement were defined as R (reinforcement) in all tables and all comparisons was done according to it.

In Free-Surface, the number of input motions and magnitudes were changed and as earthquake input motions Kobe (0.89g and 0.99g), Kocaeli (0.16g and 0.25g) and El

Centro (0.35g) were used. Sensors shown in results were selected among the sensors exhibiting maximum acceleration ones in soil for input motions.

4.4.1. Seismic Response of Free-Surface under Kobe Earthquake Motion (PGA=0.89g)

Table 4.43 shows the reduced acceleration values through all sensors comparing to unreinforced system in the soil for Free-surface under Kobe Earthquake-0.89g.

Table 4.43. Summary of all tested Cases under Kobe Earthquake Motion (PGA=0.89g).

		N=4			N=3			N=2			N=1		
		WR	R	IMP. (%)	WR	R	IMP. (%)	WR	R	IMP. (%)	WR	R	IMP. (%)
In Soil (g)	A5	1.26	1.01	24.752	1.26	1.05	20.000	1.26	1.18	6.780	1.26	1.22	3.279
	A6	1.17	0.94	24.468	1.17	0.98	19.388	1.17	1.08	8.333	1.17	1.14	2.632
	A7	1.17	0.95	23.158	1.17	0.98	19.388	1.17	1.1	6.364	1.17	1.14	2.632
	A8	1.28	1.03	24.272	1.28	1.07	19.626	1.28	1.19	7.563	1.28	1.24	3.226
	A9	1.13	0.9	25.556	1.13	0.95	18.947	1.13	1.06	6.604	1.13	1.1	2.727
	A10	1.14	0.94	21.277	1.14	0.98	16.327	1.14	1.1	3.636	1.14	1.13	0.885
	A11	0.87	0.7	24.286	0.87	0.73	19.178	0.87	0.82	6.098	0.87	0.85	2.353
	A12	0.83	0.67	23.881	0.83	0.69	20.290	0.83	0.78	6.410	0.83	0.8	3.750

In the soil, peak accelerations are 1.26g in the underside, 1.28g in the midpoint and 0.83g in the upper side. The reduction of acceleration in underside is 3%, 6%, 20% and 24%, the reduction of acceleration in midpoint is 3% 7%, 19% and 24%, the reduction of acceleration in upper side is 3%, 6%, 20% and 23% for N=1, N=2, N=3 and N=4, respectively. The maximum acceleration reduction in the soil is nearly 25%. For N=1 there is a slightly improvement in acceleration value, but between N=2 and N=3 there is a dramatic increase in the reduction of acceleration.

The sensor shown in Figure 4.71 and Figure 4.72 illustrates the improvement of sensor exhibiting maximum acceleration (A12). Figure 4.71 indicates for N=4 compared to unreinforced system and Figure 4.72 shows the comparisons of N=1, N=2, N=3 and N=4.

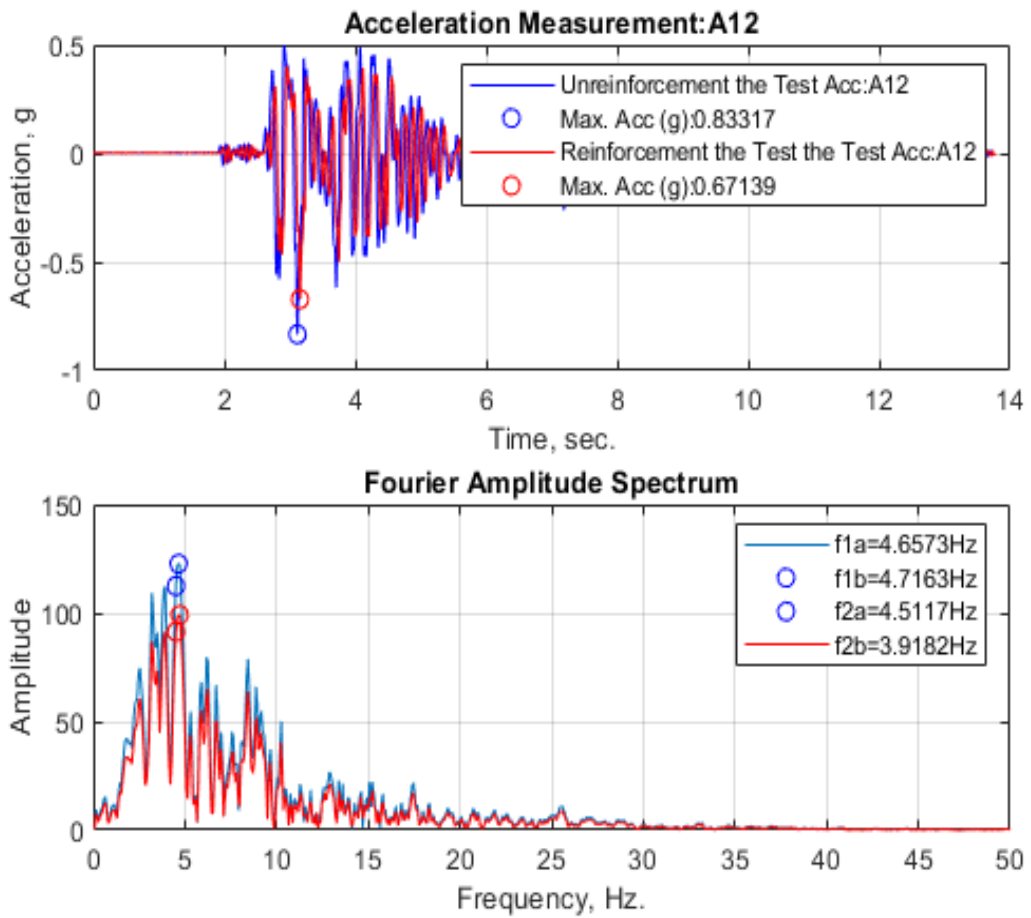


Figure 4.71. Acceleration Measurements and FAS of Soil(A12) under Kobe Earthquake Motion (PGA= 0.89 g).

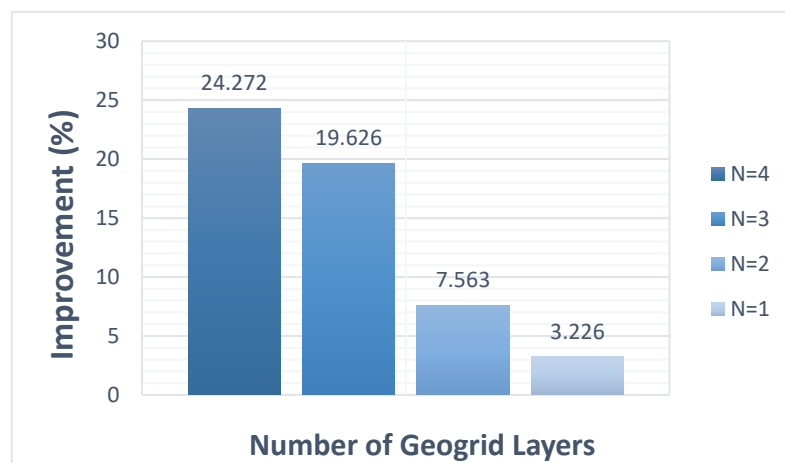


Figure 4.72. The Acceleration Improvement Graphs in Soil (A12) under Kobe Earthquake Motion (PGA= 0.89 g).

As it can be seen in Table 4.44 and Table 4.45, Arias intensity improvement for soil region is nearly 6%. RMS improvement value for soil is 12%. Also, there is no change in the natural period. The period lengthening ratio fluctuates up to 1%. Also Figure 4.73 shows Arias intensity improvement graph.

Table 4.44. Fundamental Period and Period Lengthening Ratios under Kobe Earthquake Motion (PGA= 0.89 g).

	Fundamental Period (Hz)					Period Lengthening Ratio			
	N=4	N=3	N=2	N=1	N=0	N=4	N=3	N=2	N=1
In-Soil	4.7	4.7	4.7	4.7	4.65	0.99	0.99	0.99	0.99

Table 4.45. RMS and Arias Intensity Improvement Ratios under Kobe Earthquake Motion (PGA= 0.89 g).

Root Mean Square (RSM)				Arias Intensity	
Horizontal Acceleration(g)	Peak	RSM-Rein.	RSM Imp (%)		Arias Intensity Imp (%)
In-Soil	1.28	1.14	12.7	In-Soil	24.57

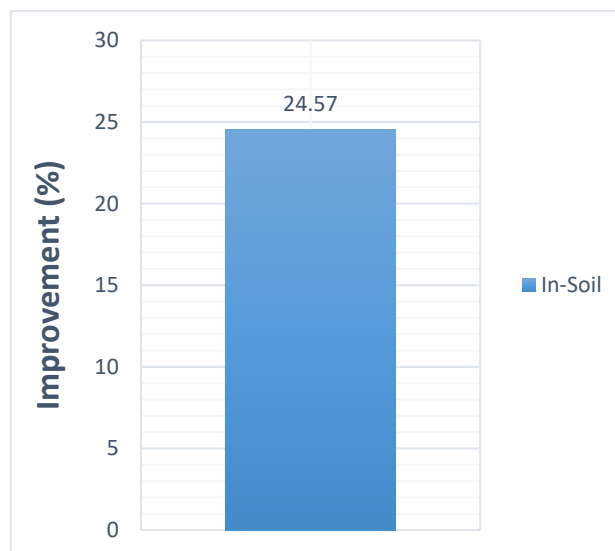


Figure 4.73. Improvement Ratios considering Arias Intensity under Kobe Earthquake Motion (PGA= 0.89 g).

4.4.2. Seismic Response of Free-Surface under Kobe Earthquake Motion (PGA=0.99 g)

Table 4.46 shows the reduced acceleration values through all sensors comparing to unreinforced system in the soil for Free-surface under Kobe Earthquake (0.99g).

Table 4.46. Summary of all tested Cases under Kobe Earthquake Motion (PGA=0.99g).

		N=4			N=3			N=2			N=1		
		WR	R	IMP. (%)	WR	R	IMP. (%)	WR	R	IMP. (%)	WR	R	IMP. (%)
In Soil (g)	A5	1.61	1.33	21.053	1.61	1.37	17.518	1.61	1.54	4.545	1.61	1.57	2.548
	A6	1.42	1.17	21.368	1.42	1.2	18.333	1.42	1.35	5.185	1.42	1.38	2.899
	A7	1.47	1.22	20.492	1.47	1.25	17.600	1.47	1.41	4.255	1.47	1.43	2.797
	A8	1.61	1.3	23.846	1.61	1.36	18.382	1.61	1.53	5.229	1.61	1.56	3.205
	A9	1.38	1.16	18.966	1.38	1.17	17.949	1.38	1.32	4.545	1.38	1.34	2.985
	A10	1.4	1.17	19.658	1.4	1.21	15.702	1.4	1.35	3.704	1.4	1.38	1.449
	A11	0.93	0.77	20.779	0.93	0.79	17.722	0.93	0.87	6.897	0.93	0.9	3.333
	A12	0.85	0.7	21.429	0.85	0.72	18.056	0.85	0.8	6.250	0.85	0.83	2.410

In the soil, peak accelerations are 1.61g in the underside and midpoint, also 0.85g in the upper side. The reduction of acceleration in underside is 2%, 4%, 17% and 21%, the reduction of acceleration in midpoint is 3%, 5%, 18% and 23%, the reduction of acceleration in upper side is 2%, 6%, 18% and 21% for N=1, N=2, N=3 and N=4, respectively. The improvements are so similar with Kobe 0.89g for free surface. The maximum acceleration reduction in the soil is nearly 24%. Between N=2 and N=3 there is a dramatic increase in the reduction of acceleration.

The sensor shown in Figure 4.74 and Figure 4.75 indicates the improvement of sensor exhibiting maximum acceleration(A8). While Figure 4.74 shows for N=4 compared to unreinforced system, Figure 4.75 compares N=1, N=2, N=3 and N=4 under Kobe Earthquake motion with 0.99 g.

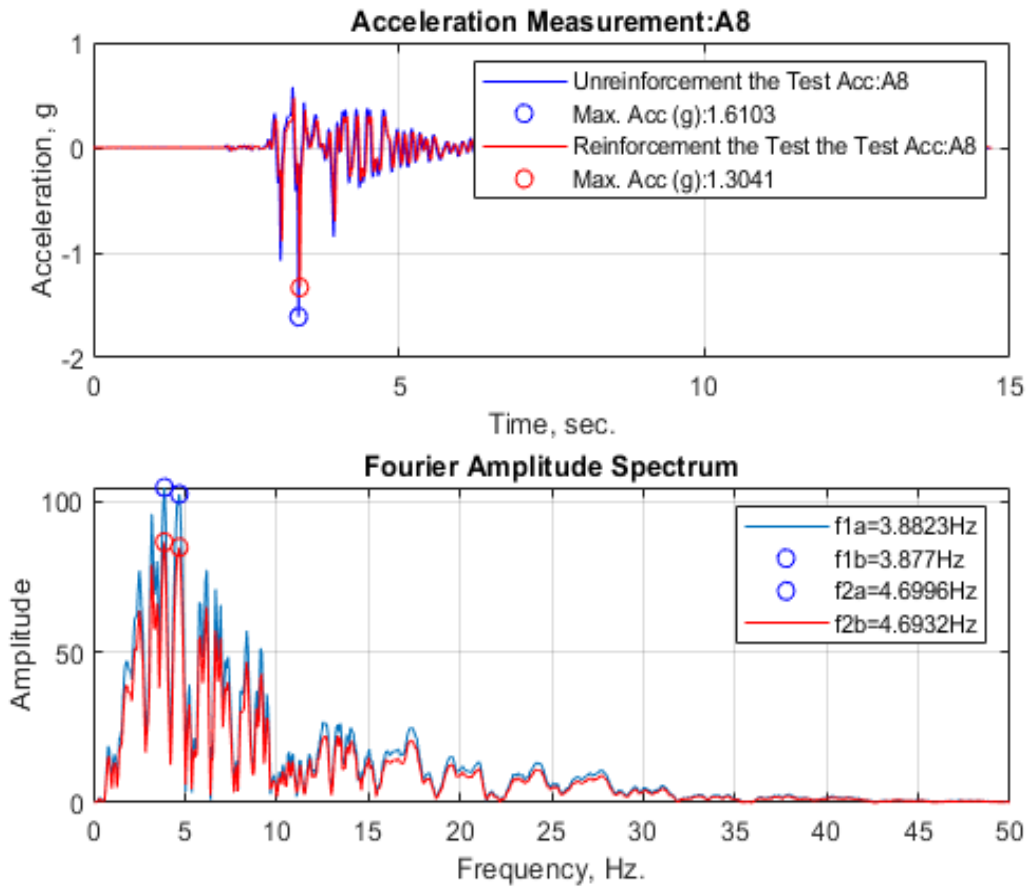


Figure 4.74. Acceleration Measurements and FAS of Soil (A8) under Kobe Earthquake Motion (PGA= 0.99 g).

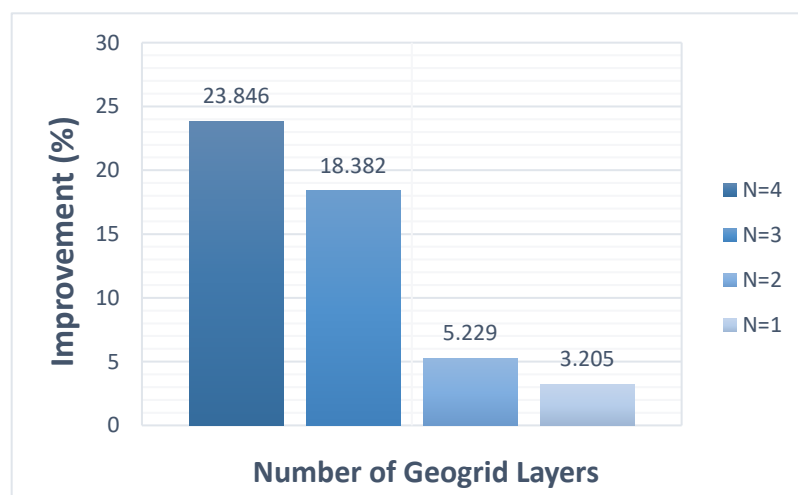


Figure 4.75. The Acceleration Improvement Graphs in Soil(A8) under Kobe Earthquake Motion (PGA= 0.99 g).

As it can be seen in Table 4.47 and 4.48, Arias intensity improvement for soil region is nearly 7%. RMS improvement value for soil is 11%. There is no change in the natural period. Also Figure 4.73 indicates Arias intensity improvement graph.

Table 4.47. Fundamental Period and Period Lengthening Ratios under Kobe Earthquake Motion (PGA= 0.99 g).

	Fundamental Period (Hz)					Period Lengthening Ratio			
	N=4	N=3	N=2	N=1	N=0	N=4	N=3	N=2	N=1
In-Soil	3.87	3.87	3.87	3.87	3.88	1.00	1.00	1.00	1.00

Table 4.48. RMS and Arias Intensity Improvement Ratios under Kobe Earthquake Motion (PGA= 0.99 g).

Root Mean Square (RSM)				Arias Intensity	
Horizontal Acceleration(g)	Peak	RSM-Rein.	RSM Imp (%)		Arias Intensity Imp (%)
In-Soil	1.61	1.44	11.67	In-Soil	21.06

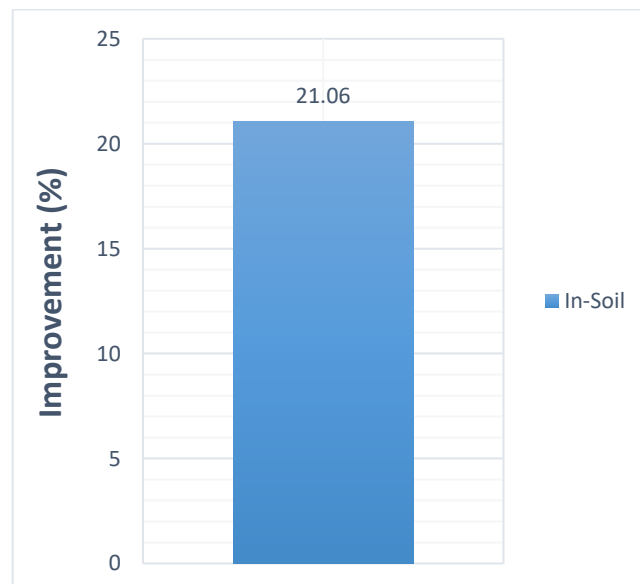


Figure 4.76. Improvement Ratios considering Arias Intensity under Kobe Earthquake Motion (PGA= 0.99 g).

4.4.3. Seismic Response of Free-Surface under Kocaeli Earthquake Motion (PGA=0.16 g)

Table 4.49 shows the reduced acceleration values through all sensors comparing to unreinforced system in the soil for Free-Surface under Kocaeli Earthquake (0.16g).

Table 4.49. Summary of all tested Cases under Kocaeli Earthquake Motion (PGA=0.16g).

		N=4			N=3			N=2			N=1		
		WR	R	IMP. (%)	WR	R	IMP. (%)	WR	R	IMP. (%)	WR	R	IMP. (%)
In Soil (g)	A5	0.14	0.11	27.273	0.14	0.12	16.667	0.14	0.13	7.692	0.14	0.13	7.692
	A6	0.17	0.14	21.429	0.17	0.15	13.333	0.17	0.16	6.250	0.17	0.17	0
	A7	0.18	0.15	20.000	0.18	0.16	12.500	0.18	0.17	5.882	0.18	0.17	5.882
	A8	0.17	0.14	21.429	0.17	0.15	13.333	0.17	0.16	6.250	0.17	0.17	0
	A9	0.19	0.15	26.667	0.19	0.16	18.750	0.19	0.17	11.765	0.19	0.18	5.556
	A10	0.2	0.16	25.000	0.2	0.17	17.647	0.2	0.19	5.263	0.2	0.2	0
	A11	0.26	0.21	23.810	0.26	0.23	13.043	0.26	0.24	8.333	0.26	0.25	4.000
	A12	0.41	0.34	20.588	0.41	0.36	13.889	0.41	0.38	7.895	0.41	0.4	2.500

In the soil, peak accelerations are 0.14g in the underside, 0.26g in the midpoint and 0.41g in the upper side. The reduction of acceleration in underside is 7%, 7%, 16% and 27%, the reduction of acceleration in midpoint is 4%, 8%, 13% and 23%, the reduction of acceleration in upper side is 2%, 7%, 13% and 20% for N=1, N=2, N=3 and N=4, respectively. The maximum acceleration reduction in the soil is nearly 27%. In the underside of soil, there is no change between N=1 and N=2 but there is significant improvement between N=3 and N=4 in the reduction of acceleration. Besides, the reduction of acceleration partly becomes zero for N=1.

The sensor shown in Figure 4.77 and Figure 4.78 indicates the improvement of sensor exhibiting maximum acceleration (A12). Figure 4.77 illustrates for N=4 compared to unreinforced system and Figure 4.78 shows the comparisons of N=1, N=2, N=3 and N=4 under Kocaeli Earthquake motion with 0.16 g.

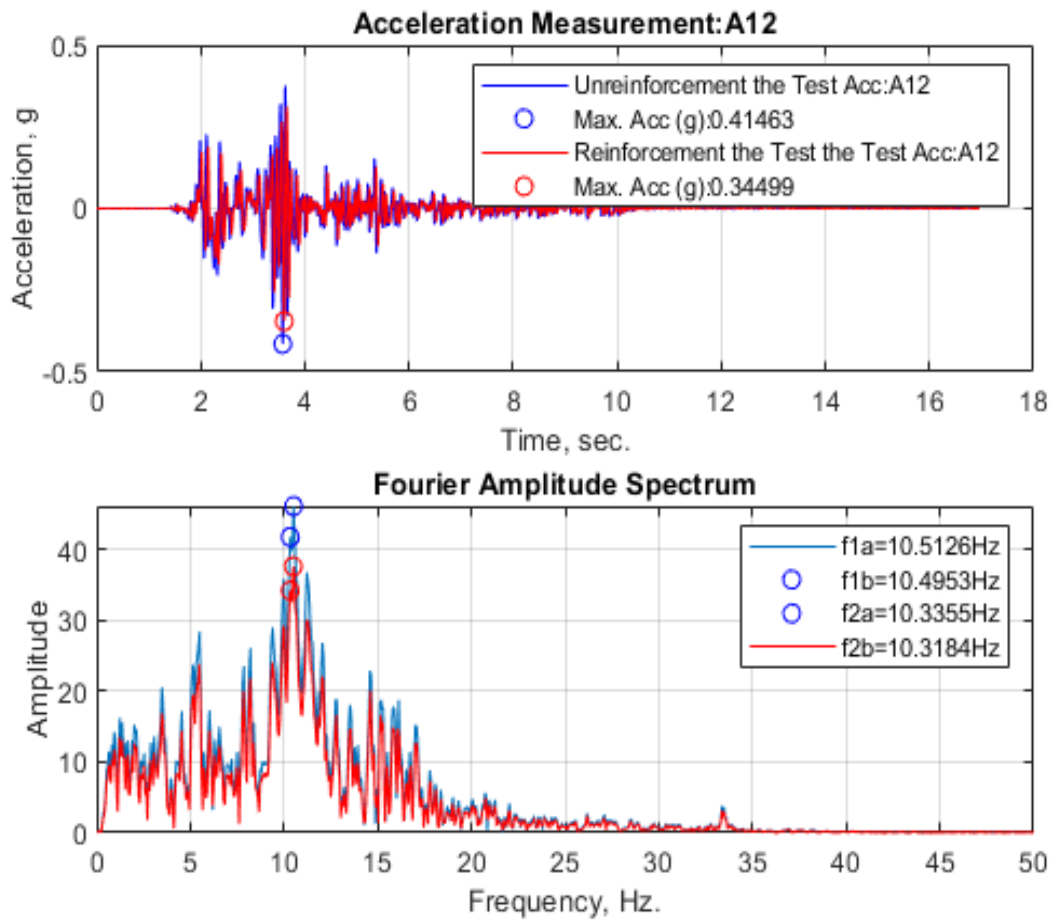


Figure 4.77. Acceleration Measurements and FAS of Soil (A12) under Kocaeli Earthquake Motion (PGA= 0.16 g).

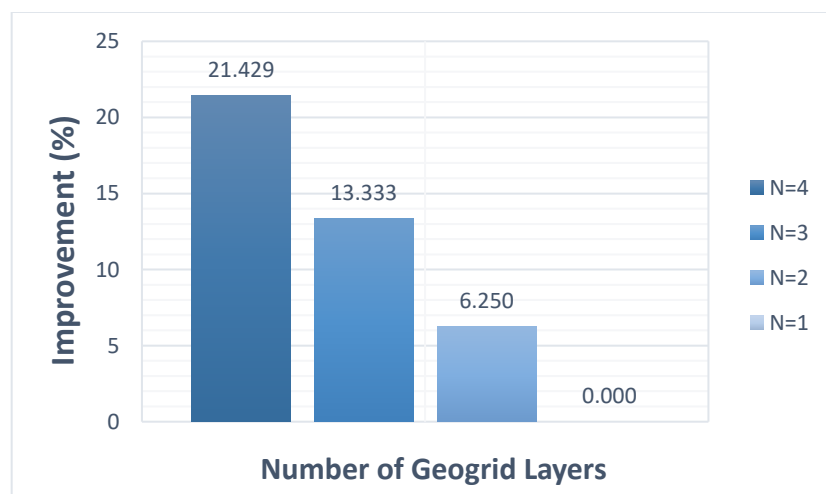


Figure 4.78. The Acceleration Improvement Graphs in Soil (A12) under Kocaeli Earthquake Motion (PGA= 0.16 g).

In Table 4.50 and Table 4.51, it can be observed Arias intensity improvement value for soil region is nearly 2%. RMS improvement for soil is 10%. Also, there is no change in the natural period. Besides, Figure 4.79 indicates Arias intensity improvement graph.

Table 4.50. Fundamental Period and Period Lengthening Ratios under Kocaeli Earthquake Motion (PGA= 0.16 g).

	Fundamental Period (Hz)					Period Lengthening Ratio			
	N=4	N=3	N=2	N=1	N=0	N=4	N=3	N=2	N=1
In-Soil	10.49	10.49	10.49	10.49	10.49	1.00	1.00	1.00	1.00

Table 4.51. RMS and Arias Intensity Improvement Ratios under Kocaeli Earthquake Motion (PGA= 0.16 g).

Root Mean Square (RSM)				Arias Intensity	
Horizontal Acceleration(g)	Peak	RSM-Rein.	RSM Imp (%)		Arias Intensity Imp (%)
In-Soil	0.41	0.37	10.61	In-Soil	28.09

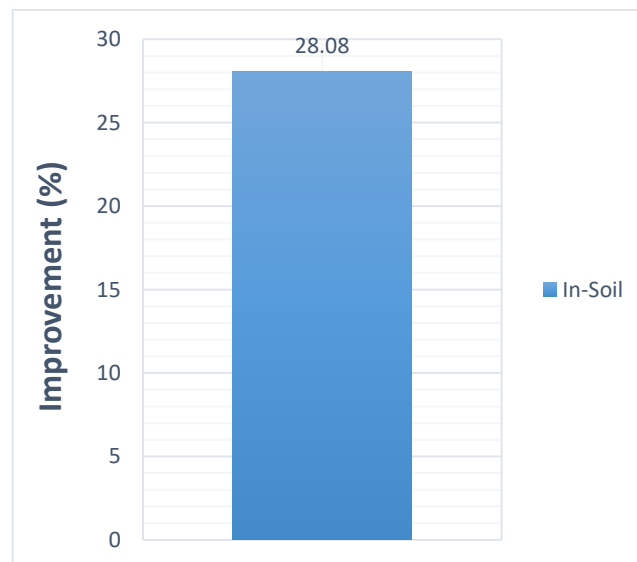


Figure 4.79. Improvement Ratios considering Arias Intensity under Kocaeli Earthquake Motion (PGA= 0.16 g).

4.4.4. Seismic Response of Free-Surface under Kocaeli Earthquake Motion (PGA=0.25 g)

Table 4.52 shows the reduced acceleration values through all sensors comparing to unreinforced system in the soil for Free-Surface under Kocaeli Earthquake (0.25g).

Table 4.52. Summary of all tested Cases under Kocaeli Earthquake motion (PGA=0.25g).

		N=4			N=3			N=2			N=1		
		WR	R	IMP. (%)	WR	R	IMP. (%)	WR	R	IMP. (%)	WR	R	IMP. (%)
In Soil	A5	0.21	0.17	23.529	0.21	0.18	16.667	0.21	0.19	10.526	0.21	0.2	5.000
	A6	0.24	0.2	20.000	0.24	0.21	14.286	0.24	0.22	9.091	0.24	0.23	4.348
	A7	0.24	0.2	20.000	0.24	0.2	20.000	0.24	0.22	9.091	0.24	0.23	4.348
	A8	0.24	0.2	20.000	0.24	0.22	9.091	0.24	0.22	9.091	0.24	0.24	0
	A9	0.25	0.21	19.048	0.25	0.22	13.636	0.25	0.24	4.167	0.25	0.24	4.167
	A10	0.25	0.2	25.000	0.25	0.21	19.048	0.25	0.24	4.167	0.25	0.25	0
	A11	0.35	0.29	20.690	0.35	0.31	12.903	0.35	0.33	6.061	0.35	0.34	2.941
	A12	0.49	0.4	22.500	0.49	0.42	16.667	0.49	0.46	6.522	0.49	0.47	4.255

In the soil, peak accelerations are 0.21g in the underside, 0.35g in the midpoint and 0.49g in the upper side. The reduction of acceleration in underside is 5%, 10%, 16% and 23%, the reduction of acceleration in midpoint is 2%, 6%, 12% and 20%, the reduction of acceleration in upper side is 4%, 6%, 16% and 22% for N=1, N=2, N=3 and N=4, respectively. The maximum acceleration reduction in the soil is nearly 25%.

The sensor shown in Figure 4.80 and Figure 4.81 represents the improvement of sensor showing maximum acceleration (A12). Figure 4.80 indicates for N=4 compared to unreinforced system and Figure 4.81 shows the comparisons of N=1, N=2, N=3 and N=4 under Kocaeli Earthquake motion with 0.25 g.

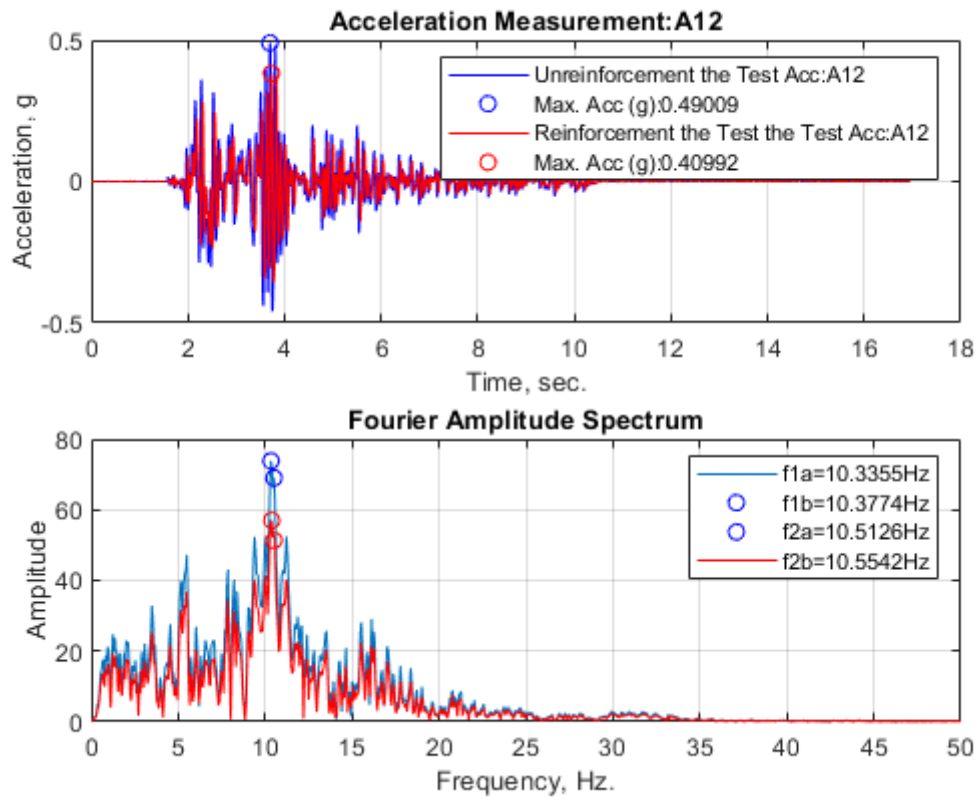


Figure 4.80. Acceleration Measurements and FAS of Soil(A12) under Kocaeli Earthquake Motion (PGA= 0.25 g).

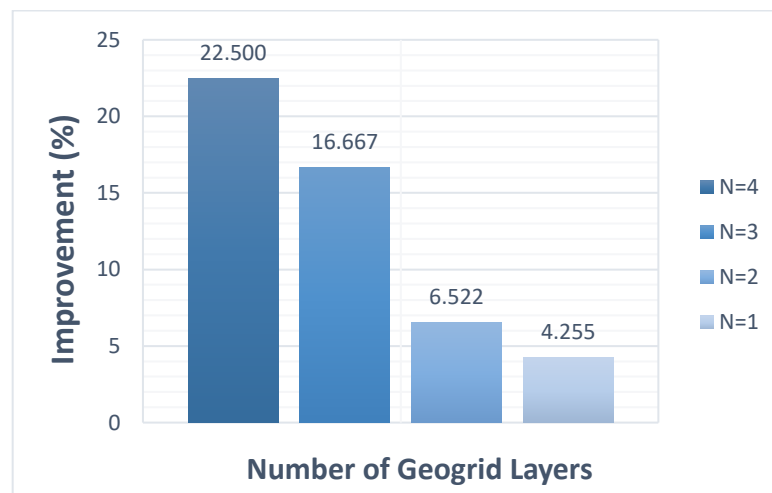


Figure 4.81. The Acceleration Improvement Graphs in Soil(A12) under Kocaeli Earthquake Motion (PGA= 0.25 g).

As it can be observed in Table 4.53 and Table 4.54, Arias intensity improvement for soil region is nearly %2. RMS improvement value for soil is %11. Also, there is no change in the natural period and Figure 4.82 shows Arias intensity improvement graph.

Table 4.53. Fundamental Period and Period Lengthening Ratios under Kocaeli Earthquake Motion (PGA= 0.25 g).

	Fundamental Period (Hz)					Period Lengthening Ratio			
	N=4	N=3	N=2	N=1	N=0	N=4	N=3	N=2	N=1
In-Soil	10.49	10.49	10.49	10.49	10.51	1.00	1.00	1.00	1.00

Table 4.54. RMS and Arias Intensity Improvement Ratios under Kocaeli Earthquake Motion (PGA= 0.25 g).

Root Mean Square (RSM)				Arias Intensity	
Horizontal Acceleration(g)	Peak	RSM-Rein.	RSM Imp (%)		Arias Intensity Imp (%)
In-Soil	0.49	0.44	11.76	In-Soil	23.38

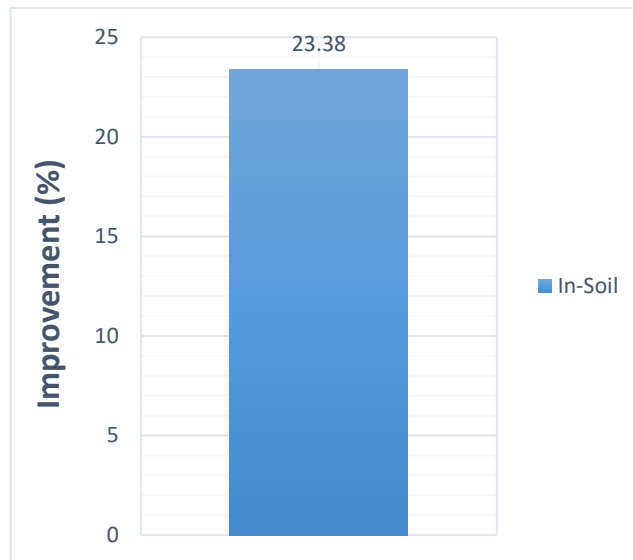


Figure 4.82. Improvement Ratios considering Arias Intensity under Kocaeli Earthquake Motion (PGA= 0.25 g).

4.4.5. Seismic Response of Free-Surface under El Centro Earthquake Motion (PGA= 0.35 g)

Table 4.55 shows the reduced acceleration values through all sensors comparing to unreinforced system in the soil for Free-Surface under El Centro Earthquake (0.35g).

Table 4.55. Summary of all tested Cases under El Centro Earthquake motion (PGA=0.35g).

		N=4			N=3			N=2			N=1		
		WR	R	IMP. (%)	WR	R	IMP. (%)	WR	R	IMP. (%)	WR	R	IMP. (%)
In Soil	A5	0.32	0.26	23.077	0.32	0.27	18.519	0.32	0.3	6.667	0.32	0.31	3.226
	A6	0.35	0.28	25.000	0.35	0.29	20.690	0.35	0.33	6.061	0.35	0.34	2.941
	A7	0.34	0.27	25.926	0.34	0.29	17.241	0.34	0.32	6.250	0.34	0.33	3.030
	A8	0.36	0.29	24.138	0.36	0.3	20.000	0.36	0.34	5.882	0.36	0.35	2.857
	A9	0.35	0.28	25.000	0.35	0.29	20.690	0.35	0.33	6.061	0.35	0.34	2.941
	A10	0.35	0.26	34.615	0.35	0.28	25.000	0.35	0.32	9.375	0.35	0.35	0
	A11	0.44	0.36	22.222	0.44	0.38	15.789	0.44	0.42	4.762	0.44	0.44	0
	A12	0.5	0.41	21.951	0.5	0.43	16.279	0.5	0.48	4.167	0.5	0.49	2.041

In the soil, peak accelerations are 0.32g in the underside, 0.44g in the midpoint and 0.5g in the upper side. The reduction of acceleration in underside is 3%, 6%, 18% and 23%, the reduction of acceleration in midpoint is 0%, 4%, 15% and 22%, the reduction of acceleration in upper side is 2%, 4%, 16% and 21% for N=1, N=2, N=3 and N=4, respectively. The maximum acceleration reduction in the soil is nearly 34%. Between N=2 and N=3 there is a dramatic increase in the reduction of accelerations.

The sensor shown in Figure 4.83 and Figure 4.84 shows the improvement of sensor giving maximum acceleration (A12). Figure 4.83 represents for N=4 compared to unreinforced system and Figure 4.84 shows the comparisons of N=1, N=2, N=3 and N=4 under El Centro Earthquake motion with 0.35 g.

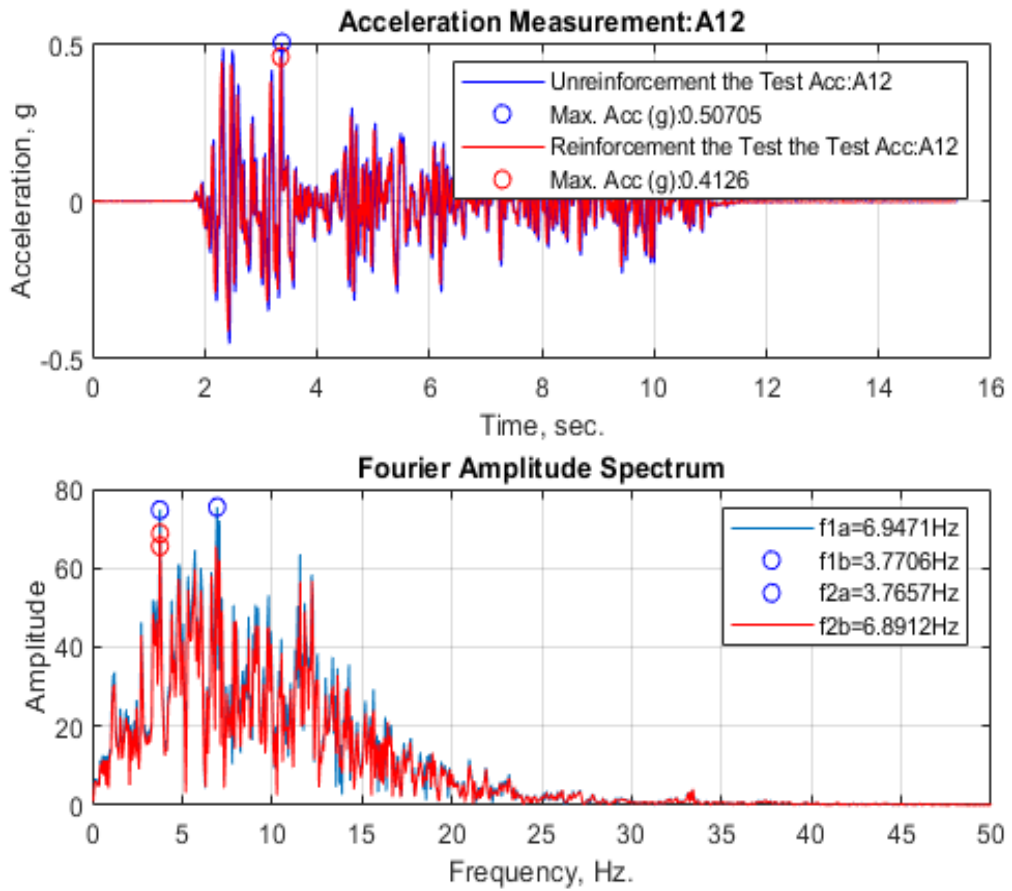


Figure 4.83. Acceleration Measurements and FAS of Soil(A12) under El Centro Earthquake Motion (PGA= 0.35 g).

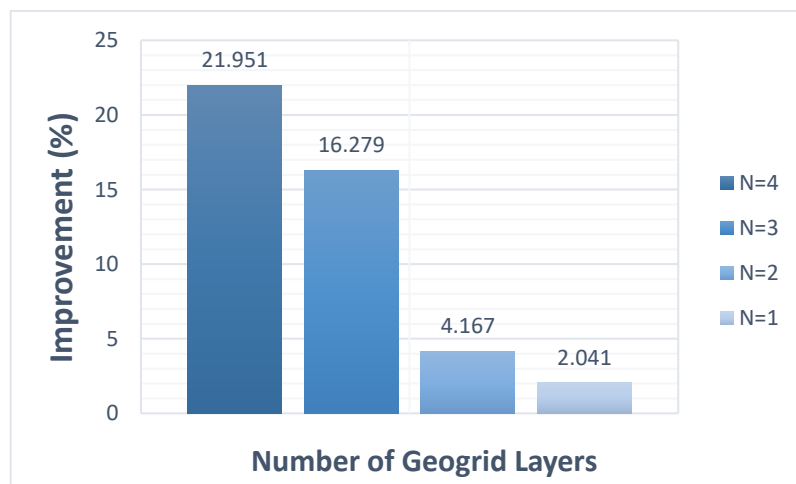


Figure 4.84. The Acceleration Improvement Graphs in Soil(A12) under El Centro Earthquake Motion (PGA= 0.35 g).

As it can be seen in Table 4.56 and Table 4.57, Arias intensity improvement for soil region is nearly 2%. RMS improvement value for soil is 10%. There is no change in the natural period. Besides, Figure 4.85 shows Arias intensity improvement graph.

Table 4.56. Fundamental Period and Period Lengthening Ratios under El Centro Earthquake Motion (PGA= 0.35 g).

	Fundamental Period (Hz)					Period Lengthening Ratio			
	N=4	N=3	N=2	N=1	N=0	N=4	N=3	N=2	N=1
In-Soil	3.77	3.77	3.77	3.77	3.76	1.00	1.00	1.00	1.00

Table 4.57. RMS and Arias Intensity Improvement Ratios under El Centro Earthquake Motion (PGA= 0.35 g).

Root Mean Square (RSM)				Arias Intensity	
Horizontal Acceleration(g)	Peak	RSM-Rein.	RSM Imp (%)		Arias Intensity Imp (%)
In-Soil	0.5	0.45	10.2	In-Soil	32.29

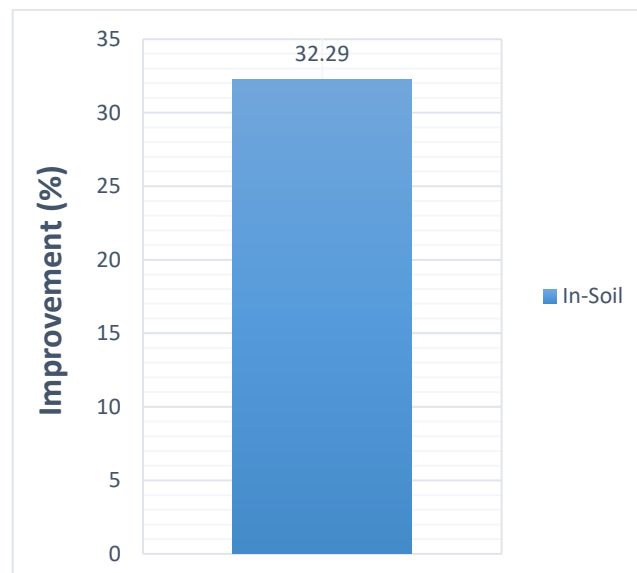


Figure 4.85. Improvement Ratios considering Arias Intensity under El Centro Earthquake Motion (PGA= 0.35 g).

4.5. Cyclic Sinusoidal Motions with Natural Frequencies

This part includes the results and comparison of cyclic sinusoidal motions with natural frequencies of the buildings that were obtained from the free-vibration tests. The natural frequencies of 5 story building were found as 2.33 Hz, 8.58 Hz, 13.34 Hz, 17.52 Hz, and 19.90 Hz and the natural frequencies of 3 story building were found as 3.93 Hz, 12.46 Hz, and 18.35Hz. Both for 3-story and 5-story building models, performance indicator parameters were investigated by considering the most dangerous frequencies to evaluate the effect of different dynamic motion characteristic on the effectiveness of proposed geogrid reinforcement system. Cyclic sinusoidal motion with 8.58 Hz frequency, which holds the first mode frequency of the 5-story building model, and 12.46 Hz frequency, which holds the second mode frequency of 3-story building model, were applied with and without geogrid reinforcement. These frequencies were the most dangerous ones and also were more effective than the earthquake motions.

4.5.1. Seismic Response of 5-Story Building Model under 8.58 Hz Cyclic Sinusoidal Motion (PGA=0.35 g)

Table 4.58 shows the reduced acceleration and displacement values through all sensors comparing to unreinforced system for 5-Storey model under 8.58 Hz-0.35g.

In the soil, peak accelerations are 0.44g in the underside and 0.47g in the midpoint and 0.49 upper side. The maximum improvements of acceleration in the underside, midpoint upper side are 29%, 53% and 8%, respectively. Also, in the soil especially for N=1 at some points there is no reduction in accelerations or improvements become negative. The reduction of foundation acceleration is 0%, 2%, 19% and 28% for N=1, N=2, N=3 and N=4, respectively.

Table 4.58. Summary of all tested Cases for 5-Story Model under 8.58 Hz-0.35g.

		N=4			N=3			N=2			N=1		
		WR	R	IMP. (%)	WR	R	IMP. (%)	WR	R	IMP. (%)	WR	R	IMP. (%)
In Soil	A5	0.4	0.31	29.032	0.4	0.38	5.263	0.4	0.39	2.564	0.4	0.4	0
	A6	0.44	0.39	12.821	0.44	0.41	7.317	0.44	0.43	2.326	0.44	0.43	2.326
	A7	0.41	0.34	20.588	0.41	0.39	5.128	0.41	0.4	2.500	0.41	0.41	0
	A8	0.43	0.28	53.571	0.43	0.4	7.500	0.43	0.42	2.381	0.43	0.42	2.381
	A9	0.46	0.37	24.324	0.46	0.43	6.977	0.46	0.45	2.222	0.46	0.45	2.222
	A10	0.44	0.37	18.919	0.44	0.39	12.821	0.44	0.44	0	0.44	0.45	-2.222
	A11	0.47	0.37	27.027	0.47	0.44	6.818	0.47	0.46	2.174	0.47	0.46	2.174
	A12	0.49	0.45	8.889	0.49	0.46	6.522	0.49	0.48	2.083	0.49	0.48	2.083
Foun.	A13	0.5	0.39	28.205	0.5	0.42	19.048	0.5	0.49	2.041	0.5	0.5	0
5 Storey Model	A14	2.6	2.19	18.721	2.6	2.38	9.244	2.6	2.55	1.961	2.6	2.56	1.563
	A15	3.61	3.01	19.934	3.61	3.37	7.122	3.61	3.53	2.266	3.61	3.56	1.404
	A16	1.69	1.4	20.714	1.69	1.65	2.424	1.69	1.65	2.424	1.69	1.67	1.198
	A17	1.67	1.35	23.704	1.67	1.56	7.051	1.67	1.63	2.454	1.67	1.65	1.212
	A18	3.56	2.97	19.865	3.56	3.4	4.706	3.56	3.48	2.299	3.56	3.51	1.425
	D20	1.66	1.26	31.746	1.66	1.41	17.730	1.66	1.63	1.840	1.66	1.64	1.220
	D21	1.79	1.52	17.763	1.79	1.66	7.831	1.79	1.75	2.286	1.79	1.77	1.130
	D22	1.28	1.06	20.755	1.28	1.24	3.226	1.28	1.25	2.400	1.28	1.27	0.787
	D23	1.35	1.15	17.391	1.35	1.2	12.500	1.35	1.31	3.053	1.35	1.33	1.504
	D24	1.79	1.67	7.186	1.79	1.69	5.917	1.79	1.75	2.286	1.79	1.77	1.130

Figure 4.86 and 4.87 show displacement and acceleration measurements and fourier amplitude spectrum of 1st and 5th Floors. Although the first floor is decreased up to 18% in acceleration value, the maximum reduction of fifth floor is 19%. The third floor' improvement is 20%. Besides, for N=1, the acceleration improvements are 1% for N=4 it reaches up to 23%.

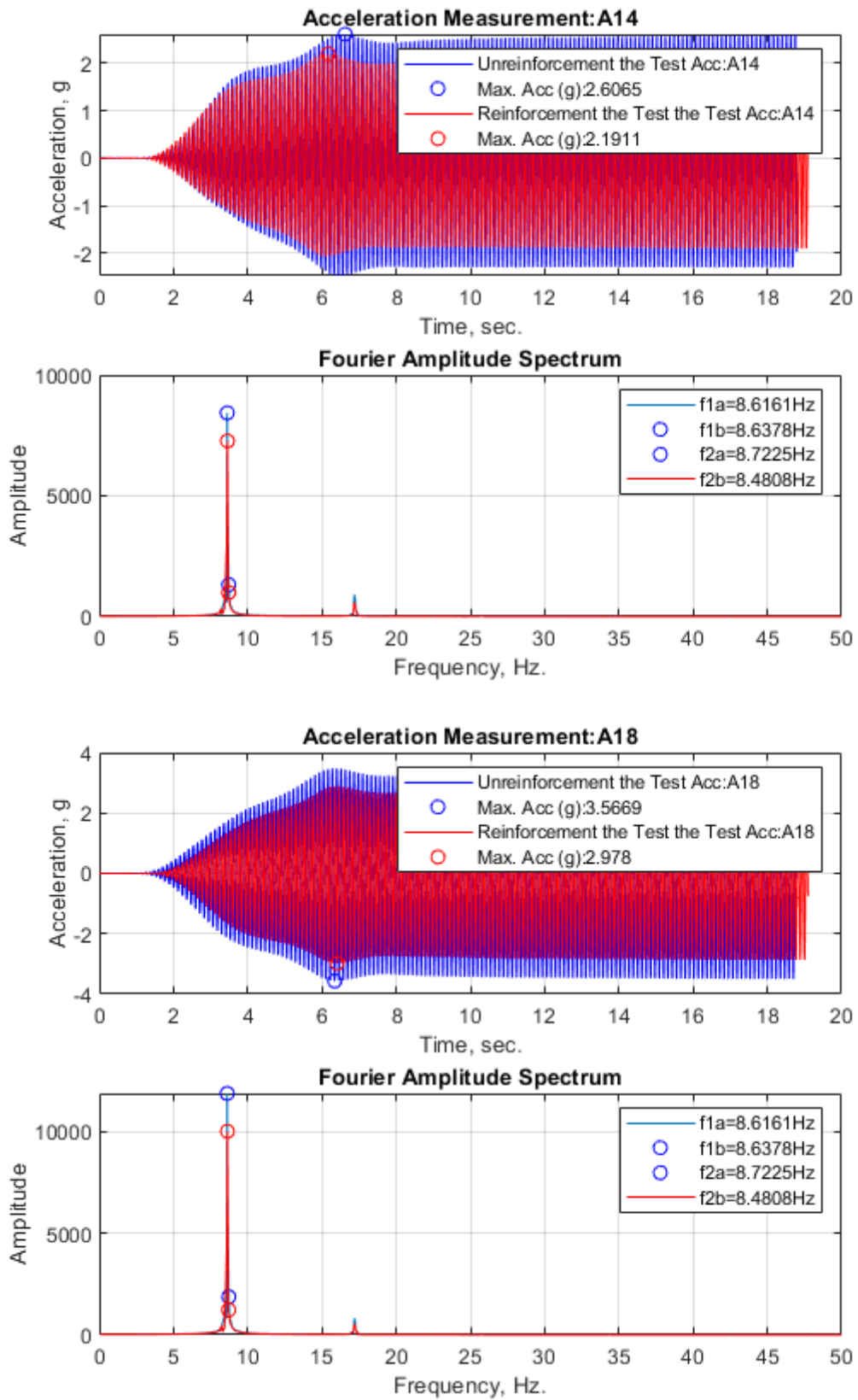


Figure 4.86. Acceleration Measurements and FAS of 1st and 5th Floors under 8.85 Hz-0.35g.

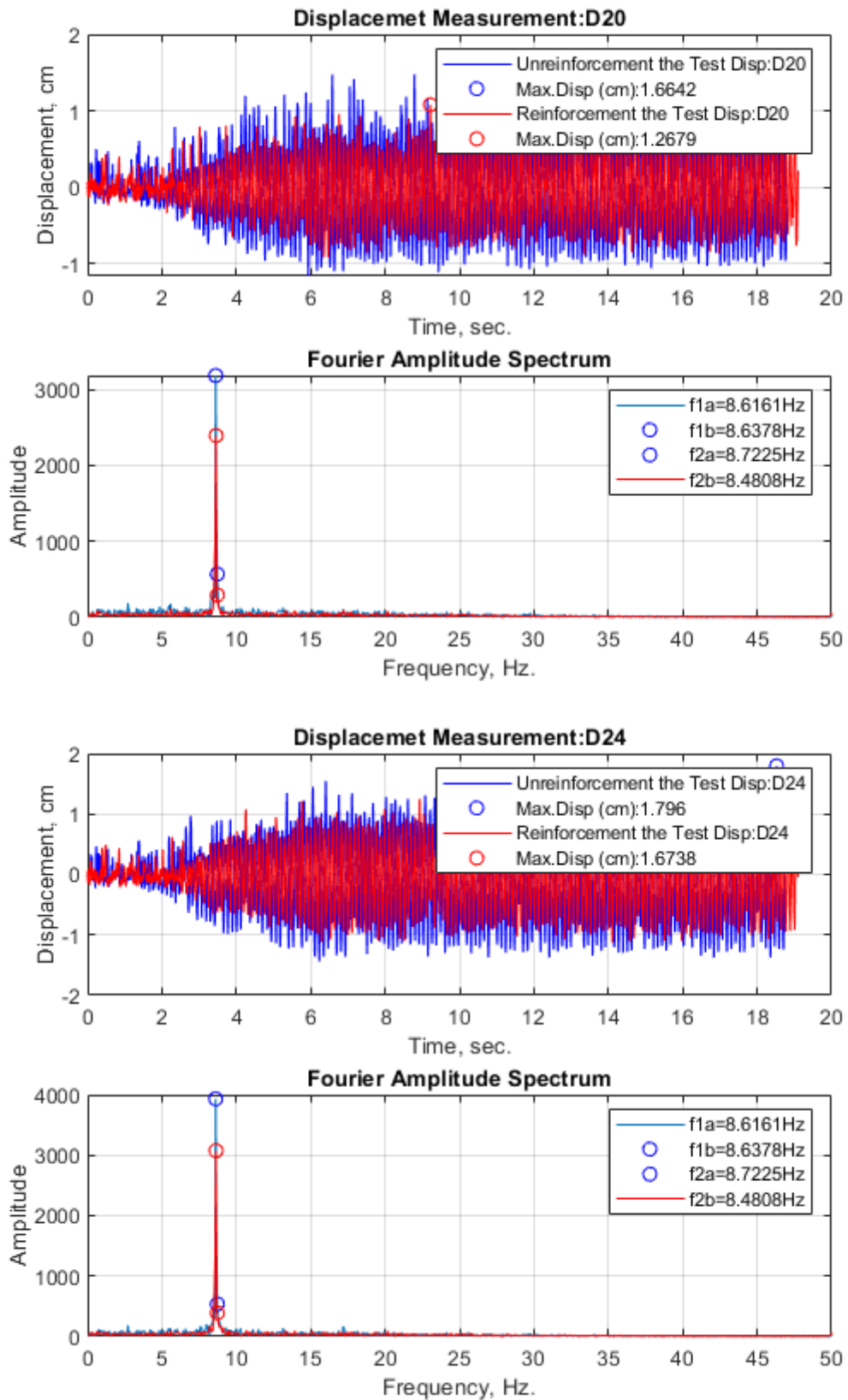


Figure 4.87. Displacement Measurements and FAS of 1st and 5th Floors under 8.58 Hz-0.35g.

In Figure 4.88 and 4.89, the acceleration and displacement improvement graphs can be observed. For all floors, in N=1 there is no notable improvement in the reduction of acceleration like in the soil, which are 1-2% or become negative. However, with the increase in the geogrid layers, the significant improvement can be observed. It becomes 2%, 8%, and 14% for the first floor 2%, 2%, and 20% for the third floor and 2%, 4%, and 19% for the fifth floor in N=2, N=3, and N=4, respectively. Approximately up to 30% the acceleration reduction can be seen comparing to unreinforced system.

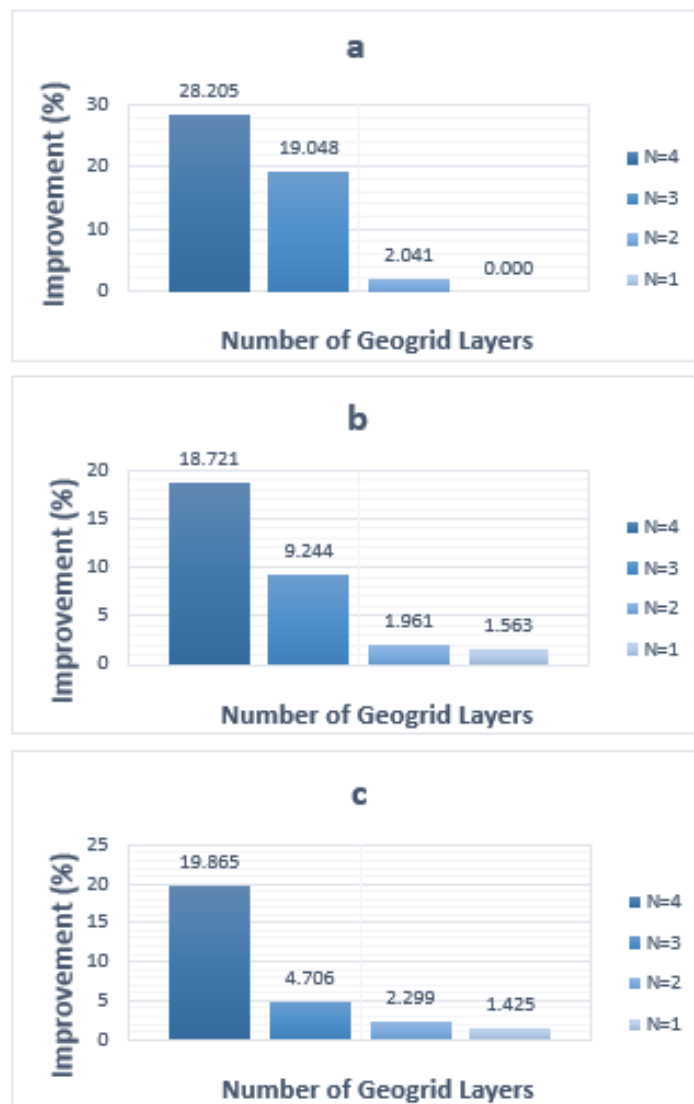


Figure 4.88. The Acceleration Improvement Graphs in Accordance with Story and Reinforcement Layers for (a) Foundation, (b) 1st Floor, (c) 5th Floor under 8.58 Hz-0.35g.

In the first, third floor and fifth floors, the maximum decrease of story's displacement is 31%, 20% and 7%, respectively. Also, just as acceleration values, there is no significant improvement in the reduce of stories displacement for N=1.

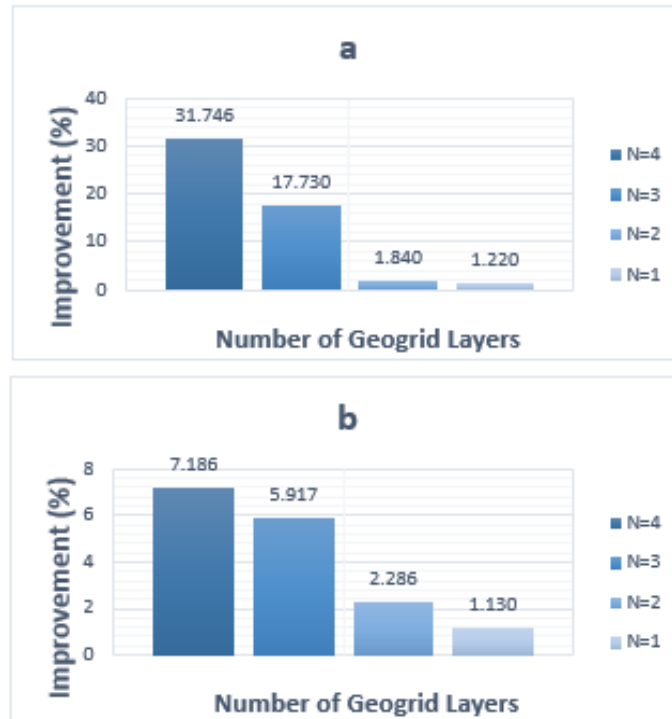


Figure 4.89. The Displacement Improvement Graphs in Accordance with Story and Reinforcement Layers for (a) 1st Floor, (b) 5th Floor under 8.58 Hz-0.35g.

In Table 4.59 and Table 4.60, Arias intensity improvements were exhibited and with the help of the fundamental period of all N values under dynamic loads for soil, foundations, floors, the period lengthening ratios were given, and also RMS of peak values were shown.

Table 4.59. Fundamental Period and Period Lengthening Ratios under 8.58 Hz-0.35g.

	Fundamental Period (Hz)					Period Lengthening Ratio			
	N=4	N=3	N=2	N=1	N=0	N=4	N=3	N=2	N=1
In-Soil	8.63	8.63	8.63	8.58	8.16	0.95	0.95	0.95	0.95
Foundation	8.63	8.63	8.63	8.58	8.16	0.95	0.95	0.95	0.95
1st Floor	8.63	8.63	8.63	8.58	8.16	0.95	0.95	0.95	0.95
2nd Floor	8.63	8.63	8.63	8.58	8.16	0.95	0.95	0.95	0.95
3rd Floor	8.63	8.63	8.63	8.58	8.16	0.95	0.95	0.95	0.95
4th Floor	8.63	8.63	8.63	8.58	8.16	0.95	0.95	0.95	0.95
5th Floor	8.63	8.63	8.63	8.58	8.16	0.95	0.95	0.95	0.95

Table 4.60. RMS and Arias Intensity Improvement Ratios under 8.58 Hz-0.35g.

Root Mean Square (RSM)				Arias Intensity	
Horizontal Acceleration(g)	Peak	RSM-Rein.	RSM Imp (%)		Arias Intensity Imp (%)
In-Soil	0.49	0.47	4.77	In-Soil	11.24
Foundation	0.5	0.45	10.53	Foundation	32.14
1st Floor	2.6	2.42	7.23	1st Floor	22.13
2nd Floor	3.61	3.37	6.98	2nd Floor	26.17
3rd Floor	1.69	1.6	5.86	3rd Floor	23.45
4th Floor	1.67	1.55	7.6	4th Floor	21.43
5th Floor	3.56	3.35	6.36	5th Floor	17.34

Arias intensity values for soil region and foundation are reduced approximately 11% and 32% and it reduces up to 26% for floors. RMS improvement values for soil, foundation and floors are 5%, 10%, 7%, 7%, 6%, 7% and 7%, respectively. There is no change in the natural period of model. The period lengthening ratio fluctuates up to %5. And also, in Figure 4.90, Story Drifts and Arias Intensity Improvement Ratios can be seen.

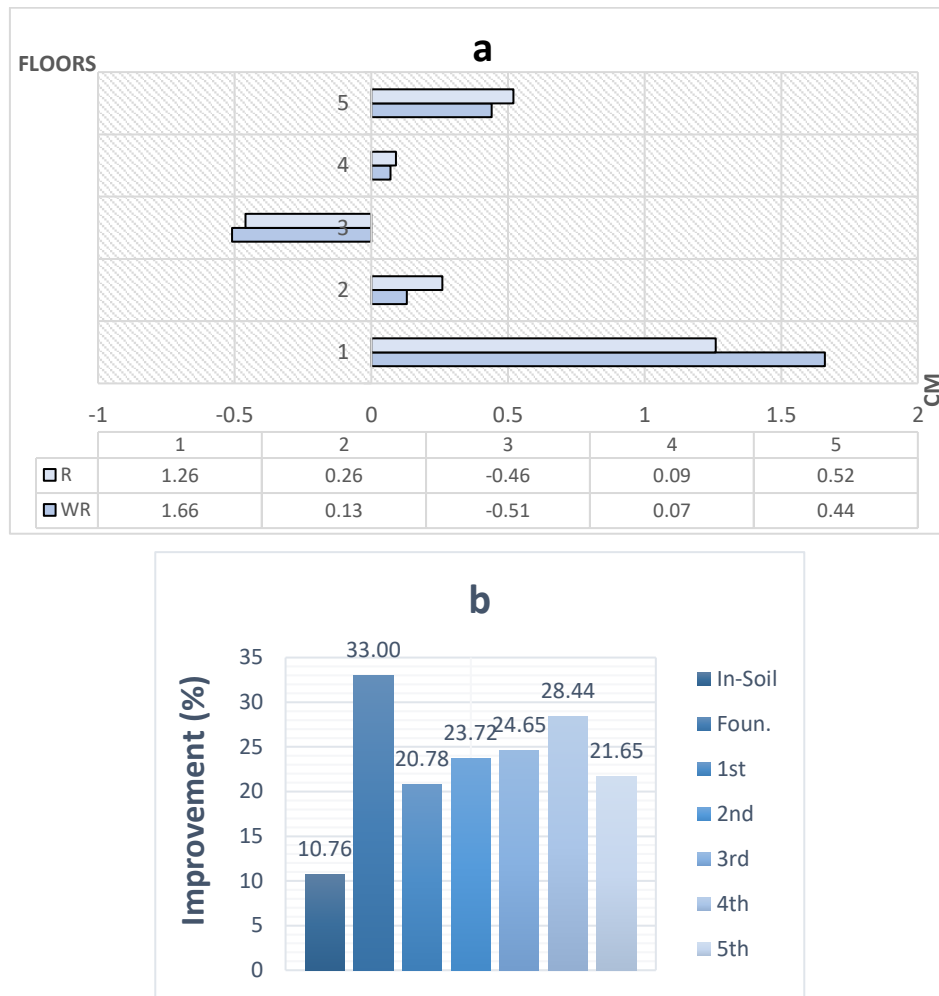


Figure 4.90. Improvement Ratios considering (a) Story drifts and (b) Arias Intensity under 8.58 Hz-0.35g

4.5.2. Seismic Response of 3-Story Building Model under 12.46 Hz Cyclic Sinusoidal Motion(PGA=0.4 g)

Table 4.61 shows the reduced acceleration and displacement values through all sensors comparing to unreinforced system for 3-Storey model under 12.46 Hz-0.4g.

Table 4.61. Summary of all tested Cases for 5-Story Model under 12.46 Hz-0.4g.

		N=4			N=3			N=2			N=1		
		WR	R	IMP. (%)	WR	R	IMP. (%)	WR	R	IMP. (%)	WR	R	IMP. (%)
In Soil (g)	A5	0.39	0.34	14.706	0.39	0.36	8.333	0.39	0.38	2.632	0.39	0.38	2.632
	A6	0.47	0.42	11.905	0.47	0.44	6.818	0.47	0.46	2.174	0.47	0.47	0
	A7	0.47	0.36	30.556	0.47	0.4	17.500	0.47	0.46	2.174	0.47	0.47	0
	A8	0.47	0.41	14.634	0.47	0.43	9.302	0.47	0.45	4.444	0.47	0.46	2.174
	A9	0.52	0.46	13.043	0.52	0.48	8.333	0.52	0.51	1.961	0.52	0.52	0
	A10	0.51	0.41	24.390	0.51	0.46	10.870	0.51	0.51	0	0.51	0.52	-1.923
	A11	0.53	0.46	15.217	0.53	0.48	10.417	0.53	0.51	3.922	0.53	0.52	1.923
	A12	0.74	0.65	13.846	0.74	0.68	8.824	0.74	0.72	2.778	0.74	0.74	0
Foun.(g)	A13	0.59	0.52	13.462	0.59	0.54	9.259	0.59	0.57	3.509	0.59	0.59	0
3 Storey Model (cm)	A14	4.13	3.32	24.398	4.13	3.58	15.363	4.13	4	3.250	4.13	4.1	0.732
	A15	1.92	1.69	13.609	1.92	1.7	12.941	1.92	1.86	3.226	1.92	1.91	0.524
	A16	3.47	3.04	14.145	3.47	3.18	9.119	3.47	3.37	2.967	3.47	3.44	0.872
	D20	1.22	1.02	19.608	1.22	1.07	14.019	1.22	1.17	4.274	1.22	1.18	3.390
	D21	0.91	0.76	19.737	0.91	0.77	18.182	0.91	0.89	2.247	0.91	0.91	0
	D22	1.08	0.95	13.684	1.08	0.99	9.091	1.08	1.05	2.857	1.08	1.07	0.935

Peak accelerations are 0.39g in the underside, 0.53g midpoint, and 0.74g in the upper side in the soil. The decrease of acceleration in underside is %2, %2, %8 and %14, the reduction of acceleration in midpoint is 1%, 3%, 10% and 15%, the reduction of acceleration in upper side is 0%, 2%, 8% and 13% roughly for N=1, N=2, N=3 and N=4. The decrease of foundation acceleration is 0%, 3%, 9% and 13% for N=1, N=2, N=3 and N=4, respectively.

Figure 4.91 and 4.92 show displacement and acceleration measurements and fourier amplitude spectrum of 1st and 3rd Floors. Although the first floor is decreased up to 18% in acceleration value, the maximum reduction of third floor is 14%. Besides, for N=1, the acceleration improvements are 0%. For N=4 it reaches up to 24%.

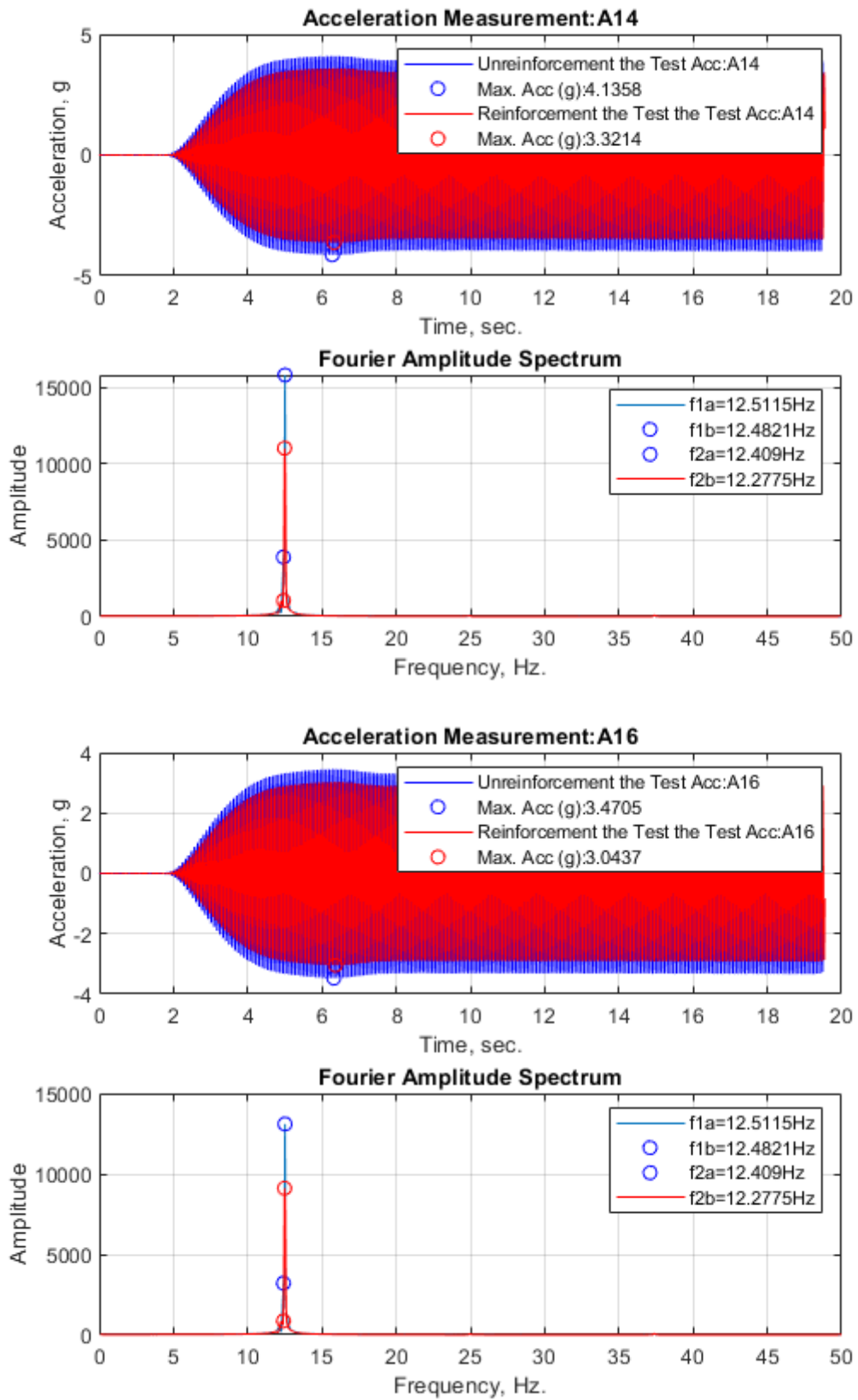


Figure 4.91. Acceleration Measurements and FAS of 1st and 3rd Floors under 12.46 Hz-0.4g.

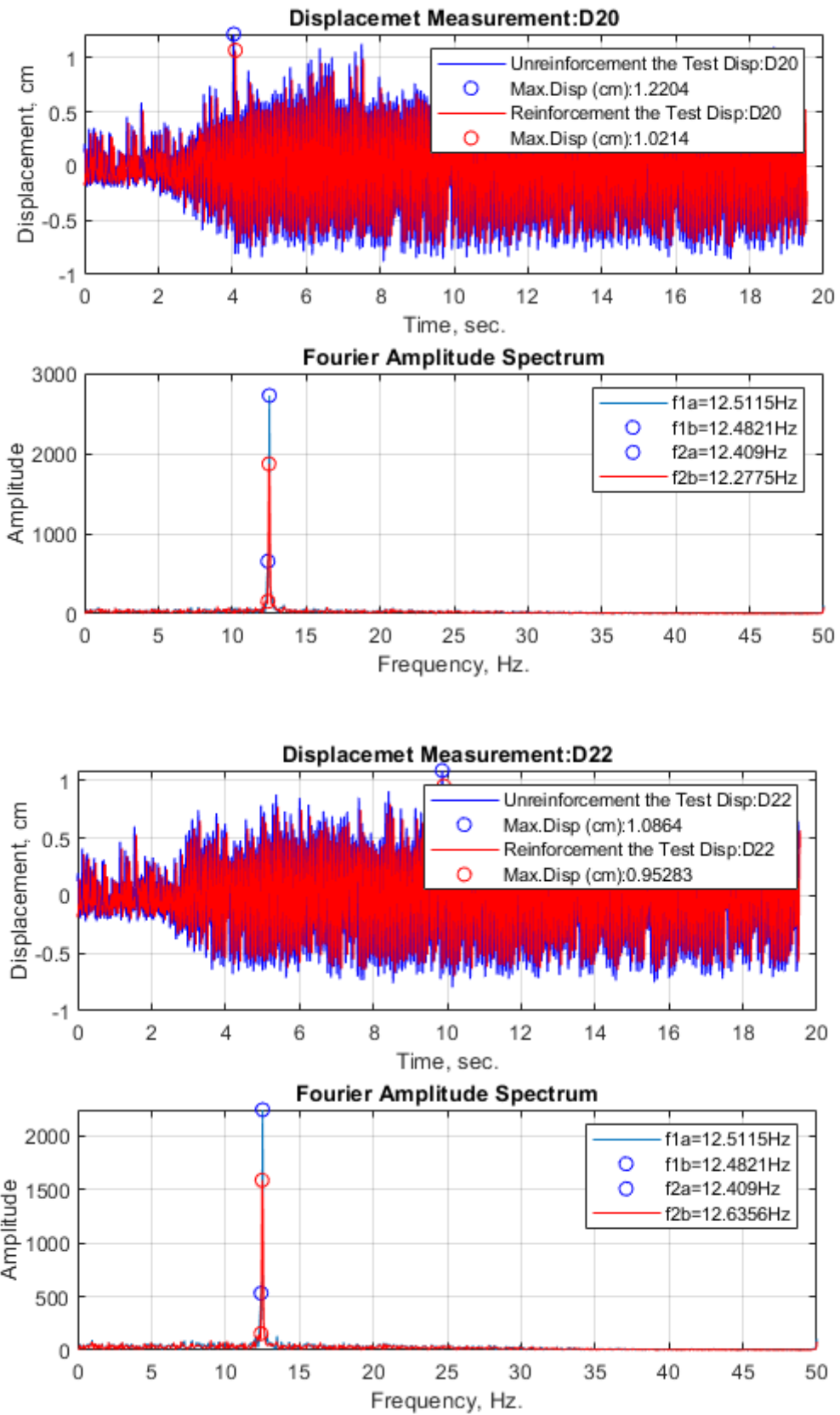


Figure 4.92. Displacement Measurements and FAS of 1st and 3rd Floors under 12.46 Hz-0.4g.

In Figure 4.93 and 4.94, the acceleration and displacement improvement graphs can be seen. The improvements in acceleration for N=1 become negative. With the increase in the geogrid layers, improvements in acceleration become 3%, 15%, and 24% on the first floor and on the third floor the acceleration values are decreased 2%, 9%, and 14% comparing to unreinforced system for N=2, N=3, and N=4, respectively.

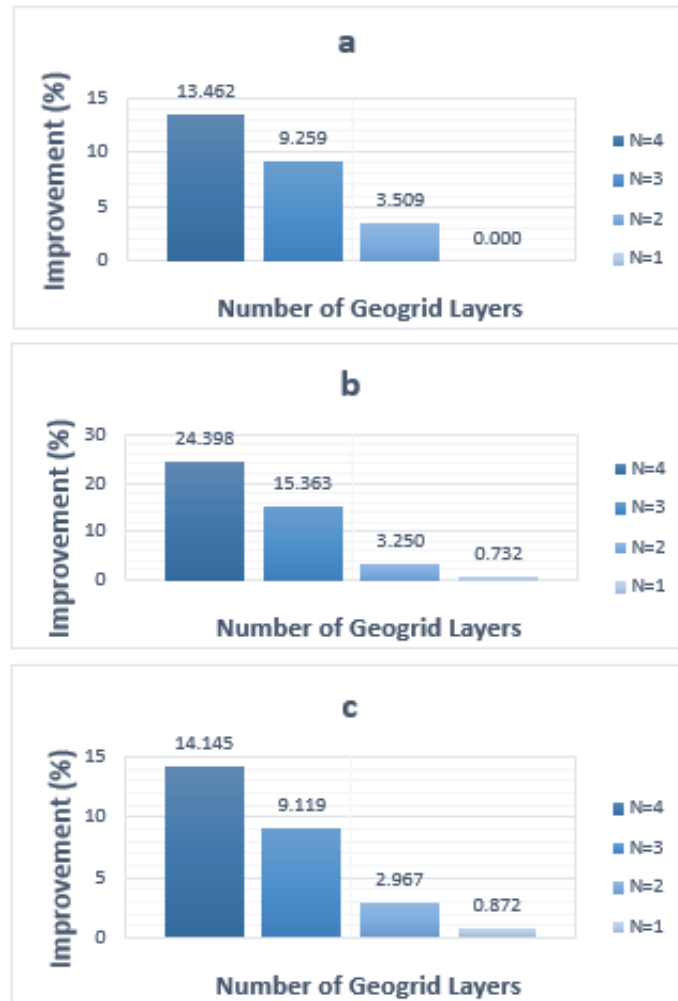


Figure 4.93. The Acceleration Improvement Graphs in Accordance with Story and Reinforcement Layers for (a) Foundation, (b) 1st Floor, (c) 3rd Floor under 12.46 Hz-0.4g.

The maximum decrease of story's displacement is 19% and 13% for the first and third floor, respectively. Besides, for the first and second floor, there is no reduction in N=1, but in N=3 the improvement values make a splash, which reaches up to 18%.

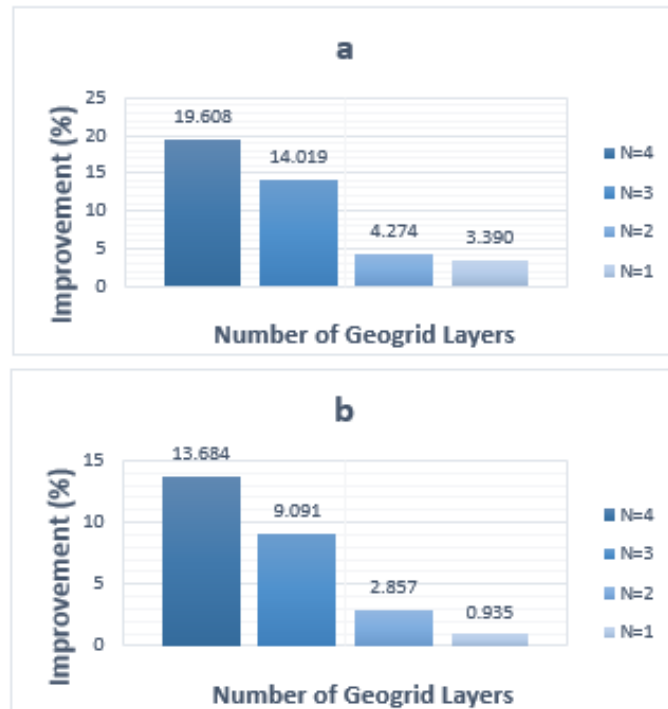


Figure 4.94. The Displacement Improvement Graphs in Accordance with Story and Reinforcement Layers for (a) 1st Floor, (b) 3rd Floor under 12.46 Hz-0.4g.

As it can be seen in Table 4.62 and 4.63, Arias intensity values for soil region and foundation are reduced nearly 11%, and 13% and it decrease up to 19% for floors. RMS improvement values for soil, foundation and floors are 5%, 6%, 9%, 7% and 6%, respectively. Also, there is no change in the natural period of model. And Figure 4.95 illustrates Story Drifts and Arias Intensity improvement ratios.

Table 4.62. Fundamental Period and Period Lengthening Ratios under 12.46 Hz-0.4g.

	Fundamental Period (Hz)					Period Lengthening Ratio			
	N=4	N=3	N=2	N=1	N=0	N=4	N=3	N=2	N=1
In-Soil	12.48	12.48	12.48	12.48	12.51	1.00	1.00	1.00	1.00
Foundation	12.48	12.48	12.48	12.48	12.51	1.00	1.00	1.00	1.00
1st Floor	12.48	12.48	12.48	12.48	12.51	1.00	1.00	1.00	1.00
2nd Floor	12.48	12.48	12.48	12.48	12.51	1.00	1.00	1.00	1.00
3rd Floor	12.48	12.48	12.48	12.48	12.51	1.00	1.00	1.00	1.00

Table 4.63. RMS and Arias Intensity Improvement Ratios under 12.46 Hz-0.4g.

Root Mean Square (RSM)				Arias Intensity	
Horizontal Acceleration(g)	Peak	RSM-Rein.	RSM Imp (%)		Arias Intensity Imp (%)
In-Soil	0.74	0.70	5.96	In-Soil	11.64
Foundation	0.59	0.56	6.18	Foundation	13.24
1st Floor	4.13	3.76	9.74	1 st Floor	19.29
2nd Floor	1.92	1.79	7.11	2 nd Floor	18.47
3rd Floor	3.47	3.26	6.40	3 rd Floor	16.20

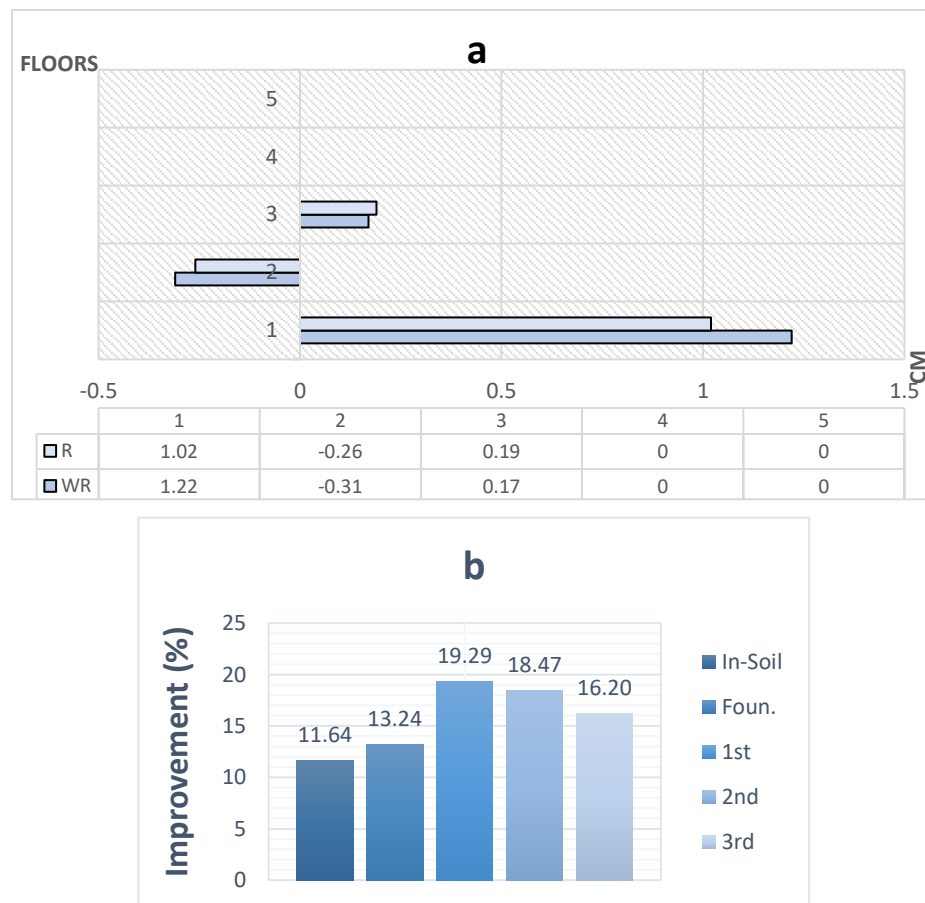


Figure 4.95. Improvement Ratios considering (a) Story drifts and (b) Arias Intensity under 12.46 Hz-0.4g.

5. DISCUSSION

Through shaking table experiments, the effects of the number of the story, the number of geogrid reinforcement layers and ground motion characteristic on effectiveness durability of the proposed geogrid reinforcement system were investigated. The percentage reduction of peak and RMS values of top floor acceleration, first floor acceleration, foundation acceleration, soil acceleration, first floor drift, top floor drift, top floor arias intensity, first floor arias intensity, foundation arias intensity was selected as performance criteria to investigate and evaluate the ultimate experimental results. The percentage reduction of selected parameters was computed based on unreinforced cases.

In order to observe ideal condition and evaluate the effect of different dynamic motion characteristic on the effectiveness of proposed geogrid reinforcement system, the obtained results of selected performance indicator were tabulated and graphed under both under earthquake records with original PGA and cyclic sinusoidal motion with the most dangerous mode frequency of the building model and different dynamic input characteristic including different scaled peak accelerations of earthquake records. Thus, effects of amplitude of the seismic motions on the effectiveness of geogrid reinforcement system were exhibited.

The figures which were exhibited below include both table and graph of alteration of the percentage reduction of values for all input motions together.

5.1. Effects of The Proposed Geogrid Reinforcement System under Earthquake Motions with Real PGA, Earthquake Motions with Increasing PGA and Cyclic Sinusoidal Motion

5.1.1. Seismic Response of The Cases For 5-Story Model

This part includes the ultimate results and comparisons of the effectiveness of proposed geogrid reinforcement system for 5-Story building model under earthquake motions with real PGA, earthquake Motions with increasing PGA and cyclic sinusoidal

motion with first mode frequency of the building model. The effect of geogrid reinforcement layers starting from without reinforcement ($N=0$) up to $N=4$ can be seen for all input motions in figures. Also, the effectiveness of proposed geogrid reinforcement was shown by considering the selected performance indicators one by one.

5.1.1.1. Effects of Proposed Geogrid Reinforcement System on Top Floor Acceleration for 5-Story Model. Figure 5.1. indicate the variations of the top floor acceleration for all input motions used through shaking table experiments and the effectiveness of proposed geogrid reinforcement system according to the number of geogrid layers. It can be seen that the proposed geogrid reinforcement system behaved better under the lower acceleration amplitude of Kocaeli and Kobe earthquakes motions. The maximum decrease in the top floor accelerations were 37% and 14% for Kobe 0.74g and Kocaeli 0.21g in $N=4$. And also, Kobe earthquake with 0.74 g was the most beneficial case among the other input motions. In contrast to Kobe and Kocaeli earthquakes, in El Centro motions the top floor acceleration exhibited preferable behavior under lower acceleration amplitude. While for El Centro earthquake with 0.89g the improvement in acceleration was %13, for El Centro earthquake with 0.35g it decreased up to %30. In cyclic sinusoidal motion with 8.58 Hz, which is the first of mode of 5-story building model, the proposed geogrid reinforcement system had limited improvement in acceleration up to $N=3$, it was 1%, 2%, and 4%, respectively. And with $N=4$ the decrease of top floor acceleration went up to 30%. It is clear that $N=4$ is the most beneficial case and increase in the number of geogrid layers resulted in better performance for top floor acceleration for all input motions including real and increasing PGA values. And also, except Kobe earthquake with 0.74g, for $N=1$ all input motions indicated slightly effect in the reduction of acceleration or improvements became negative. With $N=2$, significant increases began to be seen. However, for Kocaeli earthquake with 0.21g the reduction of acceleration continued to be 2%, 2% and 3% for $N=1$, $N=2$, and $N=3$, respectively. It became %8 for $N=4$.

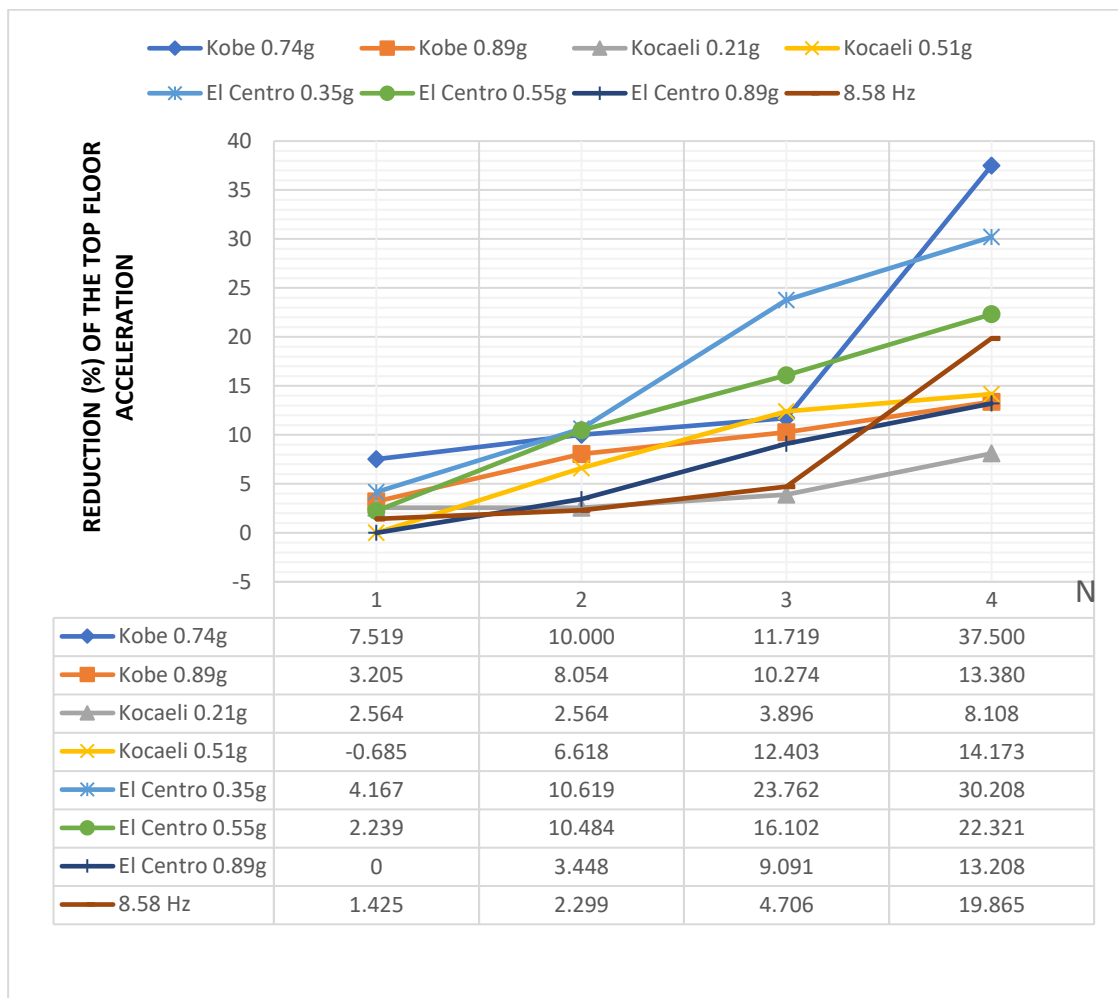


Figure 5.1. Reduction of Top Floor Acceleration under Input Motions for 5-Storey Model.

5.1.1.2. Effects of Proposed Geogrid Reinforcement System on First Floor Acceleration for 5-Story Model. Figure 5.2 represents the alteration of the first floor acceleration for all input motions used in shaking table experiments and the variations effectiveness of proposed geogrid reinforcement system by the number of geogrid layers. As can be observed the proposed geogrid reinforcement system performed better under the lower acceleration amplitude of El Centro and Kobe earthquake motions. El Centro earthquake with 0.35g and Kobe earthquake with 0.74g gave the most effective results among all El Centro and Kobe earthquake motions. The maximum reduction in the first-floor accelerations was 42% and 30%, which were obtained from Kocaeli earthquake motions. Also, Kobe earthquake with 0.89g, which was the higher amplitude earthquake motion for Kobe earthquake, was the worst input motion in the aspect of the reduction of acceleration. Its acceleration improvements were 0%, 3%, 3% and 6% for N=1, N=2, N=3 and N=4,

respectively. Unlike El Centro and Kobe earthquakes, Kocaeli Earthquake displayed better performance under higher amplitude. In Kocaeli earthquake with 0.21g and 0.51g earthquake motions, the decrease of the first-floor accelerations was %30 and %42, respectively. Cyclic sinusoidal motion with 8.58 Hz, which is the first of mode of 5-story building model, exhibited limited improvement in acceleration up to N=2, which were 1% and 1% for N=1 and N=2, respectively. And with N=3 it bounced up to 9%. For all input motions, N=4 was the most advantageous option and largely N=2 and N=3 gave quite acceptable results in reduction of the first-floor accelerations. However, except Kocaeli earthquakes there was a slight effect in reduction of acceleration values for N=1.

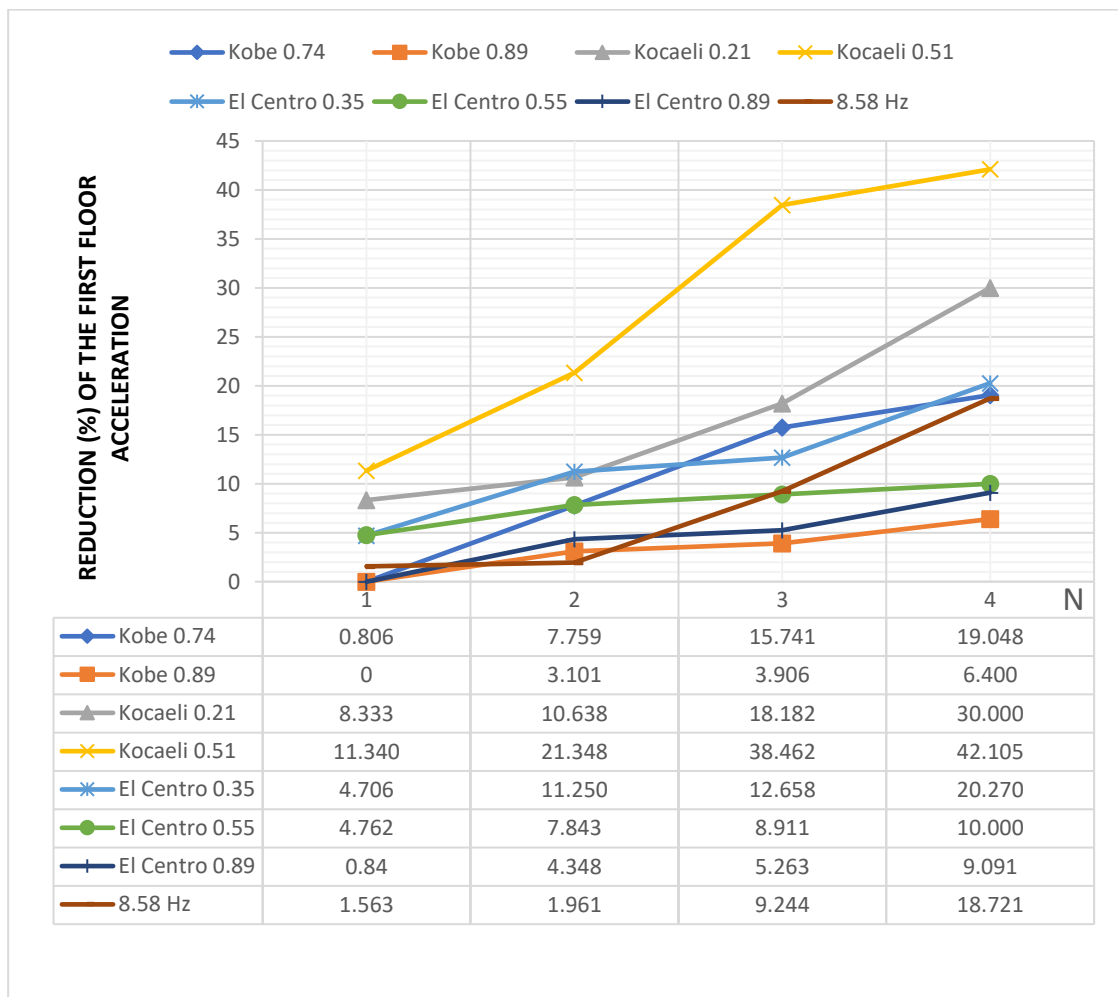


Figure 5.2. Reduction of First Floor Acceleration under Input Motions for 5-Storey Model.

5.1.1.3. Effects of Proposed Geogrid Reinforcement System on Top Floor Displacement for 5-Story Model. Variations of the top floor displacement for all input motions used through shaking table experiments and the effectiveness of proposed geogrid reinforcement

system based on the number of geogrid layers are shown in Figure 5.3. According to Figure 5.3, while Kobe earthquake behaved better under higher amplitude, El Centro Earthquake performed better under lower amplitude. The most effective results in decrease of top floor displacement for these motions were obtained from Kobe earthquake with 0.89g and El Centro earthquake with 0.35g, which were 35% and 25%. Besides, it can be seen that the change of amplitude did not significantly effect the reduction of top floor displacement for Kocaeli earthquake. The improvements were 21% and 19% for Kocaeli earthquake with 0.21g and 0.51g, respectively. Among Earthquake motions, Kobe earthquake with 0.74g gave the veriest results, which were 1%, 1%, 7% and 8% for N=1, N=2, N=3, and N=4, respectively. As expected in N=4, the most effective results were obtained for all input motions and also except Kobe earthquake with 0.89g and 0.51g. N=1 did not function to reduce top floor displacement. Cyclic sinusoidal motion with 8.58 Hz, which is the first of mode of 5-story building model, showed ineffective performance. The decrease of displacement was 1%, %2, 5% and 7% for N=1, N=2, N=3 and N=4, respectively.

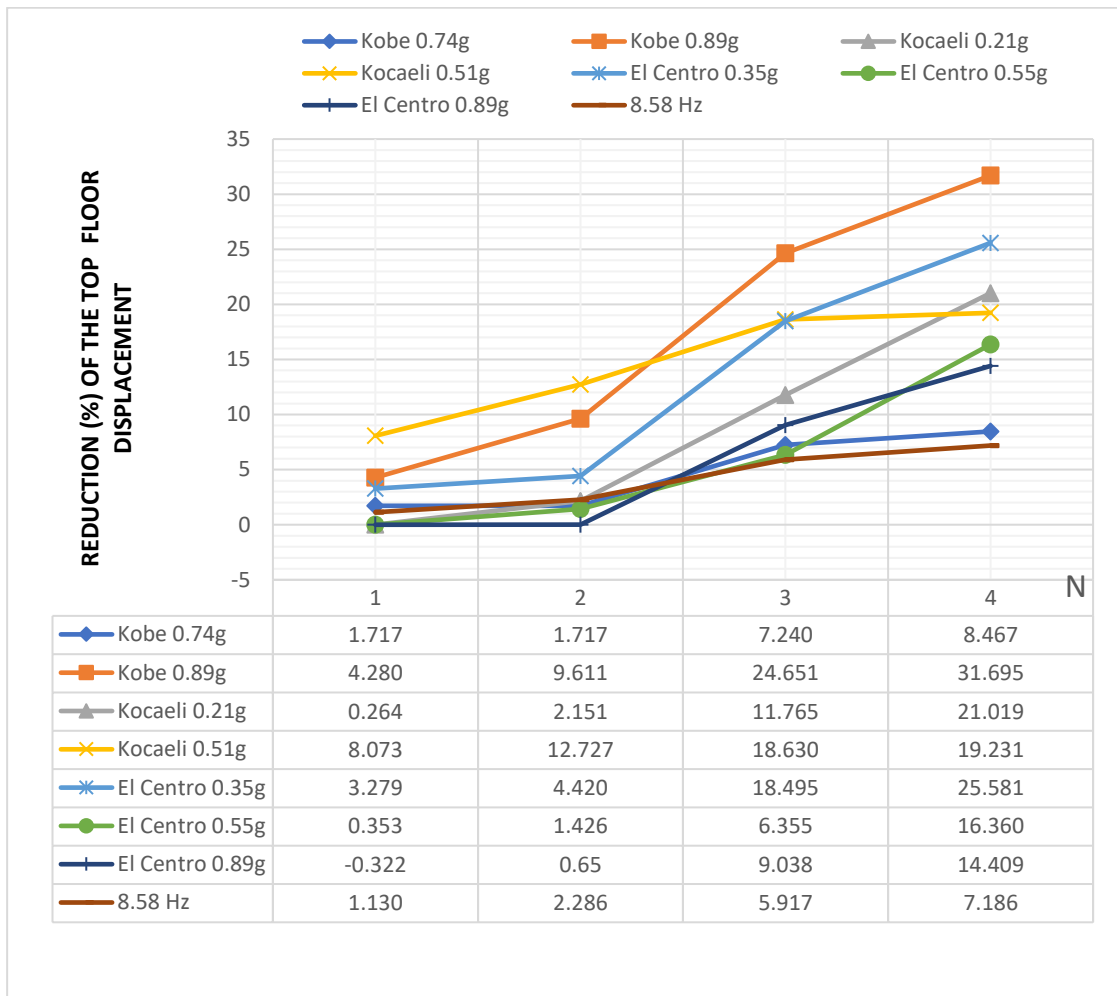


Figure 5.3. Reduction of Top Floor Displacement under Input Motions for 5-Storey Model.

5.1.1.4. Effects of Proposed Geogrid Reinforcement System on First Floor Displacement for 5-Story Model. Figure 5.4 illustrate that the variations of the top floor acceleration for all input motions used through shaking table experiments and the effectiveness of proposed geogrid reinforcement system by the number of geogrid layers. As can be observed, while for Kocaeli Earthquake motions the better improvements in the first floor displacement were under higher amplitude, for Kobe Earthquake motions, the lower amplitude was more effective. The decrease of the first floor displacement were 9%, 10%, 11%, 20% and 0%, 2%, 7%, 22% for N=1, N=2, N=3, N=4 in Kobe 0.74g and Kocaeli 0.51g respectively. Besides, the variation of amplitude of El Centro earthquake did not effect the reduction in the first floor displacement considerably. For N=4 the maximum decrease of displacements in El Centro were 22%, 25% and 24% for 0.35g, 0.55g and 0.89g

respectively. Except El Centro 0.55g and Kobe earthquake with 0.74g N=1 did not function to lessen displacement values. Cyclic sinusoidal motion with 8.58 Hz, which is the first of mode of 5-story building model, was the most effective case with 31% in the reduction of displacement among other input motions. Its improvement started with 1% for N=1 and N=2, then with significant splash the reduction values reached 17% and 31% for N=3 and N=4. Just as other indicators, for the first-floor displacement, N=4 had the most powerful impact on reduction.

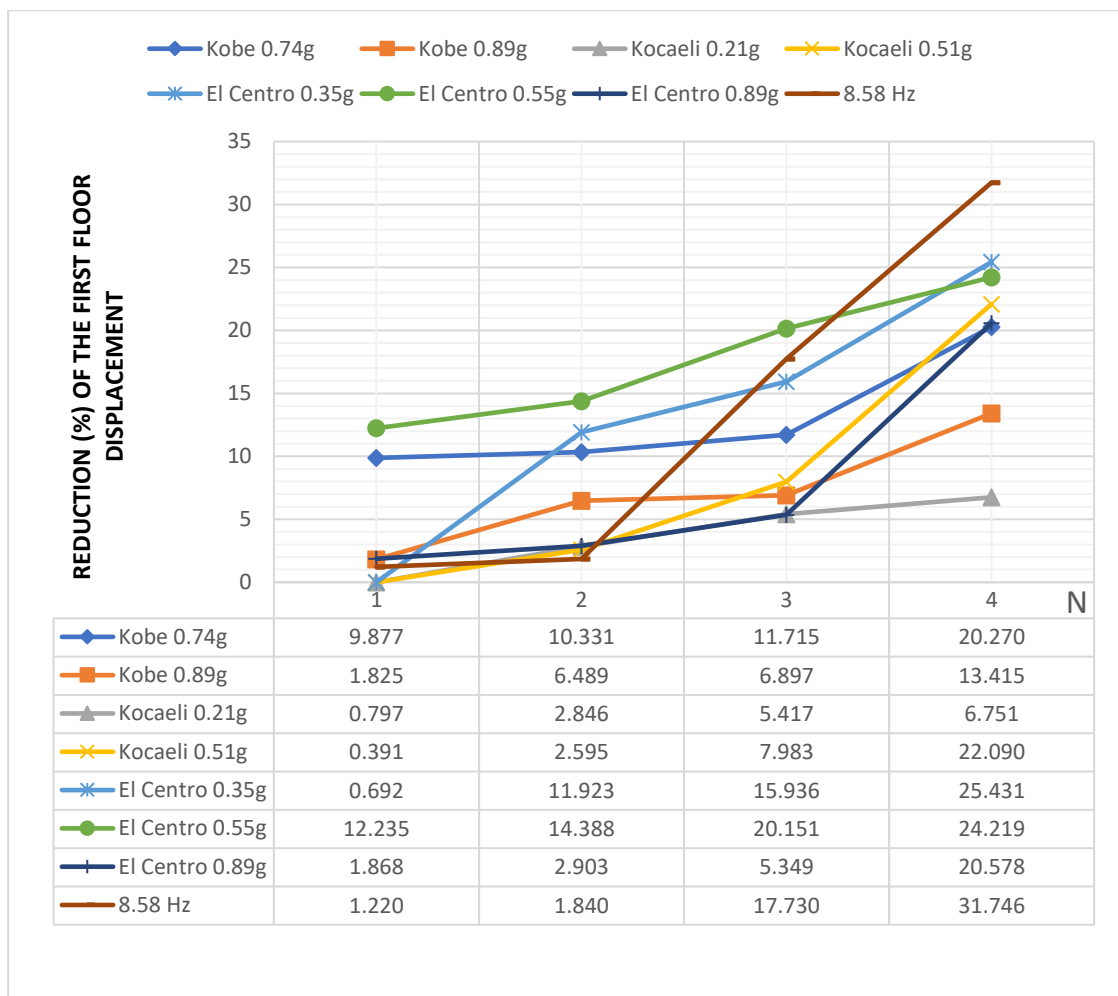


Figure 5.4. Reduction of First Floor Displacement under Input Motions for 5-Storey Model.

5.1.1.5. Effects of Proposed Geogrid Reinforcement System on Foundation Acceleration for 5-Story Model. Figure 5.5 shows the change of foundation acceleration for all input motions used throughout shaking table experiments and the effectiveness of proposed geogrid reinforcement system according to the number of geogrid layers. It can be clearly

seen that the proposed geogrid reinforcement system functioned better at Kocaeli Earthquake motions. For N=4, the reduction of foundation accelerations were 26% and 39% in Kocaeli earthquake with 0.21g and 0.51g, respectively. Also as can be observed the reinforcement system worked better at higher acceleration amplitude for Kocaeli earthquake motions and performed better at lower acceleration amplitude for Kobe and El Centro earthquake motions. The improvement in acceleration values were 6%, 7%, 15%, 18% and 2%, 5%, 9%, 14% for Kobe earthquake with 0.74g and Kobe earthquake with 0.89g. Similarly, the improvements were 4%, 9%, 17%, 20% and 2%, 4%, 4%, 12% for El Centro 0.35g and El Centro 0.89g. N=4 was the most beneficial case by far for improvement in acceleration. Cyclic sinusoidal motion with 8.58 Hz, which is the first mode of 5-story building model, showed considerable improvement in the decrease of acceleration values. It gave the second-best results. The reduction rates were 0%, 2%, 19%, 28% for N=1, N=2, N=3 and N=4, respectively. Besides, except El Centro earthquake with 0.89g, between N=2 and N=3, the effectiveness of proposed geogrid reinforcement system rose dramatically.

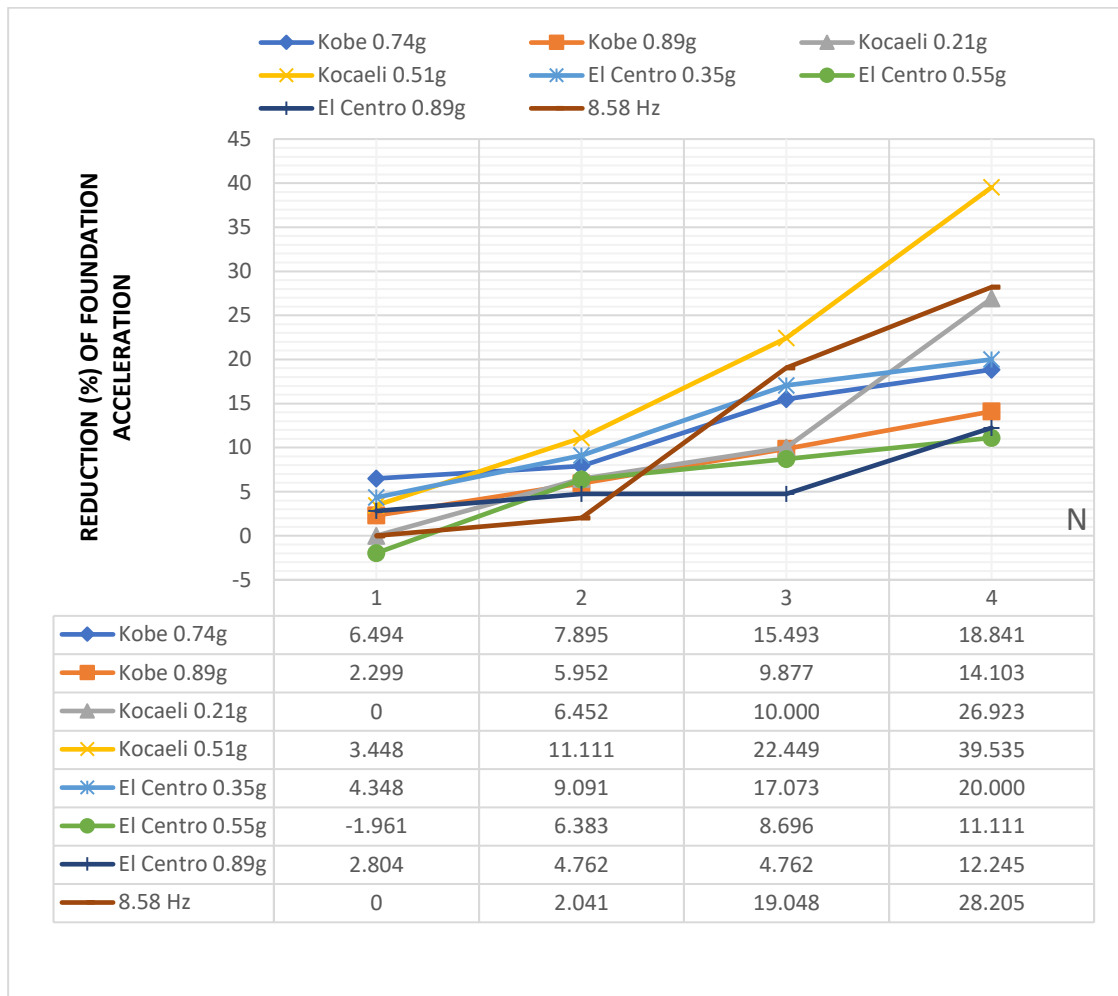


Figure 5.5. Reduction of Foundation Acceleration under Input Motions for 5-Storey Model.

5.1.1.6. Effects of Proposed Geogrid Reinforcement System on Soil Acceleration for 5-Story Model. The changing percentages of soil acceleration for all input motions used throughout shaking table experiments and the effectiveness of proposed geogrid reinforcement system with respect to the number of geogrid layers are shown in Figure 5.6. According to Figure 5.6, it can be deduced that the proposed geogrid reinforcement system functioned better at higher acceleration amplitude for El Centro and Kocaeli Earthquake motions. The decrease of soil acceleration percentages were -5%, 3%, 6%, 14% and 1%, 15%, 26%, 30% for Kocaeli 0.21g and Kocaeli 0.51g. In parallel, the reductions were 0%, 4%, 15%, 15% and 11%, 16%, 25%, 29% for El Centro 0.35g and El Centro 0.89g. In contrast to these earthquakes, in Kobe earthquake, geogrid reinforcement system was more effective under lower acceleration amplitude. Soil acceleration decreased up to 3%, 4%,

14%, 25% and 1%, 4%, 10%, 15% for Kobe earthquake with 0.74g and 0.89g. Also system showed similar performance under Kocaeli earthquake with 0.51g and El Centro earthquake with 0.89g. The maximum improvements for these Earthquake motions were 30% and 29%, respectively in N=4. In cyclic sinusoidal motion with 8.58 Hz, which is the first of mode of 5-story building model, the reinforcement system indicated poor performance compared to other input motions. The reduction percentages were 2%, 2%, 6%, 8% for N=1, N=2, N=3, N=4. As expected for all cases, N=4 was the most effective ones and N=1 nearly did not trigger reinforcement system, the improvements were faint for all input motions except El Centro earthquake with 0.89g.

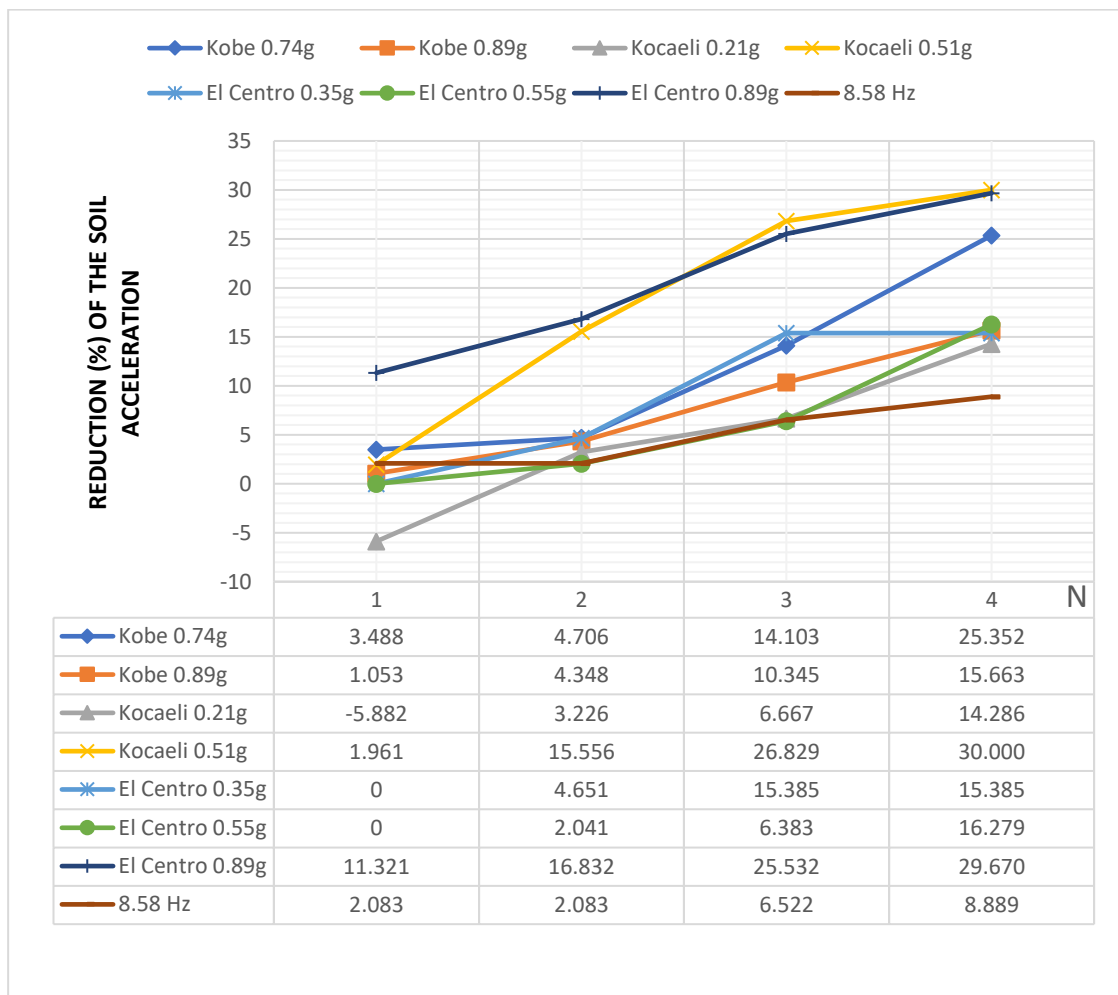


Figure 5.6. Reduction of Soil Acceleration under Input Motions for 5-Storey Model.

5.1.1.7. Effects of Proposed Geogrid Reinforcement System on Top Floor Arias Intensity for 5-Story Model. Figure 5.7 indicates the change of top floor arias intensity for all input motions used in shaking table experiments and the effectiveness of proposed geogrid

reinforcement system with according to the number of geogrid layers. It can be seen that the proposed geogrid reinforcement system apparently performed better under lower acceleration amplitude for Kobe and El Centro earthquake motions. The decrease of top floor's arias intensity were 9%, 12%, 14%, 43% and 3%, 9%, 12%, 15% for Kobe earthquake with 0.74g, and 0.89g and 5%, 13%, 29%, 34% and 0%, 4%, 11%, 15% for El Centro earthquake with 0.35g and 0.89g, respectively. In contrast to these, in Kocaeli earthquake the reinforcement system showed better performance at higher acceleration amplitude. The improvement in arias intensity were 3%, 3%, 4%, 9% and 0%, 8%, 15%, 16% for Kocaeli 0.21g and Kocaeli 0.51g. In cyclic sinusoidal motion with 8.58 Hz, which is the first mode of 5-story building model, although the reinforcement system showed poor performance up to N=3, which were 1%, 2%, 5% with N=4 improvements of it reached up %17. As expected, N=4 was the most advantageous condition by far for the reinforcement system in reduction of arias intensity and the most efficient motion was Kobe earthquake with 0.89g.

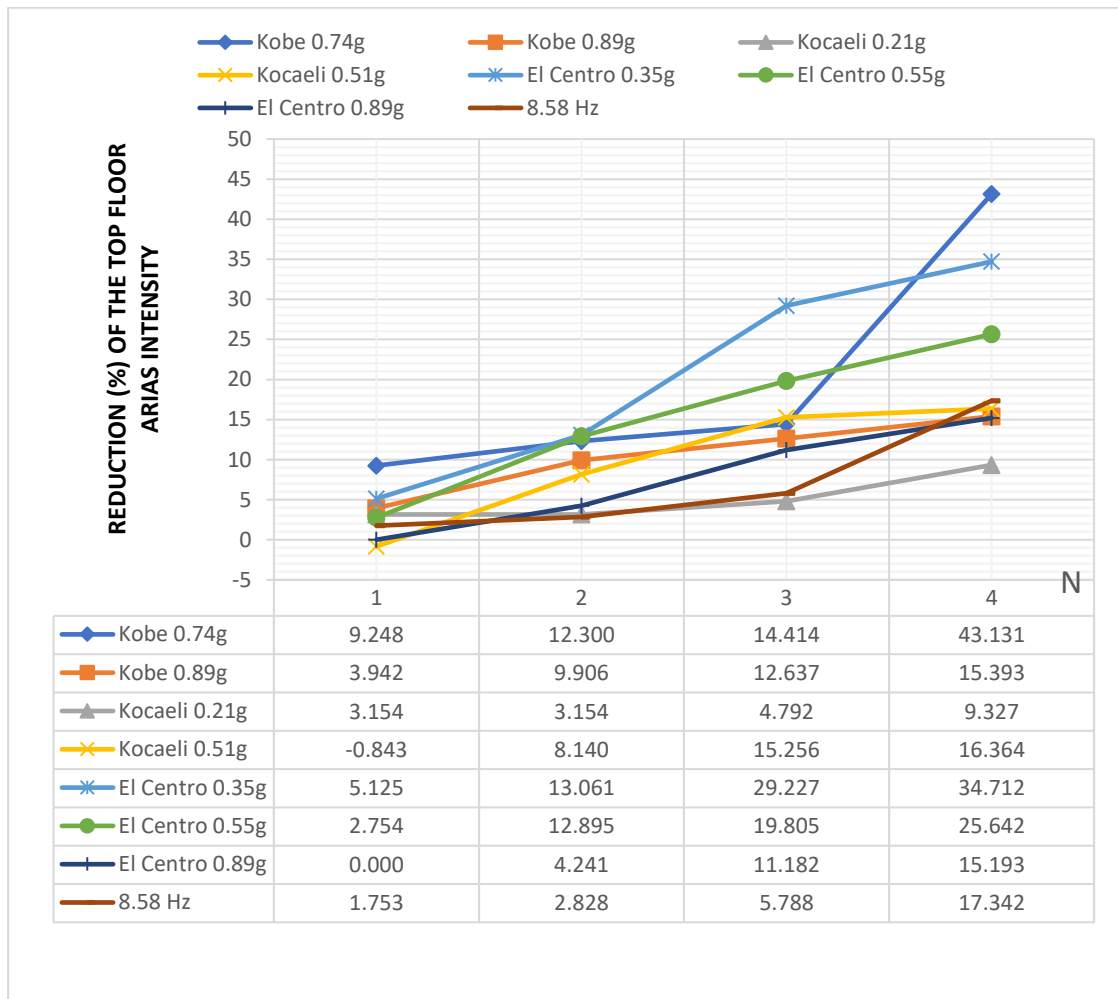


Figure 5.7. Reduction of Top Floor Arias Intensity under Input Motions for 5-Storey Model.

5.1.1.8. Effects of Proposed Geogrid Reinforcement System on Foundation Arias Intensity For 5-Story Model. The changing percentages of foundation arias intensity for all input motions used in shaking table experiments and the effectiveness of proposed geogrid reinforcement system with respect to the number of geogrid layers are exhibited in Figure 5.8. Based on Figure 5.8, it can be observed that the proposed geogrid reinforcement system functioned better under higher acceleration amplitude for Kobe Earthquake motions. The reduction in arias intensity were 7%, 9%, 18%, 22% and 2%, 7%, 11%, 16% for Kobe 0.74g and Kobe 0.89g. The most powerful case was Kocaeli earthquake with 0.51g with decrease up to %46 and for Kocaeli earthquake, system performed better at higher acceleration amplitude. The reduction of arias intensity for foundation were 0%, 7%, 11%, 31% and 4%, 13%, 26%, 46% for N=1,2,3,4, respectively. For El Centro

earthquake, the reinforcement system gave the worst performance in El Centro earthquake with 0.89g, which behaved better under lower acceleration amplitude. The arias intensity decreased up to 5%, 10%, 20%, 23% and 3%, 5%, 5%, 14% for El Centro earthquake with 0.35g and 0.89g in N=1,2,3,4 respectively. In cyclic sinusoidal motion with 8.58 Hz, which is the first of mode of 5-story building model, the decrease of acceleration was 0%, 2%, 22%, 32% for N=1,2,3,4. While until N=2 the system exhibited ineffective performance, in N=3 it ascended dramatically, which was up to 22%. As expected for all cases, N=4 was the most effective condition and N=1 did not partially trigger reinforcement system, there were improvements which were negative or zero.

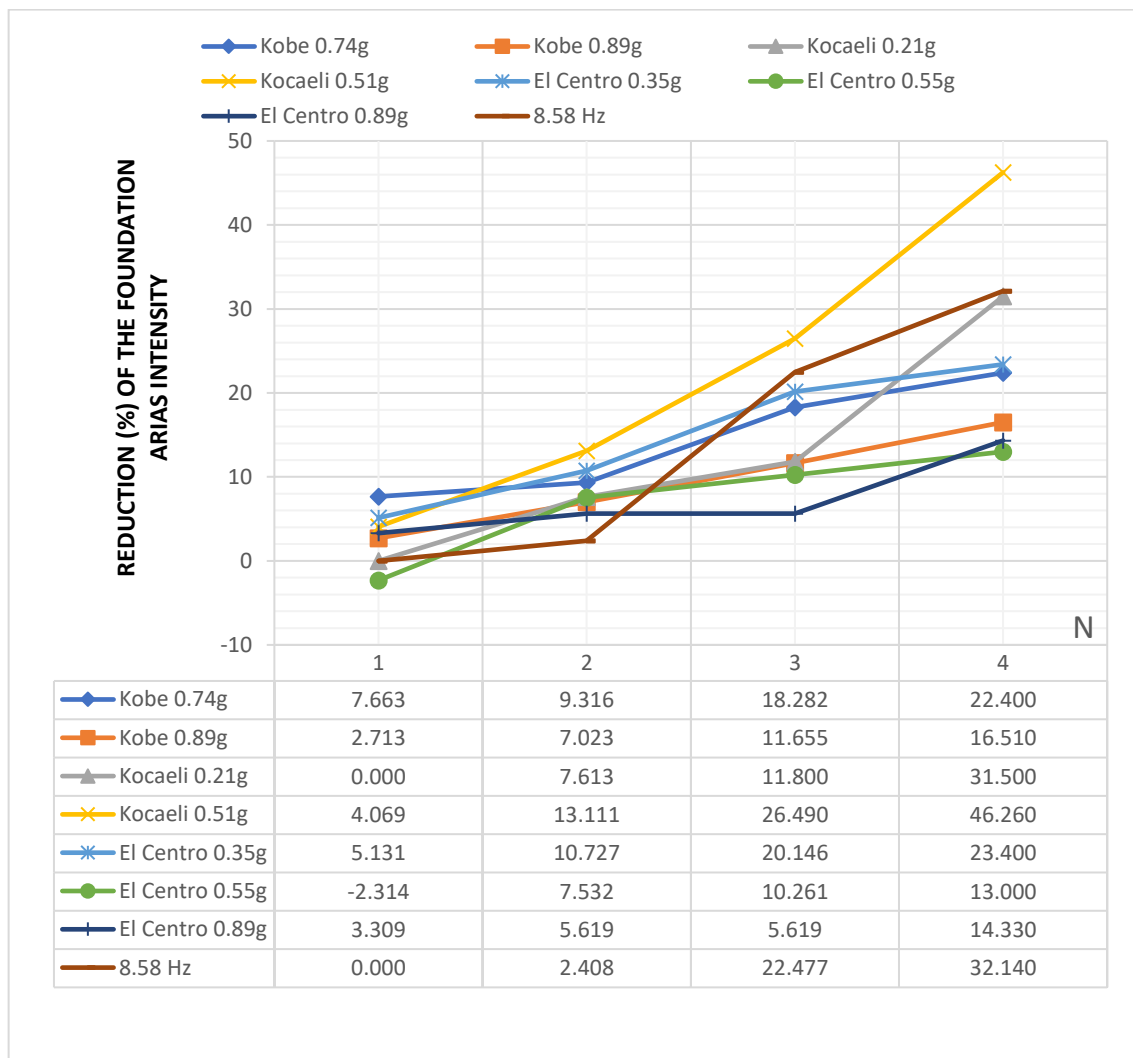


Figure 5.8. Reduction of Foundation Arias Intensity under Input Motions for 5-Storey Model.

5.1.2. Seismic Response of The Cases For 3-Story Model

This part includes the ultimate results and comparisons of the effectiveness of proposed geogrid reinforcement system for 3-Story building model under earthquake motions with real PGA, earthquake Motions with increasing PGA and cyclic sinusoidal motion with first mode frequency of the building model. The effect of geogrid reinforcement layers starting from without reinforcement (N=0) up to N=4 can be seen for all input motions in figures. Also, the effectiveness of proposed geogrid reinforcement was shown by considering the selected performance indicators one by one.

5.1.2.1. Effects of Proposed Geogrid Reinforcement System on Top Floor Acceleration for 3-Story Model. The alteration percentages of the top floor acceleration for all input motions used in shaking table experiments and the effectiveness of proposed geogrid reinforcement system according to the number of geogrid layers are shown in Figure 5.9. According to Figure 5.9. it can be seen that the proposed geogrid reinforcement system worked better at lower acceleration amplitude for Kobe and Kocaeli Earthquake motions. The reduction of top floor acceleration percentages were -1%, 6%, 17%, 25% and -3%, 6%, 10%, 19% for Kocaeli 0.21g and Kocaeli 0.51g. Similarly, the reductions were 0%, 8%, 16%, 20% and -2%, 1%, 7%, 13% for Kobe earthquake with 0.74g and 0.89g. Unlike these earthquakes, in El Centro, geogrid reinforcement system did not exhibit decisive manner for a specific acceleration amplitude. The maximum reduction of top floor acceleration was obtained from El Centro earthquake with 0.55g, which was 23% for N=4. In cyclic sinusoidal motion with 12.46 Hz, which is the second of mode of 3-story building model, although N=1 and N=2 did not have considerable improvement, with increasing the number of geogrid layers it reached up %14. As expected for all cases, N=4 was the most beneficial ones and in Kocaeli earthquake with 0.21g the improvement percentage was maximum, which was 25%. Also, for N=1 the proposed geogrid reinforcement system did not work, or the reduction of top floor acceleration became negative except El Centro earthquake motions.

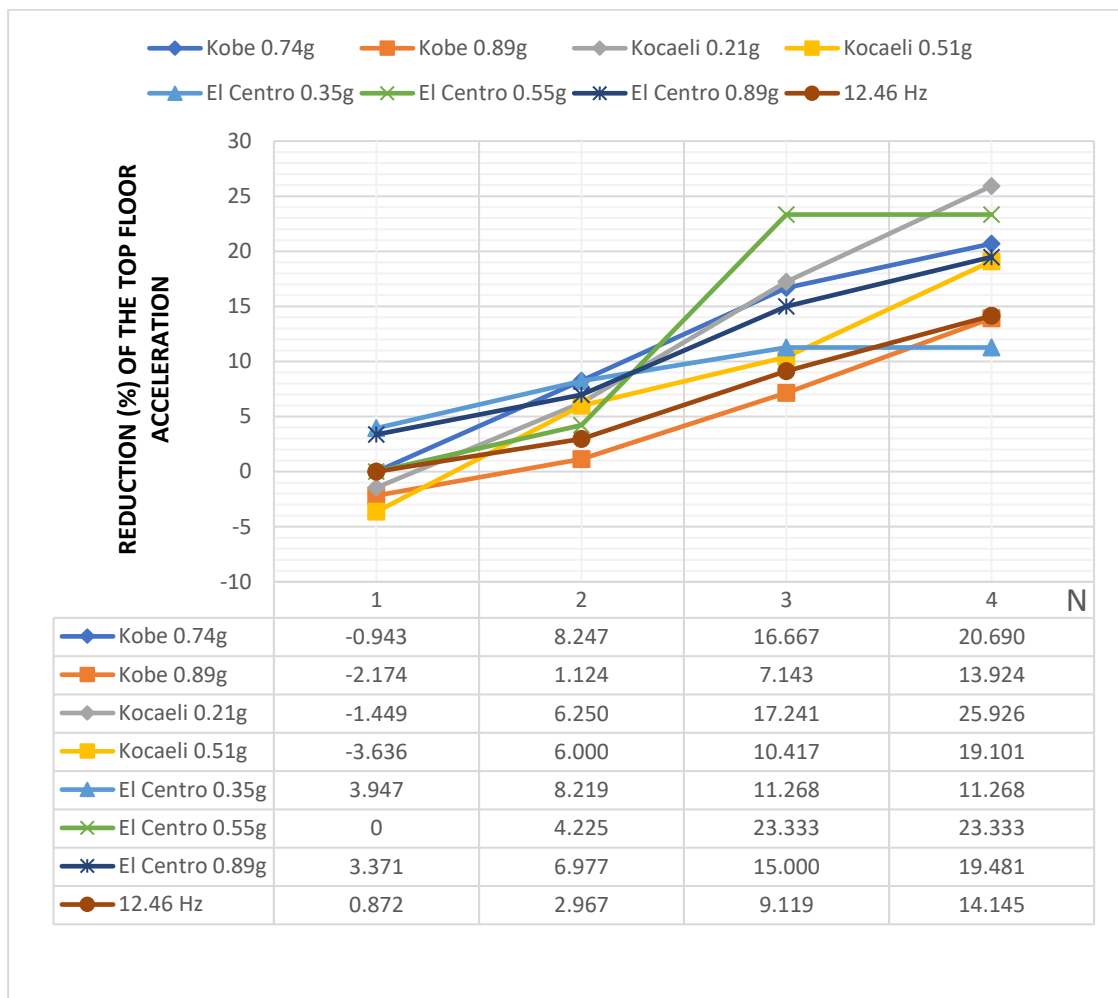


Figure 5.9. Reduction of Top Floor Acceleration under Input Motions for 3-Storey Model.

5.1.2.2. Effects of Proposed Geogrid Reinforcement System on First Floor Acceleration for 3-Story Model. Figure 5.10. shows the variations of the first floor acceleration for all input motions used during shaking table experiments and the effectiveness of proposed geogrid reinforcement system with respect to the number of geogrid layers. As can be observed that the proposed geogrid reinforcement system behaved better at the lower acceleration amplitude of Kocaeli and El Centro earthquakes motion. The reduction in first floor accelerations were 4%, 7%, 9%, 36% and 0%, 3%, 8%, 10% for Kocaeli earthquake with 0.21g and 0.51g in N=1, N=2, N=3, N=4 respectively. And also, for Kobe and El Centro Earthquakes, the changing of acceleration amplitude did not create a noteworthy difference on results. The maximum reduction in acceleration values 17%, 18%, 21% and 14%, 15% for Kobe 0.74g, Kobe 0.89g and El Centro 0.35g, El Centro earthquake with 0.55g and 0.89g, respectively for N=4. Besides Kocaeli earthquake with 0.21g was the

most effective case among the other input motions for proposed geogrid reinforcement system. In cyclic sinusoidal motion with 12.46 Hz, which is the second of mode of 3-story building model, the decrease of accelerations was 0%, 3%, 15% and 24% for N=1, N=2, N=3 N=4. It is obvious that N=4 was the most beneficial case and increasing the number of geogrid layers generated better performance for first floor acceleration reduction in all input motions and also N=1 almost all improvements became negative or 0%.

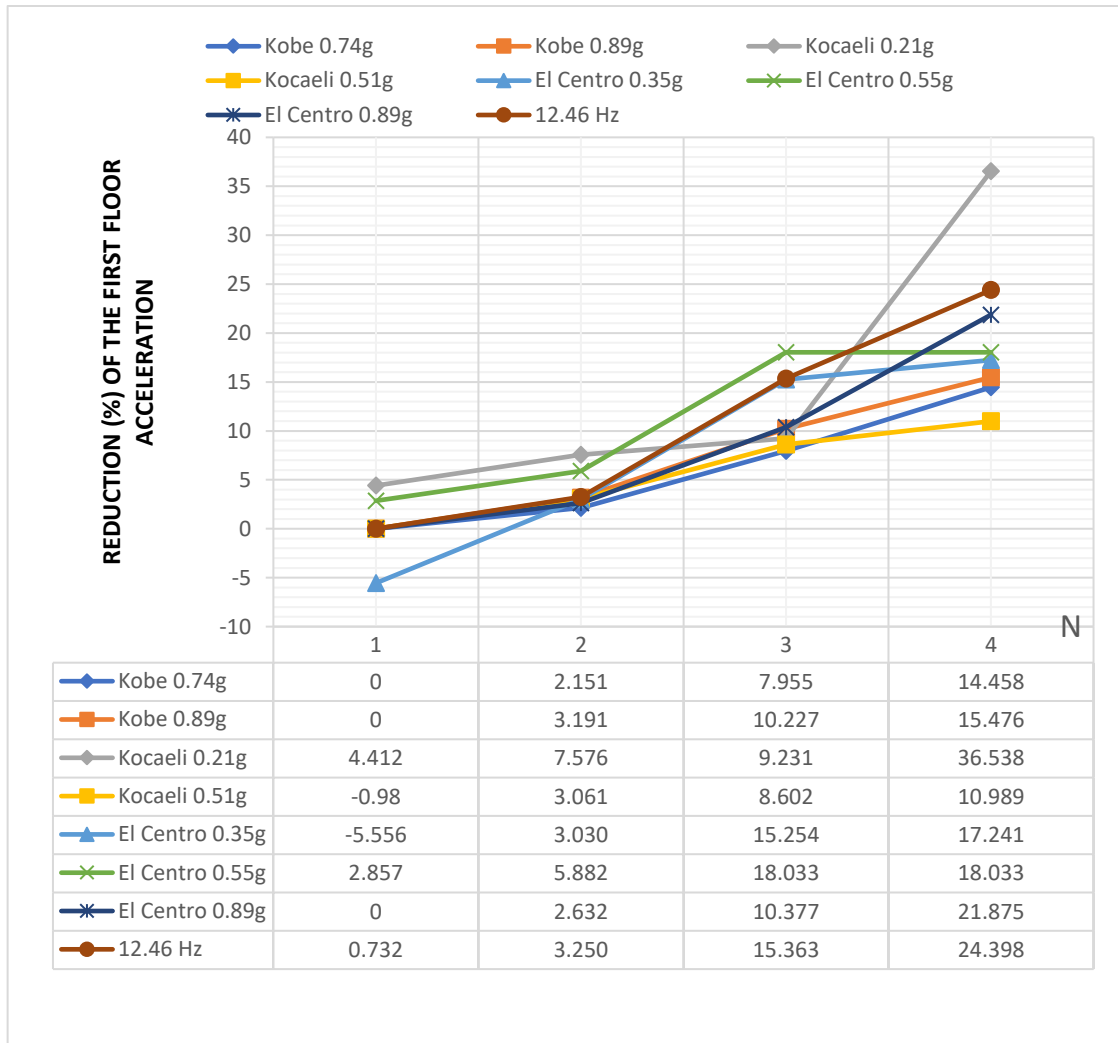


Figure 5.10. Reduction of First Floor Acceleration under Input Motions for 3-Storey Model.

5.1.2.3. Effects of Proposed Geogrid Reinforcement System on Top Floor Displacement for 3-Story Model. Figure 5.11 represents the changing of the top floor displacement for all input motions used in shaking table experiments and the effectiveness of proposed geogrid reinforcement system by the number of geogrid layers. It can be seen that the

proposed geogrid reinforcement system functioned better at the higher acceleration amplitude of El Centro earthquakes motion. The decrease of top floor displacement was 2%, 5%, 7%, 10% and 6%, 9%, 10%, 16% in N=1,2,3,4 respectively for El Centro earthquake with 0.35g and 0.89g. And the maximum improvement for Kobe and Kocaeli earthquakes were 21% and 28% in N=4, also Kocaeli earthquake with 0.51g the most beneficial case among all input motions, it decreased up to 28%. In cyclic sinusoidal motion with 12, 46 Hz, which is the second of mode of 3-story building model, the reduction of top floor displacement showed limited improvement, which were 0% and 2% and with increase of geogrid layers it reached out up to 9%, 13% for N=3 and N=4. As expected for all input motions, N=4 was the most advantageous condition and generally the results of N=2 and N=3 was acceptable in improvement of top floor displacement.

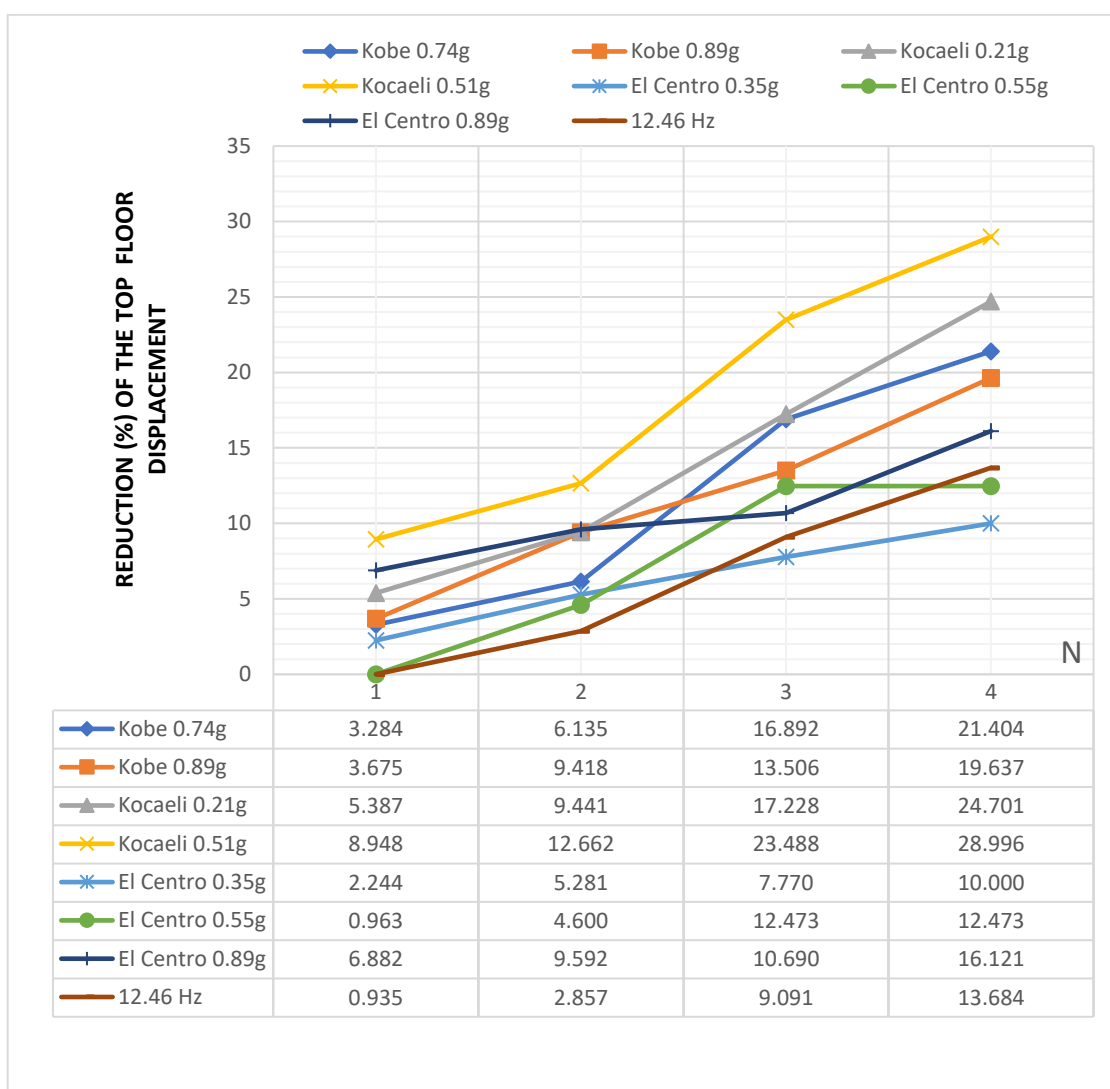


Figure 5.11. Reduction of Top Floor Displacement under Input Motions for 3-Storey Model.

5.1.2.4. Effects of Proposed Geogrid Reinforcement System on First Floor Displacement for 3-Story Model. Figure 5.12 represents the variations of the first floor displacement for all input motions used through shaking table experiments and the effectiveness of proposed geogrid reinforcement system according to the number of geogrid layers. As can be seen the proposed geogrid reinforcement system performs better under higher acceleration amplitude for Kobe Earthquake motions. The reduction of displacement in first floor were 10%, 13%, 22%, 25% and 5%, 7%, 28%, 36% for Kobe 0.74g and Kobe earthquake with 0.89g. In contrast to Kobe earthquake, for El Centro earthquake, reinforcement system functioned better at lower acceleration amplitude. The improvements were 8%, 12%, 16%, 28% and

6%, 7%, 16%, % 20% for El Centro earthquake with 0.35g and 0.89g, respectively. On the other hand, the variation of amplitude of Kocaeli earthquake did not effect improvement of the first floor displacement. The maximum reduction of displacements was 23%, 24% for Kocaeli earthquake with 0.21g and 0.51g. In cyclic sinusoidal motion with 12.46 Hz, which is the second mode of 3-story building model, the reduction of displacement was 3%, 4%, 14%, 19% for N=1,2,3,4. Besides according to results important splash happened in the reduction values between N=2 and N=3 and normally N=4 had the most powerful impact on improvement.

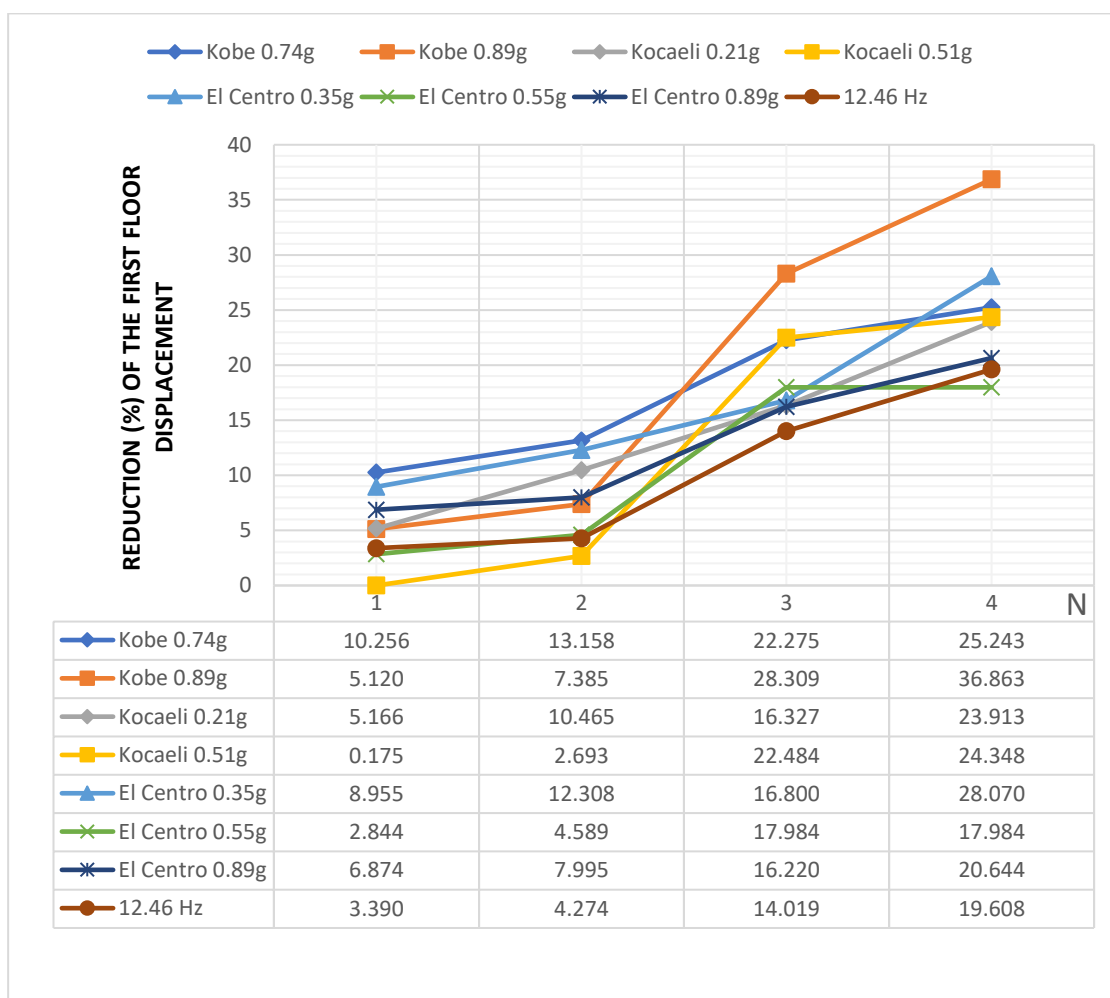


Figure 5.12. Reduction of First Floor Displacement under Input Motions for 3-Storey Model.

5.1.2.5. Effects of Proposed Geogrid Reinforcement System on Foundation Acceleration for 3-Story Model. The alteration percentages of foundation acceleration for all input motions used in shaking table experiments and the effectiveness of proposed geogrid

reinforcement system with respect to the number of geogrid layers are exhibited in Figure 5.13. According to Figure 5.13, it can be observed that the proposed geogrid reinforcement system worked better at higher acceleration amplitude for El Centro, Kocaeli, Kobe Earthquake motions. Their maximum reduction in foundation acceleration were 31%, 28%, 21%, all of them obtained from higher acceleration amplitude, which were Kobe earthquake with 0.89g, Kocaeli earthquake with 0.51g and El Centro earthquake with 0.89g, respectively. And the most beneficial cases were Kobe earthquake with 0.89g and Kocaeli earthquake with 0.51g. Their results were quite similar, which were 2%, 6%, 19%, 31% and 2%, 4%, 19%, 28% for N=1,2,3,4 respectively. And also foundation acceleration decreased up to 0%, 4%, 12%, 12% and 0%, 2%, 10%, 21% for El Centro earthquake with 0.35g and 0.89g. Also system showed similar performance under Kocaeli earthquake with 0.51g and El Centro earthquake with 0.89g. In cyclic sinusoidal motion with 12.46 Hz, which is the second of mode of 3-story building model, the decrease of acceleration was 0%, 3%, 9%, 13% for N=1,2,3,4. As expected for all cases, N=4 was the most effective ones and N=1 almost did not trigger reinforcement system, the improvements became negative or 0%.

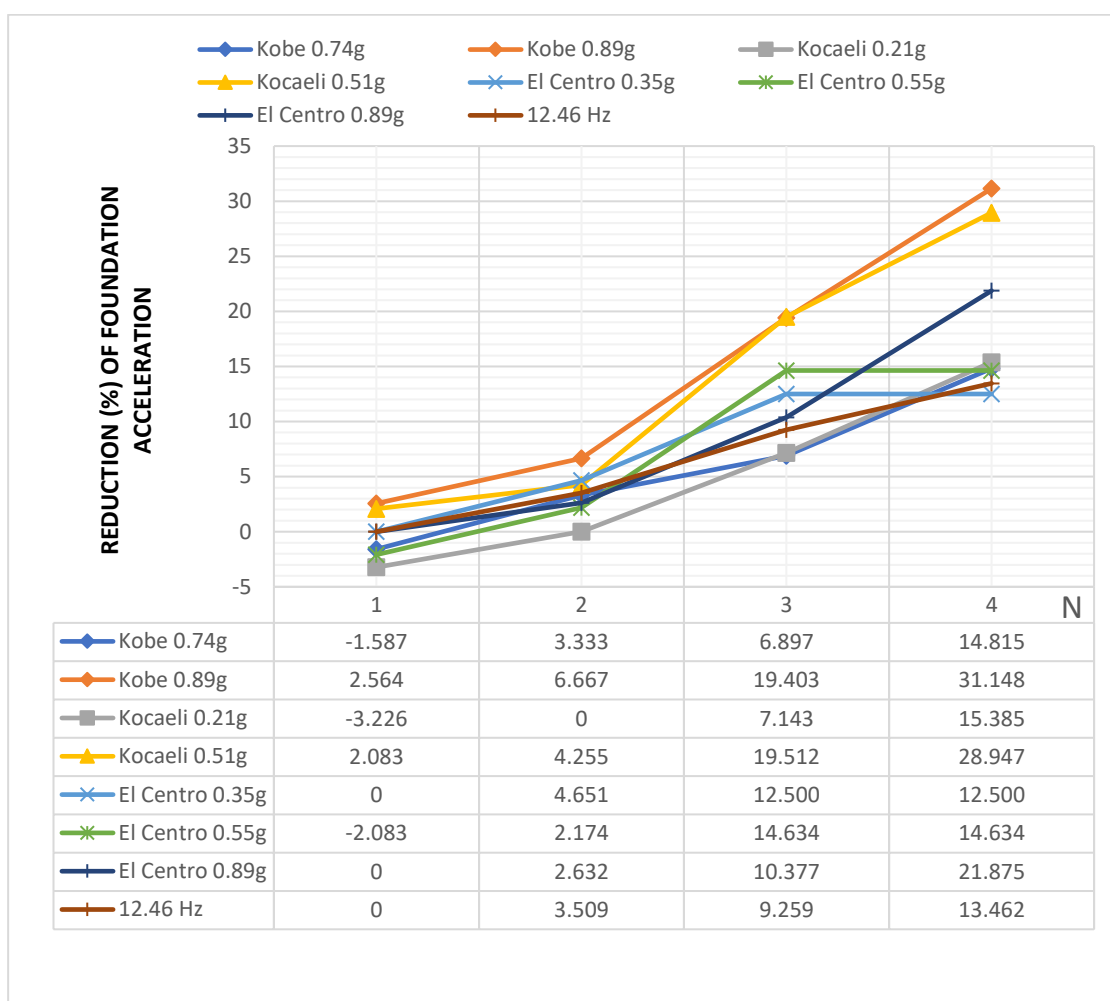


Figure 5.13. Reduction of Foundation Acceleration under Input Motions for 3-Storey Model.

5.1.2.6. Effects of Proposed Geogrid Reinforcement System on Soil Acceleration for 3-Story Model. Figure 5.14 represents the change of soil acceleration for all input motions used in shaking table experiments and the effectiveness of proposed geogrid reinforcement system according to the number of geogrid layers. It can be observed that while the proposed geogrid reinforcement system functioned better under lower acceleration amplitude for Kobe earthquake, performed better performance at higher acceleration amplitude for El Centro Earthquake. The improvement in acceleration values were 3%, 6%, 21%, 35% and 3%, 6%, 17%, 24% for Kobe earthquake with 0.74g and 0.89g. Similarly, the decrease of acceleration were 2%, 6%, 19%, 22% and 5%, 8%, 25%, 35% for El Centro earthquake with 0.35g and 0.89g. In contrast to these two earthquake motions, the reinforcement system did not show considerable difference on changing acceleration

amplitude of Kocaeli earthquake. The improvement in soil acceleration values were -6%, 7%, 11%, 20% and -1%, 4%, 15%, 21% for N=1, N=2, N=3 and N=4 respectively in Kocaeli earthquake with 0.21g and 0.51g. As expected, N=4 was the most advantageous condition by far for improvement in soil acceleration and for the reinforcement system, the best results obtained from Kobe 0.74g and El Centro earthquake with 0.35g, which were 35%. Inc cyclic sinusoidal motion with 12.46 Hz, which is the second of mode of 3-story building model, results indicated inefficient improvement compared to other input motions. The maximum improvement of it was 13%. Besides, for Kocaeli Earthquake motions, N=1 did not perform on improvement of proposed geogrid reinforcement system.

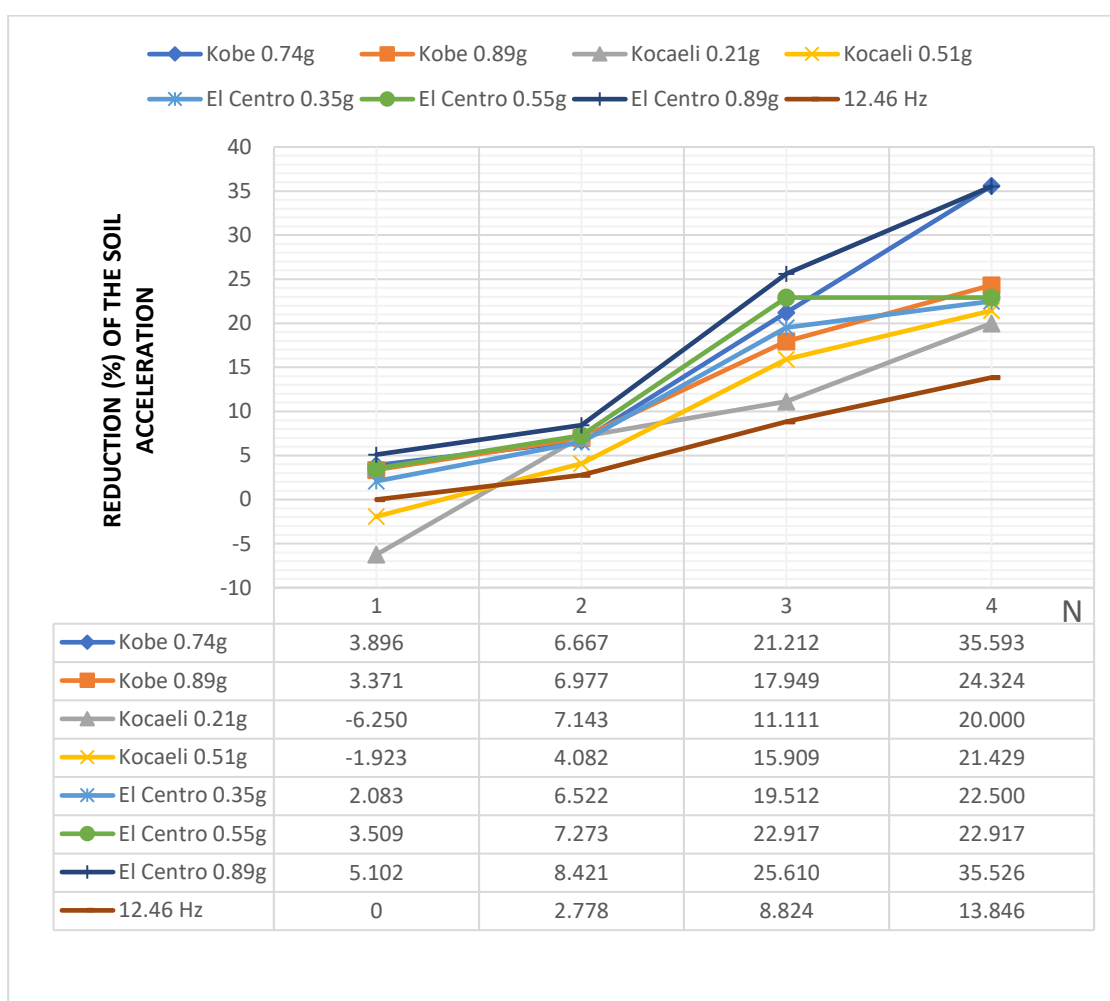


Figure 5.14. Reduction of Soil Acceleration under Input Motions for 3-Storey Model.

5.1.2.7. Effects of Proposed Geogrid Reinforcement System on Top Floor Arias Intensity for 3-Story Model. The changing of top floor arias intensity for all input motions used throughout shaking table experiments and the effectiveness of proposed geogrid

reinforcement system with respect to the number of geogrid layers are exhibited in Figure 5.15. It can be seen in Figure 5.15, the proposed geogrid reinforcement system worked more effective under lower acceleration amplitude for Kobe and Kocaeli Earthquake motions. The reduction in arias intensity were -1%, 10%, 20%, 24% and -2%, 1%, 8%, 16% for Kobe 0.74g and Kobe 0.89g. and also -1%, 7%, 21%, 30% and -4%, 7%, 13%, 22% for Kocaeli earthquake with 0.21g and 0.51g in N=1,2,3,4 respectively. Besides, the most effective results were obtained from Kocaeli earthquake with 0.21g with 30%. Besides among El Centro earthquake motions the best improvement was obtained from El Centro earthquake with 0.55g, which decreased up to 0%, 5%, 25%, 27% and the improvement of top floor arias intensity were 4%, 10%, 12%, 13% and 4%, 8%, 18%, 23% for El Centro earthquake with 0.35g and 0.89g in N=1,2,3,4 respectively. In cyclic sinusoidal motion with 12.46 Hz, which is the second of mode of 3-story building model, the decrease of arias intensity was 1%, 3%, 11%, 16% for N=1,2,3,4. For N=1 and N=2, the system functioned poorly, in N=3 it bounce up to 11% and reached 22% for N=4. As expected for all cases, N=4 was the most effective condition and in N=1 for the most part of input motions the results became negative or zero.

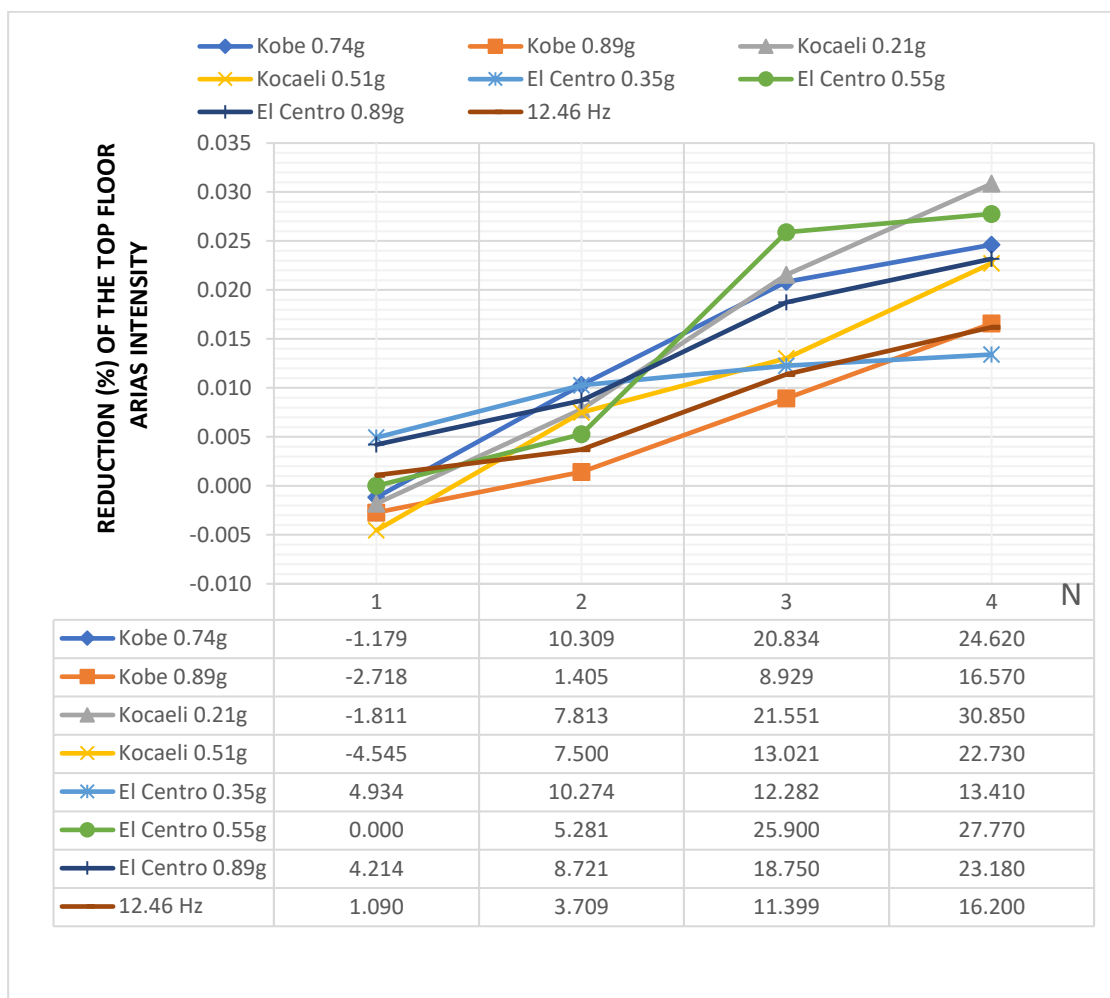


Figure 5.15. Reduction of Top Floor Arias Intensity under Input Motions for 3-Storey Model.

5.1.2.8. Effects of Proposed Geogrid Reinforcement System on Foundation Arias Intensity For 3-Story Model. Figure 5.16 shows the variations of foundation arias intensity for all input motions used in shaking table experiments and the effectiveness of proposed geogrid reinforcement system with according to the number of geogrid layers. As can be observed, the proposed geogrid reinforcement system clearly functioned far better for Kobe earthquake with 0.89g and Kocaeli earthquake with 0.51g and also these two earthquake motion gave more effective results under higher acceleration amplitudes. The decrease of foundation arias intensity were -2%, 4%, 8%, 17% and 3%, 8%, 25%, 36% for Kobe earthquake with 0.74g, and 0.89g and -4%, 0%, 9%, 18% and 2%, 5%, 25%, 33% for Kocaeli earthquake with 0.21g, and 0.51g in N=1,2,3,4, respectively. In contrast to Kocaeli and Kobe Earthquake motions in El Centro motions the proposed geogrid reinforcement

system did not fluctuate considerably according to the alteration of acceleration amplitude. The improvements in arias intensity were 0%, 6%, 13%, 14% and 0%, 4%, 12%, 18% for El Centro earthquake with 0.35g and 0.89g. In cyclic sinusoidal motion with 12.46 Hz, which is the second mode of 3-story building model, although the reinforcement system exhibited limited performance up to N=2, which were 0%, 4%, with increase in the number of geogrid layer, it reached up to 13% for N=4. Just as expected, N=4 was the most beneficial condition for the reinforcement system in reduction of arias intensity.

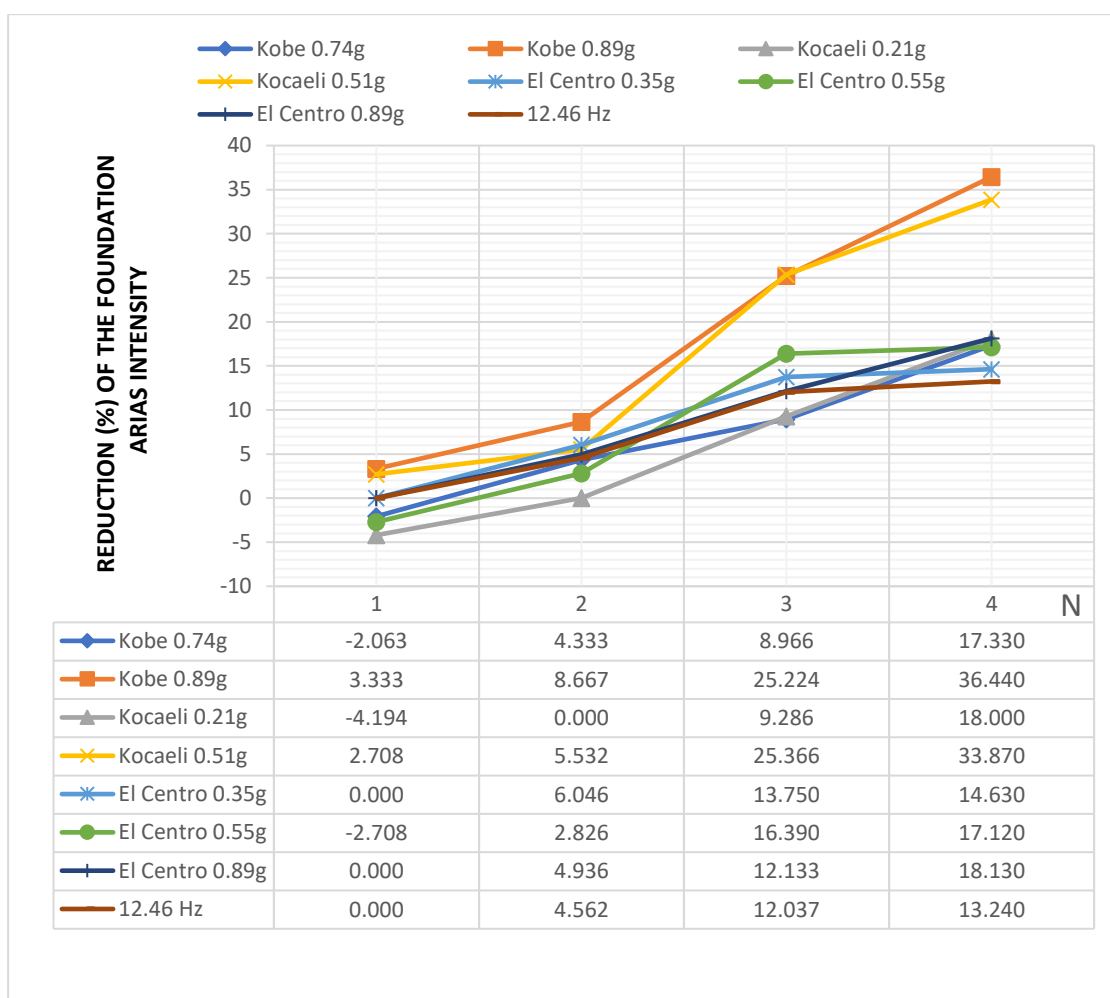


Figure 5.16. Reduction of Foundation Arias Intensity under Input Motions for 3-Storey Model.

6. SUMMARY AND CONCLUSIONS

6.1. Summary

In this study, the aim is to evaluate the behavior and effectiveness of an applicable and low-cost reinforcement system which is known as the geogrid reinforcement on the seismic performance of the low and medium rise buildings. For the sake of the content of this study, an experimental program including free-surface, a 3-storey and a 5-storey 1:10 scaled building models was designed and tested by employing earthquake and harmonic motions in the shaking table test set-up that is located in Earthquake Engineering Department of Boğaziçi University. As investigated in previous studies, the ratio of Geogrid length (L) to building foundation width (B) affects the experimental results. In this study, the L/B ratio was taken as 2.3. This value is the highest possible L/B ratio due to limitations in the experimental setup. According to some literature studies, this value is within the limits of the most effective L/B ratio. The results of this study aim to determine to what extent the seismic performance of low and medium-rise buildings can be improved when $L/B=2.3$.

The main objectives are to observe and analyze the seismic response of the models and soil with and without reinforcement. Uniaxial geogrid was selected as reinforcement material and with the help of geogrids, up to four geogrid layers was constituted in the soil. When the number of geogrid layers was determined to start establishing the experimental setup, studies related to geogrid reinforcement located at under foundation was examined and the number of geogrid layers was specified. According to previously the studies, it is clear that although it can be observed that there is significant increase in the bearing capacity and reduction in displacement and acceleration values up to four geogrid layers, there is no dramatic alteration after four layers. Also, the distance between the first geogrid layer and surface and the distances between geogrid layers were determined in the same way, by benefiting studies focusing on the optimal distances between layers (Patra et al., 2005; Omar et al., 1993). These studies and how these values were found were mentioned in previous parts elaborately.

The cases which were not used geogrid layer ($N=0$) was accepted as reference to observe the effectiveness of geogrid reinforcement system and was named as “without reinforcement (WR)” in the results. The cases with geogrid layer ($N=1,2,3,4$) was compared to the cases not used geogrid layer ($N=0$). The effects of this geogrid reinforcement system on models and soil was investigated through shaking table tests and all cases were repeated at least two times to verify and advance the reliability of the experiment and they were compared to each other.

Totally, the fourteen cases have been established in the altered base conditions and by using both earthquake and cyclic sinusoidal motions for free-surface, 3-storey and 5-storey building models, these results have been evaluated. As earthquake motions, three different earthquakes were selected, which are El Centro (Array #9 Station), Kobe (KJMA Station), and Kocaeli earthquake (Izmit Station) with the varying amplitudes ranging from 0.35g to 0.89g for El Centro earthquake, from 0.21g to 0.51g for Kocaeli earthquake and from 0.74g to 0.89g for Kobe earthquake. Moreover, cyclic sinusoidal motions with the different frequencies that were obtained from the free vibration test of the building models for 5-storey and 3-storey building models.

Through sensors placed at soil and models, accelerations and displacements at each story level were measured during tests and with the help of these data the effect of geogrid reinforcement for free-surface, 3-storey and 5-storey buildings models were examined profoundly and submitted separately. As performance indicators, horizontal acceleration responses, horizontal drifts and their peaks were presented with root-mean square (RSM) for the soil and each story. Besides, the top floor and the foundation were chosen and improvements in there was displayed. Also in the same way, the first and middle floor improvements was displayed in graphs. As additional performance indicator parameters, Arias intensity was chosen to see strength of earthquake on reinforcement and unreinforced systems. Also, in order to observe whether the natural period is shifting or not for geogrid reinforcement system, for all sensors Fourier transform graph was displayed and natural period shifting ratio were presented.

The conclusions based on the results of conducted experiments are presented in the following part of this section.

6.2. Conclusions

The major findings of this study based on performed experiments shall be summarized as follows.

- According to the results of proposed geogrid reinforcement system, it is clear that the number of geogrid layers directly affects to what extend improvements are obtained on seismic response of structure and soil.
- If beneficial effect on the seismic performance is evaluated, it can exceedingly be observed that for $N=1$ and $N=2$ there is more limited improvement in values, which is between %1-10. Also in some cases there is no improvement or values become negative for $N=1$, which means the values taken from $N=1$ is equal or a little bit worse to $N=0$ occasionally. However, this situation is not acceptable for the cases with $N=2$.
- Usually, the geogrid reinforcement system with $N=1$ can not be triggered so the results of most part of cases became negative or 0% under $N=1$.
- Generally, between $N=2$ and $N=3$ there is a considerable progress in the improvement values. According to the results of proposed geogrid reinforcement system, $N=3$ can be regarded as critical threshold for advancement.
- When evaluation of the results was examined elaborately, it may be considered that the proposed geogrid reinforcement system was more efficient under higher acceleration amplitude. However, although there were many cases that the best improvements were obtained from the earthquake motions with higher acceleration amplitude, there were the opposite cases showing better results under lower acceleration amplitude. Hence the performance of proposed geogrid reinforcement system can not be directly dependent on the acceleration amplitude of earthquake motion.
- Another noteworthy inference about the number of geogrid layers is that between $N=3$ and $N=4$ generally there is no dramatic increase in the improvement of defined parameters. Although the best improvements are obtained from $N=4$ mostly and normally, it is seen that the first remarkable splash of progression is gotten in $N=3$ for values.

- Although seismic improvement of the geogrid reinforcement system on 5-storey scaled building model looks like slightly more effective rather than 3-storey model for some cases and the opposite situation for some cases also was observed too. Hence, in general it might be said that the seismic improvement of models can be evaluated regardless of the number of stories.
- Through proposed geogrid reinforcement system, the mode of vibration profile of the structure model did not change, however as expected the magnitudes of acceleration and displacement's amplitude reduced for low-rise, mid-rise buildings and free surface.
- When the transmitted acceleration to foundation, floors and acceleration in soil are investigated, great improvements and mitigation in acceleration values can be seen. The acceleration values decreased up to 24% in Kobe Earthquake, 39% in Kocaeli Earthquake, 35% for El Centro Earthquake motions for 5-storey building model, 35% in Kobe Earthquake, 38% in Kocaeli Earthquake, 35% for El Centro Earthquake for 3-storey model and 25% in Kobe Earthquake, 27% in Kocaeli Earthquake, 34% for El Centro Earthquake for free-surface.
- During the tests the natural period of the 5-story building and 3-story building did not alter. For some cases, negligible fluctuations were detected like +/-1 or 2 %. However, in general the fact that the natural period of building model is stable and proposed geogrid reinforcement system do not change it can be accepted clearly.

In conclusion, the experimental study illustrate that the proposed geogrid reinforcement system is quite effective at the severe seismic motions. Especially, with the increase of geogrid reinforcement layers, the effectiveness of system rises considerably to mitigate earthquake effect for on low-rise and mid-rise buildings.

As a general, the results found in this study are valid for the geogrid material used and the L/B ratio. In order to determine the effect of geogrid reinforced soil on the seismic performance of low and medium-rise buildings, different geogrid properties and different L/B ratios are likely to give different results.

REFERENCES

- Abbas J. K., 2016, “Effective Length of Geogrid Reinforcement Layers under Circular Footing Resting on Sand”, *Engineering And Technology Journal* , Vol. 34, pp. 1823-1833.
- Alawaji, H. A., 2001, “Settlement and Bearing Capacity of Geogrid-Reinforced Sand over Collapsible Soil”, *Elsevier*, Vol. 19, pp.75-88.
- Day, W. R., 2001, *Geotechnical Earthquake Engineering Handbook*, McGraw Hill, New York, Ny, USA.
- Edinçliler, A., Toksoy Y., Yıldız Ö., 2017, “Parametric Study on Seismic Performance of Low and Mid-Rise Buildings on Geogrid Reinforced Sand”, *GeoAfrica 2017 Conference*, 08 – 11 October 2017, Morocco.
- Latha, M. G., Somwanshi A., 2009, “Bearing Capacity of Square Footings on Geosynthetic Reinforced Sand”, *Elsevier*, Vol. 27, pp. 281-294.
- Majedi, P., Çelik S., Akbulut S., 2018, “A Research on The Effect of The Reinforcement Geometry on The Soil bearing Capacity”, *Sigma Journal of Engineering and Natural Sciences*, Vol. 4, pp. 951-960.
- Marto, A., Oghabi M., Eisazadeh A., 2013, “The Effect of Geogrid Reinforcement on Bearing Capacity Properties of Soil Under Static Load; A Review”, *Electronic Journal of Geotechnical Engineering*, Vol. 18, pp. 1881-1898.
- Mohamed G. Arab, G. M., Omar M., Tahmaz A., 2017, “Numerical analysis of Shallow Foundations on Geogrid Reinforced Soil”, *Advances in Sustainable Construction Materials & Civil Engineering Systems (ASCMCES-17) Conference*, 18 - 20 April 2017, Sharjah City, United Arab Emirates.

Noor, I. H., Aizat M. T., Nur S. M., Muhamad R. M. Y., Azrul A. M., Dayang Z. A. H., 2020, *Effectiveness of Strip Footing with Geogrid Reinforcement for Different Types of Soils in Mosul, Iraq*, <https://doi.org/10.1371/journal.pone.0243293>, December 17, 2020.

Omar, M.T., Das B.M., Puri V.K., Yen S.C., 1993, “Ultimate Bearing Capacity of Shallow Foundations on Sand with Geogrid Reinforcement”, *Canadian Geo- technical Journal*, Vol. 30, pp. 545-549.

Patra, C. R., Das B. M., Atalar C., 2005, “Bearing Capacity of Embedded Strip Foundation on Geogrid-Reinforced Sand”, *Elsevier*, Vol. 23, pp. 454-462.

Pedley, J. M., *The Performance of Soil Reinforcement in Bending and Shear*, 1990, Ph.D. Thesis, University of Oxford, Oxford.

Santhakumar, A. R., Verma K. A., Appa Rao T. V. S. R., 2001, “Dynamic Behavior of Geogrid-Reinforced Soil”, *Fourth International Conference on Recent Advances in Geotechnical Earthquake Engineering and Soil Dynamics*, India.

Saran, Swami., 2005, *Reinforced Soil and Its Engineering Applications*, I.K. International Publishing House, New Delhi, India.

Sekman, M. 2016, *Experimental Study on Mitigation of Earthquake Hazards Using Geosynthetics*, MS. Thesis, Boğaziçi University, Istanbul.

Sharma, R., Chen Q., Farsak-Abu M., Yoon S., 2009, “Analytical Modeling of Geogrid Reinforced Soil Foundation”, *Elsevier*, Vol. 27, pp. 63-72.

Shin, E. C., Das B. M., LEE E. S., Atalar c., 2002, “Bearing Capacity of Strip Foundation on Geogrid-Reinforced Sand”, *Geotechnical and Geological Engineering*, Vol. 20, pp. 169-180.

Xu, R., Behzad Fatahi B., 2018, “Influence of Geotextile Arrangement on Seismic Performance of Mid-Rise Buildings Subjected to MCE Shaking”, *Elsevier*, Vol. 46, pp. 511-528.

Yadu, L., Tripathi R. K., 2013, “Effect of The Length of Geogrid Layers in The Bearing Capacity Ratio of Geogrid Reinforced Granular Fill-Soft Subgrade Soil System”, *Social and Behavioral Sciences*, Vol. 104, pp. 225-234.

Yetimoğlu, T., Jonathan T. H. W., Sağlamer A., 1994, “Bearing Capacity of Rectangular Footings on Geogrid-Reinforced Sand”, *Journal of Geotechnical Engineering*, Vol. 12, pp. 2083-2099.

Zhang, L., Wang J., Victor N. K., TANG Y., 2020, “Load Bearing Characteristics of Square Footing on Geogrid-Reinforced Sand subjected to Repeated Loading”, *Journal of Central South University*, Vol 2, pp. 920–936.